Nanoparticles as advanced treatment modalities to disinfect the root canal system

Amir I.O. Ibrahim

A thesis submitted in fulfillment of the requirement for the degree of

Doctor of Philosophy

Department of Restorative Dentistry

Faculty of Dentistry

University of the Western Cape

Supervisors: Dr. Desigar Moodley

Professor Leslie F. Petrik

Keywords

Endodontics

Intra-canal medicament

Nanoparticles

Chitosan nanoparticles

Chitosan hydrogel

Zeolite

Streptococcus mutans

Enterococcus faecalis

Candida albicans

Abstract

Introduction: Persistent root canal pathogens are one of the main causes of endodontic treatment failure. These pathogens are usually isolated in areas within the root canals that are inaccessible to mechanical instrumentation, chemical irrigants and medicaments resulting in incomplete sterilization of the root canal system. Furthermore, the development of resistant microbial species renders it difficult to disinfect the root canal system using commonly available root canal irrigants and intra-canal medicaments. Intra-canal medicaments are antimicrobial agents that are placed inside the root canal system in order to eliminate the remaining microorganisms that persist after mechanical instrumentation and irrigation. However, their antimicrobial efficacy is effective only against some of the root canal pathogens. Furthermore, the presence of tissue inhibitory factors such as dentine powder and serum albumine within the root canal system inhibits their antimicrobial activity. The use of nanoparticles as antimicrobial agents has recently attracted considerable attention especially in the medical field as a result of their unique antibacterial properties. These properties include their ability to use multiple mechanisms to eradicate microbial cells and their low potentiality to produce microbial resistance. Polymeric nanoparticles such as chitosan nanoparticles (Ch-Np) gained significant interest as a result of their biocompatible and antimicrobial properties. In medicine, several vehicles were designed to carry these antibacterial nanoparticles. Zeolites (Ze) are microporous crystalline hydrated sodium aluminosilicate material that is utilized in the chemical sciences as a carrier for various nanoparticles. **Aim:** The aim of this study was to create a novel bioactive

nanocomposite intra-canal medicament using chitosan nanoparticles (Ch-Np), loaded into Zeolite-Y as a carrier and evaluate its antimicrobial and biological properties against root canal pathogens. **Methods:** The antimicrobial activity of low molecular weight chitosan (LMW-Ch) was first evaluated against *Streptococcus mutans, Enterococcus faecalis* and *Candida albicans* in a planktonic state using a Time-Kill Test performed by broth micro-dilution technique. Chitosan nanoparticles were synthesized from LMW-Ch using electrospraying technique. Ch-Np were characterized for their size, surface charge, morphology and chemical structure. The antimicrobial efficacy of Ch-Np was then evaluated against *S. mutans*, *E. faecalis* and *C. albicans* in a planktonic state using a Time-Kill Test performed using broth micro-dilution technique and against biofilm biomass using a microtiter plate biofilm assay. The newly created chitosan nanoparticle based intra-canal medicament was created by loading Ch-Np onto Zeolite and its antimicrobial activity evaluated using agar diffusion test. Additionally, the effect of tissue inhibitors (dentine powder and serum albumin) on the antibacterial activity of the novel Ch-Np-Zeolite nanocomposite was evaluated using a Time-Kill Test performed by broth micro-dilution technique. Finally, the cytotoxicity of LMW-Ch, Ch-Np, Zeolite-Y and Ch-Np-Zeolite nanocomposite was evaluated against 3T3 mouse fibroblast cells. **Results:** LMW-Ch showed bactericidal effect against *S. mutans* and *E. faecalis* and showed fungistatic effect against *C. albicans*. Electrospraying of LMW-Ch produced Ch-Np with average particle size of 430 nm and a surface charge of 51.7 mV. Ch-Np completely eradicated *S. mutans* and *E. faecalis* in planktonic state within 30 minutes and 1 hour respectively and showed fungistatic activity of *C. albicans*. Furthermore, Ch-Np produced significant reduction in the biofilm biomass for all tested pathogens. Ch-Np when loaded onto Zeolite produced a paste like material

was created to serve as a novel intra-canal medicament, and showed a mean diameter inhibition zone of 9.6 mm for *S. mutans* and 7.8 mm for *E. faecalis*. The presence of tissue inhibitors did not affect the antibacterial efficacy of Ch-Np-Zeolite nanocomposite. When tested for cytotoxicity using 3T3 cells none of the tested materials was shown to be cytotoxic. **Conclusions:** The novel Ch-Np-Zeolite nanocomposite completely eradicated *S. mutans* and *E. faecalis* even in the presence of tissue inhibitors and showed fungistatic activity and great reduction in the biofilm biomass of *C. albicans*. Furthermore it promoted the growth of 3T3 fibroblast cell suggesting its capability to heal the injured periapical tissue.

Publications, presentations and awards

Articles relevant to the thesis and published in scientific journals

- Ibrahim, A.I.O., Moodley, D.S., Petrik, L. and Patel, N., 2017. Use of antibacterial nanoparticles in Endodontics. *South African Dental Journal*, 72(3), pp.105-112.
- Moodley, D.S., Ibrahim, A.I.O., Petrik, L.F., Maboza, E.J.M., Olivier, A., The antimicrobial activity of chitosan against endodontic pathogens (Submitted).
- Ibrahim, A.I.O., Moodley, D.S., and Petrik, L. Synthesis and antimicrobial properties of chitosan nanoparticles against endodontic pathogens. Ready for submission)
- Ibrahim, A.I.O., Moodley, D.S., and Petrik, Antimicrobial propeties of chitosan laoded in Zeolite nanoparticles as a novel intracanal medicament (Ready for submission).

Presentations at scientific congresses

- Antimicrobial properties of a novel chitosan nanoparticle based intra-canal medicament (2018). Ibrahim, A.I.O., Moodley, D., Petrik, L., Maboza, E .J., Olivier, A., *48th Scientific meeting of the South African division of the International Association of Dental Research*. South Africa. Cape Town. Abstract no. 3005589.

- Antimicrobial properties of Zeolite and Titanium Dioxide containing nanoparticles (2016). Ibrahim, A.I.O., Moodley, D., Petrik, L., Missengue, R. N.M., Patel, N., Osman, Y., 47th *Scientific meeting of the South African division of the International Association of Dental Research*. South Africa. Cape Town. Abstract no. 2590091.

Awards and Achievements

- Best postgraduate research paper presented on the 48th Scientific Meeting of the South African Division of the International Association of Dental Research, 2018, Pretoria, South Africa.

- Best presentation by postgraduate student. 2018. Research Day. Faculty of Dentistry. University of the Western Cape, Cape Town, South Africa.

Declaration

I declare that: "*Nanoparticles as advanced treatment modalities to disinfect the root canal system"* is my own work, that it has not been submitted for any degree or examination in any other university, and that all the sources I have used or quoted have been indicated and acknowledged by complete references.

Signed: 

Full name: Amir Isam Omer Ibrahim Date: …6/11/2018…….

Acknowledgement

First and foremost, I would like to thank Allah for His endless mercy, blessings and gifts. I thank Allah for His grace that enabled me to successfully complete this thesis.

There are no proper words to convey my deep gratitude and respect for my supervisor **Dr. Desigar Moodley** for his invaluable guidance, advice, support, criticism and encouragement throughout this project. It is an honor to know him as a supervisor and researcher and to have him as a supervisor for my thesis. I will always be indebted to him.

My sincerest gratitude is extended to my thesis co-supervisor **Prof. Leslie F Petrik** for her continuous support, guidance, cooperation, encouragement and for facilitating all the requirements, going out of her way. No words can convey my sincere gratitude.

I owe my deepest gratitude towards my better half and beloved wife **Rasha Medhat** for her support and understanding of my goals and aspirations. Her love and support has always been my strength. Her patience and sacrifice will remain my inspiration throughout my life. Without her help, this thesis could not be completed. I love you.

I would like to express my gratitude to **Mr. Ernest J. Maboza** for his valuable guidance, timely suggestions and support. His technical and editorial advice was essential to the completion of the microbiology part of this thesis.

I greatly appreciate all the hard work and the tremendous support of **Mrs. Annette Olivier** for her extensive help with the *in vitro* cytotoxicity testing and for always providing me with a positive energy through my PhD journey.

My special words of thanks should also go to **Mrs. Reneda Basson**, Oral and Dental Research Institute, for providing me with invaluable assistance and support. She always helped and supported me in various ways. Words cannot express my gratitude. I also like to thank her for the proof reading of the thesis.

I also thank **Prof. Herman W. Kruijsse**. Most of the results described in this thesis would not have been obtained without his assistance and support for the statistical analysis.

I gratefully acknowledge the **Oral and Dental Research Institute** staff, Faculty of Dentistry, University of the Western Cape, for providing me with all the facilities, support and to allow me to carry out my research in this esteemed institute. I also extend my appreciation to **Dr. Nicky Basson** and **Prof. Sias Renier Grobler**.

I also thank my colleagues **Mr. Cosmas C. Uche**, **Dr. Roland Missengue**, **Dr. Mazin Sirry**, and **Mr. Ahmed Aldood** for their great assistance.

I greatly appreciate and acknowledge the support received from the **Environmental Nanoscience Research group**, Department of Chemistry, Faculty of Natural Science, University of the Western Cape. Most of the results described in this thesis would not have been obtained without their support.

Last but not least I greatly appreciate the fund that I received from **AgriProtein** that enables me to complete this project.

Dedication

I dedicate this thesis to my lovely wife Rasha, My mother and to the soul of my father

Contents

List of Figures

List of Tables

Abbreviations

Ch	Chitosan
LMW	Low molecular weight
HMW	High molecular weight
ATCC	America type culture collection
BHI	brain heart infusion broth
Mcf	McFarland standard
PBS	Phosphate buffer saline solution
CFU	Colony forming units
Np	Nanoparticle
Ze	Zeolite
FTIR	Fourier transform infrared
SEM	Scanning electron microscopy
TFA	Trifluoroacetic acid
PDI	Polydispersity index

Chapter 1
Background

1.1 Introduction

Persistent root canal pathogens are one of the main causes of endodontic treatment failure (Ricucci *et al.*, 2015; Endo *et al.*, 2013; Lin *et al.*, 1992). These pathogens are usually isolated in areas within the root canals that are inaccessible to mechanical instrumentation, chemical irrigants and intra-canal medicaments and resulting in incomplete sterilization of the root canal system (Nair *et al.*, 2005). Such areas include the deeper parts of the dentinal tubules and the isthmus area (Lin *et al.*, 1991).

Numerous root canal irrigants are currently available. Although their use showed some effectiveness against some pathogens, none of them have the ability to completely eradicate the persistent pathogens from the root canal system (Stuart *et al.*, 2006). In addition, mature microbial biofilm has the ability to resist the antibacterial action of commonly used root canal irrigants (Stojicic *et al.*, 2013).

Intra-canal medicaments are antimicrobial agents that are placed inside the root canal system in order to eradicate the remaining microorganisms that persist after mechanical instrumentation and irrigation (Mohammadi and Dummer, 2011). Calcium hydroxide is the most commonly used intra-canal medicament, however its antimicrobial activity is only effective against some of the root canal pathogens (Ørstavik and Haapasalo, 1990).

In addition, the presence of factors such as dentine powder, dentine matrix and remnants of pulp tissue within the root canal system was shown to inhibit the antimicrobial properties of calcium hydroxide (Haapasalo *et al.*, 2007; Haapasalo *et al.*, 2000) as a result of the buffering action against its alkalinity (Portenier *et al.*, 2001). Furthermore, the development of resistant microbial species renders it difficult to disinfect the root canal system using commonly available root canal irrigants and intra-canal medicaments (Wang *et al.*, 2012; Evans *et al.*, 2002).

Several studies have attempted to find an effective way to eradicate persistent endodontic pathogens from the root canal system by optimizing the role of mechanical preparation and by using different treatment modalities (Elakanti *et al.*, 2015; Estrela *et al.*, 2008; Shabahang and Torabinejad, 2003). The use of nanoparticles as antimicrobial agents has recently attracted considerable attention in Pharmaceutical Sciences as a result of their superior antibacterial properties (Seil and Webster, 2012). Although most of the nanoparticles possess the same unique properties which are their ability to activate multiple mechanisms to eradicate microbial cells and their low potentiality to produce microbial resistance, there may be slight differences in the antimicrobial mechanism among different types of nanoparticles (Beyth *et al.*, 2015). In medicine several antimicrobial nanoparticles such as silver (Ag) and zinc oxide (ZnO) were evaluated against various microbial species. These nanoparticles showed a promising effect against persistent microorganisms as they overcome antimicrobial resistance (Wu *et al.*, 2014; Guerreiro-Tanomaru *et al.*, 2013). However, their application as antimicrobial agents against endodontic pathogens is an area that requires further investigation starting from evaluation of their antimicrobial activity in various conditions to how they can be applied clinically.

In medicine, several vehicles were designed to carry these antibacterial nanoparticles. The new materials that resulted from incorporation of nanoparticles with other carrier materials are known as nanocomposites (Evanoff and Chumanov, 2005). Several types of nanocomposites are available, such as incorporation of metallic nanoparticles into polymer and metal into clay (Shameli *et al.*, 2010; Balan and Burget, 2006).

Chitosan (Ch) is a natural polysaccharide (Şenel *et al.*, 2000) obtained by deacetylation of chitin (Silva *et al.*, 2013). Chitosan is characterized by its antimicrobial properties against different microbial species (Palmeira-de-Oliveira *et al.*, 2010; Tayel *et al.*, 2010; Helander *et al.*, 2001). The antimicrobial mechanism of chitosan results from several interacting factors. The particle size of chitosan was reduced into nanoparticles using different techniques to expand their areas of application and to enhance their antimicrobial activity (MubarakAli *et al.*, 2018; Divya and Jisha, 2018).

Zeolites (Ze) are microporous crystalline hydrated sodium aluminosilicate materials (Gougazeh and Buhl, 2014). Several nanoparticles can be added to zeolites as a result of their porous structure which allows controlled size and distribution of nanoparticles (Talebi *et al.*, 2010). In the chemical sciences, incorporation of antimicrobial nanoparticles into different types of zeolites and their antimicrobial properties were recently evaluated against multiple microorganisms (Missengue *et al.*, 2016). The results of these studies show that different types of zeolites can controllably leach the loaded antimicrobial nanoparticles whilst maintaining their antimicrobial properties (Ferreira *et al.*, 2016; Missengue *et al.*, 2016).

1.2 Rationale of the study

Complete eradication of endodontic pathogens from the root canal system has not been shown in the literature. In medicine, several nanocomposite materials are available as effective antimicrobial agents; however their use against endodontic pathogens has not been fully investigated.

In this study, a novel bioactive chitosan nanoparticle-zeolite nanocomposite material was created to be used as an intra-canal medicament in order to overcome some of the shortcomings of current intra-canal medicaments.

1.3 Aims and objectives of the study

The aim of this study was to create a novel bioactive nanocomposite intra-canal medicament using Chitosan nanoparticles (Ch-NP), loaded into Zeolite-Y as a carrier and to evaluate its antimicrobial and biological properties.

The objectives of the study were:

i. To evaluate the antimicrobial effect of low molecular weight chitosan (LMW-Ch) against *Streptococcus mutans, Enterococcus faecalis* and *Candida albicans* at two different concentrations.
ii. To evaluate the antimicrobial effect of chitosan nanoparticles against *Streptococcus mutans, Enterococcus faecalis,* and *Candida albicans* over time and compare its effect with low molecular weight chitosan.
iii. To evaluate the antibacterial effect of Ch-Np when loaded into Zeolite-Y against *Streptococcus mutans, Enterococcus faecalis,* and *Candida albicans.*

iv. To evaluate the effect of tissue inhibitor factors such as dentin powder and serum albumin on the antibacterial effect of the novel Ch-Np-Zeolite nanocomposite.

v. To evaluate the cytotoxicity of the LMW-Ch, Ch-Np, Zeolite-Y and the novel Ch-Np-Zeolite nanocomposite.

1.4 Research approach

In order to achieve the above-mentioned aim and objectives, the thesis was divided into two phases (Figure 1-1). The first phase included evaluation of the antimicrobial properties of LMW-Ch against samples of endodontic pathogens. Chitosan nanoparticles were synthesized using the LMW-Ch and characterized using scanning electron microscopy, Zetasizer, Zeta potential and Fourier-transform infrared spectroscopy.

The second phase of this study included evaluation of the antimicrobial effect of using Ch-Np against selected endodontic pathogens in a planktonic state and against their biofilm biomass. Additionally, Ch-Np was loaded into Zeolite-Y to form a novel Ch-Np-Zeolite nanocomposite in a paste form to be used as an intra-canal medicament and its antimicrobial effect was evaluated. The effect of tissue inhibitors on the antimicrobial activity of Ch-Np-Zeolite nanocomposite was also evaluated. The use of non-toxic material is one of the main requirements of any material when used *in vivo*, thus the cytotoxic effect of the novel Ch-Np-Zeolite nanocomposite was evaluated against mouse fibroblast cells (3T3).

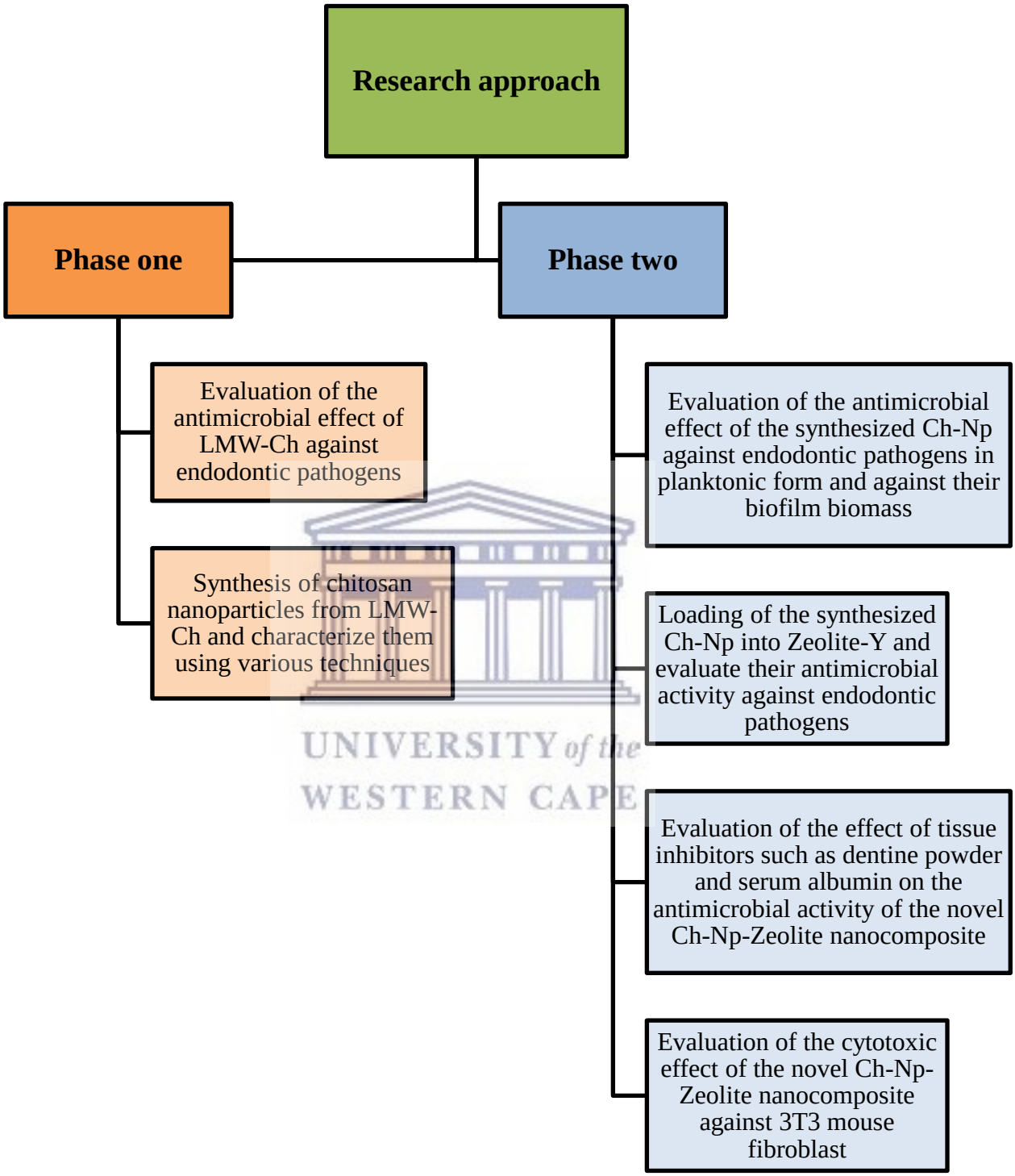

Figure 1-1: Flow chart showing the two phases of the research approach

1.5 Null hypothesis

i. Ch-Np does not have any effect on endodontic pathogens and cannot reduce the biofilm biomass.
ii. The antimicrobial effect of Ch-Np-Zeolite nanocomposite is affected by the presence of tissue inhibitors.
iii. There is a cytotoxic effect when using Ch-Np-Zeolite nanocomposite.

1.6 Thesis outline

This thesis is divided into seven chapters and is designed as follows:

Chapter 1: This chapter is an introduction presenting a brief overview of the literature regarding the microbial role as one of the factors causing endodontic failure. Furthermore, it provides a brief review on the current treatment modalities used to disinfect the root canal system and the new developments in antimicrobial agents that may be used in endodontics. The rationale and objective for conducting this thesis as well as the research question are outlined and finally the framework of the thesis design is provided.

Chapter 2: This chapter provides a review of the literature. It reviews the role of microorganisms as a primary aetiological factor in endodontic diseases. Furthermore, it outlines the different treatment protocols currently available to treat endodontic diseases and to combat these endodontic pathogens. Finally it outlines the role of nanotechnology on synthesizing nanoparticles that have the potential to act as antimicrobial agents. The current studies that used nanoparticles to combat persistent endodontic pathogens were also reviewed.

Chapter 3: This chapter aims to evaluate the antimicrobial effect of LMW-Ch against endodontic pathogens and to determine whether it could serve as an effective precursor to synthesize Ch-Np for the intended application within the root canal system. It also provides a review of the literature on the use of chitosan as an antimicrobial agent and its suggested mechanism of action as antimicrobial agent.

Chapter 4: This chapter aims to synthesize water soluble chitosan nanoparticles and characterize them using different characterization methods such as zeta-sizer, zeta-potential, Fourier-transform infrared spectroscopy and scanning electron microscopy. It also provides a literature review on the different techniques used to synthesize Ch-Np and provides the advantage of the selected method used in this study compared to other methods available in the literature.

Chapter 5: This chapter presents the findings of the conducted experiment which evaluated the antimicrobial effect of the synthesized Ch-Np against endodontic pathogens in a planktonic state and against its ability to reduce the biofilm biomass of endodontic pathogens. Furthermore, it illustrates the difference between the antimicrobial effect of the synthesized Ch-Np in Chapter 3 and LMW-Ch.

Chapter 6: This chapter describes the method used to load the synthesized Ch-Np into Zeolite-Y to form a novel nanocomposite to serve as intra-canal medicament. Furthermore, it evaluates its antimicrobial effect against endodontic pathogens in the presence and absence of tissue inhibitors such as dentine powder and serum albumin.

Chapter 7: This chapter aims to evaluate the cytotoxicity of LMW-Ch, Ch-Np, Zeolite-Y and the novel Ch-Np-Zeolite nanocomposite by evaluating its effect on the growth rate of mouse 3T3 fibroblast cells in culture.

Chapter 8: This chapter summarizes the findings of this thesis, shows the recommendations and provides the prospective studies that can be generated from this thesis.

1.7 References

Balan, L., and Burget, D. (2006). Synthesis of metal/polymer nanocomposite by UV-radiation curing. *European Polymer Journal*, 42(12): 3180-3189.

Beyth, N., Houri-Haddad, Y., Domb, A., Khan, W., and Hazan, R. (2015). Alternative antimicrobial approach: Nano-antimicrobial materials. *Evidence-Based Complementary and Alternative Medicine*, 2015: 1-16.

Divya, K., and Jisha, M. S. (2018). Chitosan nanoparticles preparation and applications. *Environmental Chemistry Letters*, 16(1): 101-112.

Elakanti, S., Cherukuri, G., Rao, V. G., Chandrasekhar, V., Rao, A. S., and Tummala, M. (2015). Comparative evaluation of antimicrobial efficacy of QMix 2 in 1, sodium hypochlorite, and chlorhexidine against *Enterococcus faecalis* and *Candida albicans*. *Journal of Conservative Dentistry*, 18(2): 128-131.

Endo, M. S., Ferraz, C. C. R., Zaia, A. A., Almeida, J. F. A., and Gomes, B. P. F. A. (2013). Quantitative and qualitative analysis of microorganisms in root-filled teeth with persistent infection: Monitoring of the endodontic retreatment. *European Journal of Dentistry*, 7(3): 302-309.

Estrela, C., Silva, J. A., Alencar, A. H. G. d., Leles, C. R., and Decurcio, D. A. (2008). Efficacy of sodium hypochlorite and chlorhexidine against *Enterococcus faecalis*: a systematic review. *Journal of Applied oral science*, 16(6): 364-368.

Evanoff, D. D., and Chumanov, G. (2005). Synthesis and optical properties of silver nanoparticles and arrays. *ChemPhysChem*, 6(7): 1221-1231.

Evans, M., Davies, J. K., Sundqvist, G., and Figdor, D. (2002). Mechanisms involved in the resistance of *Enterococcus faecalis* to calcium hydroxide. *International Endodontic Journal*, 35(3): 221-228.

Ferreira, L., Guedes, J. F., Almeida-Aguiar, C., Fonseca, A. M., and Neves, I. C. (2016). Microbial growth inhibition caused by Zn/Ag-Y zeolite materials with different amounts of silver. *Colloids and Surfaces B: Biointerfaces*, 142(1): 141-147.

Gougazeh, M., and Buhl, J. C. (2014). Synthesis and characterization of zeolite A by hydrothermal transformation of natural Jordanian kaolin. *Journal of the Association of Arab Universities for Basic and Applied Sciences*, 15(1): 35-42.

Guerreiro-Tanomaru, J. M., Figueiredo Pereira, K., Almeida Nascimento, C., Basso Bernardi, M. I., and Tanomaru-Filho, M. (2013). Use of nanoparticulate zinc oxide as intracanal medication in endodontics: ph and antimicrobial activity. *Acta Odontológica Latinoamericana*, 26(3): 167-172.

Haapasalo, H. K., Sirén, E. K., Waltimo, T. M. T., Òrstavik, D., and Haapasalo, M. P. P. (2000). Inactivation of local root canal medicaments by dentine: an *in vitro* study. *International Endodontic Journal*, 33(2): 126-131.

Haapasalo, M., Qian, W., Portenier, I., and Waltimo, T. (2007). Effects of dentin on the antimicrobial properties of endodontic medicaments. *Journal of Endodontics*, 33(8): 917-925.

Helander, I., Nurmiaho-Lassila, E.-L., Ahvenainen, R., Rhoades, J., and Roller, S. (2001). Chitosan disrupts the barrier properties of the outer membrane of Gram-negative bacteria. *International Journal of Food Microbiology*, 71(2): 235-244.

Lin, L. M., Pascon, E. A., Skribner, J., Gängler, P., and Langeland, K. (1991). Clinical, radiographic, and histologic study of endodontic treatment failures. *Oral Surgery, Oral Medicine, Oral Pathology*, 71(5): 603-611.

Lin, L. M., Skribner, J. E., and Gaengler, P. (1992). Factors associated with endodontic treatment failures. *Journal of Endodontics*, 18(12): 625-627.

Missengue, R. N., Musyoka, N. M., Madzivire, G., Babajide, O., Fatoba, O. O., Tuffin, M., and Petrik, L. F. (2016). Leaching and antimicrobial properties of silver nanoparticles loaded onto natural zeolite clinoptilolite by ion exchange and wet impregnation. *Journal of Environmental Science and Health, Part A*, 51(2): 97-104.

Mohammadi, Z., and Dummer, P. M. H. (2011). Properties and applications of calcium hydroxide in endodontics and dental traumatology. *International Endodontic Journal*, 44(8): 697-730.

MubarakAli, D., LewisOscar, F., Gopinath, V., Alharbi, N. S., Alharbi, S. A., and Thajuddin, N. (2018). An inhibitory action of chitosan nanoparticles against pathogenic bacteria and fungi and their potential applications as biocompatible antioxidants. *Microbial Pathogenesis*, 114: 323-327.

Nair, P., Henry, S., Cano, V., and Vera, J. (2005). Microbial status of apical root canal system of human mandibular first molars with primary apical periodontitis after "one-visit" endodontic treatment. *Oral Surgery, Oral Medicine, Oral Pathology, Oral Radiology, and Endodontology*, 99(2): 231-252.

Ørstavik, D., and Haapasalo, M. (1990). Disinfection by endodontic irrigants and dressings of experimentally infected dentinal tubules. *Endodontics & Dental Traumatology*, 6(4): 142-149.

Palmeira-de-Oliveira, A., Ribeiro, M., Palmeira-de-Oliveira, R., Gaspar, C., Costa-de-Oliveira, S., Correia, I., Pina Vaz, C., Martinez-de-Oliveira, J., Queiroz, J., and Rodrigues, A. (2010). Anti-Candida activity of a chitosan hydrogel: mechanism of action and cytotoxicity profile. *Gynecologic and Obstetric Investigation*, 70(4): 322-327.

Portenier, I., Haapasalo, H., Rye, A., Waltimo, T., Ørstavik, D., and Haapasalo, M. (2001). Inactivation of root canal medicaments by dentine, hydroxylapatite and bovine serum albumin. *International Endodontic Journal*, 34(3): 184-188.

Ricucci, D., Siqueira, J. F., Lopes, W. S., Vieira, A. R., and Rôças, I. N. (2015). Extraradicular infection as the cause of persistent symptoms: a case series. *Journal of Endodontics*, 41(2): 265-273.

Seil, J. T., and Webster, T. J. (2012). Antimicrobial applications of nanotechnology: methods and literature. *International Journal of Nanomedicine*, 7: 2767-2781.

Şenel, S., İkinci, G., Kaş, S., Yousefi-Rad, A., Sargon, M. F., and Hıncal, A. A. (2000). Chitosan films and hydrogels of chlorhexidine gluconate for oral mucosal delivery. *International Journal of Pharmaceutics*, 193(2): 197-203.

Shabahang, S., and Torabinejad, M. (2003). Effect of MTAD on *Enterococcus faecalis*-contaminated root canals of extracted human teeth. *Journal of Endodontics*, 29(9): 576-579.

Shameli, K., Ahmad, M. B., Yunus, W. Z. W., Ibrahim, N. A., and Darroudi, M. (2010). Synthesis and characterization of silver/talc nanocomposites using the wet chemical reduction method. *International Journal of Nanomedicine*, 5: 743-751.

Silva, P. V., Guedes, D. F. C., Nakadi, F. V., Pécora, J. D., and Cruz-Filho, A. M. (2013). Chitosan: a new solution for removal of smear layer after root canal instrumentation. *International Endodontic Journal*, 46(4): 332-338.

Stojicic, S., Shen, Y., and Haapasalo, M. (2013). Effect of the source of biofilm bacteria, level of biofilm maturation, and type of disinfecting agent on the susceptibility of biofilm bacteria to antibacterial agents. *Journal of Endodontics*, 39(4): 473-477.

Stuart, C. H., Schwartz, S. A., Beeson, T. J., and Owatz, C. B. (2006). *Enterococcus faecalis*: Its Role in Root Canal Treatment Failure and Current Concepts in Retreatment. *Journal of Endodontics*, 32(2): 93-98.

Talebi, J., Halladj, R., and Askari, S. (2010). Sonochemical synthesis of silver nanoparticles in Y-zeolite substrate. *Journal of Materials Science*, 45(12): 3318-3324.

Tayel, A. A., Moussa, S., Wael, F., Knittel, D., Opwis, K., and Schollmeyer, E. (2010). Anticandidal action of fungal chitosan against *Candida albicans*. *International Journal of Biological Macromolecules*, 47(4): 454-457.

Wang, Z., Shen, Y., and Haapasalo, M. (2012). Effectiveness of endodontic disinfecting solutions against young and old *Enterococcus faecalis* biofilms in dentin canals. *Journal of Endodontics*, 38(10): 1376-1379.

Wu, D., Fan, W., Kishen, A., Gutmann, J. L., and Fan, B. (2014). Evaluation of the antibacterial efficacy of silver nanoparticles against *Enterococcus faecalis* biofilm. *Journal of Endodontics*, 40(2): 285-290.

Chapter 2

Literature review

2.1 Root canal infection

The role of microorganisms as a primary etiological factor in pulp diseases and apical periodontitis was recognized by Kakehashi *et al* (1965). They showed a direct correlation between the presence of microbial cells within the pulp tissue and the presence of an inflammatory process in the dental pulp and around the root apex if the microbial cells passed beyond the periapical foramen (Kakehashi *et al.*, 1965).

Furthermore, the ability of different microbial species to invade the dentinal tubules was observed in 1890 by Miller (Love, 2004). This invasion plays an important role in the initiation of pulpal and periradicular diseases. Multiple pathways are available for the microorganisms to invade the root canal system. However, the crown of the tooth is the main portal of entry for infection of the root canal space (Tronstad and Sunde, 2003). Microbial invasion can occur through carious lesions, faulty restorations, tooth wear and enamel and dentine cracks (Haapasalo *et al.*, 2003). Additionally, other portals of microbial entry to the pulp space may also occur through invasion of microorganisms from periodontal pockets and from the blood stream (Narayanan and Vaishnavi, 2010; Love, 2004). Microorganisms can invade the dentinal tubules to varying depths (Love,

2004) and can extend into the periapical area causing periapical periodontitis (Nair, 2004; Kakehashi *et al.*, 1965).

The presence of microorganisms in the dentinal tubules of the coronal part of the root canal system are mainly associated with pulpal and periradicular disease, while those present in the radicular dentinal tubules are associated mainly with root canal infection (Love, 2004).

2.1.1 Endodontic microbiology

Endodontic infections are polymicrobial in nature (Sundqvist and Figdor, 2003) and more than 400 microbial species have been identified from endodontic samples (Jhajharia *et al.*, 2015). α-hemolytic streptococci, ϒ-streptococci, and enterococci are the most commonly isolated bacteria from infected root canals (Farber and Seltzer, 1988). However, other bacterial species are also observed in an infected root canal. In addition to that, other microorganisms can also be found in endodontic infections such as archaea and fungi (Siqueira and Sen, 2004; Siqueira, 2002; Waltimo *et al.*, 1997). There are several factors that determine the type of bacteria that can be recovered from an infected root canal system such as: the method of sampling; the timing of sampling; duration till cultivation; type of transportation in cultivation media; the incubation condition; the use of microscopy and the use of bacterial smear (Baumgartner and Falkler, 1991).

Narayanan and Vaishnavi (2010) listed endodontic pathogens and classified them into intra-radicular, extra-radicular and persistent pathogens. The intra-radicular pathogens are mainly Gram negative species (*Prevotella* species, *Prophyromonas* species, *Tannerella forsythia*, *Dialister* species, *Fusobacterium* and *Spirochetes*), Gram positive

anaerobic rods and Gram positive cocci (*Parvimanas micra*, *Streptococcus anginosus*, *Streptococcus mitisi*, *Streptococcus Sanguinis*, and *Enterococcus faecalis*). In addition, fungi like *Candida* species and viruses were also reported as intra-radicular pathogens.

Extra-radicular pathogens are those pathogens that spread to the periapical area from an infected root canal system or a periodontal lesion (Kawashima *et al.*, 2009). The most common bacteria that are isolated from the periapical area are anaerobic bacteria such as *Actinomyces* species, *Propionibacterium propionicum*, *Treponema* species, *Prophyromonas gingivalis*, *Prophyromonas endodontalis*, *Treponema forsythia*, *Prevotella* species and *Fusobacterium nucleatum* (Narayanan and Vaishnavi, 2010).

Persistent endodontic pathogens are those microorganisms retained in the apical third of the root canal system following root canal treatment and represent the primary microbial species that are responsible for secondary endodontic infection (Evans *et al.*, 2002a; Baumgartner and Falkler, 1991). The most predominant bacterial species that were observed in a secondary endodontic infection are *Streptococcus* species, *Lactobacilli* species, *Staphylococci*, *Enterococcus faecalis*, *Olsenella uli*, *Parvimonas micra*, *Pseudoramibacterium* species, *Actinomyces* species, *Bifidobacterium* species and *Eubacterium* species. Additionally, Gram-negative anaerobic rods such as *Fusobacterium nucleatum*, *Prevotella* species and *Campylobacter rectus* were also isolated from secondary infection. Yeasts such as *Candida albicans* are also present in secondary root canal infections (Narayanan and Vaishnavi, 2010).

2.1.2 Primary and secondary endodontic infection

Root canal infections are classified into primary or secondary infections. Primary infection is usually associated with symptomatic or asymptomatic periradicular disease

while the secondary infection is usually associated with persistent infection or failed root canal treated teeth (Siqueira, 2002).

There are varieties between the microbial species isolated from primary endodontic infection compared to those isolated from secondary endodontic infection. In primary infection, obligate anaerobic bacterial species are the most predominant bacterial species while, in secondary infection, the facultative anaerobic bacterial species are found in higher percentages (Gomes *et al.*, 2004). This transition between different bacterial species results from the changes in nutritional and environmental status inside the root canal system as the infection progresses. This will create a more anaerobic environment with depletion of nutrition, which offers a tough ecological niche for the surviving microorganisms (Sundqvist and Figdor, 2003).

Furthermore, the literature showed that the microbial species in primary endodontic infections differ for symptomatic and asymptomatic infections in which Gram-negative anaerobic species are found to be more predominant in symptomatic periradicular lesions (Gomes *et al.*, 2004).

Generally, the microorganisms observed in primary endodontic infections are anaerobic bacteria (Fabricius *et al.*, 1982) with *Bacteriodes*, *Prophyromonas*, *Provtella*, *Fusobacterium*, *Treponema*, *Peptostreptococcus*, *Eubacterium* and *Campolylobacter* as the predominant species (Nair, 2004; Siqueira, 2002).

Secondary endodontic infection is caused by persistent pathogens within the root canal system or the periapical area following completed root canal treatment. These microorganisms can be present in the root canal system as a result of inadequate root

canal disinfection, improper access to the cavity, missed canal during treatment and leaking of microorganisms through defective restorations (Peciuliene *et al.*, 2008).

Gram-positive facultative species are shown to present at a higher percentage in secondary endodontic infections compared to primary infections (Siqueira, 2001a). Additionally, Gram-positive facultative bacterial species have the ability to resist the commonly used root canal antimicrobial agents (Peciuliene *et al.*, 2008; Pinheiro *et al.*, 2003).

Generally, *Enterococcus* species (*Enterococcus faecalis*), *Actinomyces, Peptostreptococcus,* and *Propionibacterium,* are the most common microbial species that are present in secondary endodontic infections (Nair, 2004). Also present in higher concentrations in secondary root canal infection are fungi like *Candida albicans* (Kumar *et al.*, 2015; Waltimo *et al.*, 1997; Nair *et al.*, 1990).

Among these microorganisms *Enterococcus faecalis* and *Candida albicans* are the most predominant microorganisms in cases of root canal failure (Kumar *et al.*, 2015; Tennert *et al.*, 2014; Pinheiro *et al.*, 2003; Waltimo *et al.*, 2003; Peciuliene *et al.*, 2001; Peciuliene *et al.*, 2000).

E. faecalis are Gram positive cocci that are found as normal intestinal organisms. Their presence in an infected root canal is probably not derived from the patient's own microflora indicating that endodontic infection with *E. faecalis* is of an exogenous origin (Vidana *et al*, 2011). They are highly associated with endodontic failure and secondary root canal infection following root canal treatment (Colaco, 2018). They represent about 67 – 77 % of the total microbial species isolated from secondary root

canal infection (Stuart *et al.*, 2006). Furthermore, they have the ability to survive as a single species or as a major component of the mixed flora (Evans *et al*, 2002).

There are several factors that are associated with the virulence of *E. faecalis* inside the root canal system including its ability to bind to the dentin wall through serine protease gelatinase and collagen binding protein (Hubble *et al.*, 2003), ability to invade into various depths inside the dentinal tubules as a result of its small size (Nair *et al.*, 2017) and its ability to withstand starvation for extended periods until an adequate nutritional supply is available (Figdor *et al.*, 2003).

E. faecalis has the ability to resist the commonly used root canal irrigants such as different concentrations of sodium hypochlorite, chlorhexidine and Qmix 2 in1 (Wang *et al.*, 2012). Furthermore, it also has the ability to resist the commonly used intra-canal medicaments such as calcium hydroxide (Evans *et al.*, 2002b). Furthermore, *E. faecalis* biofilm can resist the destruction caused by lymphocyte phagocytosis and other antimicrobial agents to a larger extent than other biofilm producing organisms (Stuart *et al*, 2006).

2.1.3 Ecology system of root canal pathogens

Initially, endodontic pathogens survive within the root canal system utilizing the remnants of pulp tissue as a nutrient media. As the infection advances, environmental factors such as the oxygen tension, pH, temperature and type of available nutrients in the root canal system change. As a result, the invading microorganisms will change their virulence factors in an attempt to accommodate the new environmental changes (Siqueira, 2002).

Endodontic diseases are biofilm-induced diseases (Siqueira *et al.*, 2010). This form of microbial colonization inside the root canal was initially identified by Nair (1987). It appears as a surface-attached microbial community which is defined by Mohammadi *et al.*, (2013) as "a sessile multicellular microbial community characterized by cells that are firmly attached to a surface and enmeshed in a self-produced matrix of extracellular polymeric substance" (Mohammadi *et al.*, 2013). However, certain microorganisms are also present in a planktonic state within the root canal system (Usha, 2010; Svensäter and Bergenholtz, 2004).

Microbial biofilm consists of approximately 10-15% microbial content and 85-90% extracellular matrix (Kokare *et al.*, 2009). The extracellular matrix is composed of a conglomeration of various types of hydrated biopolymers known as the extracellular polymeric substance (EPS) (Flemming and Wingender, 2010).

Root canal biofilm can be categorized into three categories according to their location inside the root canal system; intra-canal biofilms, extra-radicular biofilms, periapical biofilms, and biomaterial-centred infections.

Biofilm formation generally occurs in phases in the presence of a microbial element, aqueous environment and solid surface (Dua *et al.*, 2012). The steps of biofilm formation include deposition of thin film as a conditioning for adhesion and colonization of planktonic microorganisms that float in the fluid media. Following microbial adhesion, the microorganisms start growing to form the biofilm. There can be detachment of some parts of the biofilm into the surrounding environment (Dua *et al.*, 2012).

Formation of endodontic biofilm starts gradually, from the coronal pulp chamber and migrates apically to the apical foramen (Svensäter and Bergenholtz, 2004). Most of the microorganisms that contaminate the pulp originate from coronal carious lesions. As the carious lesion extends to the pulp chamber exposing the pulp tissue, the carious biofilm contaminates the coronal pulp tissue causing inflammation and an exudate which provides liquefied media for biofilm formation and a source of nutrition for the invading microorganisms (Siqueira *et al.*, 2010). This theory was supported by the similarity between the microbial community found in deep carious lesions and the one found in primary endodontic infection (Siqueira *et al.*, 2010).

2.1.4 Evidence of biofilm formation in endodontic infection

The first observation of the presence of biofilm was noted by Ramachandran Nair within the root canal system of a large carious tooth associated with a periapical inflammatory process, using transmission electron microscopy (Nair, 1987). The presence of microbial deposits in the apical 2 mm of infected root canal systems consisting of cocci and rods with or without spirochetes similar in their structure to those found in dental plaque, was observed by Molven *et al*., (1991). The presence of endodontic biofilm within the dentinal tubules up to depth varying between 10 to 150 µm was also recognized by Sen *et al*., (1995).

Additionally, Ricucci and Siqueria (2010) evaluated the prevalence of microbial biofilm based on a histological evaluation of biopsies obtained either during apical surgery or from recently extracted teeth in treated and untreated root canals associated with apical periodontitis. This histological evaluation demonstrated the presence of microbial biofilm within the radicular root canal system and isthmus area. The percentage of biofilm was 80% in untreated cases and 77% for failed root canals in treated cases.

Distel *et al*., (2002) showed that *Enterococcus faecalis* forms biofilm within two days of microbial contamination even in the presence of a calcium hydroxide intra-canal medicament.

The presence of endodontic biofilm on the external surface of the apical foramen of the root canal system was also evaluated by Tronstad *et al*., (1990) where they evaluated root tips resected during periapical surgery, using scanning electron microscopy, and showed the presence of a microbial community in a plaque like structure in the irregularities of the root tips. The plaque was dominated by cocci and rod types of microorganisms attached together by an extracellular matrix structure giving the appearance of a biofilm. Leonardo *et al*., (2002) also observed the apex of teeth with pulpal necrosis associated with or without radiographic radiolucency following their extraction. Biofilm consisting of cocci and bacilli were always observable on necrotic teeth that are associated with radiographic radiolucency (Leonardo *et al.*, 2002).

Thus, endodontic pathogens always seem to be present in a biofilm state within root canal infections, whether the infection is primary or secondary (Ricucci *et al.*, 2009; Carr *et al.*, 2009; Siqueira *et al.*, 2002).

2.1.5 Influence of biofilm in endodontic infection

Endodontic pathogens in a biofilm state within the root canal system show enhanced pathogenicity since the biofilm facilitates a different behaviour from those microorganisms found in a planktonic state, as it provides several virulence factors not present in the planktonic state (Siqueira and Rôças, 2014; Flemming and Wingender, 2010; Kolenbrander *et al.*, 2010; Tronstad and Sunde, 2003).

Kishen (2010) listed the mechanisms by which endodontic pathogens can resist the commonly used root canal irrigants and medicaments. These mechanisms are usually associated with the extracellular polymeric matrix, rate of growth, availability of nutrients and ability to adopt a resistance phenotype.

The extracellular polymeric matrix provides a number of essential functions to the microbial community (Flemming and Wingender, 2010). It facilitates adhesion of the biofilm to the surfaces and presents mechanical stability to the biofilm. It also has the ability to retain moisture to maintain a highly hydrated environment around the biofilm. Additionally, it accumulates extracellular enzymes around the biofilm which in turn allow the availability of nutrients around it. It can also serve as a source of nutrients in case of starvation. Moreover, it has a protective role by protecting the microbial cell from the host immune response and antimicrobial agents. Finally, it maintains the biofilm cell in close proximity to facilitate different microbial communication methods such as genetic exchange, communication between cells (quorum sensing) and pathogenic synergism (Flemming and Wingender, 2010). All these factors can contribute to the high resistance of biofilm to the antimicrobial agent. Additionally, the extracellular polymeric matrix can facilitate a decrease in the penetration rate of the antimicrobial agents (Costerton *et al.*, 1999).

About 20% to 70% of microorganisms in biofilms demonstrate dissimilar gene expression patterns compared to those microorganisms found in a planktonic state. Thus, microbial biofilm can be more resistant to antimicrobial agents compared to equivalent microorganisms found in a planktonic state (Beloin *et al.*, 2004; Sauer *et al.*, 2002).

Another hypothesis for the low susceptibility of biofilm to antimicrobial agents is that the presence of slow-growing microbial cells in the biofilm is the result of nutrition limitation, making them more resistant to antimicrobial agents (Brown *et al.*, 1988).

2.2 Treatment of root canal infection

The main goal in treating root canal infection is to eliminate the microbial contamination within the entire root canal system (Carrotte, 2004a). This goal is achieved by fully debriding the root canal system from any infectious microorganisms. The debridement is done through root canal cleaning and shaping in which all the necrotic tissue and the infected root canal dentine is removed from the root canal system (Hülsmann *et al.*, 2005). Thereafter the root canal system is finally sealed "obturated" three dimensionally to prevent any reinfection (Torabinejad *et al.*, 2003).

As a result of the complex anatomy of the root canal system, eradication of endodontic pathogens should be done with the use of both mechanical and chemical root canal preparation (Siqueira, 2001b). Both methods are used simultaneously and cannot be considered separately, hence it is referred to as chemomechanical or biomechanical preparation (Hülsmann *et al.*, 2005).

2.2.1 Role of mechanical preparation

The role of mechanical preparation in root canal disinfection is to mechanically remove part of the infected dentine and at the same time provide room for the antimicrobial irrigant solutions and intra-canal medicament to act against the remaining different pathogens and thus enhance the eradication of endodontic pathogens (Vaudt *et al.*, 2007). The techniques used for the mechanical preparation include manual and automated root canal preparation, sonic and ultrasonic preparation, use of laser, and a

nickel titanium rotary system. Hülsmann *et al*., (2005) listed the goals of mechanical preparation of the root canal system, namely: removal of the vital and necrotic tissue from the main root canal, creation of sufficient space for irrigation and medication, preservation of the integrity and location of the apical anatomy, avoidance of iatrogenic damage to the canal system and root structure, facilitation of the canal filling, avoidance of further irritation and/or infection of the peri-radicular tissue, and preservation of sound root dentine to allow long-term functioning of the tooth (Hülsmann *et al.*, 2005).

Although there is advancement in the technology of mechanical instrumentation as new instruments are introduced to the dental market, these instruments do not have the ability to clean the entire root canal system as a result of the complex anatomy of the root canal system and the presence of isthmus and lateral canals which are difficult to instrument (Del Fabbro *et al.*, 2018; Siqueira *et al.*, 2017).

2.2.2 Role of biological preparation

Since large areas of the main root canal wall remain untouched by the advanced root canal instrument (Peters *et al.*, 2001), an antibacterial root canal irrigant should be used to maximize bacterial elimination from the root canal system (Siqueira, 2001b).

2.2.2.1 Root canal irrigants

Haapasalo *et al*., (2010) listed the requirement of ideal root canal irrigants. The irrigants should have a flushing action thereby facilitating removal of microorganisms, tissue remnants and dentin chips from the root canal thus preventing blockage of the apical third of the canal by preventing packing or compaction of the hard tissue in the apical third of the canal. They should have the ability to dissolve the organic and inorganic tissue of the root canal and possess an antimicrobial action. There are several root canal

irrigants currently available. However, there are no irrigants that possess all ideal requirements for root canal irrigants (Haapasalo *et al.*, 2010).

Sodium hypochlorite is the most commonly used root canal irrigant due to its mechanism of action. It is commonly used in concentrations between 0.5% and 6%. It has a strong antimicrobial action and has the ability to dissolve the organic tissue and pulp remnants (Haapasalo *et al.*, 2010). However, it does not remove the smear layer (Carrotte, 2004b).

BioPure MTAD (Dentsply Tulsa) is a mixture of doxycycline, citric acid and detergent that was found to be a potent antibacterial agent against *E. faecalis* and less potent against *C. albicans* compared to sodium hypochlorite (Misuriya *et al.*, 2014). Additionally, others found no difference in the antibacterial action against *E. feacalis* when 5.25% sodium hypochlorite/15% EDTA and 1.3% sodium hypochlorite/MTAD was used (Kho and Baumgartner, 2006).

Qmix 2 in 1 (Dentsply Sirona) is a mixture of a bisdiguanide antimicrobial agent, a polycarboxylic acid, calcium-chelating agent, saline, and surfactant and was introduced as root canal irrigant (Dai *et al.*, 2011). It was found that the antibacterial action against *E. faecalis* of Qmix 2 in 1 is superior to that of MTAD and chlorhexidine (Stojicic *et al.*, 2012).

Other materials that can be used as root canal irrigant material such as: chlorhexidine digluconate; iodine compound; and hydrogen peroxide have also been evaluated, but none of these irrigants were able to eliminate all endodontic pathogens (Stojicic *et al.*, 2013).

Hence root canal irrigants are used as an adjunct treatment protocol to facilitate the removal of remaining debris and act as antimicrobial agents in the root canal system. Although a variety of root canal irrigants are used today, none of them have the ability to completely eradicate the root canal pathogens due to several factors, such as bacterial resistance (Wang *et al.*, 2012). In spite of the various activation protocols used to activate the root canal irrigants they are still unable to completely remove all the debris from the root canal system (Leoni *et al.*, 2017).

2.2.2.2 Intra-canal medicaments

The use of intra-canal medicaments as antimicrobial agents, especially in multiple visit root canal treatments, are mandatory as they have the ability to disinfect the remaining root canal pathogens following mechanical preparation (McGurkin-Smith *et al.*, 2005), act as physical barrier and prevent the penetration of other microbes into the root canal system through a defective coronal restoration (Kawashima *et al.*, 2009), act as anti-inflammatory materials and reduce the inflammation in the periapical area and help to dry wet canals (Chong and Ford, 1992). Accordingly, Kawashima *et al.*, (2009) defined intra-canal medicaments as " temporary placement of strong disinfection medical agents in an attempt to sterilize the intra-canal space and to act as a physical and chemical blockage against coronal leakage from temporary filling material and at the same time to be biocompatible". Intra-canal medicaments include: volatile intra-medicaments, steroid-antibiotic base intra-canal medicaments and calcium hydroxide.

a) Volatile medicaments

In the past, volatile materials such as formocresol, metacresylacetate and camphorated monoparachlorophenol were used as intra-canal medicaments. However, their use is

limited as a result of the questionable antibacterial effectiveness in clinical cases and their short duration of action (Gatewood, 2007). Additionally, the toxic effect of these materials limited their usage (Al-Haj Ali *et al.*, 2015).

b) Antibiotics

The first use of an antibiotic as intra-canal medicament was introduced by Grossman (1951). This medicament was in the form of a paste in a silicon vehicle that contained a combination of penicillin, streptomycin, bacitracin and caprylate sodium at various concentrations and became known as Grossman's medicament (Grossman, 1951). However, its use as intra-canal medicament was restricted by the Food and Drug Administration (FDA) due to the potential for developing sensitivity and allergic reaction (Balasubramaniam and Jayakumar, 2017).

Generally, the use of antibiotic based intra-canal medicaments has the advantage of having a localized effect without the potentiality of developing the systemic adverse effect of using antibiotics. This may, in turn increase the efficacy of disinfection of the root canal system. However, antibiotic based intra-canal medicaments should be used with care due to their drawbacks such as development of more resistant bacterial strains, ability to stain the tooth structure and development of allergic reactions (Balasubramaniam and Jayakumar, 2017).

Currently, different antibiotic based intra-canal medicaments are available such as Odontopaste (Australian Dental Manufacturing), Pulpomixine (Septodont), Septomixine (Septodont) and Ledermix (Riemser Pharma GmbH).

Odontopaste is an intra-canal medicament in which 5% clindamycin hydrochloride and 1% triamcinolone acetonide is added to zinc oxide (Balasubramaniam and Jayakumar,

2017). The incorporation of triamcinolone acetonide reduces the inflammation and post-operative pain (Athanassiadis *et al.*, 2011). However, some studies showed that clindamycin hydrochloride had no effect on *E. faecalis*, a persistent root canal pathogen (Rams *et al.*, 2013; Addy and Martin, 2005).

Pulpomixine is a steroid-antibiotic based intra-canal medicament, but showed no effect in inhibiting the residual root canal pathogens, such as *S. mutans, E. faecalis* and *C. albicans*.(Attia *et al.*, 2015).

Septomixine (Septodont) is an antibiotic based intra-canal medicament consisting of dexamethasone, polymyxin B sulphate, tiotrichine, neomycine sulfate, haletazole terate and a radiopaque contrast agent. The presence of dexamethasone aids in reducing the inflammation in the periapical tissue (Nobuhara *et al.*, 1993). However, Tang *et al.*, (2004) showed that it was not effective in eradicating the residual root canal pathogens.

Ledermix is the most commonly used antibiotic-steroid based intra-canal medicament. It was initially developed in 1960 by Schroeder and Triadan in an attempt to reduce the postoperative pain and inflammation (Murvindran and James, 2014). An antibiotic was added initially in the form of chloramphenicol to boost the host immune response and to counteract the effect of steroid. Currently it consists of tetracycline, demeclocycline HCl and triamcinolone acetonide as steroid in a polyethylene glycol base (Murvindran and James, 2014). The antimicrobial efficacy of Ledermix is determined by demeclocycline and tetracycline. The antibacterial efficacy of demeclocycline is concentration dependent (0.05-128 mg/L) (Abbott, 1990). It is more effective against microbial species in the lumen of the root canal system because they are subjected to a higher concentration of demeclocyline than the microbial species at the periphery of the

root canal (Abbott, 1990). Additionally, the use of tetracycline produces a bacteriostatic rather than a bactericidal effect against the endodontic pathogens and it is ineffective against fungi (Abbott, 1990; Ehrmann, 1965).

c) Calcium hydroxide

Calcium hydroxide ($CaOH_2$) is the most commonly used intra-canal medicament. It was initially used as a pulp capping material by Herman in 1920 (Fava and Saunders, 1999). It is an odorless white powder with poor water solubility and a pH of 12.5 – 12.8 (Siqueira and Lopes, 1999). The use of calcium hydroxide as intra-canal medicament can be ascribed to the following biological properties: antimicrobial function (Shuping *et al.*, 2000; Sjögren *et al.*, 1991); reduced dental hard tissue resorption (Tronstad, 1988); stimulation of reparative tissue formation (Song *et al.*, 2017; Mohammadi and Shalavi, 2016; Gandolfi *et al.*, 2015); ability to dissolve tissue (Wadachi *et al.*, 1998; Andersen *et al.*, 1992); and anti-inflammatory effect (Valera *et al.*, 2016; Safavi and Nichols, 1993).

The antimicrobial efficacy of calcium hydroxide is well known in the literature (Shokraneh *et al.*, 2014; Kim and Kim, 2014; Mohammadi *et al.*, 2012; Sjögren *et al.*, 1991). Siqueira and Lopes (1999) listed several factors that contribute to the antimicrobial activity of calcium hydroxide which are mainly divided into either chemical activity or physical activity. The chemical effect of calcium hydroxide is mainly due to the release of hydroxyl ions from the calcium hydroxide when it comes into contact with an aqueous medium (Siqueira and Lopes, 1999). The hydroxyl ions are one of the highly reactive oxidant free radicals that have the ability to damage the bacterial cytoplasmic cell membrane, damage the bacterial cell membrane and cause

protein denaturation. The physical effects of calcium hydroxide include its ability to act as a physical barrier and prevent the ingress of microorganisms into the root canal system by narrowing the space available within the root canal system for the bacteria to multiply (Siqueira and Lopes, 1999). The antimicrobial mechanism of calcium hydroxide depends on several factors. The major factor is the highly alkaline environment that is provided when calcium hydroxide is applied which renders the bacteria unable to survive (Byström *et al.*, 1985).

An important factor that determines the efficacy of calcium hydroxide is its ability to remain in close proximity to the root canal wall and thus the endodontic pathogens (Siqueira and Lopes, 1999). However, the penetration of the hydroxyl ions into the dentinal tubules has a limited depth which in turn limits the effect of calcium hydroxide to be concentrated in the most superficial layers of the dentinal wall (Tronstad *et al.*, 1981). Additionally, the action of the hydroxyl ions is buffered as it penetrates into the dentinal tubules and contacts the bicarbonate, phosphate and acid proteins of the dentine structure (Siqueira and de Uzeda, 1998).

An important shortcoming of $CaOH_2$ in endodontic failure is commonly associated with *E.* faecalis (Delboni *et al.*, 2017; Murad *et al.*, 2014; Stuart *et al.*, 2006), Calcium hydroxide is unable to eliminate *E. faecalis* from an infected root canal system (Valera *et al.*, 2016; Kurian *et al.*, 2016; Cwikla *et al.*, 2005; Gomes *et al.*, 2003; Evans *et al.*, 2002a).

Multiple mechanisms are involved in the resistance of *E faecalis* to the antibacterial effect of calcium hydroxide. *E. faecalis* has the ability to withstand the high pH value of calcium hydroxide (McHugh *et al.*, 2004; Evans *et al.*, 2002a). Additionally, *E. faecalis*

is able to maintain its internal pH to produce enzymes and proteins thereby maintaining its normal function by controlling the proton pump to maintain its cytoplasmic pH by controlling the transport of minerals such as potassium and sodium through its cell membrane (Estrela and Holland, 2003; Evans *et al.*, 2002a; Estrela *et al.*, 1995).

In an attempt to overcome this disadvantage of calcium hydroxide, other materials such as chlorhexidine gluconate were mixed with it. However, mixing calcium hydroxide with chlorhexidine did not improve its antibacterial efficacy against *E. faecalis* (Schäfer and Bössmann, 2005). Saatchi *et al*., (2014) in a systematic review and meta-analysis concluded that mixing calcium hydroxide with chlorhexidine did not improve its antimicrobial efficacy against *E. faecalis*.

The limitations of commercial intra-canal medicaments have promoted researchers to focus on nanotechnology in an attempt to improve the antimicrobial effect of these agents.

2.3 Nanotechnology in endodontics

The word "nano" originated from a Greek word which means "dwarf" (Bhardwaj *et al.*, 2014). The philosophy of nanotechnology was first described by Richard P. Feynman, a Nobel Prize winner, in his lecture "There's Plenty of Room at the Bottom" (Feynman, 1960). Since then, the concept of nanotechnology has been applied in numerous scientific fields such as physics, engineering as well as in the medical field. Nanotechnology is defined as a science that deals with the development of new materials with new properties and functions through controlling and restructuring of the materials on a nanometer scale and hence the name nanomaterials (Sanchez and Sobolev, 2010). The term is applied, according to the European commission, to "any

natural, incidental or manufactured material containing particles, in an unbound state or as an aggregate or as an agglomerate and where, for 50% or more of the particles in the number size distribution, one or more external dimensions are in the size range 1 nm – 100 nm". However, there is no scientific evidence to support this value according to the European commission (2011), for instance, polymeric nanoparticles are usually in the range of 10 – 1000 nm (Jahangiri and Barghi, 2018).

Nanomaterials exist in various forms and shapes. They are categorized according to their dimensions into: zero dimensions such as nanoparticles, one dimension such as nanorods, two dimensions such as thin films and three dimensions such as nanocones (Tiwari *et al.*, 2012).

The term nanodentistry is defined as "the science and technology of diagnosis, treating and preventing oral diseases, relieving pain, reserving and improving dental health using nanostructured material" (Mantri and Mantri, 2013). Nanodentistry is applied in different areas, for example: manufacturing of dental materials, prevention of oral diseases such as dental caries and periodontal diseases, as therapeutic agents for the treatment of dentin hypersensitivity, oral cancer and endodontic diseases in the technology of tissue engineering and as a diagnostic aid to identify certain diseases such as oral cancer (Neel *et al.*, 2015).

Currently the application of nanomaterial in endodontics is limited to a few studies (Afkhami *et al.*, 2015; Kishen *et al.*, 2008) that evaluated the antimicrobial properties of some nanomaterials in different forms against endodontic pathogens.

2.3.1 Antibacterial mechanisms of nanoparticles

The use of nanoparticles as antimicrobial agents has recently attracted considerable attention in the medical field as a result of their superior antibacterial properties compared to those of other antimicrobial agents with low potential to produce microbial resistance (Seil and Webster, 2012). The antimicrobial activity of nanoparticles against different microorganisms differs from its original bulk state (Seil and Webster, 2012) and may vary according to the different types of nanoparticles (Beyth *et al.*, 2015).

The efficacy of the nanoparticles to eradicate bacterial cells is attributed to the effect of two different mechanisms that work concurrently (Figure 2-1). One involves the binding of nanoparticles to the targeted bacterial cell membrane through electrostatic forces, causing an alteration in the membrane potential, depolarization and eventually loss of membrane integrity (Pelgrift and Friedman, 2013). This results in disturbance of major bacterial cell functions such as respiration, transportation of nutrients and disturbance of the energy transduction leading subsequently to bacterial cell death (Pelgrift and Friedman, 2013).

The second mechanism includes production of reactive oxygen species (ROS) that can influence survival of the bacterial cell by blocking the protein function, destroying DNA and resulting in excess radical production (Valko *et al.*, 2007).

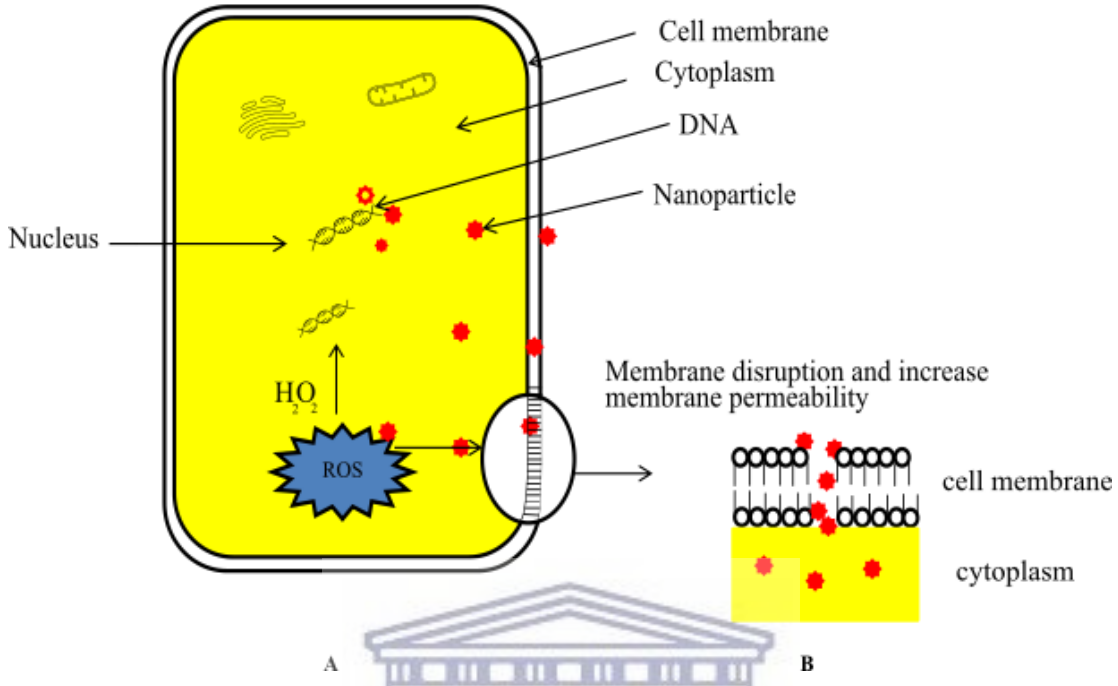

Figure 2-1: Diagram adapted from Hajipour *et al.*, (2012) representing the antibacterial mechanisms of nanoparticles, (A) Toxicity through production of reactive-oxygen species (ROS), (B) Nanoparticles attach to bacterial cell membranes causing toxicity through cell damage.

2.3.2 Antimicrobial efficacy of nanoparticles in endodontics

Various nanoparticles have been investigated recently in different forms in *in vitro* studies to evaluate their efficacy against endodontic pathogens (Bhardwaj *et al.*, 2014; Guerreiro-Tanomaru *et al.*, 2013; Shrestha *et al.*, 2010). The nanoparticles used in these studies can be broadly classified into three categories according to their chemistry: metallic or inorganic, polymeric and bioactive non-organic nanoparticles.

2.3.3 Antibacterial efficacy of metallic or inorganic nanoparticles

The antibacterial effect of metallic or inorganic nanoparticles such as silver, magnesium and zinc oxide against endodontic pathogens has been evaluated in many *in vitro* studies (Monzavi *et al.*, 2015; Wu *et al.*, 2014; Kishen *et al.*, 2008). Among these metallic nanoparticles, the antibacterial effect of silver nanoparticles was most commonly considered in the literature.

a. Silver nanoparticles (Ag-Np)

The antimicrobial properties of silver nanoparticles were first demonstrated by Morones *et al.*, (Morones *et al.*, 2005). Silver nanoparticles have the ability to bind to the negatively charged part of the bacterial cell membrane disturbing its functions such as permeability and respiration, causing leaking of the cytoplasmic content and eventually rupture of the bacterial cell (Kim *et al.*, 2007). As a result, the nanoparticles will infiltrate inside the cytoplasmic content and interact with sulfur - and phosphorus - containing proteins such as DNA and RNA, causing further damage to the bacterial cell (Morones *et al.*, 2005). Additionally, the silver nanoparticles release silver ions when in contact with aqueous media, further disturbing the bacterial functions (Abbasi *et al.*, 2014; Prabhu and Poulose, 2012; Sotiriou and Pratsinis, 2010; Morones *et al.*, 2005; Sondi and Salopek-Sondi, 2004).

Wu *et al.*, (2014) evaluated the effect of silver nanoparticles in a concentration of 0.1% as an irrigant solution and as a gel in two different concentrations (0.02% and 0.1%) against *E. faecalis* biofilm. The solution did not cause any major change to the structure of *E. faecalis* biofilm. However, the use of silver nanoparticles in a gel form with a concentration of 0.02% had the ability to disrupt the structural integrity of the

E. faecalis biofilm more than a 0.01% silver nanoparticle gel and thus decreased the number of viable bacteria.

The antibacterial effect of silver nanoparticles as an intra-canal medicament in a paste form was evaluated by Buruniera *et al*., (2014). The antibacterial efficacy of these new materials was evaluated against different bacterial species such as *E. faecalis*, *P. areuginosa*, *S. mutans*, *E. coli* and *S. aureus*. Silver nanoparticles demonstrated antibacterial activity against the tested bacterial species. Additionally, the use of hydroxyethylcellulose polymer gel as a vehicle for silver nanoparticles provides the maximum homogeneity and fluidity as a carrier compared with the other materials and thus resulted in improved antibacterial properties (Bruniera *et al.*, 2014).

Silver nanoparticles may hold different surface charges and the effect of these variations on their antibacterial efficacy was evaluated by Abbaszadegan *et al*., (2015). The efficacy of three preparations having surface charges of neutral, negatively-charged and positively-charged against planktonic cells of *E. faecalis* was compared with that of sodium hypochlorite and chlorhexidine. Positively-charged silver nanoparticles showed the lowest minimal inhibitory concentration against the tested bacterial species. However, unlike with neutral and negatively-charged silver nanoparticles, sodium hypochlorite and chlorhexidine, the minimal bacterial effect was still shown with the positively charged silver nanoparticles at lower concentrations. Additionally, some tissue inhibitors, such as dentin powder or the remnants of pulp tissue, that have the ability to inhibit the antibacterial effect of root canal medicaments (Siqueira and Rôças, 2008), were shown to have no such effect on the antibacterial properties of the positively-charged silver nanoparticles even after 24 hours contact time. The study concluded that the growth of *E. faecalis* was prevented when exposed for 5 minutes to

positively-charged silver nanoparticles at 5.7×10^{-10} mol L^{-1} (Abbaszadegan *et al.*, 2015). Furthermore, silver nanoparticles were shown to enhance the antibacterial properties of some intra-canal medicaments such as calcium hydroxide against *E. faecalis* (Afkhami *et al.*, 2015).

The main disadvantages that limit the use of silver nanoparticles in endodontics are its ability to cause dentinal discoloration (Besinis *et al.*, 2014) and possible cytotoxic effect on human cells (Gliga *et al.*, 2014).

b. Magnesium-containing nanoparticles (Mg-Np)

Magnesium-containing nanoparticles were suggested for use as antimicrobial agents against endodontic pathogens due to their known antibacterial properties against gram-positive and gram-negative bacteria, spores and viruses (Beyth *et al.*, 2015). Magnesium-containing nanoparticles are either magnesium-oxide nanoparticles or magnesium-halogen-containing nanoparticles such as chlorine, bromine and fluorine (Pelgrift and Friedman, 2013; Blecher *et al.*, 2011). The antimicrobial properties of magnesium containing nanoparticles were thought to be due to multiple mechanisms. Similar to the common antimicrobial mechanisms of nanoparticles, magnesium-halogen containing nanoparticles infiltrate inside the bacterial cell, resulting in a disturbance in the membrane potential. The penetration facilitates the DNA binding and lipid peroxidation effects on the nanoparticles causing more destruction of the bacterial cells (Lellouche *et al.*, 2009). Magnesium-oxide nanoparticles were found to be bactericidal when present in an aqueous form as a result of the action of superoxide anions that form on the bacterial surface (Huang *et al.*, 2005).

The antibacterial efficacy of different concentrations of magnesium oxide nanoparticles (5 mg/L and 10 mg/L), 5.25% sodium hypochlorite and 2% chlorhexidine against endodontic pathogens such as *E. faecalis*, *S. aureus* and *C. albicans* was studied by Monzavi *et al*., (2015). There was no significant difference in the antimicrobial efficacies among the solutions used against the tested endodontic pathogens. However, the inclusion of magnesium oxide nanoparticles in a solution produced extended antibacterial activity when compared with sodium hypochlorite (Monzavi *et al.*, 2015).

c. Zinc oxide nanoparticles (ZnO-Np)

Zinc oxide nanoparticles possess high antibacterial effectiveness (Sirelkhatim *et al.*, 2015; Liu *et al.*, 2009), destroying microbial cells in a higher pH environment (Yamamoto, 2001). The antibacterial mechanism of zinc oxide nanoparticles is similar to that of other types of nanoparticles, causing increased permeability of the cell wall membrane, a release of cytoplasmic content and cell death (Huang *et al.*, 2008). The bactericidal effect of zinc oxide nanoparticles is related to size; the smaller the size the higher the antibacterial effect and the production of reactive oxygen species such as hydrogen peroxide when in contact with an aqueous medium (Blecher *et al.*, 2011; Jalal *et al.*, 2010; Zhang *et al.*, 2008; Padmavathy and Vijayaraghavan, 2008; Yamamoto, 2001). Additionally, zinc oxide nanoparticles can produce zinc ions within the bacterial cell causing disturbance in its enzymatic system and the mechanism of amino acid metabolism, resulting in further damage (Song *et al.*, 2010). The antibacterial effect of zinc oxide nanoparticles has been shown to depend on concentration, higher levels resulting in the maximum antibacterial effect (Yamamoto, 2001).

The antibacterial and antibiofilm efficacy of zinc oxide nanoparticles against some endodontic pathogens such as *E. faecalis* was assessed by Kishan *et al*., (2008). Zinc oxide nanoparticles reduce the colony forming unit of *E. faecalis* in a biofilm state which was evident when zinc oxide nanoparticles were incorporated into resin based root canal sealer (Kishen *et al.*, 2008). A 95% reduction in the ability of *E. faecalis* to adhere and form biofilm in a dentinal wall was also shown by Kishen *et al* (2008).

Another study found that the thickness and structure of the *E. faecalis* biofilm was reduced and disrupted after 72 hours contact time with zinc oxide nanoparticles but concluded that zinc oxide nanoparticles have the ability to eliminate *E.* faecalis in a planktonic state only (Shrestha *et al.*, 2010). Varying degrees of antibacterial effects against *P. aeruginosa, E. faecalis, C. albicans, S. aureous* and *K. rhizophila* were shown when zinc oxide nanoparticles were incorporated into polyethylene glycol to form a creamy mix used as an intra-canal medicament (Guerreiro-Tanomaru *et al.*, 2013). Several studies also showed the antibacterial effect of using metallic nanoparticles against endodontic pathogens (Table 1-1).

Table 1-1: Summary of studies that evaluated the antimicrobial effect of metallic nanoparticles against some endodontic pathogens

Nanoparticles used	**Microorganism tested**	**Test mechanism**	**Results**	**Reference**
Ag-Np	*E. faecalis* biofilm	As an irrigant and as a gel	Use of Ag-Np as irrigant does not change biofilm structure. 0.02% Ag-Np in a gel form can disrupt the structural integrity of the biofilm.	Wu *et al*., (2014)
Ag-Np	*E. faecalis*	Added to calcium hydroxide	Ag-Np enhanced the antibacterial properties of calcium hydroxide	Afkhami *et al*., (2015)
Ag-Np	*E. coli*, *P. aeruinosa*, *S.mutuns*, *S, aureus*	As intra-canal medicament using different carriers	Ag-Np have antibacterial properties against the tested microorganisms in the three carrier	Buruniera *et al*., (2014)
Ag-Np	Planktonic *E. faecalis*	With different surface charges (neutral, positive and negative)	Positively charged Ag-Np have low antibacterial properties, however it is more effective in lower concentrations than neutral and negative surface charges in diluted concentrations. Antibacterial properties were not affected by the inhibitory effect	Abbaszadegan *et al*., (2015)

			of dentin powder.	
Mg-Np	*E. faecalis, S. aureus, C. albicans*	As an irrigant solution	Mg-Np showed extended antibacterial action over time.	Monzavi *et al*., (2015)
ZnO-Np	*E. faecalis* biofilm	As an irrigant solution and when added to zinc oxide based sealer.	ZnO-Np decreased the number of colony forming units of the tested bacteria. ZnO-Np enhanced the antibacterial property of zinc oxide based sealer. Dentine treated with zinc oxide nanoparticles reduces bacterial adhesion to dentin wall by 95%.	Kishan *et al*., (2008)
ZnO-Np	*E. faecalis* in planktonic and biofilm state	As an irrigant solution	ZnO-Np completely eliminates planktonic bacteria while that of biofilm could survive up to 72 hours. The biofilm thickness was reduced.	Shertha *et al.*, (2010)
ZnO-Np	*P. aeruinosa, C. albicans, S, aureus, K. rhizophila, E.*	As intra-canal medicament when incorporated	ZnO-Np with calcium hydroxide has a higher inhibitory effect against *P.*	Guerreiro-Tanomaru *et al*., (2013)

	faecalis	to polyethylene glycol with and without calcium hydroxide.	*aeruinosa* and lower effect against *E. faecalis* and varying degrees of effective ness against the other tested microorganisms.	

2.3.4 Bioactive glass

In 1971 a new material was developed by Professor Hench with antibacterial properties that can bond to the bone structure which consisted of 45% SiO_2, 24% Na_2O, 24.5% CaO and 6% P_2O_5 and became known as Bioglass (Hench, 2006). According to Stoore *et al* (1998) the antimicrobial property of bioactive glass material was ascribed to its ability to:

i. Release ions when it comes into contact with an aqueous medium,
ii. Increase the surrounding pH,
iii. Increase the osmotic pressure around the bacterial cell causing inhibition of bacterial growth,
iv. Precipitate calcium and phosphate ions in the bacterial cell membrane disturbing its functions.

The use of 45S5 bioactive glass nanoparticles was found to produce a better antibacterial effect against *E. faecalis* than micro-sized bioactive glass particles (Waltimo *et al.*, 2007). However, Zehnder *et al* (2006) showed that calcium hydroxide is more effective than 20-60 nm sized bioglass nanoparticles against *E. faecalis*.

Additionally, Mohn *et al* (2010) added bismuth oxide into bioactive glass nanoparticles in an attempt to increase its radiopacity and alkalinity for use as an intra-canal medicament or a root canal filling material. The newly synthesized material was radiopaque and highly alkaline which in turn increases the antimicrobial properties of bioactive glass nanoparticles (Mohn *et al.*, 2010).

The use of bioactive glass nanoparticles as an antimicrobial agent as a replacement for the commonly used endodontic disinfectants are still an area of controversy as a result of the variation in results obtained by different studies regarding their antimicrobial efficacy against endodontic pathogens.

Thus, the large numbers of nanoparticles available today provide multiple choices for their use in the medical field. Current endodontic research is focused on evaluating the antimicrobial property of some nanoparticles as new agents against endodontic pathogens. Available studies show that there is promise in the use of different types of nanoparticles as antimicrobial agents especially against persistent endodontic pathogens such as *E. faecalis*. Whilst it appears that some of the shortcomings of traditional root canal irrigants and medicaments can be overcome, more *in vitro* and *in vivo* studies are needed to evaluate which nanoparticles are more appropriate for use as a root canal irrigant solution or intra-canal medicament. Indeed, more studies are needed to evaluate the biocompatibility, safety, cost and ease of use of these innovative materials.

It appears that nanoparticles are providing the answer to the resistant microbial species, especially *E. faecalis*, as traditional intra-canal medicaments do not seem to be effective. Therefore the interest of many researchers is starting to focus on the process

of finding a new nanoparticle based intra-canal medicament by means of testing various nanoparticles on resistant endodontic pathogens.

2.4 References

Abbasi, E., Milani, M., Fekri Aval, S., Kouhi, M., Akbarzadeh, A., Tayefi Nasrabadi, H., Nikasa, P., Joo, S. W., Hanifehpour, Y., and Nejati-Koshki, K. (2014). Silver nanoparticles: synthesis methods, bio-applications and properties. *Critical Reviews in Microbiology*, 42(2): 173-180.

Abbaszadegan, A., Nabavizadeh, M., Gholami, A., Aleyasin, Z., Dorostkar, S., Saliminasab, M., Ghasemi, Y., Hemmateenejad, B., and Sharghi, H. (2015). Positively charged imidazolium-based ionic liquid-protected silver nanoparticles: a promising disinfectant in root canal treatment. *International Endodontic Journal*, 48(8): 790-800.

Abbott, P. V. (1990). Medicaments: aids to success in endodontics. Part 1. A review of the literature. *Australian Dental Journal*, 35(5): 438-448.

Addy, L., and Martin, M. (2005). Clindamycin and dentistry. *British Dental Journal*, 199(1): 23-26.

Afkhami, F., Pourhashemi, S. J., Sadegh, M., Salehi, Y., and Fard, M. J. K. (2015). Antibiofilm efficacy of silver nanoparticles as a vehicle for calcium hydroxide medicament against *Enterococcus faecalis*. *Journal of Dentistry*, 43(12): 1573-1579.

Al-Haj Ali, S. N., Al-Jundi, S. H., and Ditto, D. J. (2015). *In vitro* toxicity of formocresol, ferric sulphate, and grey MTA on human periodontal ligament fibroblasts. *European Archives of Paediatric Dentistry*, 16(1): 51-55.

Andersen, M., Lund, A., andreasen, J. O., and Andreasen, F. M. (1992). *In vitro* solubility of human pulp tissue in calcium hydroxide and sodium hypochlorite. *Endodontics & Dental Traumatology*, 8(3): 104-108.

Athanassiadis, M., Jacobsen, N., and Parashos, P. (2011). The effect of calcium hydroxide on the steroid component of Ledermix and Odontopaste. *International Endodontic Journal*, 44(12): 1162-1169.

Attia, D. A., Farag, A. M., Afifi, I. K., and Darrag, A. M. (2015). Antimicrobial effect of different intracanal medications on various microorganisms. *Tanta Dental Journal*, 12(1): 41-47.

Balasubramaniam, R., and Jayakumar, S. (2017). Antibiotics in endodontics-A concise review. *International Journal of Applied Dental Sciences*, 3(4): 323-329.

Baumgartner, C. J., and Falkler, W. A. (1991). Bacteria in the apical 5 mm of infected root canals. *Journal of Endodontics*, 17(8): 380-383.

Beloin, C., Valle, J., Latour-Lambert, P., Faure, P., Kzreminski, M., Balestrino, D., Haagensen, J. A., Molin, S., Prensier, G., and Arbeille, B. (2004). Global impact of mature biofilm lifestyle on *Escherichia coli* K-12 gene expression. *Molecular Microbiology*, 51(3): 659-674.

Besinis, A., De Peralta, T., and Handy, R. D. (2014). Inhibition of biofilm formation and antibacterial properties of a silver nano-coating on human dentine. *Nanotoxicology*, 8(7): 745-754.

Beyth, N., Houri-Haddad, Y., Domb, A., Khan, W., and Hazan, R. (2015). Alternative antimicrobial approach: Nano-antimicrobial materials. *Evidence-Based Complementary and Alternative Medicine*, 2015: 1-16.

Bhardwaj, A., Bhardwaj, A., Misuriya, A., Maroli, S., Manjula, S., and Singh, A. K. (2014). Nanotechnology in dentistry: Present and future. *Journal of International Oral Health*, 6(1): 121-126.

Blecher, K., Nasir, A., and Friedman, A. (2011). The growing role of nanotechnology in combating infectious disease. *Virulence*, 2(5): 395-401.

Brown, M. R., Allison, D. G., and Gilbert, P. (1988). Resistance of bacterial biofilms to antibiotics a growth-rate related effect? *Journal of Antimicrobial Chemotherapy*, 22(6): 777-780.

Bruniera, J. F. B., Silva-Sousa, Y. T. C., Lara, M. G., Pitondo-Silva, A., Marcaccini, A. M., and Miranda, C. E. S. (2014). Development of intracanal formulation containing silver nanoparticles. *Brazilian Dental Journal*, 25(4): 302-306.

Byström, A., Claesson, R., and Sundqvist, G. (1985). The antibacterial effect of camphorated paramonochlorophenol, camphorated phenol and calcium hydroxide in the treatment of infected root canals. *Dental Traumatology*, 1(5): 170-175.

Carr, G. B., Schwartz, R. S., Schaudinn, C., Gorur, A., and Costerton, J. W. (2009). Ultrastructural Examination of Failed Molar Retreatment with Secondary Apical Periodontitis: An Examination of Endodontic Biofilms in an Endodontic Retreatment Failure. *Journal of Endodontics*, 35(9): 1303-1309.

Carrotte, P. (2004a). Endodontics: Part 1 The modern concept of root canal treatment. *British Dental Journal*, 197(4): 181-183.

Carrotte, P. (2004b). Endodontics: Part 7 Preparing the root canal. *British Dental Journal*, 197(10): 603-613.

Chong, B. S., and Ford, T. R. P. (1992). The role of intracanal medication in root canal treatment. *International Endodontic Journal*, 25(2): 97-106.

Colaco, A. S. (2018). Extreme resistance of Enterococcus faecalis and its role in endodontic treatment failure. *Progress in Medical Sciences*, 2(1): 9-13.

Commission, E. (2011). Commission recommendation of 18 october 2011 on the definition of nanomaterial (2011/696/EU). *Official Journal of the European Communities: Legis*.

Costerton, J. W., Stewart, P. S., and Greenberg, E. P. (1999). Bacterial biofilms: a common cause of persistent infections. *Science*, 284(5418): 1318-1322.

Cwikla, S. J., Bélanger, M., Giguère, S., Progulske-Fox, A., and Vertucci, F. J. (2005). Dentinal tubule disinfection using three calcium hydroxide formulations. *Journal of Endodontics*, 31(1): 50-52.

Dai, L., Khechen, K., Khan, S., Gillen, B., Loushine, B. A., Wimmer, C. E., Gutmann, J. L., Pashley, D., and Tay, F. R. (2011). The effect of QMix, an experimental antibacterial root canal irrigant, on removal of canal wall smear layer and debris. *Journal of Endodontics*, 37(1): 80-84.

Del Fabbro, M., Afrashtehfar, K. I., Corbella, S., El-Kabbaney, A., Perondi, I., and Taschieri, S. (2018). *In vivo* and *in vitro* effectiveness of rotary nickel-titanium vs manual stainless steel instruments for root canal therapy: systematic review and meta-analysis. *Journal of Evidence Based Dental Practice*, 18(1): 59-69.

Delboni, M. G., Gomes, B. P. F. A., Francisco, P. A., Teixeira, F. B., and Drake, D. (2017). Diversity of *Enterococcus faecalis* genotypes from multiple oral sites associated with endodontic failure using repetitive sequence-based polymerase chain reaction and arbitrarily primed polymerase chain reaction. *Journal of Endodontics*, 43(3): 377-382.

Distel, J. W., Hatton, J. F., and Gillespie, M. J. (2002). Biofilm formation in medicated root canals. *Journal of Endodontics*, 28(10): 689-693.

Dua, K., Singh, G., Goel, M., and Sachdeva, G. (2012). Endodontic biofilm and its relevance in endodontic infection. *Indian Journal of Dental Sciences*, 4(5): 110-114.

Ehrmann, E. H. (1965). The effect of triamcinolone with tetracycline on the dental pulp and apical periodontium. *The Journal of Prosthetic Dentistry*, 15(1): 144-152.

Estrela, C., and Holland, R. (2003). Calcium hydroxide: study based on scientific evidences. *Journal of Applied Oral Science*, 11(4): 269-282.

Estrela, C., Sydney, G. B., Bammann, L. L., and Felippe Jr, O. (1995). Mechanism of action of calcium and hydroxyl ions of calcium hydroxide on tissue and bacteria. *Brazilian Dental Journal*, 6(2): 85-90.

Evans, M., Davies, J., Sundqvist, G., and Figdor, D. (2002a). Mechanisms involved in the resistance of Enterococcus faecalis to calcium hydroxide. *International Endodontic Journal*, 35(3): 221-228.

Evans, M., Davies, J. K., Sundqvist, G., and Figdor, D. (2002b). Mechanisms involved in the resistance of *Enterococcus faecalis* to calcium hydroxide. *International Endodontic Journal*, 35(3): 221-228.

Fabricius, L., Dahlén, G., Öhman, A. E., and Möller, Å. J. R. (1982). Predominant indigenous oral bacteria isolated from infected root canals after varied times of closure. *Scandinavian Journal of Dental Research*, 90(2): 134-144.

Farber, P. A., and Seltzer, S. (1988). Endodontic microbiology. I. Etiology. *Journal of Endodontics*, 14(7): 363-371.

Fava, L., and Saunders, W. (1999). Calcium hydroxide pastes: classification and clinical indications. *International Endodontic Journal*, 32(4): 257-282.

Feynman, R. P. (1960). There's plenty of room at the bottom. *Engineering and Science*, 23(5): 22-36.

Figdor, D., Davies, J., and Sundqvist, G. (2003). Starvation survival, growth and recovery of Enterococcus faecalis in human serum. *Oral Microbiology and Immunology*, 18(4): 234-239.

Flemming, H. C., and Wingender, J. (2010). The biofilm matrix. *Nature Reviews Microbiology*, 8(9): 623-633.

Gandolfi, M. G., Siboni, F., Botero, T., Bossù, M., Riccitiello, F., and Prati, C. (2015). Calcium silicate and calcium hydroxide materials for pulp capping: biointeractivity, porosity, solubility and bioactivity of current formulations. *Journal of Applied Biomaterials & Functional Materials*, 13(1): 43-60.

Gatewood, R. S. (2007). Endodontic materials. *Dental Clinics of North America*, 51(3): 695-712.

Gliga, A. R., Skoglund, S., Wallinder, I. O., Fadeel, B., and Karlsson, H. L. (2014). Size-dependent cytotoxicity of silver nanoparticles in human lung cells: the role of cellular uptake, agglomeration and Ag release. *Particle and Fibre Toxicology*, 11(1): 11-27.

Gomes, B., Souza, S., Ferraz, C., Teixeira, F., Zaia, A., Valdrighi, L., and Souza-Filho, F. (2003). Effectiveness of 2% chlorhexidine gel and calcium hydroxide against *Enterococcus faecalis* in bovine root dentine *in vitro*. *International Endodontic Journal*, 36(4): 267-275.

Gomes, B. P. F. A., Pinheiro, E. T., Gadê-Neto, C. R., Sousa, E. L. R., Ferraz, C. C. R., Zaia, A. A., Teixeira, F. B., and Souza-Filho, F. J. (2004). Microbiological examination of infected dental root canals. *Oral Microbiology & Immunology*, 19(2): 71-76.

Grossman, L. I. (1951). Polyantibiotic Treatment of Pulpless Teeth. *The Journal of the American Dental Association*, 43(3): 265-278.

Guerreiro-Tanomaru, J. M., Figueiredo Pereira, K., Almeida Nascimento, C., Basso Bernardi, M. I., and Tanomaru-Filho, M. (2013). Use of nanoparticulate zinc oxide as intracanal medication in endodontics: ph and antimicrobial activity. *Acta Odontológica Latinoamericana*, 26(3): 167-172.

Haapasalo, M., Shen, Y., Qian, W., and Gao, Y. (2010). Irrigation in endodontics. *Dental Clinics of North America*, 54(2): 291-312.

Haapasalo, M., Udnæs, T., and Endal, U. (2003). Persistent, recurrent, and acquired infection of the root canal system post-treatment. *Endodontic Topics*, 6(1): 29-56.

Hajipour, M. J., Fromm, K. M., Ashkarran, A. A., de Aberasturi, D. J., de Larramendi, I. R., Rojo, T., Serpooshan, V., Parak, W. J., and Mahmoudi, M. (2012). Antibacterial properties of nanoparticles. *Trends in Biotechnology*, 30(10): 499-511.

Hench, L. L. (2006). The story of Bioglass. *Journal of Materials Science: Materials in Medicine*, 17(11): 967-978.

Huang, L., Li, D.-Q., Lin, Y.-J., Wei, M., Evans, D. G., and Duan, X. (2005). Controllable preparation of Nano-MgO and investigation of its bactericidal properties. *Journal of Inorganic Biochemistry*, 99(5): 986-993.

Huang, Z., Zheng, X., Yan, D., Yin, G., Liao, X., Kang, Y., Yao, Y., Huang, D., and Hao, B. (2008). Toxicological effect of ZnO nanoparticles based on bacteria. *Langmuir*, 24(8): 4140-4144.

Hubble, T., Hatton, J., Nallapareddy, S., Murray, B., and Gillespie, M. (2003). Influence of Enterococcus faecalis proteases and the collagen-binding protein, Ace, on adhesion to dentin. *Oral Microbiology and Immunology*, 18(2): 121-126.

Hülsmann, M., Peters, O. A., and Dummer, P. M. (2005). Mechanical preparation of root canals: shaping goals, techniques and means. *Endodontic Topics*, 10(1): 30-76.

Jahangiri, A., and Barghi, L. (2018). Polymeric nanoparticles: review of synthesis methods and applications in drug delivery. *Journal of Advanced Chemical and Pharmaceutical Materials*, 1(2): 38-47.

Jalal, R., Goharshadi, E. K., Abareshi, M., Moosavi, M., Yousefi, A., and Nancarrow, P. (2010). ZnO nanofluids: Green synthesis, characterization, and antibacterial activity. *Materials Chemistry and Physics*, 121(1–2): 198-201.

Jhajharia, K., Parolia, A., Vikram Shetty, K., and Mehta, L. K. (2015). Biofilm in endodontics: A review. *Journal of International Society of Preventive & Community Dentistry*, 5(1): 1-12.

Kakehashi, S., Stanley, H. R., and Fitzgerald, R. J. (1965). The effects of surgical exposures of dental pulps in germ-free and conventional laboratory rats. *Oral Surgery, Oral Medicine, Oral Pathology*, 20(3): 340-349.

Kawashima, N., Wadachi, R., Suda, H., Yeng, T., and Parashos, P. (2009). Root canal medicaments. *International Dental Journal*, 59(1): 5-11.

Kho, P., and Baumgartner, J. C. (2006). A comparison of the antimicrobial efficacy of NaOCl/Biopure MTAD versus NaOCl/EDTA against Enterococcus faecalis. *Journal of Endodontics*, 32(7): 652-655.

Kim, D., and Kim, E. (2014). Antimicrobial effect of calcium hydroxide as an intracanal medicament in root canal treatment: a literature review-Part I. *In vitro* studies. *Restorative Dentistry & Endodontics*, 39(4): 241-252.

Kim, J. S., Kuk, E., Yu, K. N., Kim, J.-H., Park, S. J., Lee, H. J., Kim, S. H., Park, Y. K., Park, Y. H., and Hwang, C.-Y. (2007). Antimicrobial effects of silver nanoparticles. *Nanomedicine: Nanotechnology, Biology and Medicine*, 3(1): 95-101.

Kishen, A. (2010). Advanced therapeutic options for endodontic biofilms. *Endodontic Topics*, 22(1): 99-123.

Kishen, A., Shi, Z., Shrestha, A., and Neoh, K. G. (2008). An investigation on the antibacterial and antibiofilm efficacy of cationic nanoparticulates for root canal disinfection. *Journal of Endodontics*, 34(12): 1515-1520.

Kokare, C., Chakraborty, S., Khopade, A., and Mahadik, K. (2009). Biofilm: Importance and applications. *Indian Journal of Biotechnology*, 8(2): 159-168.

Kolenbrander, P. E., Palmer, R. J., Periasamy, S., and Jakubovics, N. S. (2010). Oral multispecies biofilm development and the key role of cell–cell distance. *Nature Reviews Microbiology*, 8(7): 471-480.

Kumar, J., Sharma, R., Sharma, M., Prabhavathi, V., Paul, J., and Chowdary, C. D. (2015). Presence of *Candida albicans* in root canals of teeth with apical periodontitis and evaluation of their possible role in failure of endodontic treatment. *Journal of International Oral Health*, 7(2): 42-45.

Kurian, B., Swapna, D., Nadig, R. R., Ranjini, M., Rashmi, K., and Bolar, S. R. (2016). Efficacy of calcium hydroxide, mushroom, and Aloe vera as an intracanal medicament against *Enterococcus faecalis*: An *in vitro* study. *Endodontology*, 28(2): 137-142.

Lellouche, J., Kahana, E., Elias, S., Gedanken, A., and Banin, E. (2009). Antibiofilm activity of nanosized magnesium fluoride. *Biomaterials*, 30(30): 5969-5978.

Leonardo, M. R., Rossi, M. A., Silva, L. A. B., Ito, I. Y., and Bonifácio, K. C. (2002). EM evaluation of bacterial biofilm and microorganisms on the apical external root surface of human teeth. *Journal of Endodontics*, 28(12): 815-818.

Leoni, G., Versiani, M., Silva-Sousa, Y., Bruniera, J., Pécora, J., and Sousa-Neto, M. (2017). *Ex vivo* evaluation of four final irrigation protocols on the removal of hard-tissue debris from the mesial root canal system of mandibular first molars. *International Endodontic Journal*, 50(4): 398-406.

Liu, Y., He, L., Mustapha, A., Li, H., Hu, Z., and Lin, M. (2009). Antibacterial activities of zinc oxide nanoparticles against *Escherichia coli* O157: H7. *Journal of Applied Microbiology*, 107(4): 1193-1201.

Love, R. M. (2004). Invasion of dentinal tubules by root canal bacteria. *Endodontic Topics*, 9(1): 52-65.

Mantri, S. S., and Mantri, S. P. (2013). The nano era in dentistry. *Journal of Natural Science, Biology, and Medicine*, 4(1): 39-44.

McGurkin-Smith, R., Trope, M., Caplan, D., and Sigurdsson, A. (2005). Reduction of intracanal bacteria using GT rotary instrumentation, 5.25% NaOCl, EDTA, and $Ca(OH)_2$. *Journal of Endodontics*, 31(5): 359-363.

McHugh, C. P., Zhang, P., Michalek, S., and Eleazer, P. D. (2004). pH required to kill *Enterococcus faecalis in vitro*. *Journal of Endodontics*, 30(4): 218-219.

Misuriya, A., Bhardwaj, A., Bhardwaj, A., Aggrawal, S., Kumar, P. P., and Gajjarepu, S. (2014). A comparative antimicrobial analysis of various root canal irrigating solutions on endodontic pathogens: An *in vitro* study. *The Journal of Contemporary Dental Practice*, 15(2): 153-160.

Mohammadi, Z., Palazzi, F., Giardino, L., and Shalavi, S. (2013). Microbial biofilms in endodontic infections: an update review. *Biomedical Journal*, 36(2): 59-70.

Mohammadi, Z., and Shalavi, S. (2016). Managing root resorption using calcium hydroxide: A review. *International Journal of Clinical Dentistry*, 9(4): 247-254.

Mohammadi, Z., Shalavi, S., and Yazdizadeh, M. (2012). Antimicrobial activity of calcium hydroxide in endodontics: a review. *Chonnam Medical Journal*, 48(3): 133-140.

Mohn, D., Zehnder, M., Imfeld, T., and Stark, W. J. (2010). Radio-opaque nanosized bioactive glass for potential root canal application: evaluation of radiopacity, bioactivity and alkaline capacity. *International Endodontic Journal*, 43(3): 210-217.

Molven, O., Olsen, I., and Kerekes, K. (1991). Scanning electron microscopy of bacteria in the apical part of root canals in permanent teeth with periapical lesions. *Endodontics & Dental Traumatology*, 7(5): 226-229.

Monzavi, A., Eshraghi, S., Hashemian, R., and Momen-Heravi, F. (2015). *In vitro* and *ex vivo* antimicrobial efficacy of nano-MgO in the elimination of endodontic pathogens. *Clinical Oral Investigations*, 19(2): 349-356.

Morones, J. R., Elechiguerra, J. L., Camacho, A., Holt, K., Kouri, J. B., Ramírez, J. T., and Yacaman, M. J. (2005). The bactericidal effect of silver nanoparticles. *Nanotechnology*, 16(10): 2346.

Murad, C. F., Sassone, L. M., Faveri, M., Hirata, R., Figueiredo, L., and Feres, M. (2014). Microbial diversity in persistent root canal infections investigated by checkerboard DNA-DNA hybridization. *Journal of Endodontics*, 40(7): 899-906.

Murvindran, V., and James, D. (2014). Antibiotics as an intracanal medicament in Endodontics. *Journal of Pharmaceutical Sciences and Research*, 6(9): 297-301.

Nair, P. (2004). Pathogenesis of apical periodontitis and the causes of endodontic failures. *Critical Reviews in Oral Biology & Medicine*, 15(6): 348-381.

Nair, P. N. R., Sjögren, U., Krey, G., Kahnberg, K.-E., and Sundqvist, G. (1990). Intraradicular bacteria and fungi in root-filled, asymptomatic human teeth with therapy-resistant periapical lesions: A long-term light and electron microscopic follow-up study. *Journal of Endodontics*, 16(12): 580-588.

Nair, R. P. N. (1987). Light and electron microscopic studies of root canal flora and periapical lesions. *Journal of Endodontics*, 13(1): 29-39.

Nair, V. S., Nayak, M., Ramya, M., Sivadas, G., Ganesh, C., Devi, S. L., and Vedam, V. (2017). Detection of adherence of Enterococcus faecalis in infected dentin of extracted human teeth using confocal laser scanning microscope: An In vitro Study. *Journal of Pharmacy & Bioallied Sciences*, 9(Suppl 1): S41.

Narayanan, L. L., and Vaishnavi, C. (2010). Endodontic microbiology. *Journal of Conservative Dentistry*, 13(4): 233-239.

Neel, E. A. A., Bozec, L., Perez, R. A., Kim, H.-W., and Knowles, J. C. (2015). Nanotechnology in dentistry: prevention, diagnosis, and therapy. *International Journal of Nanomedicine*, 10: 6371-6394.

Nobuhara, W. K., Carnes, D. L., and Gilles, J. A. (1993). Anti-inflammatory effects of dexamethasone on periapical tissues following endodontic overinstrumentation. *Journal of Endodontics*, 19(10): 501-507.

Padmavathy, N., and Vijayaraghavan, R. (2008). Enhanced bioactivity of ZnO nanoparticles-an antimicrobial study. *Science and Technology of Advanced Materials*, 9(3): 035004.

Peciuliene, V., Balciuniene, I., Eriksen, H. M., and Haapasalo, M. (2000). Isolation of *Enterococcus faecalis* in previously root-filled canals in a lithuanian population. *Journal of Endodontics*, 26(10): 593-595.

Peciuliene, V., Maneliene, R., Balcikonyte, E., Drukteinis, S., and Rutkunas, V. (2008). Microorganisms in root canal infections: a review. *Stomatologija*, 10(1): 4-9.

Peciuliene, V., Reynaud, A. H., Balciuniene, I., and Haapasalo, M. (2001). Isolation of yeasts and enteric bacteria in root-filled teeth with chronic apical periodontitis. *International Endodontic Journal*, 34(6): 429-434.

Pelgrift, R. Y., and Friedman, A. J. (2013). Nanotechnology as a therapeutic tool to combat microbial resistance. *Advanced Drug Delivery Reviews*, 65(13): 1803-1815.

Peters, O., Schönenberger, K., and Laib, A. (2001). Effects of four Ni–Ti preparation techniques on root canal geometry assessed by micro computed tomography. *International Endodontic Journal*, 34(3): 221-230.

Pinheiro, E., Gomes, B., Ferraz, C., Sousa, E., Teixeira, F., and Souza-Filho, F. (2003). Microorganisms from canals of root-filled teeth with periapical lesions. *International Endodontic Journal*, 36(1): 1-11.

Prabhu, S., and Poulose, E. K. (2012). Silver nanoparticles: mechanism of antimicrobial action, synthesis, medical applications, and toxicity effects. *International Nano Letters*, 2(1): 1-10.

Rams, T. E., Feik, D., Mortensen, J. E., Degener, J. E., and van Winkelhoff, A. J. (2013). Antibiotic susceptibility of periodontal *Enterococcus faecalis*. *Journal of Periodontology*, 84(7): 1026-1033.

Ricucci, D., and Siqueira, J. F. (2010). Biofilms and apical periodontitis: study of prevalence and association with clinical and histopathologic findings. *Journal of Endodontics*, 36(8): 1277-1288.

Ricucci, D., Siqueira Jr, J. F., Bate, A. L., and Pitt Ford, T. R. (2009). Histologic investigation of root canal–treated teeth with apical periodontitis: A retrospective study from twenty-four patients. *Journal of Endodontics*, 35(4): 493-502.

Saatchi, M., Shokraneh, A., Navaei, H., Maracy, M. R., and Shojaei, H. (2014). Antibacterial effect of calcium hydroxide combined with chlorhexidine on *Enterococcus faecalis*: a systematic review and meta-analysis. *Journal of Applied Oral Science*, 22(5): 356-365.

Safavi, K. E., and Nichols, F. C. (1993). Effect of calcium hydroxide on bacterial lipopolysaccharide. *Journal of Endodontics*, 19(2): 76-78.

Sanchez, F., and Sobolev, K. (2010). Nanotechnology in concrete–a review. *Construction and Building Materials*, 24(11): 2060-2071.

Sauer, K., Camper, A. K., Ehrlich, G. D., Costerton, J. W., and Davies, D. G. (2002). *Pseudomonas aeruginosa* displays multiple phenotypes during development as a biofilm. *Journal of Bacteriology*, 184(4): 1140-1154.

Schäfer, E., and Bössmann, K. (2005). Antimicrobial Efficacy of Chlorhexidine and Two Calcium Hydroxide Formulations Against *Enterococcus faecalis*. *Journal of Endodontics*, 31(1): 53-56.

Seil, J. T., and Webster, T. J. (2012). Antimicrobial applications of nanotechnology: methods and literature. *International Journal of Nanomedicine*, 7: 2767-2781.

Sen, B. H., Piskin, B., and Demirci, T. (1995). Observation of bacteria and fungi in infected root canals and dentinal tubules by SEM. *Endodontics & Dental Traumatology*, 11(1): 6-9.

Shokraneh, A., Farhad, A. R., Farhadi, N., Saatchi, M., and Hasheminia, S. M. (2014). Antibacterial effect of triantibiotic mixture versus calcium hydroxide in combination with active agents against *Enterococcus faecalis* biofilm. *Dental Materials Journal*, 33(6): 733-738.

Shrestha, A., Zhilong, S., Gee, N. K., and Kishen, A. (2010). Nanoparticulates for antibiofilm treatment and effect of aging on its antibacterial activity. *Journal of Endodontics*, 36(6): 1030-1035.

Shuping, G. B., Ørstavik, D., Sigurdsson, A., and Trope, M. (2000). Reduction of intracanal bacteria using nickel-titanium rotary instrumentation and various medications. *Journal of Endodontics*, 26(12): 751-755.

Siqueira, J., and Lopes, H. (1999). Mechanisms of antimicrobial activity of calcium hydroxide: a critical review. *International Endodontic Journal*, 32(5): 361-369.

Siqueira, J., Perez, A., Marceliano-Alves, M., Provenzano, J., Silva, S., Pires, F., Vieira, G., Rocas, I., and Alves, F. (2017). What happens to unprepared root canal walls: a correlative analysis using micro-computed tomography and histology/scanning electron microscopy. *International Endodontic Journal*, 51(5): 501-508.

Siqueira, J. F. (2001a). Aetiology of root canal treatment failure: why well-treated teeth can fail. *International Endodontic Journal*, 34(1): 1-10.

Siqueira, J. F. (2001b). Strategies to treat infected root canals. *Journal of the California Dental Association*, 29(12): 825-838.

Siqueira, J. F. (2002). Endodontic infections: Concepts, paradigms, and perspectives. *Oral Surgery, Oral Medicine, Oral Pathology, Oral Radiology, and Endodontology*, 94(3): 281-293.

Siqueira, J. F., and de Uzeda, M. (1998). Influence of different vehicles on the antibacterial effects of calcium hydroxide. *Journal of Endodontics*, 24(10): 663-665.

Siqueira, J. F., and Rôças, I. N. (2008). Clinical implications and microbiology of bacterial persistence after treatment procedures. *Journal of Endodontics*, 34(11): 1291-1301.

Siqueira, J. F., and Rôças, I. N. (2014). Present status and future directions in endodontic microbiology. *Endodontic Topics*, 30(1): 3-22.

Siqueira, J. F., Rôças, I. N., and Lopes, H. P. (2002). Patterns of microbial colonization in primary root canal infections. *Oral Surgery, Oral Medicine, Oral Pathology, Oral Radiology, and Endodontology*, 93(2): 174-178.

Siqueira, J. F., Rôças, I. N., and Ricucci, D. (2010). Biofilms in endodontic infection. *Endodontic Topics*, 22(1): 33-49.

Siqueira, J. F., and Sen, B. H. (2004). Fungi in endodontic infections. *Oral Surgery, Oral Medicine, Oral Pathology, Oral Radiology, and Endodontology*, 97(5): 632-641.

Sirelkhatim, A., Mahmud, S., Seeni, A., Kaus, N. H. M., Ann, L. C., Bakhori, S. K. M., Hasan, H., and Mohamad, D. (2015). Review on zinc oxide nanoparticles: antibacterial activity and toxicity mechanism. *Nano-Micro Letters*, 7(3): 219-242.

Sjögren, U., Figdor, D., Spångberg, L., and Sundqvist, G. (1991). The antimicrobial effect of calcium hydroxide as a short-term intracanal dressing. *International Endodontic Journal*, 24(3): 119-125.

Sondi, I., and Salopek-Sondi, B. (2004). Silver nanoparticles as antimicrobial agent: a case study on *E. coli* as a model for Gram-negative bacteria. *Journal of Colloid and Interface Science*, 275(1): 177-182.

Song, M., Yu, B., Kim, S., Hayashi, M., Smith, C., Sohn, S., Kim, E., Lim, J., Stevenson, R. G., and Kim, R. H. (2017). Clinical and molecular perspectives of reparative dentin formation: lessons learned from pulp-capping materials and the emerging roles of calcium. *Dental Clinics*, 61(1): 93-110.

Song, W., Zhang, J., Guo, J., Zhang, J., Ding, F., Li, L., and Sun, Z. (2010). Role of the dissolved zinc ion and reactive oxygen species in cytotoxicity of ZnO nanoparticles. *Toxicology Letters*, 199(3): 389-397.

Sotiriou, G. A., and Pratsinis, S. E. (2010). Antibacterial activity of nanosilver ions and particles. *Environmental Science & Technology*, 44(14): 5649-5654.

Stojicic, S., Shen, Y., and Haapasalo, M. (2013). Effect of the source of biofilm bacteria, level of biofilm maturation, and type of disinfecting agent on the susceptibility of biofilm bacteria to antibacterial agents. *Journal of Endodontics*, 39(4): 473-477.

Stojicic, S., Shen, Y., Qian, W., Johnson, B., and Haapasalo, M. (2012). Antibacterial and smear layer removal ability of a novel irrigant, QMiX. *International Endodontic Journal*, 45(4): 363-371.

Stoor, P., Söderling, E., and Salonen, J. I. (1998). Antibacterial effects of a bioactive glass paste on oral microorganisms. *Acta Odontologica Scandinavica*, 56(3): 161-165.

Stuart, C. H., Schwartz, S. A., Beeson, T. J., and Owatz, C. B. (2006). *Enterococcus faecalis*: Its Role in Root Canal Treatment Failure and Current Concepts in Retreatment. *Journal of Endodontics*, 32(2): 93-98.

Sundqvist, G., and Figdor, D. (2003). Life as an endodontic pathogen. *Endodontic Topics*, 6(1): 3-28.

Svensäter, G., and Bergenholtz, G. (2004). Biofilms in endodontic infections. *Endodontic Topics*, 9(1): 27-36.

Tang, G., Samaranayake, L. P., and Yip, H. K. (2004). Molecular evaluation of residual endodontic microorganisms after instrumentation, irrigation and medication with either calcium hydroxide or Septomixine. *Oral Diseases*, 10(6): 389-397.

Tennert, C., Fuhrmann, M., Wittmer, A., Karygianni, L., Altenburger, M. J., Pelz, K., Hellwig, E., and Al-Ahmad, A. (2014). New bacterial composition in primary and persistent/secondary endodontic infections with respect to clinical and radiographic findings. *Journal of Endodontics*, 40(5): 670-677.

Tiwari, J. N., Tiwari, R. N., and Kim, K. S. (2012). Zero-dimensional, one-dimensional, two-dimensional and three-dimensional nanostructured materials for advanced electrochemical energy devices. *Progress in Materials Science*, 57(4): 724-803.

Torabinejad, M., Shabahang, S., Aprecio, R. M., and Kettering, J. D. (2003). The Antimicrobial Effect of MTAD: An In Vitro Investigation. *Journal of Endodontics*, 29(6): 400-403.

Tronstad, L. (1988). Root resorption - etiology, terminology and clinical manifestations. *Endodontics & Dental Traumatology*, 4(6): 241-252.

Tronstad, L., Andreasen, J. O., Hasselgren, G., Kristerson, L., and Riis, I. (1981). pH changes in dental tissues after root canal filling with calcium hydroxide. *Journal of Endodontics*, 7(1): 17-21.

Tronstad, L., Barnett, F., and Cervone, F. (1990). Periapical bacterial plaque in teeth refractory to endodontic treatment. *Endodontics & Dental Traumatology*, 6(2): 73-77.

Tronstad, L., and Sunde, P. T. (2003). The evolving new understanding of endodontic infections. *Endodontic Topics*, 6(1): 57-77.

Usha, H. (2010). Biofilm in endodontics: New understanding to an old problem. *International Journal of Contemporary Dentistry*, 1(3): 44-51.

Valera, M. C., Oliveira, S., Maekawa, L., Cardoso, F., Chung, A., Silva, S., and Carvalho, C. (2016). Action of chlorhexidine, Zingiber officinale, and calcium hydroxide on *Candida albicans*, *Enterococcus faecalis*, *Escherichia coli*, and endotoxin in the root canals. *The Journal of Contemporary Dental Practice*, 17(2): 114-8.

Valko, M., Leibfritz, D., Moncol, J., Cronin, M. T., Mazur, M., and Telser, J. (2007). Free radicals and antioxidants in normal physiological functions and human disease. *The International Journal of Biochemistry & Cell Biology*, 39(1): 44-84.

Vaudt, J., Bitter, K., and Kielbassa, A. M. (2007). Evaluation of rotary root canal instruments in vitro: a review. *Endodontic Practice Today*, 1(3): 189-203.

Wadachi, R., Araki, K., and Suda, H. (1998). Effect of calcium hydroxide on the dissolution of soft tissue on the root canal wall. *Journal of Endodontics*, 24(5): 326-330.

Waltimo, T., Brunner, T., Vollenweider, M., Stark, W., and Zehnder, M. (2007). Antimicrobial effect of nanometric bioactive glass 45S5. *Journal of Dental Research*, 86(8): 754-757.

Waltimo, T., Sen, B., Meurman, J. H., Ørstavik, D., and Haapasalo, M. (2003). Yeasts in apical periodontitis. *Critical Reviews in Oral Biology & Medicine*, 14(2): 128-137.

Waltimo, T. M. T., Sirén, E. K., Torkko, H. L. K., Olsen, I., and Haapasalo, M. P. P. (1997). Fungi in therapy-resistant apical periodontitis. *International Endodontic Journal*, 30(2): 96-101.

Wang, Z., Shen, Y., and Haapasalo, M. (2012). Effectiveness of endodontic disinfecting solutions against young and old *Enterococcus faecalis* biofilms in dentin canals. *Journal of Endodontics*, 38(10): 1376-1379.

Wu, D., Fan, W., Kishen, A., Gutmann, J. L., and Fan, B. (2014). Evaluation of the antibacterial efficacy of silver nanoparticles against *Enterococcus faecalis* biofilm. *Journal of Endodontics*, 40(2): 285-290.

Yamamoto, O. (2001). Influence of particle size on the antibacterial activity of zinc oxide. *International Journal of Inorganic Materials*, 3(7): 643-646.

Zehnder, M., Luder, H. U., Schätzle, M., Kerosuo, E., and Waltimo, T. (2006). A comparative study on the disinfection potentials of bioactive glass S53P4 and calcium hydroxide in contra-lateral human premolars ex vivo. *International Endodontic Journal*, 39(12): 952-958.

Zhang, L., Ding, Y., Povey, M., and York, D. (2008). ZnO nanofluids – A potential antibacterial agent. *Progress in Natural Science*, 18(8): 939-944.

Chapter 3
Antimicrobial effects of low molecular weight chitosan

3.1 Review of the literature

The use of natural polysaccharides for hydrogel formation gained increased attention and replaced the use of synthetic polymers due to the fact that they are easily accessible in nature where they can be extracted from both animals and plants. Additionally, natural polymers are usually less toxic and more biocompatible compared to synthetic polymers (Coviello *et al.*, 2007).

Synthesis of chitosan hydrogel became more popular recently as a result of its antimicrobial properties (Yoshimura *et al.*, 2006; Helander *et al.*, 2001), biocompatibility (Kumar, 2000), various medical applications such as drug delivery vehicles (Agnihotri *et al.*, 2004) and use as a possible scaffold for tissue engineering (VandeVord *et al.*, 2002).

Chitosan is a natural polysaccharide that is obtained by deacetylation of chitin (Rinaudo, 2006) which is one of the most abundant polysaccharides in nature (Rinaudo, 2006). Chemically, chitin is composed of (1-4)-linked 2-acetamido-2-deoxy-β-D-glucose (Park and Kim, 2010). It is a hydrophobic material that is insoluble in water or

organic solvents (Kumar, 2000). To overcome this disadvantage, the chemical structure of chitin is modified by reducing the acetyl group (*N*-deacetylation) by 40 to 35% through chemical hydrolysis in an alkaline solution and high temperature, producing a new chemical formula that consists of a copolymer of (1-4)-2-amine-2-deoxy-β-D-glucan and (1-4)-2-acetamide-2-deoxy-β-D-glucan which is known as chitosan (Ch) (Goy *et al.*, 2009) (Figure 3-1). Furthermore, the deacetylation of chitin creates multiple reactive functional groups that increase its reactivity and thus expand their possible applications (Prashanth and Tharanathan, 2007).

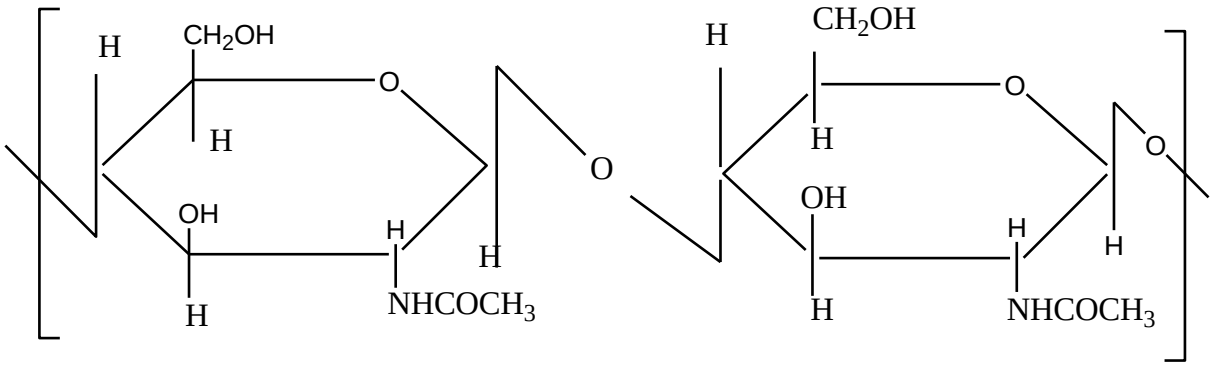

(A)

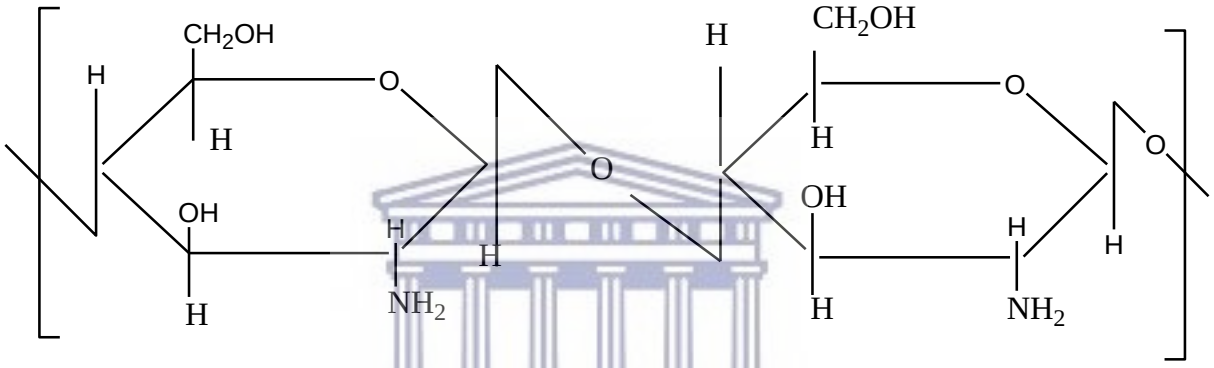

(B)

Figure 3-1: The chemical structure of (A) chitin, (B) chitosan in which the acetyl group was removed from chitin (chemical structure adapted from Kumar, 2000)

3.1.1 Antimicrobial properties of chitosan

Chitosan possesses antimicrobial properties against some Gram-positive and Gram-negative bacterial species (Helander *et al.*, 2001) as well as fungal species (Palmeira-de-Oliveira *et al.*, 2010; Tayel *et al.*, 2010). The antimicrobial mechanism of chitosan results from several interacting factors. Kong *et al.*, (2010) classified these factors as follows: factors related to the microbial species; factors related to chitosan structure and

chemistry; physical state in which the chitosan material is applied; and environmental factors such as the pH.

The antibacterial effect of chitosan varies from one bacterial species to another depending on the bacterial cell membrane structure (Chung *et al.*, 2004). The antibacterial mechanism of chitosan was suggested to be due to the ability of the chitosan to bind to the bacterial cell membrane, thus disturbing its permeability, causing lysis of its content and eventually death of the bacteria (Qi *et al.*, 2004; Rabea *et al.*, 2003). However, controversy still exists regarding the degree of potency and effect of chitosan against different bacterial cell walls and thus different bacterial species such as Gram positive and Gram negative (Chung *et al.*, 2004; No *et al.*, 2002) .

Several factors are associated with the antimicrobial effect of chitosan such as its degree of deacetylation, molecular weight and the capacity of chitosan to chelate metallic ions from the microbial cell walls.

The degree of deacetylation of chitosan is determined by its degree of solubility and its charge density, in which chitosan with a high degree of deacetylation showed a high percentage of the free amino group (NH_2) and hydroxyl group (OH) (Goy *et al.*, 2009). The influence of the degree of deacetylation on the antimicrobial effect of chitosan is related to the electrostatic interaction between the positively charged chitosan (free amino group and hydroxyl group) and the negatively charged bacterial cell wall, in which the higher the degree of deacetylation, the stronger the electrostatic interaction and eventually the maximum antimicrobial effect (Kong *et al.*, 2010; Andres *et al.*, 2007; Chung *et al.*, 2003). Wang *et al.*, (2004) and Chen *et al.*, (2005) incorporated zinc

(Zn^{+}) and silver ions (Ag^{+}) into chitosan structures to increase their positively charged density which resulted in higher antimicrobial effect compared to chitosan itself.

The antimicrobial effect of chitosan is also affected by its molecular weight (No *et al.*, 2002). Lower molecular weight (LMW) chitosan has stronger antimicrobial properties compared to chitosan with high molecular weight (HMW) (Tikhonov *et al.*, 2006). Kumar *et al* suggested that it is possibly due to the ability of the short structural chain of the LMW-Ch to adhere to the bacterial cell wall, thus disturbing its function (Kumar *et al.*, 2005). However, the effect of the molecular weight of chitosan on its antibacterial effect was found to be related to the type of microorganism (Gram-positive or Gram-negative) (Zheng and Zhu, 2003). HMW-Ch was found to have a potent effect against *Staphylococcus aureus* (Gram-positive), while LMW-Ch was found to have a potent effect against *Escherichia coli* (Gram-negative) (Zheng and Zhu, 2003). According to Zheng and Zhu (2003) this could be due to the ability of the HMW-Ch to form a film in the bacterial cell wall, altering its ability to absorb nutrients from the surrounding media, while the LMW-Ch can penetrate the bacterial cell membrane, easily disturbing its metabolic activities.

Chitosan also possesses chelating capacity to various metallic ions in acidic and neutral conditions (Kong *et al.*, 2008; Kurita, 1998). This property can influence the antimicrobial effect of chitosan as it chelates the metallic ions that are present in the microbial cell wall, disturbing the stability of the microbial cell wall membrane (Rabea *et al.*, 2003).

The physical state in which the chitosan molecules present (soluble or solid) can influence their antimicrobial properties (Kong *et al.*, 2010). Unlike solid chitosan that

contacts the surrounding media through its surface only, the soluble chitosan can form better contact with the surrounding environment as it disassociates equally into the surrounding media causing maximum contact with the microorganisms and eventually a higher antimicrobial effect compared to chitosan in a solid or insoluble state (Kong *et al.*, 2010). However, this effect is dependent on different factors such as the pH of the surrounding media, chitosan molecular weight and degree of deacetylation (Qin *et al.*, 2006).

Furthermore, chitosan showed higher antimicrobial properties in an acidic environment (Kong *et al.*, 2008; Rabea *et al.*, 2003; Fei Liu *et al.*, 2001). The presence of chitosan in an acidic medium will increase the positively charged amino groups in the chitosan structure that facilitate the interaction between the positively charged chitosan and the negatively charged bacterial cell wall (Raafat *et al.*, 2008; Je and Kim, 2006; Helander *et al.*, 2001).

3.1.2 Chitosan hydrogels

Chitosan is soluble in an acidic medium (Dutta *et al.*, 2004; Kumar, 2000). The presence of chitosan in acidic media will change its form to hydrogel form (entangled chitosan). The formation of chitosan hydrogel in acidic medium will result from repulsion of the chitosan molecules while keeping their surface charge (Fan *et al.*, 2012).

Hydrogel generally is defined as a three-dimensional network of a single polymer (homopolymer) or more than one polymer (copolymer) that is cross linked and has the ability to absorb fluids (Peppas *et al.*, 2000) 400 times more than their original weight (Yoshimura *et al.*, 2006). The process of fluids absorption by hydrogels is known as

swelling. During this process, the fluids are linked to a hydrophilic group such as hydroxyl (-OH), amine (NH_2), sulphate ($-SO_3H$) and amide (-CONH-, $-CONH_2$) of the polymer forming hydrogel, causing expansion and an increase in the volume of the hydrogel (Ahmadi *et al.*, 2015). The destruction or solubility of the hydrogel structure during the swelling process is prevented by the cross-linked structure of the polymers forming the hydrogel (Peppas *et al.*, 2000). The absorbed fluid molecule can present as bonded to the hydrophilic polymer chain, as unbounded "free molecules" inside the network structure, or form a weakly bonded hydrophilic group to the polymer (Ahmadi *et al.*, 2015).

The polymeric network can be formed either by chemical or physical reaction and thus the formed hydrogel can be classified accordingly into either chemical cross-linked, physical cross-linked hydrogels or as a combination of chemical and physical cross-linked hydrogels (Coviello *et al.*, 2007).

Physical cross-linked hydrogels are weaker and can be degraded easily (Bhattarai *et al.*, 2010). It results from a physical reaction such as crystal formation or electrostatic bond (Berger *et al.*, 2004). Chemical cross-linked hydrogels are more stable and less degradable as a result of permanent network formation (Ahmadi *et al.*, 2015). Chemical cross-linking can result from several reactions such as enzymatic reactions, radical polymerization, photopolymerization or through the use of linkers that result in covalent crosslinking (Ahmadi *et al.*, 2015; Kızılel *et al.*, 2006; Kim *et al.*, 2005).

The simplest method to prepare a chitosan hydrogel is through cross-linking with itself in the presence of an acidic solution without any presence of other cross-linkers (Sayyar *et al.*, 2015; Felt *et al.*, 1999). Since chitosan is soluble in an acidic medium (Dutta *et*

al., 2004; Kumar, 2000) this will cause interaction between the chitosan molecules as a result of inter-chain hydrogen bonding (Fan *et al.*, 2012). This will cause the chitosan to be in a hydrogel form (entangled chitosan) which is a weaker and easily soluble form of chitosan (Berger *et al.*, 2004).

3.2 Rationale of the study

With the increased number of studies that evaluated the antimicrobial effect of chitosan, it seems that there are various factors that affect its antimicrobial efficacy. Furthermore, its degree of efficacy varies among different microbial species. In this study the effect of low molecular weight chitosan was evaluated against endodontic pathogens to overcome the shortcoming of the current endodontic antimicrobial agents.

3.3 Aim of the study

The aim of this study was to evaluate the antimicrobial effect of low molecular weight chitosan against three endodontic pathogens, namely *S. mutans*, *E. faecalis* and *C. albicans* in a planktonic state.

3.4 Objectives

i. To evaluate and compare the effect of LMW-Ch on the survival time of three different microbial planktonic cells namely *S. mutans*, *E. faecalis* and *C. albicans* using the Time-Kill Test.

ii. To evaluate and compare the effect of two different concentrations of LMW-Ch on the survival time of planktonic cells of *S. mutans*, *E. faecalis* and *C. albicans*.

3.5 Null hypothesis

i. LMW-Ch cannot eradicate *S. mutans*, *E. faecalis* and *C. albicans*.

ii. The concentration of LMW-CH has no effect on the eradication time of *S. mutans*, *E. faecalis* and *C. albicans*

3.6 Methodology

3.6.1 Preparation of chitosan hydrogels

Chitosan with a low molecular weight of 50 – 190 KDa and 75 – 85% degree of deacetylation was purchased from Sigma-Aldrich Inc, South Africa (batch number: 448869) and used for preparation of two different concentrations of chitosan hydrogels namely 1% and 3% (w/v) (Figure 3-2). The selection of these two concentrations was based on the fact that as the concentration of the chitosan increase the viscosity of the hydrogel increases (Şenel *et al.*, 2000) which render it difficult to be handle.

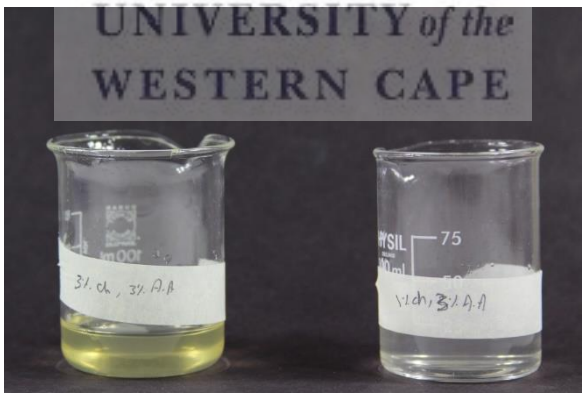

Figure 3-2: Prepared Chitosan hydrogels in two concentrations 1% and 3%. The colour of the hydrogel changed to yellow as the concentration increased.

For preparation of 1% (w/v) chitosan hydrogel, 300 mg of chitosan was dissolved in 3% (v/v) glacial acetic acid (pH = 2.25) and stirred for 24 hours using a magnetic stirrer to allow complete dissolution of the chitosan powder. The pH of the resulted hydrogel was 3.30. Similarly, for preparation of 3% (w/v) of chitosan hydrogel, 900 mg of the chitosan was dissolved in 3% (v/v) glacial acetic acid (pH = 2.25) and stirred for 24 hours using a magnetic stirrer to allow complete dissolution of the chitosan powder. The pH of the resulted hydrogel was 3.58.

3.6.2 Antimicrobial effect of LMW-Ch against endodontic pathogens in a planktonic state

a. Preparation of microbial cultures

The two bacterial species, *Streptococcus mutans* (ATCC 25175) and *Enterococcus faecalis* (ATCC 29212) and one fungal species, *Candida albicans* (ATCC 90028) were obtained from American type culture collections (USA).

The microbial species were incubated in brain heart infusion broth (BHI) at 37°C for 24 hours. Following the overnight culture, *S. mutans*, *E. faecalis* and *C. albicans* were subcultured in brain heart infusion agar plates and incubated overnight at 37°C. The microbial cells were then suspended in phosphate buffer saline solution (PBS) and the concentration was adjusted to 0.5 McFarland standard (Mcf) using DensiCHEK Plus (BioMérieux, Inc Durham, USA) (Figure 3-3).

Figure 3-3: DensiCHEK Plus BioMerieuc, Inc Durham, USA showing the concentration of the microbial suspension of 0.5 McFarland standard.

b. Antimicrobial assay

A Time-Kill Test (Balouiri *et al.*, 2016) was performed using a broth microdilution technique to evaluate the antimicrobial effect of LMW chitosan against the three pathogens. 100 µL from each hydrogel (1% and 3%) was dispensed in a sterile well of a 12-well cell culture plate to which 200 µL of 0.5 Mcf from each tested microbial species suspension and 1700 µL of BHI as a growth medium were added in each well and labelled as experimental groups (A; *S. mutans*, B; *E. faecalis*, C; *C. albicans*). The positive control group (D) consisted of 200 µL of the tested microbial species suspension added to 1700 µL of BHI and placed in a 12-well cell culture plate. The effect of acetic acid was evaluated as a negative control group (E) which consisted of 100 µL of 3% (v/v) acetic acid (pH = 2.25), 200 µL of the tested microbial species suspension and 1700 µL of BHI (Figure 3-4). The 12 well plate was incubated in an Orbital Shaker Incubator (Biocom Biotech, USA) at 37°C in an aerobic condition.

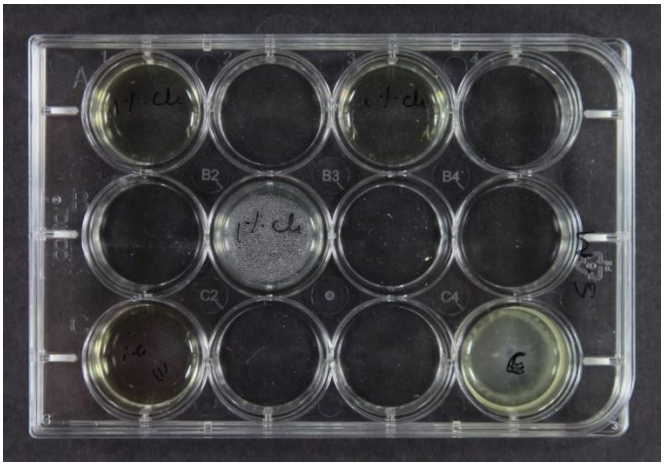

Figure 3-4: 12-well cell culture plate showing different wells contain samples from the experimental group (BHI, microbial suspension and LMW-Ch) and control group (BHI and microbial suspension).

50 µL of PBS was added to each well and then 100 µL from each group was transferred and placed in a sterile 96-well microtiter plate (Figure 3-5). The suspension was diluted two-fold by transferring 50 µL from the first well to the second well proceeding up to the sixth well.

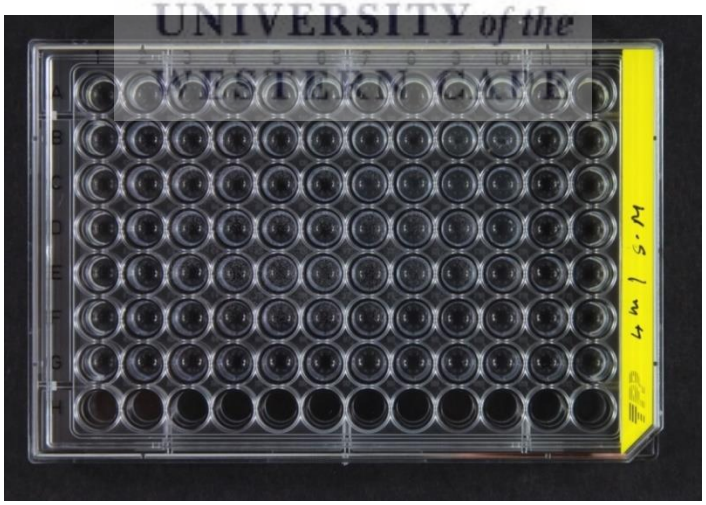

Figure 3-5: A 96-well mictrotiter plate showing different wells contains 100 µL pipetted from a group sample and placed in the first row (A) of the 96-well plate. 50 µL from the first well (A) was transferred to the second well (A) which previously contained 50 µL of PBS. The serial dilution continued until the 6th well (G).

The final volume of the last well was 100 µL. 2 µL from the final dilution of each group was then transferred and streaked in a brain heart infusion agar plate and incubated at 37°C for 24 hours in an aerobic condition. The procedure of serial dilution was done at zero minute, 30 minutes, 1, 2, 4, 6, 8 and 24 hours respectively. After a 24 hour incubation period, the numbers of the colony forming units (CFU) in each plate were counted using an automated colony counter (Gerber, Switzerland) (Figure 3-6). The test was repeated in triplicate.

The numbers of colony forming units that exceeded 300 were considered as too numerous to count (TNTC) and recorded as 300 (CFU), while those less than 30 were considered as too low to count (TLTC) and recorded as zero (Sutton, 2011). The number of the colony forming units that are less than 30 are considered as insignificant to produce illness (Sutton, 2011). The number of CFU/mL less than 30 was considered and counted for the *C. albicans* group in this study. This was done to standardize the laboratory procedure in evaluating the antimicrobial efficacy of commercial LMW–Ch against *E. faecalis*, *S. mutans* and *C. albicans* by using the 0.5 Mcf for all microorganisms and plating from the 6th dilution. The 0.5 McFarland standard was considered as a starting concentration for all microorganisms tested, although for *C. albicans* it is less (1.5×10^6 CFU/mL) than that of *E. faecalis* and *S. mutans*, (1.2×10^8 CFU/mL). This factor resulted in a lower number of colony forming units in *C. albicans* compared to that of *E. faecalis* and *S. mutans* at the same dilution factor.

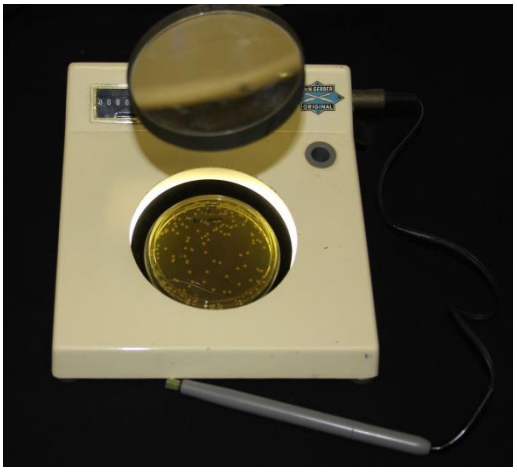

Figure 3-6: Automated colony counter used to count the number of the microbial colonies in the agar plates.

3.7 Data analysis

All results for each group were transferred to an Excel spreadsheet (Microsoft Corporation 2010, USA) The data was expressed in Log CFU/mL and then analyzed using IBM SPSS statistical software (version 25, IBM, USA).

The antimicrobial effect of LMW-Ch against *S. mutans*, *E. faecalis* and *C. albicans* was evaluated by measuring the survival time of each microbial species when exposed to LMW-Ch. The survival time was tested using the Kaplan-Meier test. In addition, the effect of the concentration of LMW-Ch on its antimicrobial efficacy was evaluated by comparing the difference in the survival time of each micro-organism in the two concentrations to the controls.

The antimicrobial effect of using 3% acetic acid as a solvent for LMW-Ch was evaluated by comparing the number of the Log CFU/mL in the positive control group (BHI) and the negative control group (3% acetic acid) for each microbial species.

3.8 Results

3.8.1 Effect of 1% and 3% LMW-Ch against endodontic pathogens in a planktonic state

The effect of LMW-Ch against *S. mutans*, *E. faecalis* and *C. albicans* was evaluated using the Time-Kill Test. The mean, median and standard error of the survival rate of each microbial species when exposed to different concentration of LMW-Ch is shown in Table 3-1.

Table 3-1: The Mean, median and standard error for the survival time of *S. mutans*, *E. faecalis* and *C. albicans* when exposed to 1% and 3% LMW-Ch.

Means and Medians for Survival Time									
Microorganism	LMW-Ch concentration	Mean				Median			
		Estimate	Std. Error	95% Confidence Interval		Estimate	Std. Error	95% Confidence Interval	
				Lower Bound	Upper Bound			Lower Bound	Upper Bound
S. mutans	1%	9.65	1.56	6.6	12.7	6	0.85	4.33	7.67
	3%	8.03	1.37	5.34	10.73	6	0.91	4.21	7.79
	Overall	8.82	1.03	6.8	10.83	6	0.62	4.78	7.22
E. faecalis	1%	11.94	1.85	8.31	15.58	8	0.68	6.67	9.33
	3%	9.69	1.56	6.62	12.75	6	0.85	4.34	7.66
	Overall	10.78	1.2	8.43	13.12	8	0.49	7.04	8.96
C. albicans	1%	10.69	1.75	7.27	14.12	6	1.62	2.83	9.17
	3%	11.65	1.85	8.02	15.27	8	1.34	5.37	10.63
	Overall	11.19	1.26	8.72	13.65	6	1.02	4	8
Overall	Overall	10.24	0.67	8.92	11.56	6	0.39	5.23	6.77

a. Effect of 1% and 3% MW-Ch against planktonic cells of *S. mutans*

The Kaplan-Meir survival function curve showed that *S. mutans* was observed at zero minute, 30 minutes, 1 hour and 2 hours only when it was exposed to 1% and 3% LMW- Ch (Figure 3-7). The figure represents the cumulative survival rate of *S. mutans* which is defined as the estimated survival probability according to Goel *et al* (2010).

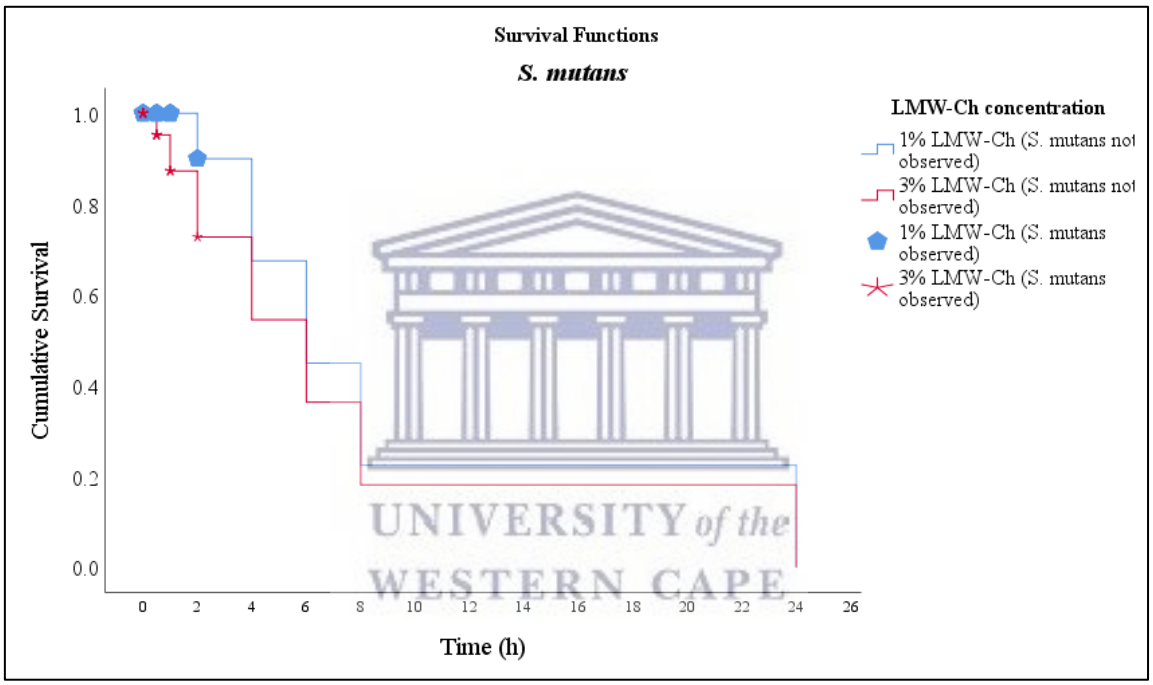

Figure 3-7: Survival function curve of *S. mutans* showing the time at which it was observed when it was exposed to LMW-Ch at 1% and 3%.

The number of the Log CFU/mL for both concentrations at zero minute was 6.72. The 3% LMW-Ch showed a steeper decline in the colony count within the first 2 hours compared to 1% LMW-Ch. Both concentrations eradicated *S. mutans* at 4 hour contact time. The mean number of the CFU/mL of both concentrations at different times compared to the positive control group is shown in Table 3-2.

Table 3-2: The mean number of the Log CFU/mL of *S. mutans* when exposed to 1% and 3% LMW-Ch compared to the positive control group.

Time (h)	1% LMW-Ch	3% LMW-Ch	(+ve) Control
0	6.75	6.72	6.97
0.5	6.58	4.30	6.86
1	6.37	3.20	6.83
2	3.14	1.03	6.92
4	0.00	0.00	6.97
6	0.00	0.00	6.94
8	0.00	0.00	6.98
24	0.00	0.00	6.98

Although both concentrations showed complete eradication of *S. mutans* at 4 hours contact time, *S. mutans* showed greater reduction in the mean Log CFU/mL when exposed to 3% LMW-Ch compared to 1% LMW-Ch in the first 4 hours. The mean Log CFU/mL is shown in Figure 3-8. Complete eradication of *S. mutans* occurred at 4 hours contact time for both concentrations. However, the use of 3% LMW-Ch showed steeper decline in the colony count within the first 2 hours compare to 1% LMW-Ch. The colony forming units of *S. mutans* when exposed to 1% and 3% LMW-Ch are shown in Figure 3-9.

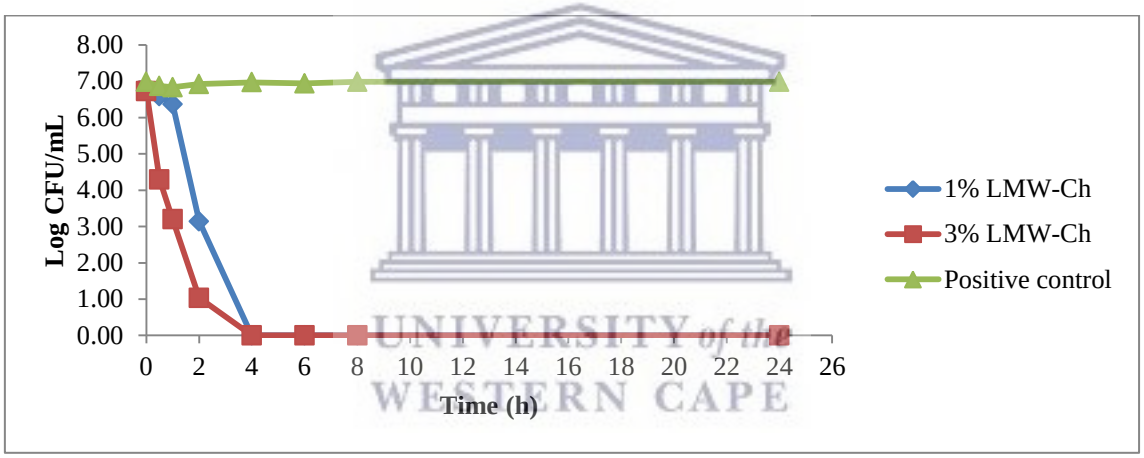

Figure 3-8: The mean Log CFU/mL of *S. mutans* following its exposure to 1% and 3% LMW-Ch over time.

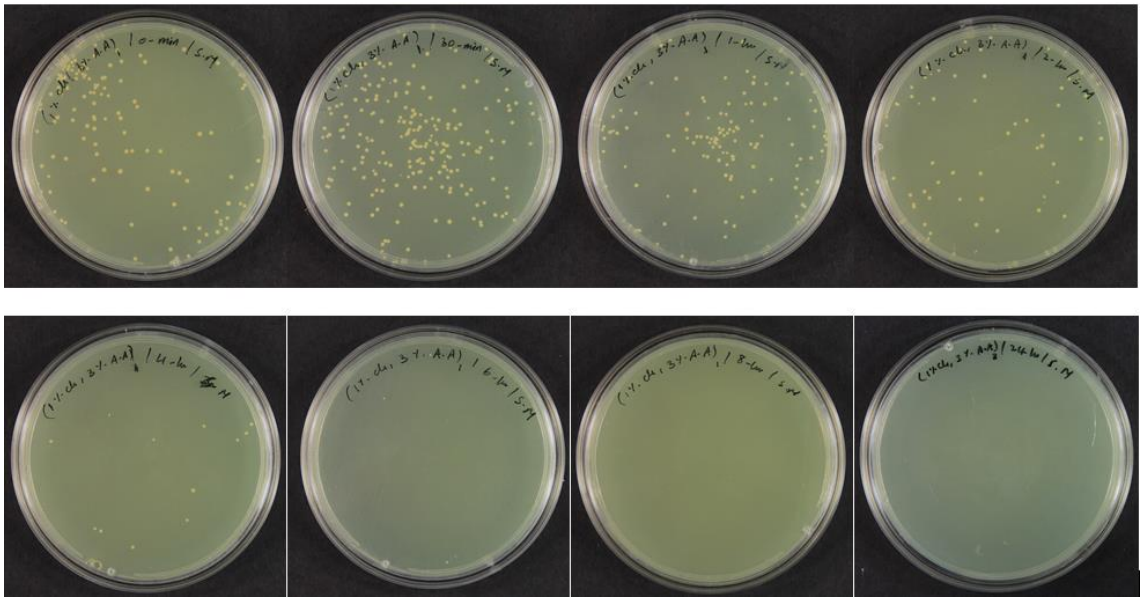

(A)

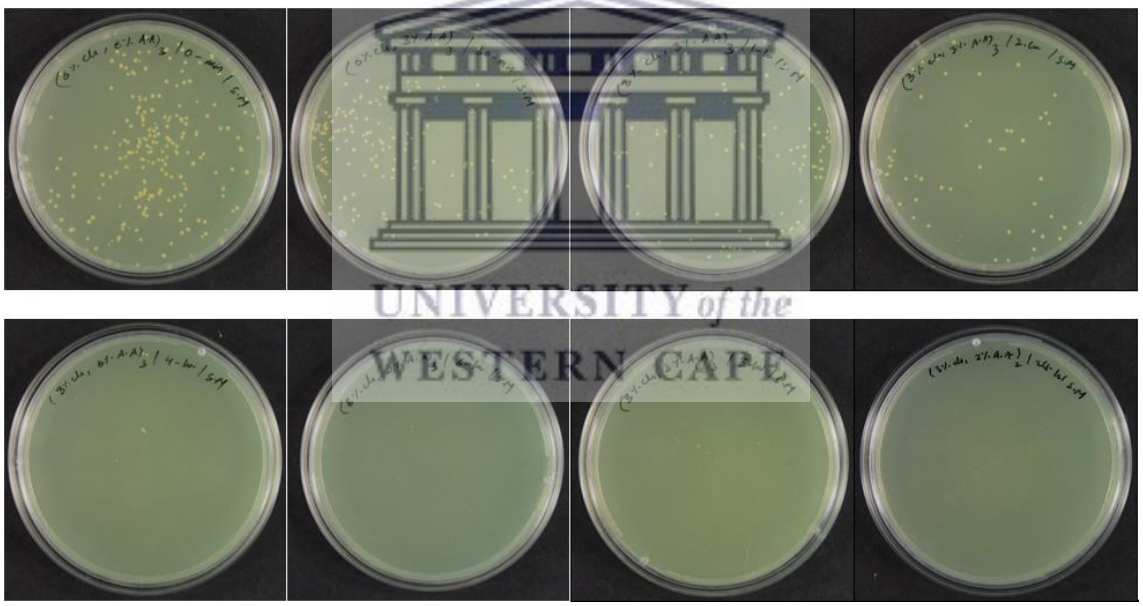

(B)

Figure 3-9: The colony forming units of *S. mutans* when exposed to (A) 1% LMW-Ch, (B) 3% LMW-Ch over time.

b. Effect of 1% and 3% LMW-Ch against planktonic cells of *E. faecalis*

The Kaplan-Meir survival function curve showed that *E. faecalis* was observed at zero minute, 30 minutes, 1, 2 and 4 hours when exposed to 1% LMW-Ch. It was also exposed to 3% LMW-Ch, observed at zero minute, 30 minutes, 1 and 2 hours and showed complete eradication after 2 hours (Figure 3-10).

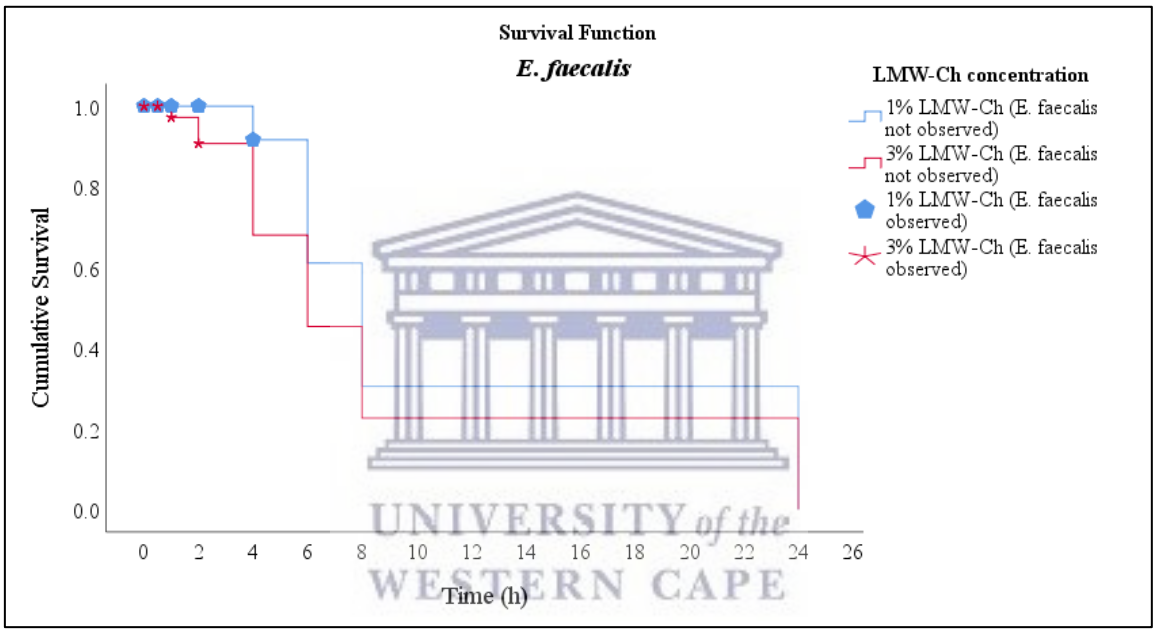

Figure 3-10: Survival function curve of *E. faecalis* showing the time at which it was observed when it was exposed to LMW-Ch at 1% and 3%.

The mean number of the Log CFU/mL was less in the 3% LMW-Ch group compared to the 1% LMW-Ch group at various time intervals. The mean number of the CFU/mL of each concentration at different times compared to the positive control group is shown in Table 3-3.

Table 3-3: The mean number of the CFU/mL of *E. faecalis* when exposed to 1% and 3% LMW-Ch compared to the positive control group.

Time (h)	1% LMW-Ch	3% LMW-Ch	(+ve) Control
0	6.98	6.98	6.98
0.5	6.98	6.86	6.98
1	6.98	5.48	6.98
2	6.91	4.11	6.98
4	4.27	0.00	6.98
6	0.00	0.00	6.98
8	0.00	0.00	6.98
24	0.00	0.00	6.98

There was a difference in the survival time of *E. faecalis* when exposed to different concentrations of LMW-Ch. The use of 3% LMW-Ch showed greater bactericidal effect against *E. faecalis* where it was completely eradicated at 4 hours contact time compared to 6 hours contact time for the 1% LMW-Ch. The mean Log CFU/mL is shown in Figure 3-11. There was complete eradication of *E. faecalis* at 6 hours contact time when it was exposed to 1% LMW-Ch compared to 4 hours when exposed to 3% LMW-Ch. The colony forming units of *E. faecalis* when exposed to 1% and 3% LMW-Ch are shown in Figure 3-12.

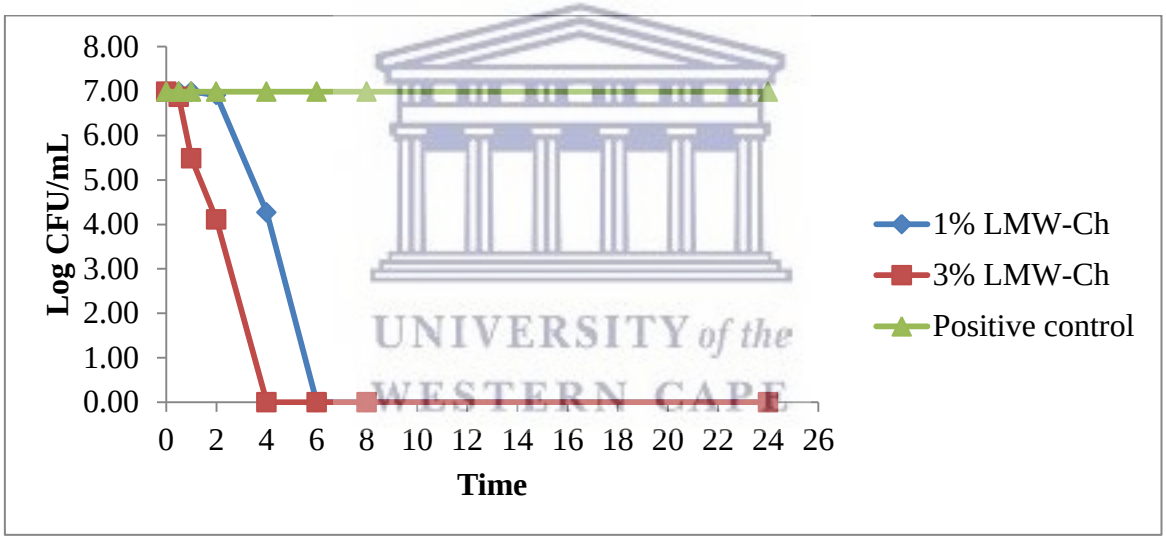

Figure 3-11: The mean Log CFU/mL of *E. faecalis* following its exposure to 1% and 3% LMW-Ch over time.

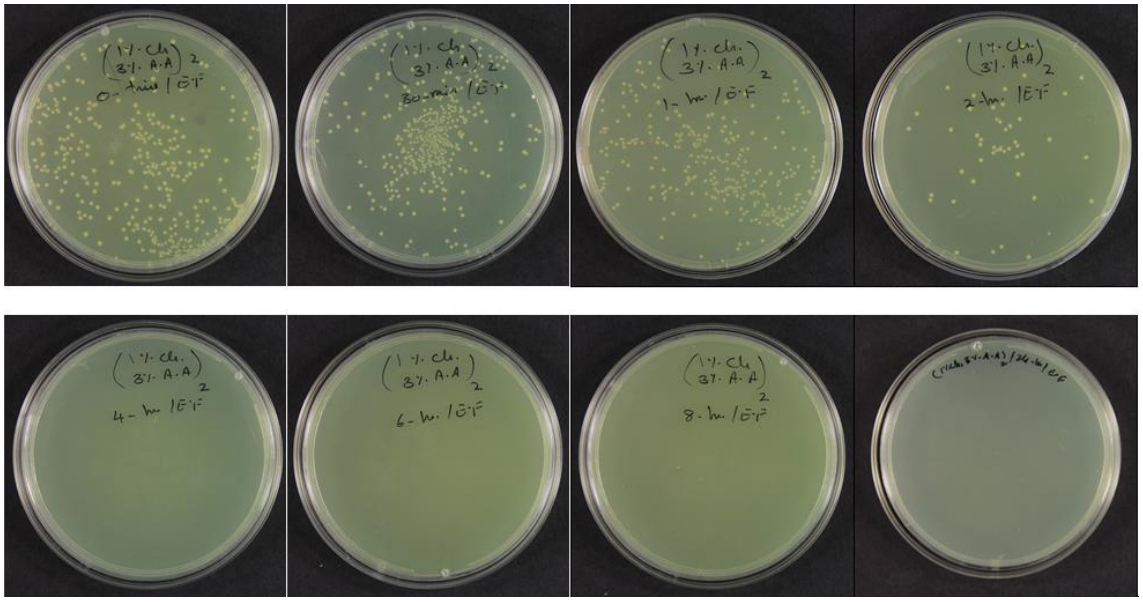

(A)

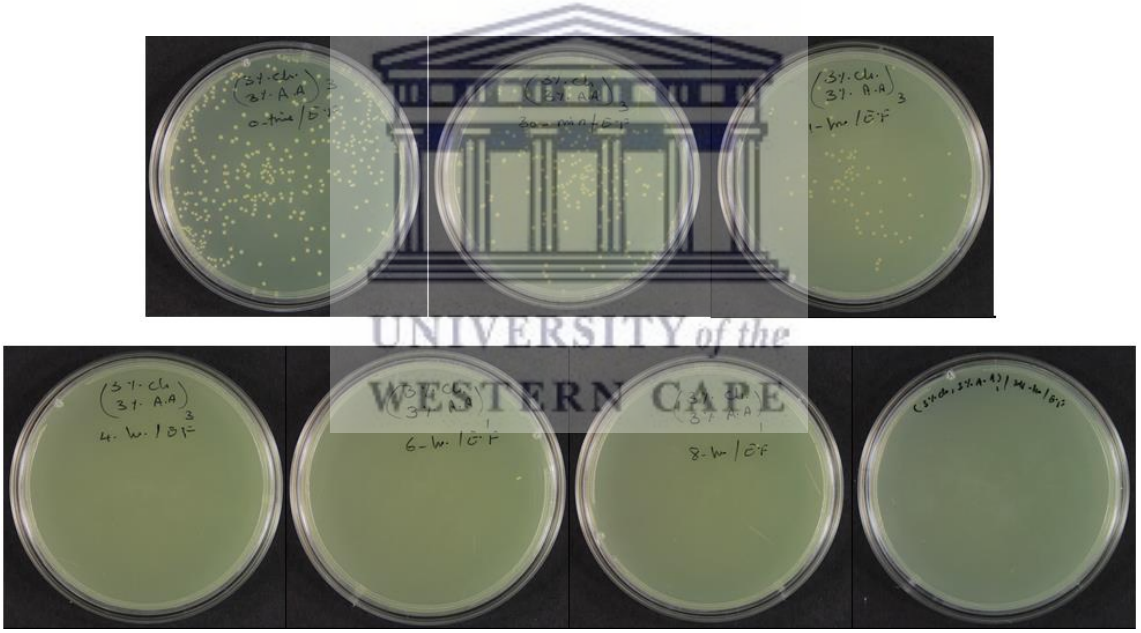

(B)

Figure 3-12: The colony forming units of E. faecalis when exposed to (A) 1% LMW-Ch, (B) 3% LMW-Ch over time.

c. Effect of LMW-Ch against planktonic cells of *C. albicans*

The Kaplan-Meir survival function curve showed that *C. albicans* was observed at all times when exposed to 1% LMW-Ch. However, in the 3% LMW-Ch it was not observed at 4 hours contact time and re-observed again at 6 hours and continued to be observed up to 24 hours (Figure 3-13).

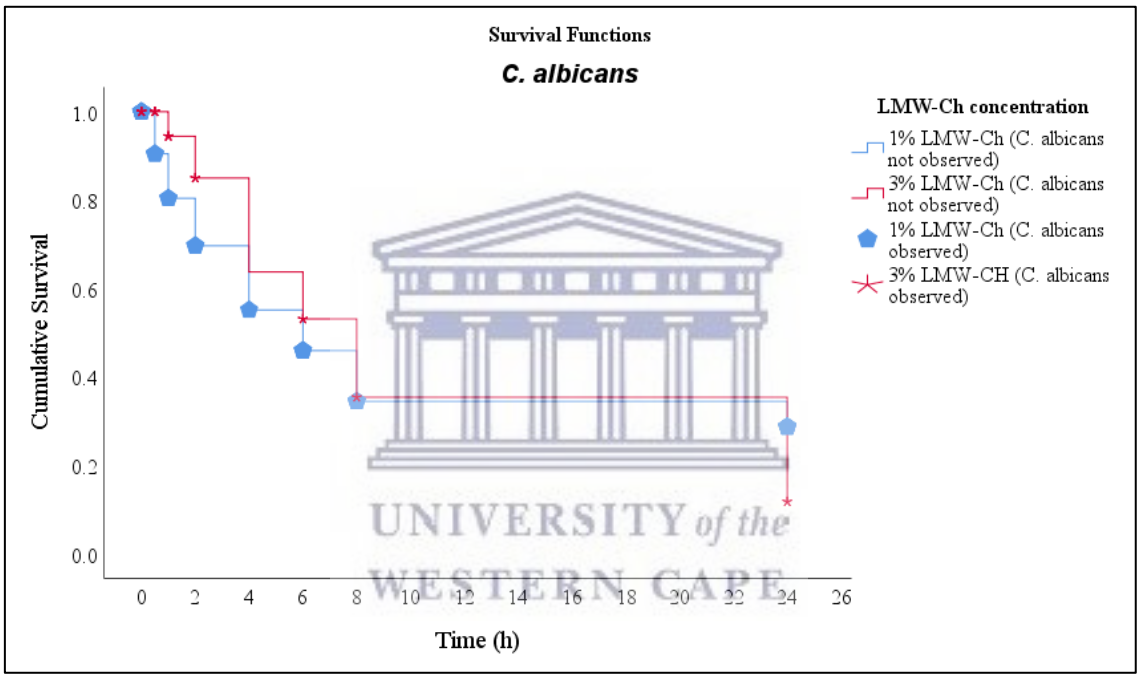

Figure 3-13: Survival function curve of *C. albicans* showing the time at which it was observed when it was exposed to LMW-Ch at 1% and 3%.

The mean number of the Log CFU/mL of *C. albicans* was different at different times and as the concentration of LMW-Ch changed. The mean number of the Log CFU/mL was less in the 1% LMW-Ch group compared to the 1% LMW-Ch group at zero minute, 30 minute, 1 and 2 hours. At 4 hours contact time the mean number of the Log CFU/mL was 0.87. However, this number was zero at the 3% LMW-Ch group at the same time. At 6 hours contact time the mean number of the Log CFU/mL increased again to 2.62 and continued to increase although it was less compared to the 1% LMW-Ch group. The mean number of the CFU/mL of each concentration at different time compared to the positive control group is shown in Table 3-4.

Table 3-4: The mean number of the CFU/mL of *C. albicans* when exposed to 1% and 3% LMW-Ch compared to the positive control group.

TIME	1% LMW-Ch	3% LMW-Ch	(+ve) Control
0	4.98	5.10	5.41
0.5	1.70	5.09	5.28
1	1.50	3.16	5.11
2	1.60	2.33	4.51
4	0.87	0.00	5.51
6	2.77	2.62	6.65
8	3.07	1.62	6.98
24	5.32	2.22	6.98

The 3% LMW-Ch showed better antifungal effect against *C. albicans* compared to 1% LMW-Ch. The mean Log CFU/mL is shown in Figure 3-14. The figure shows a reduction in the mean Log CFU/mL in both groups with greater effect when 3% LMW-Ch was used. The colony forming units of *C. albicans* when exposed to 1% and 3% LMW-Ch are shown in Figure 3-15.

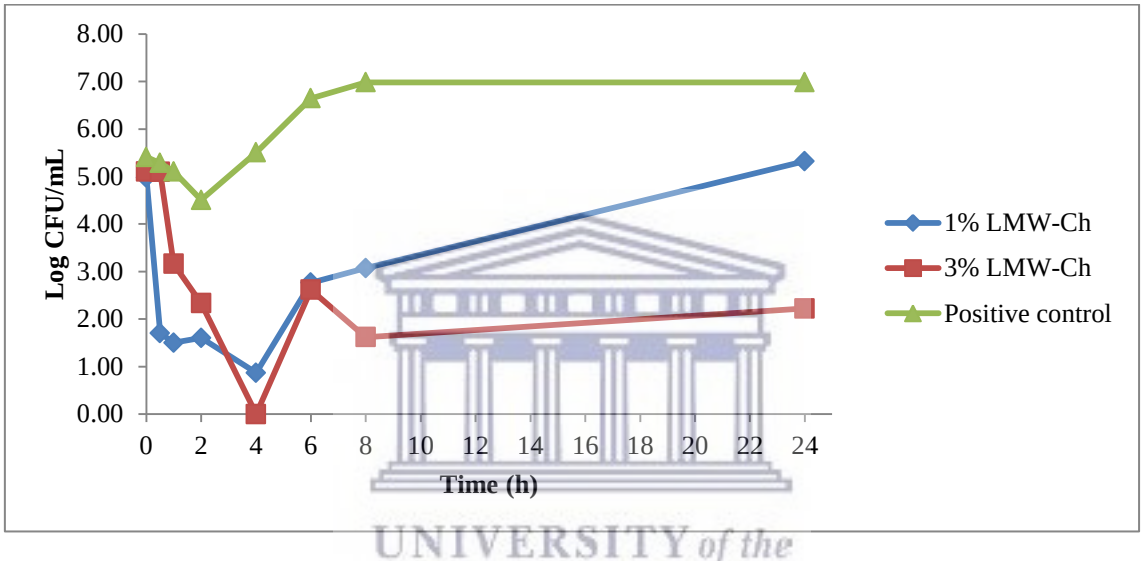

Figure 3-14: The of the mean Log CFU/mL of *C. albicans* following its exposure to 1% and 3% LMW-Ch over time.

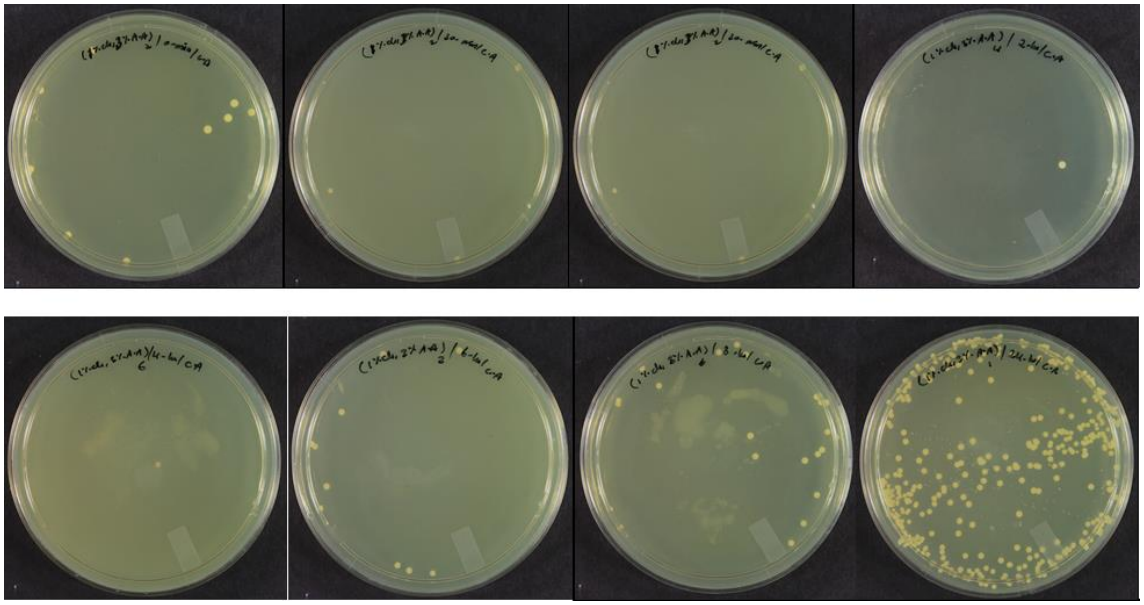

(A)

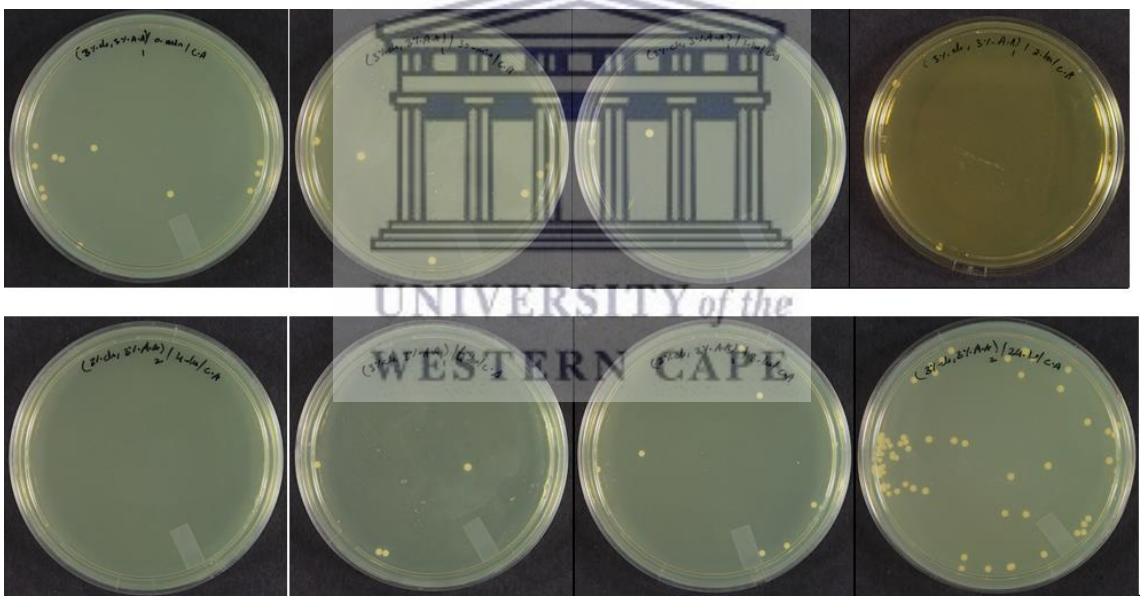

(B)

Figure 3-15: The colony forming units of *C. albicans* when exposed to (A) 1% LMW-Ch, (B) 3% LMW-Ch over time.

Comparison between the effect of 1% and 3% LMW-Ch among each microbial species was tested using the Breslow (Generalized Wilcoxon) test. The results of the three tests showed no statistical difference between the use of 1% and 3% LMW-Ch as antimicrobial agent against *S. mutans, E. faecalis* and *C. albicans* (p. 0.05) (Table 3-5).

Table 3-5: Pairwise comparison between the antimicrobial effect of different LMW-Ch concentrations against *S. mutans, E. faecalis* and *C. albicans*.

Pairwise Comparisons						
	Microorganism	LMW-Ch concentration	1%		3%	
			Chi-Square	Sig.	Chi-Square	Sig.
Breslow (Generalized Wilcoxon)	*S. mutans*	1%			2.83	0.09
		3%	2.83	0.09		
	E. faecalis	1%			3.49	0.06
		3%	3.49	0.06		
	C. albicans	1%			1.72	0.19
		3%	1.72	0.19		

3.8.2 Effect of acetic acid against endodontic pathogens in a planktonic state

The exposure of *S. mutans, E. faecalis* and *C. albicans* to 3% acetic acid did not eradicate them as the mean number of the Log CFU/mL was not reduced to zero in all times excluding any antimicrobial effect of using 3% acetic acid as a solvent for LMW-Ch.

a. Effect of acetic acid against planktonic cells of *S. mutans*

The mean number of the Log CFU/mL in the positive control group and when *S. mutans* was exposed to 3% acetic acid (negative control group) at zero minute was 6.97 and 6.93 respectively. The mean number of the Log CFU/mL continued to be similar until 4 hours contact time. At 4 hours contact time the mean number of the Log CFU/mL started decreasing from 6.97 to 6.65 when it was exposed to 3% acetic acid. The mean number of the Log CFU/mL continued to reduce at 6 hours (6.57) and 8 hours (6.52) in the negative control group compared to 6.94 CFU/mL at 6 and 6.98 CFU/mL at 8 hours in the positive control group. The mean number of the Log CFU/mL of the negative control group became similar to the positive control group at 24 hours contact time (6.98) (Figure 3-16). The colony forming units of *S. mutans* in the positive and negative control groups are shown in Figure 3-17.

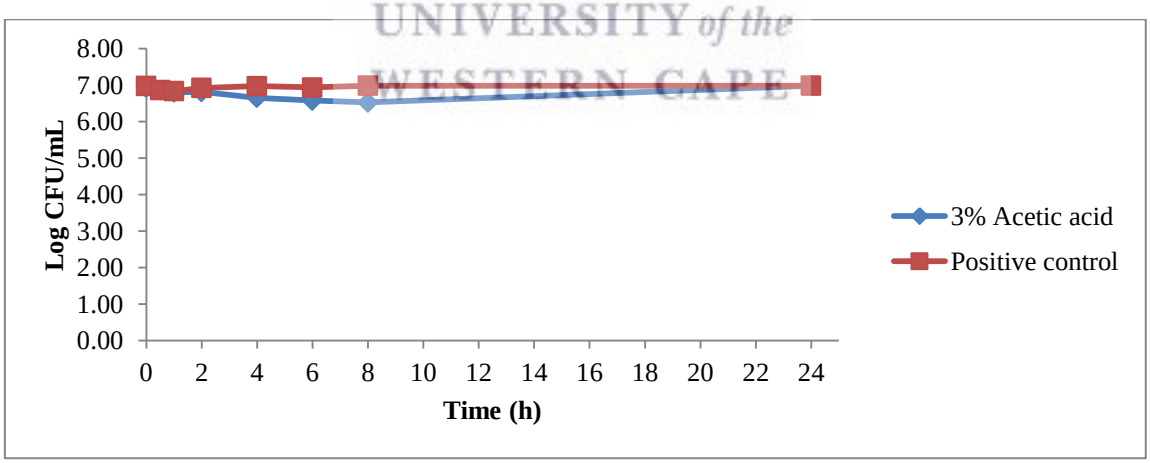

Figure 3-16: The mean Log CFU/mL of *S. mutans* at normal growth rate (positive control) and following its exposure to 3% acetic acid over time.

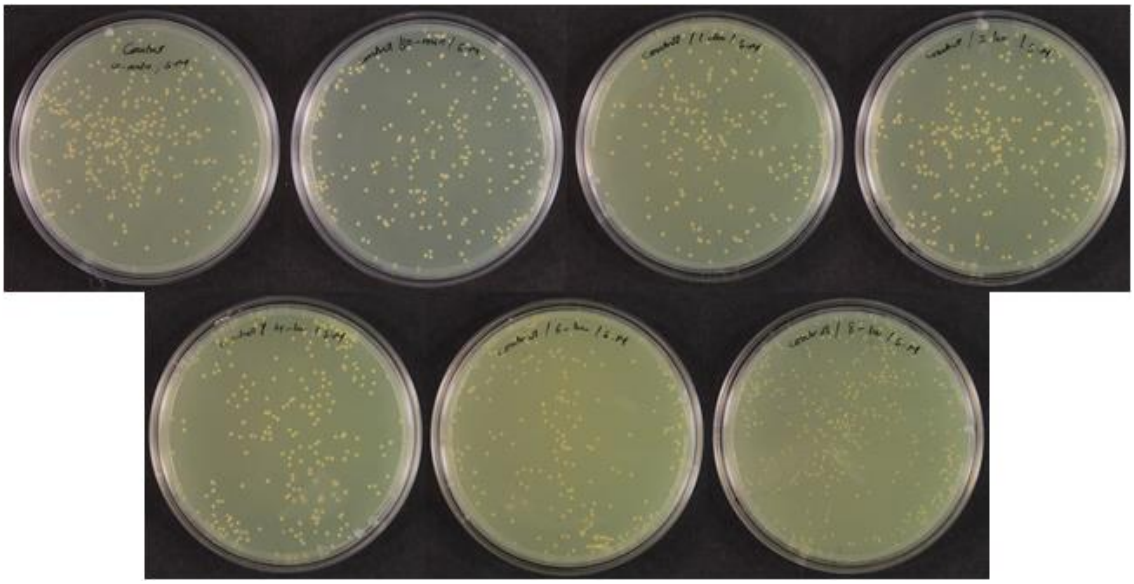

(A)

(B)

Figure 3-17: The colony forming units of *S. mutan*s over time (A) positive control group, (B) negative control group.

b. Effect of acetic acid against planktonic cells of *E. faecalis*

The use of 3% acetic acid did not affect the number of the Log CFU/mL of *E. faecalis*. The number of the Log CFU/mL of *E. faecalis* was similar (6.98) in positive and negative control groups at all times (Figure 3-18). The colony forming units of *E. faecalis* in the positive and negative control groups are shown in Figure 3-19.

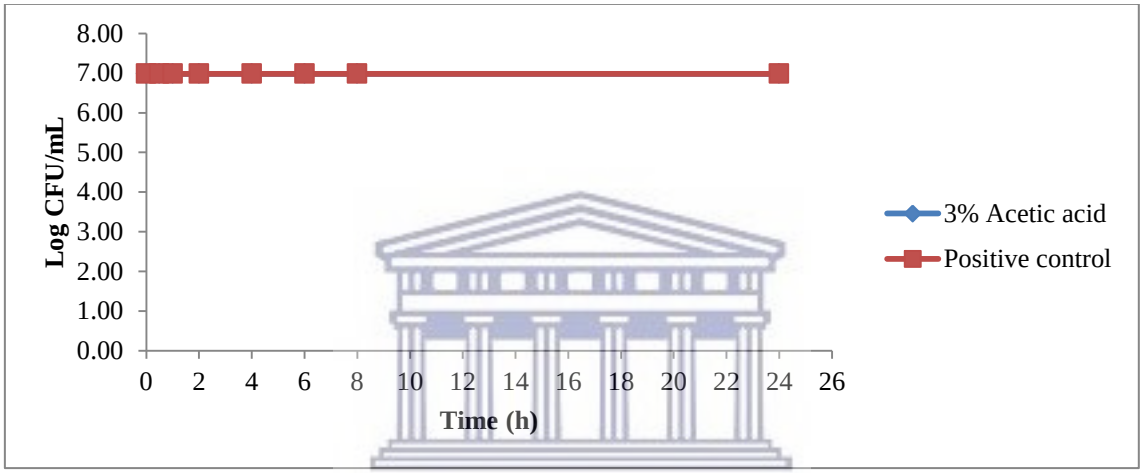

Figure 3-18: The mean Log CFU/mL of *E. faecalis* at normal growth rate (positive control) and following its exposure to 3% acetic acid over time. The number of the Log CFU/mL of the two control groups grow at the same rate hence the two lines in the graph were superimposed.

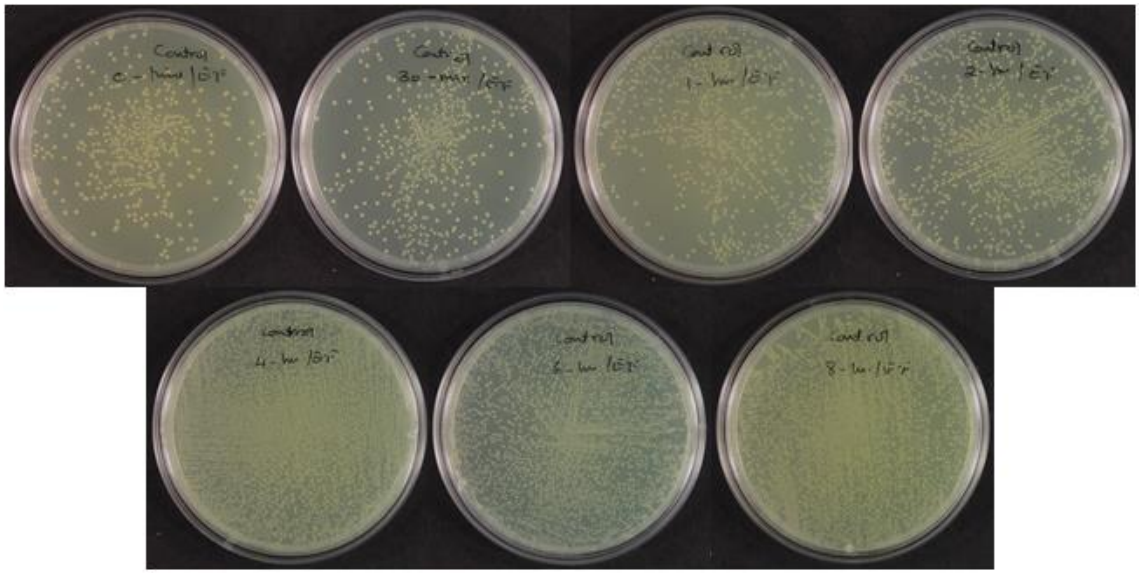

(A)

(B)

Figure 3-19: The colony forming units of *E. faecalis* over time (A) positive control group, (B) negative control group.

c. Effect of acetic acid against planktonic cells of *C. albicans*

The effect of 3% acetic acid was different for *C. albicans*. When *C. albicans* was in a nutrient medium (positive control group), the number of the Log CFU/mL was 5.41 at zero minute which decreased slightly (4.51) at 2 hours and then started to increase gradually until it became too numerous to count within 24 hours. When *C. albicans* was exposed to 3% acetic acid (negative control group) the number of the Log CFU/mL at zero minute was 5.47. This number decreased slightly (3.72) at 4 hours contact time and started to increase gradually until it became almost similar to the number of the Log CFU/mL of the positive control group (6.57) at 6 hours contact time. At 24 hours contact time the number of the Log CFU/mL decreased slightly (6.42). Although there was a reduction in the Log CFU/mL of *C. albicans* when exposed to 3% acetic acid, this reduction did not reduce the number of the Log CFU/mL to zero after 24 hours contact time (Figure 3-20). The colony forming units of *C. albicans* in the positive and negative control groups are shown in Figure 3-21.

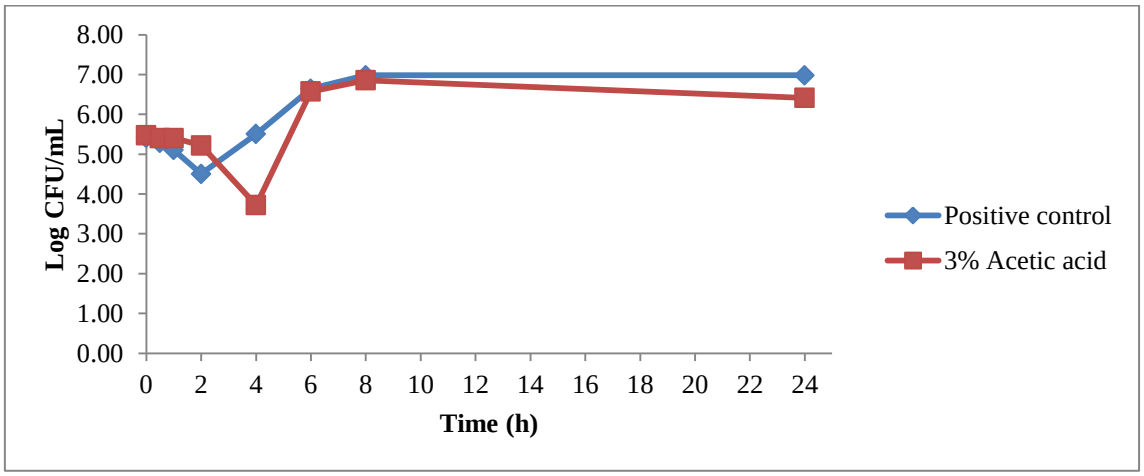

Figure 3-20: The mean Log CFU/mL of *C. albicans* in normal growth rate (+ve control) and following its exposure to 3% acetic acid over time.

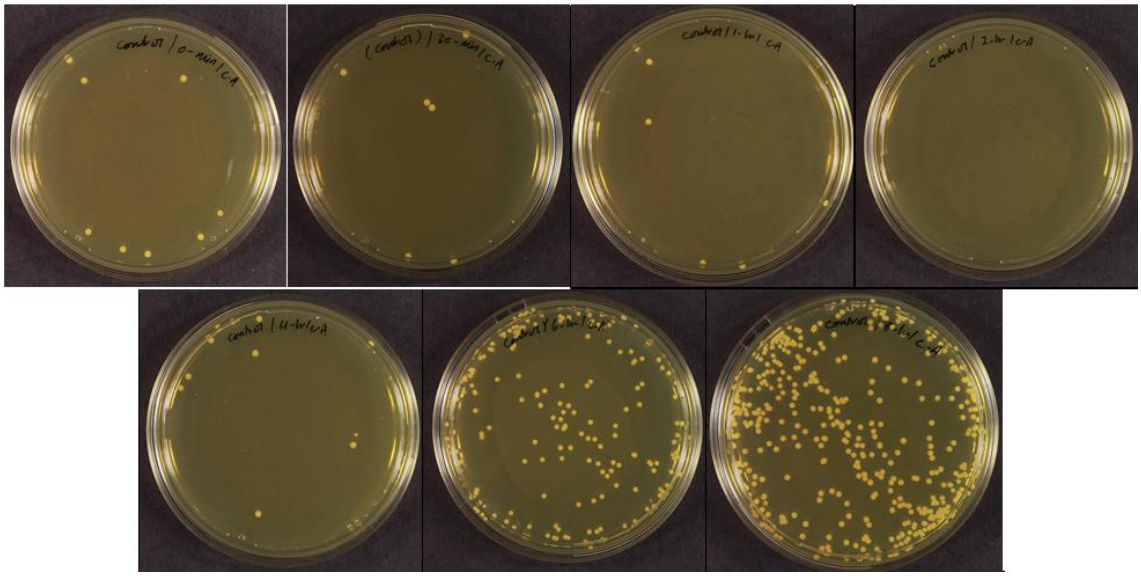

(A)

(B)

Figure 3-21: The colony forming units of *C. albicans* over time (A) positive control group, (B) negative control group.

3.9 Discussion

Chitosan showed antimicrobial activity against various microbial species (Kong *et al.*, 2010). However, only a few studies have evaluated its activity against endodontic pathogens. The purpose of this study was to evaluate whether there is any antimicrobial effect of using LMW-Ch against two endodontic bacteria namely; *S. mutans* and *E. faecalis* and one fungal species namely *C. albicans*. Additionally, this study evaluated the effect of chitosan concentration on its antimicrobial potency. The selection of chitosan was based on its ability to produce an antimicrobial effect against various microbial species in addition to its promising antimicrobial effect in medicine.

S. mutans was selected as it represents one of the main endodontic pathogens isolated from primary endodontic infections, while *E. faecalis* and *C. albicans* were selected as representative endodontic pathogens mainly isolated from secondary infection (Zehnder, 2006) which also showed resistance to the traditional intra-canal medicaments (Valera *et al.*, 2016).

The survival time of the three microbial species when exposed to LMW-Ch was evaluated using the Time-kill Test. This test was used to determine the time required to kill a microorganism when subjected to an antimicrobial agent following carefully controlled conditions (Barry *et al.*, 1999). The advantage of using this test compared to other tests used to evaluate the antimicrobial properties of a material such as the agar diffusion test, is its ability to provide information regarding the type of antimicrobial mechanism, whether it is bactericidal, bacteriostatic, fungicidal or fungistatic (Balouiri *et al.*, 2016). Additionally, it provides information regarding whether the killing time of a material is affected by its concentration (Pfaller *et al.*, 2004). As a result of these

advantages, the Time-kill Test was used to evaluate whether LMW-Ch has a bacteriostatic, bactericidal, fungistatic or fungicidal effect on *E. faecalis*, *S. mutans* and *C. albicans* and to determine the effect of the concentration on its activity.

Furthermore, the difference between the method used in this study compared to most of the studies that evaluated the antimicrobial effect of chitosan is that, the other studies evaluated the minimal inhibitory concentrations (MIC) of chitosan (Costa *et al.*, 2014; Younes *et al.*, 2014) which is defined as the minimal concentration of chitosan that is required to only inhibit the growth of a microorganism regardless of the type of inhibition (bacteriostatic, bactericidal, fungistatic or fungicidal) or the time required to produce the inhibition.

LMW–Ch was dissolved in 3% acetic acid as chitosan is soluble in acidic medium (Dutta *et al.*, 2004). To exclude the effect of using 3% acetic acid on the survival rate of *S. mutans*, *E. faecalis* and *C. albicans* it was used as negative control group and the growth rate (mean number of the Log CFU/mL) of each microbial species was compared to that of the positive control group. The results showed that the use of acetic acid as a solvent, did not affect the growth of the three tested pathogens indicating that any antimicrobial effect of the chitosan hydrogel resulted from the chitosan itself rather than any other component in the hydrogel.

Although the presence of the three tested pathogens in acidic medium (low pH) did not affect their growth rate, this may enhance the antimicrobial activity of chitosan due to the protonation of the amino group of chitosan that occurred at a low pH. The protonation of the amino group will render the chitosan more attractive to any negatively charged compound such as the microbial cell wall (Costa *et al.*, 2014). This

assumption was also supported by other studies (Rabea *et al.*, 2003; No *et al.*, 2002; Fei Liu *et al.*, 2001).

3.9.1 Effect of LMW-Ch against planktonic cells of *S. mutans* and *E. faecalis*

Although, *S. mutans* and *E. faecalis* are both Gram positive bacteria which possess a single cell wall characterized by its thickness and insolubility in different solvents (Cummins and Harris, 1956), they behaved differently when exposed to LMW-Ch. This may be due to the difference in the genetic mapping between the two pathogens (Hardie and Whiley, 1997) which could be reflected in their defence mechanisms against LMW-Ch used in this experiment.

The survival time of *S. mutans* and *E. faecalis* was affected by the concentration of chitosan. This effect could be due to the increased number of the protonated amino group and free radicals that attach to and attack the bacterial cell wall causing lysis and destruction. In this study *S. mutans* and *E. faecalis* showed a lower number of the Log CFU/mL when the concentration of the LMW-Ch increased at the same time. The mean number of the Log CFU/mL of *S. mutans* was 3.14 at 2 hours following its contact with 1% LMW-Ch. This number was less (1.03) when the concentration of LMW-Ch increased to 3% at 2 hours contact time. However, *S. mutans* showed no change in their survival time when the concentration of chitosan was increased from 1% to 3%. Furthermore, the mean number of the Log CFU/mL of *E. faecalis* at 4 hours following its contact with 1% LMW-Ch was 4.27. However, when the concentration of LMW-Ch increased to 3%, *E. faecalis* was completely eradicated at 4 hours contact time.

The effect of concentration on the antibacterial efficacy of LMW-Ch was supported by many authors (Andres *et al.*, 2007; Zheng and Zhu, 2003). Additionally, Liu *et al.*,

(2006) showed that the antibacterial efficacy of chitosan increased as the concentration increased as long as the molecular weight of chitosan was between 55 to 155 KDa.

In this study, chitosan with low molecular weight was used. This was based on the evidence found in the literature showing the ability of LMW-Ch to produce a bactericidal effect against Gram positive and negative bacteria as a result of its ability to bind to the bacterial cell wall, thus disturbing its function (Kumar *et al*., 2005). This was also shown in this study as chitosan with molecular weight of 50 – 190 KDa showed a bactericidal effect against *S. mutans* and *E. faecalis*.

The results of this study were also supported by a study which showed that LMW–Ch produced higher antibacterial activity against Gram positive bacteria such as *Bacillus subtilis* and Gram negative bacteria such as *E. clio* and *Pseudomonas aureofasien* (Tikhonov *et al*., 2006).

Younes *et al*., (2014) reported an antibacterial effect against Gram positive and Gram negative bacterial when chitosan was used at both high and low molecular weight. However, the antibacterial effect of chitosan against Gram positive bacteria such as *E. faecalis* was found to be enhanced by increasing the molecular weight of chitosan. A similar effect was also reported by Zheng and Zhu (2003).

3.9.2 Effect of LMW-Ch against planktonic cells of *C. albicans*

The use of low molecular weight chitosan showed a fungistatic effect against *C. albicans* compared to its effect on bacterial cells such as *S. mutans* and *E. faecalis*. This may be due to the difference in the structural anatomy of both pathogens. The bacterial cell wall is composed mainly of peptidoglycan while the fungal cell wall is composed mainly of chitin, chitosan, glucan and mannan (Russell, 2003). However, it is clear that

there was a decrease in the number of the CFU/mL of *C. albicans* over time when it was exposed to LMW–Ch, suggesting its antifungal effect.

Furthermore, the antifungal effect of LMW-Ch is suggested to be related to its concentration. The use of 3% LMW-Ch produced increased antifungal effect compared to 1%. This is clear at 4 hours contact time where *C. albicans* showed a mean number of the Log CFU/mL of 0.87 when exposed to 1% LMW-Ch compared to zero when exposed to 3% LMW-Ch at the same time. The absence of *C. albicans* at 4 hours following their exposure to 3% LMW-Ch indicates that the concentration was strong enough to cause injury to *C. albicans* which was reflected by the presence of zero colonies at that time. However, the re-observation of *C. albicans* at 6 hours can be explained by the ability of *C. albicans* to adapt to the new stressed environment (presence of chitosan) and start to regrow. The inability of the injured microorganism to grow in a culture medium was described by Bogosian and Bourneuf (2001). This effect is usually seen in *in vitro* studies where there is highly nutrient media which enhances the recoverability of the injured *C. albicans* which may be different clinically.

The failure to obtain a durable fungicidal effect is considered due to either the ability of *C. albicans* to utilize chitosan at their cell wall instead of destroying it or it could be due to the development of a resistance mechanism by *C. albicans* over time. The development of a resistance mechanism may be supported by the reduction of the mean number of the Log CFU/mL when *C. albicans* was exposed to LMW-Ch compared to the control group.

This study showed that the use of chitosan with molecular weight of 50 – 190 KDa had an antifungal activity by arresting the growth but did not completely eradicate

C. albicans for a period of time before it started to regrow again. The effect of chitosan molecular weight on its antifungal activity is controversial. Tayel *et al*., (2010) showed that chitosan produced an antifungal effect in ultralow molecular weight (32 KDa). Costa *et al*., (2014) showed that chitosan with molecular weight of 624 KDa can inhibit the growth of *C. albicans* more effectively compared to LMW–Ch of 107 KDa. Furthermore, Sanel *et al*., (2000) showed that chitosan with a molecular weight of 1000 KDa can inhibit candida growth in a concentration of 10 mg/mL.

Costa *et al* (2014) suggested that this diversity in the effect of different molecular weights of chitosan on their antifungal properties against *C. albicans* was related to chitosan's degree of deacetylation in which a very high degree of deacetylation and very low molecular weight produce maximum antifungal effect.

Kanafani and Perfect (2008) suggested that the susceptibility of *C. albicans* to various antifungal agent may be different with different type strains of *C. albicans* which could be a possible explanation for the growth behaviour of *C. albicans* when exposed to LMW-Ch.

3.10 Conclusion

- LMW-Ch completely eradicated planktonic cells of *S. mutans* and *E. faecalis*.
- The use of 3% LMW-Ch eradicated *S. mutans* and *E. faecalis* more rapidly compared to 1% LMW-Ch.
- The use of 3% LMW-Ch inhibited the growth of *C. albicans* for a period of time before it started to re-grow, showing a possible resistance mechanism.
- 3% LMW-Ch had better antimicrobial effect against endodontic pathogens compared to1% LMW-Ch.

- LMW-Ch can be considered a plausible candidate to function as a precursor for nanoparticles acting as a new antimicrobial agent for a novel chitosan nanoparticle based intra-canal medicament to combat endodontic pathogens.

3.11 References

Agnihotri, S. A., Mallikarjuna, N. N., and Aminabhavi, T. M. (2004). Recent advances on chitosan-based micro-and nanoparticles in drug delivery. *Journal of Controlled Release*, 100(1): 5-28.

Ahmadi, F., Oveisi, Z., Samani, S. M., and Amoozgar, Z. (2015). Chitosan based hydrogels: characteristics and pharmaceutical applications. *Journal of Research in Pharmaceutical Sciences*, 10(1): 1-16.

Andres, Y., Giraud, L., Gerente, C., and Le Cloirec, P. (2007). Antibacterial effects of chitosan powder: mechanisms of action. *Environmental Technology*, 28(12): 1357-1363.

Balouiri, M., Sadiki, M., and Ibnsouda, S. K. (2016). Methods for *in vitro* evaluating antimicrobial activity: A review. *Journal of Pharmaceutical Analysis*, 6(2): 71-79.

Barry, A. L., Craig, W. A., Nadler, H., Reller, L. B., Sanders, C. C., and Swenson, J. M. (1999). Methods for determining bactericidal activity of antimicrobial agents: approved guideline. *National Committe for Clinical Laboratory Standard Document M26-A*, 19(18).

Berger, J., Reist, M., Mayer, J. M., Felt, O., and Gurny, R. (2004). Structure and interactions in chitosan hydrogels formed by complexation or aggregation for biomedical applications. *European Journal of Pharmaceutics and Biopharmaceutics*, 57(1): 35-52.

Bhattarai, N., Gunn, J., and Zhang, M. (2010). Chitosan-based hydrogels for controlled, localized drug delivery. *Advanced Drug Delivery Reviews*, 62(1): 83-99.

Bogosian, G., and Bourneuf, E. V. (2001). A matter of bacterial life and death. *EMBO Reports*, 2(9): 770-774.

Chen, S., Wu, G., and Zeng, H. (2005). Preparation of high antimicrobial activity thiourea chitosan–Ag^{+} complex. *Carbohydrate Polymers*, 60(1): 33-38.

Chung, Y.-C., Su, Y. P., Chen, C.-C., Jia, G., Wang, H. L., Wu, J. G., and Lin, J. G. (2004). Relationship between antibacterial activity of chitosan and surface characteristics of cell wall. *Acta Pharmacologica Sinica*, 25(7): 932-936.

Chung, Y.-C., Wang, H.-L., Chen, Y.-M., and Li, S.-L. (2003). Effect of abiotic factors on the antibacterial activity of chitosan against waterborne pathogens. *Bioresource Technology*, 88(3): 179-184.

Costa, E., Silva, S., Tavaria, F., and Pintado, M. (2014). Antimicrobial and antibiofilm activity of chitosan on the oral pathogen *Candida albicans*. *Pathogens*, 3(4): 908-919.

Coviello, T., Matricardi, P., Marianecci, C., and Alhaique, F. (2007). Polysaccharide hydrogels for modified release formulations. *Journal of Controlled Release*, 119(1): 5-24.

Cummins, C., and Harris, H. (1956). The chemical composition of the cell wall in some gram-positive bacteria and its possible value as a taxonomic character. *Microbiology*, 14(3): 583-600.

Dutta, P. K., Dutta, J., and Tripathi, V. (2004). Chitin and chitosan: Chemistry, properties and applications. *Journal of Scientific and Industrial Research*, 63(1): 20-31.

Fan, W., Yan, W., Xu, Z., and Ni, H. (2012). Formation mechanism of monodisperse, low molecular weight chitosan nanoparticles by ionic gelation technique. *Colloids and Surfaces B: Biointerfaces*, 90: 21-27.

Fei Liu, X., Lin Guan, Y., Zhi Yang, D., Li, Z., and De Yao, K. (2001). Antibacterial action of chitosan and carboxymethylated chitosan. *Journal of Applied Polymer Science*, 79(7): 1324-1335.

Felt, O., Furrer, P., Mayer, J. M., Plazonnet, B., Buri, P., and Gurny, R. (1999). Topical use of chitosan in ophthalmology: tolerance assessment and evaluation of precorneal retention. *International Journal of Pharmaceutics*, 180(2): 185-193.

Goel, M. K., Khanna, P., and Kishore, J. (2010). Understanding survival analysis: Kaplan-Meier estimate. *International Journal of Ayurveda Research*, 1(4): 274 - 278.

Goy, R. C., Britto, D. d., and Assis, O. B. (2009). A review of the antimicrobial activity of chitosan. *Polímeros*, 19(3): 241-247.

Hardie, J., and Whiley, R. (1997). Classification and overview of the genera *Streptococcus* and *Enterococcus*. *Journal of Applied Microbiology*, 83(S1): 1-11.

Helander, I., Nurmiaho-Lassila, E.-L., Ahvenainen, R., Rhoades, J., and Roller, S. (2001). Chitosan disrupts the barrier properties of the outer membrane of Gram-negative bacteria. *International Journal of Food Microbiology*, 71(2): 235-244.

Je, J.-Y., and Kim, S.-K. (2006). Chitosan derivatives killed bacteria by disrupting the outer and inner membrane. *Journal of Agricultural and Food Chemistry*, 54(18): 6629-6633.

Kanafani, Z. A., and Perfect, J. R. (2008). Resistance to antifungal agents: mechanisms and clinical impact. *Clinical Infectious Diseases*, 46(1): 120-128.

Kim, K. H., Kim, J., and Jo, W. H. (2005). Preparation of hydrogel nanoparticles by atom transfer radical polymerization of N-isopropylacrylamide in aqueous media using PEG macro-initiator. *Polymer*, 46(9): 2836-2840.

Kızılel, S., Sawardecker, E., Teymour, F., and Pérez-Luna, V. H. (2006). Sequential formation of covalently bonded hydrogel multilayers through surface initiated photopolymerization. *Biomaterials*, 27(8): 1209-1215.

Kong, M., Chen, X. G., Liu, C. S., Liu, C. G., Meng, X. H., and Yu, L. J. (2008). Antibacterial mechanism of chitosan microspheres in a solid dispersing system against *E. coli*. *Colloids and Surfaces B: Biointerfaces*, 65(2): 197-202.

Kong, M., Chen, X. G., Xing, K., and Park, H. J. (2010). Antimicrobial properties of chitosan and mode of action: a state of the art review. *International Journal of Food Microbiology*, 144(1): 51-63.

Kumar, A. B. V., Varadaraj, M. C., Gowda, L. R., and Tharanathan, R. N. (2005). Characterization of chito-oligosaccharides prepared by chitosanolysis with the aid of papain and Pronase, and their bactericidal action against *Bacillus cereus* and *Escherichia coli*. *Biochemical Journal*, 391(2): 167-175.

Kumar, M. N. R. (2000). A review of chitin and chitosan applications. *Reactive and Functional Polymers*, 46(1): 1-27.

Kurita, K. (1998). Chemistry and application of chitin and chitosan. *Polymer Degradation and Stability*, 59(1–3): 117-120.

Liu, N., Chen, X.-G., Park, H.-J., Liu, C.-G., Liu, C.-S., Meng, X.-H., and Yu, L.-J. (2006). Effect of MW and concentration of chitosan on antibacterial activity of *Escherichia coli*. *Carbohydrate Polymers*, 64(1): 60-65.

No, H. K., Park, N. Y., Lee, S. H., and Meyers, S. P. (2002). Antibacterial activity of chitosans and chitosan oligomers with different molecular weights. *International Journal of Food Microbiology*, 74(1): 65-72.

Palmeira-de-Oliveira, A., Ribeiro, M., Palmeira-de-Oliveira, R., Gaspar, C., Costa-de-Oliveira, S., Correia, I., Pina Vaz, C., Martinez-de-Oliveira, J., Queiroz, J., and Rodrigues, A. (2010). Anti-Candida activity of a chitosan hydrogel: mechanism of action and cytotoxicity profile. *Gynecologic and Obstetric Investigation*, 70(4): 322-327.

Park, B. K., and Kim, M.-M. (2010). Applications of chitin and its derivatives in biological medicine. *International Journal of Molecular Sciences*, 11(12): 5152-5164.

Peppas, N. A., Bures, P., Leobandung, W., and Ichikawa, H. (2000). Hydrogels in pharmaceutical formulations. *European Journal of Pharmaceutics and Biopharmaceutics*, 50(1): 27-46.

Pfaller, M., Sheehan, D., and Rex, J. (2004). Determination of fungicidal activities against yeasts and molds: lessons learned from bactericidal testing and the need for standardization. *Clinical Microbiology Reviews*, 17(2): 268-280.

Prashanth, K. V. H., and Tharanathan, R. N. (2007). Chitin/chitosan: modifications and their unlimited application potential—an overview. *Trends in Food Science & Technology*, 18(3): 117-131.

Qi, L., Xu, Z., Jiang, X., Hu, C., and Zou, X. (2004). Preparation and antibacterial activity of chitosan nanoparticles. *Carbohydrate Research*, 339(16): 2693-2700.

Qin, C., Li, H., Xiao, Q., Liu, Y., Zhu, J., and Du, Y. (2006). Water-solubility of chitosan and its antimicrobial activity. *Carbohydrate Polymers*, 63(3): 367-374.

Raafat, D., Von Bargen, K., Haas, A., and Sahl, H.-G. (2008). Insights into the mode of action of chitosan as an antibacterial compound. *Applied and Environmental Microbiology*, 74(12): 3764-3773.

Rabea, E. I., Badawy, M. E.-T., Stevens, C. V., Smagghe, G., and Steurbaut, W. (2003). Chitosan as antimicrobial agent: applications and mode of action. *Biomacromolecules*, 4(6): 1457-1465.

Rinaudo, M. (2006). Chitin and chitosan: properties and applications. *Progress in Polymer Science*, 31(7): 603-632.

Russell, A. (2003). Similarities and differences in the responses of microorganisms to biocides. *Journal of Antimicrobial Chemotherapy*, 52(5): 750-763.

Sayyar, S., Murray, E., Thompson, B., Chung, J., Officer, D. L., Gambhir, S., Spinks, G. M., and Wallace, G. G. (2015). Processable conducting graphene/chitosan hydrogels for tissue engineering. *Journal of Materials Chemistry B*, 3(3): 481-490.

Şenel, S., İkinci, G., Kaş, S., Yousefi-Rad, A., Sargon, M. F., and Hıncal, A. A. (2000). Chitosan films and hydrogels of chlorhexidine gluconate for oral mucosal delivery. *International Journal of Pharmaceutics*, 193(2): 197-203.

Sutton, S. (2011). Accuracy of plate counts. *Journal of Validation Technology*, 17(3): 42-46.

Tayel, A. A., Moussa, S., Wael, F., Knittel, D., Opwis, K., and Schollmeyer, E. (2010). Anticandidal action of fungal chitosan against *Candida albicans*. *International Journal of Biological Macromolecules*, 47(4): 454-457.

Tikhonov, V. E., Stepnova, E. A., Babak, V. G., Yamskov, I. A., Palma-Guerrero, J., Jansson, H.-B., Lopez-Llorca, L. V., Salinas, J., Gerasimenko, D. V., and Avdienko, I. D. (2006). Bactericidal and antifungal activities of a low molecular weight chitosan and its N-/2 (3)-(dodec-2-enyl) succinoyl/-derivatives. *Carbohydrate Polymers*, 64(1): 66-72.

Valera, M. C., Oliveira, S., Maekawa, L., Cardoso, F., Chung, A., Silva, S., and Carvalho, C. (2016). Action of chlorhexidine, Zingiber officinale, and calcium hydroxide on *Candida albicans*, *Enterococcus faecalis*, *Escherichia coli*, and endotoxin in the root canals. *The Journal of Contemporary Dental Practice*, 17(2): 114-8.

VandeVord, P. J., Matthew, H. W., DeSilva, S. P., Mayton, L., Wu, B., and Wooley, P. H. (2002). Evaluation of the biocompatibility of a chitosan scaffold in mice. *Journal of Biomedical Materials Research Part A*, 59(3): 585-590.

Wang, X., Du, Y., and Liu, H. (2004). Preparation, characterization and antimicrobial activity of chitosan–Zn complex. *Carbohydrate Polymers*, 56(1): 21-26.

Yoshimura, T., Matsuo, K., and Fujioka, R. (2006). Novel biodegradable superabsorbent hydrogels derived from cotton cellulose and succinic anhydride: Synthesis and characterization. *Journal of Applied Polymer Science*, 99(6): 3251-3256.

Younes, I., Sellimi, S., Rinaudo, M., Jellouli, K., and Nasri, M. (2014). Influence of acetylation degree and molecular weight of homogeneous chitosans on antibacterial and antifungal activities. *International Journal of Food Microbiology*, 185: 57-63.

Zehnder, M. (2006). Root Canal Irrigants. *Journal of Endodontics*, 32(5): 389-398.

Zheng, L.-Y., and Zhu, J.-F. (2003). Study on antimicrobial activity of chitosan with different molecular weights. *Carbohydrate Polymers*, 54(4): 527-530.

Chapter 4
Synthesis and characterization of chitosan nanoparticles

4.1 Review of the literature

The use of materials on nano-scale level compared to their use in larger sizes has recently gained considerable attention due to their improved properties compared to the bulk materials (Feynman, 1960). Various materials can be used as a precursor to nanoparticles. They are mainly categorized as organic (polymeric) or inorganic, based on their origin. Inorganic nanoparticles have been investigated intensively because of their possible antibacterial effect and their ability to endure adverse processing conditions (Hajipour *et al.*, 2012; Dizaj *et al.*, 2014). Organic nanoparticles have also gained significant interest from researchers as a result of their potential biocompatible and antimicrobial properties (Virlan *et al.*, 2016).

Various techniques can be used to synthesize nanoparticles. These techniques are mainly classified as either top-down or bottom-up techniques (Bhardwaj *et al.*, 2014). The bottom-up technique is based on the theory that nanoparticles are synthesized or built-up from atoms that are transformed into clusters and eventually nanoparticles (Ealia and Saravanakumar, 2017). Different methods are available based on the bottom-up approach, such as; sol-gel, spinning, chemical vapour deposition, pyrolysis and

biosynthesis. The top-down approach is based on reducing the size of a bulk material to a nano-scale level. The methods available for the top-down technique are mechanical milling, nanolithography, laser ablation, sputtering and thermal deposition (Ealia and Saravanakumar, 2017).

Chitosan nanoparticles

Chitosan nanoparticles (Ch-Np) can be synthesized using different techniques based on the bottom-up approach. The differences between these techniques are related to the size of the synthesized nanoparticles, chemical and thermal stability and toxicity that may develop from the materials used during the synthesizing process (Agnihotri *et al.*, 2004). Ahmed and Aljaeid (2016) categorized the techniques used to prepare Ch-Np into two main techniques; cross-linking and the drying technique. Each technique involves using different methods that can be used to synthesize Ch-Np.

1. Cross-linking technique:
    a) Chemical cross-linking:
        i. Emulsion cross-linking [(water/oil) emulsion].
        ii. Emulsion droplet coalescence method.
    b) Physical cross-linking:
        i. Ionic gelation.
        ii. Thermal cross-linking.
2. Drying technique:
    a) Spray drying.
    b) Supercritical drying.
    c) Reverse micellar technique.

d) Sieving method.

e) Solvent evaporation.

Chitosan nanoparticles could by synthesized through either the chemical or physical cross-linking method. Ch-Np produced via the chemical cross-linking method utilizes chemical agents to be cross-linked via the amino groups of the chitosan and eventually Ch-Np is formed (Croisier and Jérôme, 2013). The drawback of using this method is the risk of synthesizing toxic and chemically less stable nanoparticles as a result of the effect of the different types of solvents or cross-linkers used (Croisier and Jérôme, 2013).

Synthesis of Ch-Np via the physical cross-linking method is a simple technique based on physical interaction between the cationic nature of chitosan and other anion macromolecule cross-linkers (Zhao *et al.*, 2011). One of the main advantages of using this method is the elimination of possible toxicity that can be generated from using other chemical reagents (Agnihotri *et al.*, 2004).

The use of the drying technique to synthesize Ch-Np is based on elimination of the water or solvent content from chitosan solution in a liquid, semi solid or solid form through evaporation and vacuuming of the vapor (Dizaj *et al.*, 2014).

a. Ionic gelation method

The ionic gelation method was first introduced by Calvo *et al.*, (1997). It is the most commonly used method to synthesize Ch-Np as a result of its simplicity and ability to synthesize non-toxic Ch-Np, as it avoids the use of different reagents used in chemical cross-linking (Fan *et al.*, 2012)

In this method the nanoparticles are produced through physical, non-covalent electrostatic reaction between two differently charged macromolecules (Zhao *et al.*, 2011). Tripolyphosphate (Figure 4-1) polyanion is used to react with the positively charged chitosan solution. The electrostatic reaction between the chitosan and the tripolyphosphate changes the surface charge and structure of the chitosan resulting in the formation of Ch-Np (Qi *et al.*, 2004).

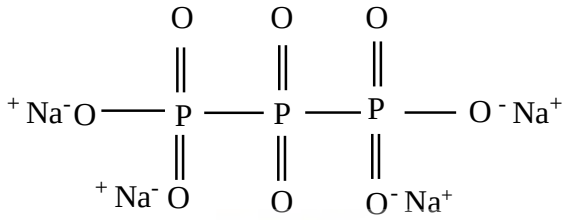

Figure 4-1: Chemical sturucture of sodium tripolyphosphate. Chemical structure adapted from Zhao *et al.*, (2011).

This reaction is pH sensitive and the positive charge density of the chitosan amine group is greater when the chitosan is dissolved in an acidic media (Gan *et al.*, 2005). The high charge density of chitosan will facilitate the electrostatic interaction between the amine group of chitosan and the tripolyphosphate (Gan *et al.*, 2005). At a lower pH the force of attraction between the chitosan and the tripolyphosphate is decreased and results in a loose network and Ch-Np structure (Kawashima *et al.*, 1985). At a higher pH the reaction between the chitosan amino groups and the anionic groups of the tripolyphosphate will be facilitated resulting in gel formation and ionic interaction causing nanoparticle formation (Shweta and Sonia, 2013). However, a very high pH value will cause the nanoparticles to aggregate (Gan *et al.*, 2005).

The size of the particles yielded with this method varies. Different authors reported an average size of 321 nm (Liu and Gao, 2009), 300 to 400 nm (Fernández-Urrusuno *et al.*, 1999), 20 to 200 nm (Xu and Du, 2003), 40 nm (Qi *et al.*, 2004), 20-80 nm (Wu *et al.*, 2005) and 53.99 nm (Du *et al.*, 2009).

Several factors can influence the large diversity in the size of the nanoparticles obtained with the ionic gelation method. According to Calvo *et al.*, (1997), the concentrations of chitosan and tripolyphosphate are important parameters that influence the size of the Ch-Np obtained by ionic gelation. They also reported that when chitosan was used at lower concentrations, the size of the nanoparticle yield was smaller. This result was supported by Fan *et al* (2012) who showed that the use of low concentrations of chitosan and tripolyphosphate can produce smaller size nanoparticles with an average size of 138 nm. Additionally, they reported that the maximum concentration of chitosan should be 1.5 mg/mL and 1.0 mg/mL for the tripolyphosphate. As the concentration of the chitosan increased, the distance between the chitosan molecules decreased resulting in limited intermolecular cross-linking, producing larger particle size (Fan *et al.*, 2012).

Another factor that influences the size of the Ch-Np is the ratio of chitosan to tripolyphosphate. As this ratio increased, the size of the nanoparticles produced increased (Helander *et al.*, 2001; Wang *et al.*, 2004; Fan *et al.*, 2012).

The chemical property of the chitosan used, such as the molecular structure can also play a role in the size and the charge density of the nanoparticles. It was found that the use of low molecular weight chitosan tends to produce small Ch-Np followed by medium and finally high molecular weight. However, among the different molecular

weights used, the size of the nanoparticles increased as the concentration of the chitosan increased (Xu and Du, 2003; Gan *et al.*, 2005; Wu *et al.*, 2005).

The limitations of using the ionic-gelation method to produce Ch-Np are that there is a tendency for the Ch-Np to aggregate upon the addition of another polymer to produce the nanoparticles (Gan *et al.*, 2005; Fan *et al.*, 2012) and the inability to produce water soluble Ch-Np (Qi *et al.*, 2004).

b. Electrospraying

Electrospraying is a simple single method used to produce solid nanoparticles from a liquid by means of an electrical force and hence the name electrohydrodynamic spraying (Jaworek and Sobczyk, 2008).

The use of the electrospraying technique to produce nanomaterials has several advantages that include; its simplicity, reproducibility and minimum experimental setup required; different materials can be used to produce nano-scale particles; its ability to produce nanoparticles with little tendency of agglomeration; and its ability to produce charged particles as a result of the electrical current applied during synthesis (Jaworek, 2007; Nguyen *et al.*, 2016).

According to Bock *et al.*, (2011), the mechanism of nanoparticles formation through electrospraying (Figure 4-2) depends on the force that acts on the bulk liquid while it is passing through a needle at a constant rate and a high electrical potential. The passage of the electrical current through a liquid droplet is able to create an electrical force "Coulomb force" inside the droplet (Bock *et al.*, 2011). This electrical force will act against the cohesive force of the droplet caused by the surface tension of the dissolving liquid. Nanoparticles are formed when the Coulomb force exceeds the cohesive force,

resulting in breaking the droplets into small particles on a nano-scale level, while the solvent evaporates from the droplet (Jadhav *et al.*, 2013).

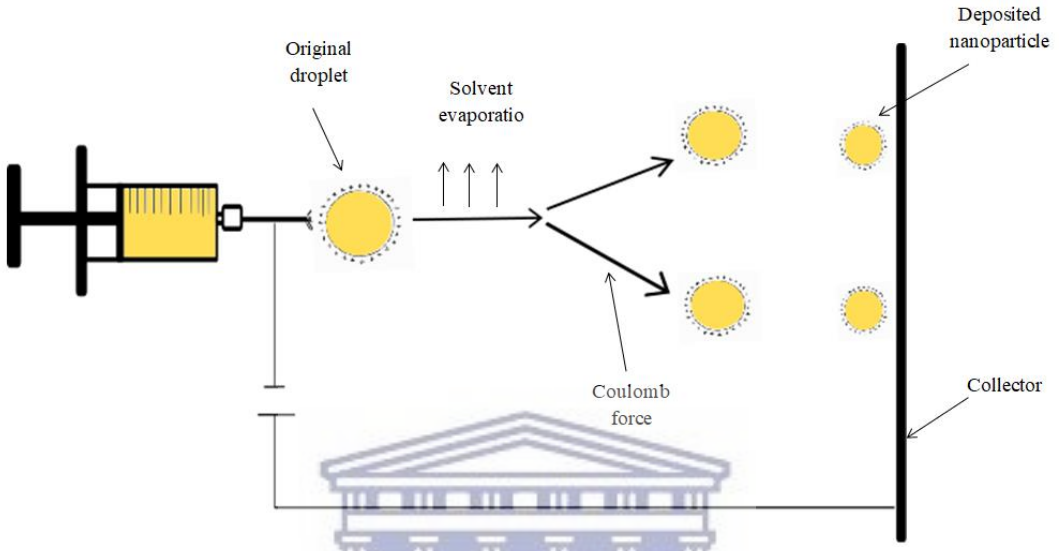

Figure 4-2: Mechanism of electrospraying. Diagram adapted from Nguyen *et al.*,.(2016).

The size and morphology of the electrosprayed nanoparticles is determined by the ability of the polymer chain to elongate, the ability of the solvent to evaporate and the degree of polymer diffusion (Guarino *et al.*, 2015).

One of the most important parameters that influence the electrospraying process is the type of solvent used. In addition to its ability to dissolve the electrosprayed material, the type of solvent will determine the viscosity, surface tension, vapour pressure and conductivity of the electrosprayed solution and thus determine the spraying manner (Jaworek, 2007). Several properties should be considere during selection of a solvent used for electrospraying, namely; its volatility, conductivity, viscosity and possibility of

interaction with the electrosprayed material (Nguyen *et al.*, 2016). Among these properties, the ability of the solvent to evaporate during electrospraying is the most crucial factor that determines the properties of the electrosprayed particles. The degree of evaporation is important since a solvent with a low evaporation rate will result in wet particles that tend to fuse, causing particles to have an irregular size and shape. On the other hand, solvents with a high vapour rate will result in the drying of the electrosprayed particles before reaching the collector. In such a case the particles produced have a porous morphology (Tapia-Hernández *et al.*, 2015; Nguyen *et al.*, 2016).

The most important parameters for synthesis of nanoparticles of polymers using the electrospraying technique are; the type of polymer, its concentration, molecular weight and ability of the solvent to dissolve the polymer (Wu *et al.*, 2005).

The synthesis of Ch-Np using electrospraying was evaluated by several researchers. The effect of different parameters such as the viscosity and surface tension of the primary chitosan solution was evaluated by Pancholi *et al.*, (2009).. They prepared chitosan solution by dissolving chitosan powder with a molecular weight of 731 g/mol in acetic acid. The produced nanoparticles were influenced by the viscosity and the surface tension of the chitosan solution in which the higher the viscosity, the larger the particle size produced and the lower the surface tension, the smaller the particles produced. They also showed that, in optimal conditions for the viscosity and the surface tension, the size of chitosan was reduced from 2500 nm to 500 nm when electrosprayed.

Other factors, such as the concentration of the chitosan and acetic acid solutions, the needle size and the distance between the needle and the collector, was evaluated by

Arya *et al*., (2009). They showed that Ch-Np with an average size less than 1000 nm was obtained when the concentration of chitosan was 2% and the concentration of acetic acid was 90%. Additionally, the optimal size was obtained when the size of the needle was a 26 gauge and the distance between the needle tip and the collector was 7 cm.

Zhang and Kawakami (2010) synthesized Ch-Np using the electrospraying technique. They used acetic acid to prepare a chitosan solution that was mixed with ethanol. Ethanol was added to control the viscosity, conductivity and surface tension of the solution. The solution was sprayed from a needle with a 0.65 mm diameter at a flow rate of 8.3 µL / minute and a distance of 7 cm between the needle and the collector. The electrospraying was done with an electrical current of 25 KV. Their study showed that addition of ethanol affects the size and homogeneity of the produced nanoparticles. The average size of the nanoparticles was 124 nm. They concluded that the nanoparticles produced by electrospraying depend on the chitosan concentration, the flow rate, the acetic acid concentration and the viscosity, which can be controlled by addition of ethanol.

Research studies that synthesized Ch-Np using the electrospraying technique are limited in number. Most of these studies used acetic acid as a solvent with the addition of surfactant to enable its evaporation to form dry chitosan nanoparticles. Furthermore, the use of acetic acid as a solvent will not convert the Ch-Np into water soluble Ch-Np, which is an important requirement of the intra-canal medicament.

4.2 Rationale of the study

There is a need to synthesize water soluble Ch-Np to facilitate its use in endodontics. Furthermore, the use of highly surface charged Ch-Np is essential to enhance its antimicrobial properties.

4.3 Aim of the study

The aim of this study was to synthesize water soluble Ch-Np from LMW-Ch to act as an antimicrobial agent.

4.4 Objectives

i. To synthesize water soluble Ch-NP from LMW-Ch using the electrospraying method.
ii. To evaluate the hydrodynamic size and zeta potential of the prepared Ch-Np using a zetasizer.
iii. To identify the different functional groups of the synthesized nanoparticles using Fourier-transform infrared spectroscopy (FTIR) and compare them to that of chitosan.
iv. To evaluate the morphology of the synthesized nanoparticles using scanning electron microscopy.

4.5 Methodology

4.5.1 Materials

The following materials were used to synthesize Ch-Np.

i. Chitosan with low molecular weight of 50 – 190 KDa and 75 – 85% degree of deacetylation was purchased from Sigma-Aldrich Inc, South Africa (batch number: 448869).

ii. Trifluoroacetic acid ReagentPlus ® 99% were purchased from Sigma-Aldrich Inc, South Africa (batch number T6508).

4.5.2 Preparation of chitosan solution

20 mL of 90% (v/v) Trifluoroacetic acid (TFA) solution was prepared by mixing 18.2 mL of 99% (TFA) into 1.8 mL deionized water. 6% chitosan solution by mass was prepared by dissolving 1.90 g LMW-Ch in 20 mL of the previously prepared 90% (TFA) using a magnetic stirrer for 4 hours at 50 °C.

4.5.3 Electrospraying

The electrospraying procedure was adapted from Zhang and Kawakami (2010) with minor modifications (trifluoroacetic acid was used as a solvent for chitosan instead of acetic acid, the flow rate and the distance between the needle and the collector).

For electrospraying, a total volume of 20 mL of chitosan solution was dispensed in a 20 mL disposable syringe with a 19 mm gauge needle. The syringe was placed and fixed in a 33 DDS dual drive independent channel syringe pump (Harvard apparatus, USA) (Figure 4-3). A collector (aluminum foil) was placed 12 cm away from the tip of the needle and perpendicular to it. A 25 kV voltage current was generated between the

needle and the collector using a high voltage generator in which the high negative voltage was applied to the aluminum foil and the positive voltage was applied to the needle tip. The chitosan solution was dispersed in droplets at a rate of 0.4 mL/h. The solvent evaporated before reaching the aluminum foil where the nanoparticles collected. The electrospraying technique was carried out at room temperature. The deposited nanoparticles were then characterized.

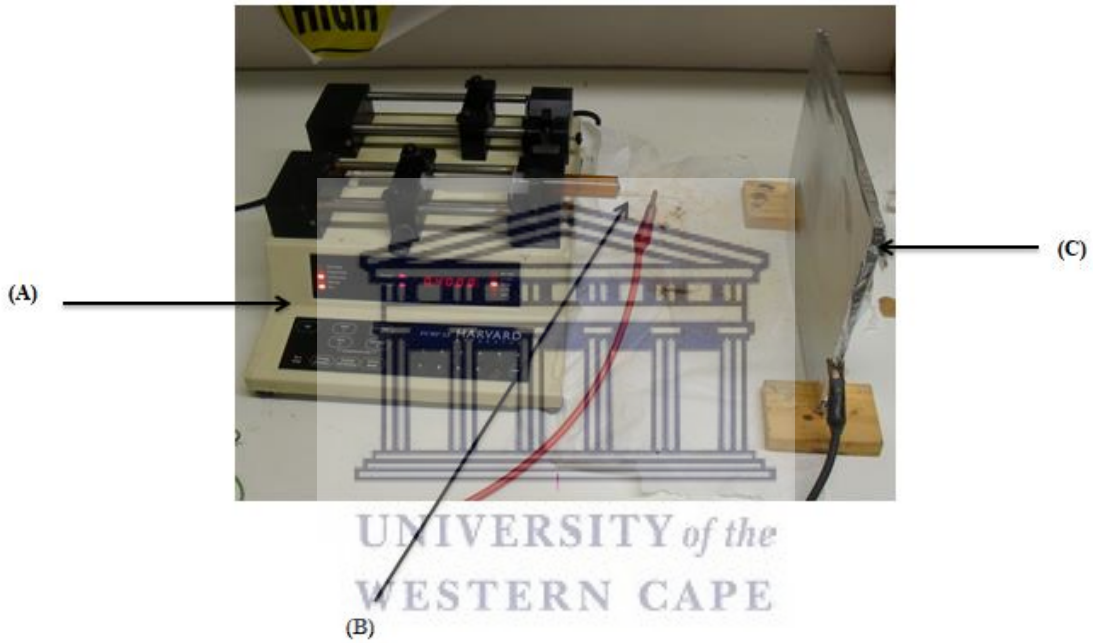

Figure 4-3: Photograph showing experimental setup of electrospraying technique.
(A) 33 DDS dual drive independent channel syringe pump to which (B) 19 mm needle containing the chitosan solution was mounted and connected to a high voltage machine. The Ch-Np was collected in (C) collector (aluminium foil).

4.5.4 Evaluation of the hydrodynamic particle size, particle distribution and surface charge

The hydrodynamic size, particle distribution or the polydispersity index (PDI) and surface charge (zeta potential) of LMW-Ch and the electrosprayed Ch-Np were evaluated using the dynamic light scattering (DLS) method (Zetasizer Nano instrument, Nano S90, Malvern instruments Ltd, England).

The samples were prepared by suspending 0.005 g of LMW-Ch and electrosprayed Ch-Np in 1 mL of deionized water. The samples were vortexed for 2 minutes to assure complete dissolution and distribution of the materials before testing. 1 mL of each sample was placed in a UV- transparent disposable low volume cuvette for the analysis. The scattered light was collected at an angle of 90° at 25°C. The measurements were run in triplicate.

4.5.5 Fourier-transform infrared spectroscopy analysis

Fourier-transform infrared (FTIR) spectroscopy was done using a 400 FTIR/FT-NIR Spectrophotometer equipped with universal ATR sampling accessory by PerkinElmer to evaluate the changes in the chemical structure of LMW-Ch before and after electrospraying, by comparing the functional groups of the synthesized Ch-Np to the functional groups of LMW-Ch and TFA.

0.01 g of LMW-Ch, Ch-Np and a drop of TFA was placed on the sample holder (crystal) of the PerkinElmer Spectrum 400 FTIR/FT-NIR Spectrophotometer. The LMW-Ch and Ch-Np powder were pressed by turning the tuning gauge until the force reading reached 60%. A drop of the TFA was placed on the surface of the highly polished sample holder. All samples were evaluated by collecting the signals in 32

scans of the infrared spectra within a range of 4000 – 650 cm^{-1} in transmittance (%), at room temperature.

4.5.6 Scanning electron analysis

The changes in the morphology and particle size of LMW-Ch following electrospraying was evaluated using high resolution scanning electron microscopy (HR-SEM). High resolution scanning electron microscopy images of LMW-Ch before and after electrospraying were generated using a Zeiss Gemini Auriga Scanning Electron Microanalyser equipped with a CDU – led detector at 3.00 kV with tungsten filament. A small amount of LMW-Ch and the synthesized Ch-Np were placed on stubs coated with carbon and the samples were then coated with a thin gold film to make the surface conductive, prevent charging in the samples' morphology and to enhance the resolution of the samples' images. SEM images were taken at different magnification levels and at various points of the samples with the following parameters:

- Current: 10mA
- Magnification: Various
- Resolution: 100 nm but sometimes varies.
- Working distance: 4.8 mm.
- Voltage: 3.00 kV.
- Signal A: InLens.

4.6 Results

Electrospraying of LMW-Ch resulted in deposition of small particles in the collectors (Figure 4-4) which were further characterized using the various characterization methods.

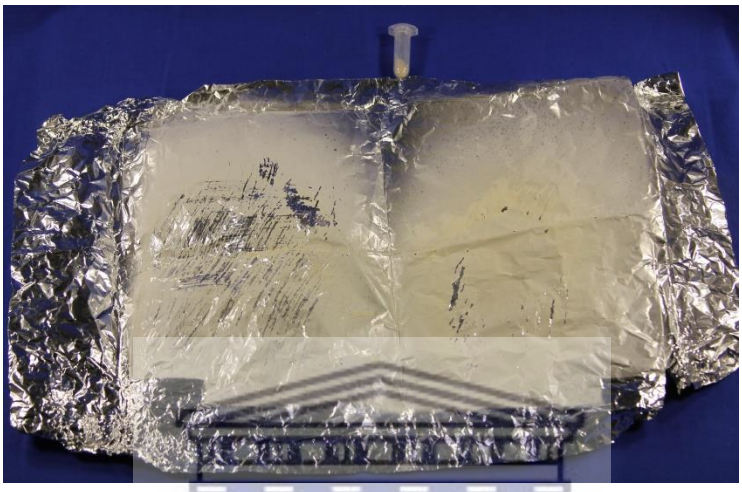

Figure 4-4: Aluminium foil (collector) showing the deposited Ch-Np.

4.6.1 Hydrodynamic particle size, particle distribution and surface charge

a. Hydrodynamic particle size

The use of a Zetasizer Nano instrument, Nano S90, showed an average hydrodynamic particle size distribution of the LMW-Ch of 3435 nm. However, when LMW-Ch was electrosprayed, the size decreased to an average particle size of 419.1 nm forming Ch-Np (Figure 4-5).

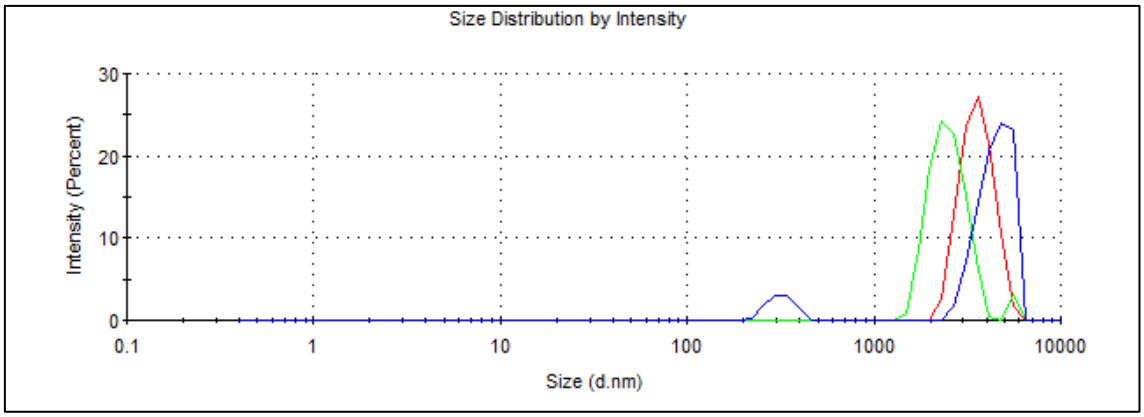

(A)

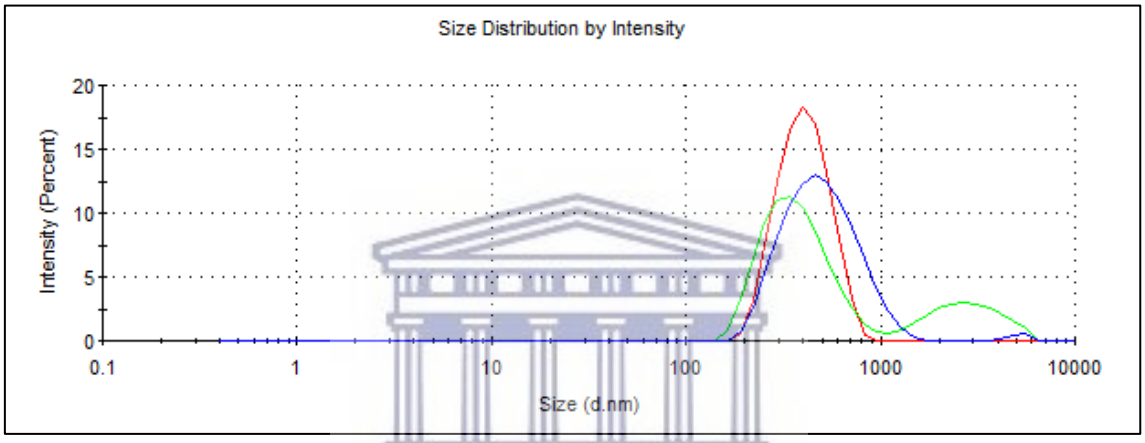

(B)

Figure 4-5: Hydrodynamic particle size distribution of (A) LMW-Ch, (B) Electrosprayed Ch-Np showing reduction in the average hydrodynamic size.

b. Particle distribution (polydispersity index)

LMW-Ch showed an average polydispersity index value of 0.469. The polydispersity index of the electrosprayed Ch-Np was reduced to an average of 0.254.

c. Surface charge (Zeta potential)

The LMW-Ch showed an average zeta potential of 25.6 mV compared to 53.7 mV in electrosprayed Ch-Np when tested using a Zetasizer Nano instrument, Nano S90 (Figure 4-6).

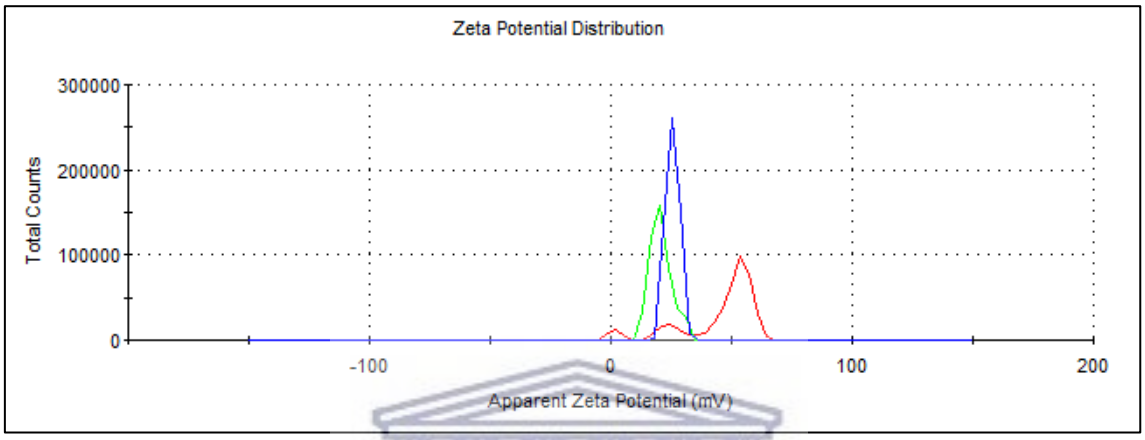

(A)

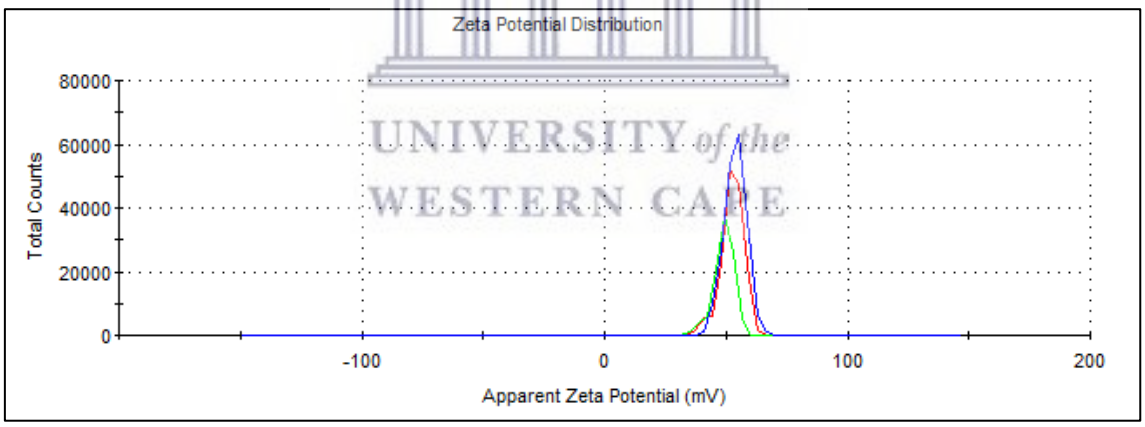

(B)

Figure 4-6: Zeta potential value distribution of (A) LMW-Ch, (B) Ch-Np showing increase in the zeta potential of the Ch-Np.

4.6.2 Fourier transform infrared spectroscopy analysis

a. Low molecular weight chitosan FTIR analysis

The FTIR spectrum of the LMW-Ch surface is shown in Figure 4-7. The spectrum confirms the presence of the main characteristic absorption peak of the Chitosan. The peak at 3370 cm^{-1} was assigned as O-H stretching vibration while the peak at 2869 cm^{-1} was assigned as CH_3 symmetric stretch (methylene group). The peak at 1643 cm^{-1} represents the carbonyl group (C=O) vibration and stretching secondary amide (amide I), while the peak at 1568 cm^{-1} was assigned as N-H bend, CH_3 stretch (amide II). The sharp medium peak at 1370 cm^{-1} was assigned to CH bend, CH_3 symmetric distortion. The CH_2 wagging (C-N vibration from amide) amide III functional group was identified at peak 1311 cm^{-1}. The peak, strong at 1025 cm^{-1}, was assigned to C-O-C symmetric stretch in phase ring (saccharide ring).

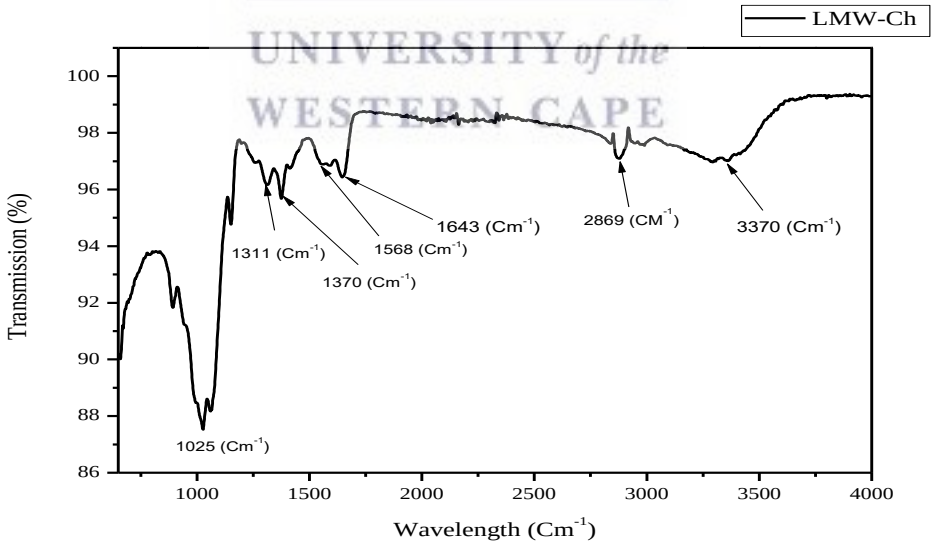

Figure 4-7: FTIR spectrum of LMW-Ch showing the transmission peak of different functional groups.

b. Chitosan nanoparticles FTIR analysis

The FTIR spectrum of the electrosprayed Ch-NP surface is shown in

Figure 4-8. The spectrum confirms the presence of the main characteristic absorption peak of LMW-Ch in the electrosprayed Ch-Np. The peak at 1669 cm^{-1} was assigned to the carbonyl group (C=O) vibration and stretching secondary amide (amide I). The peak at 1529 cm^{-1} was assigned to N-H bend, C-N stretch (amide II), while the peak at 1319 cm^{-1} was assigned to CH_2 bend, CH_3 symmetric distortion (amide III). The peak at 1130 cm^{-1} was assigned to asymmetries in the phase ring stretch mode, while the peak at 1062 cm^{-1} was assigned to C-O-C symmetric stretch in phase (glucoseamine) ring.

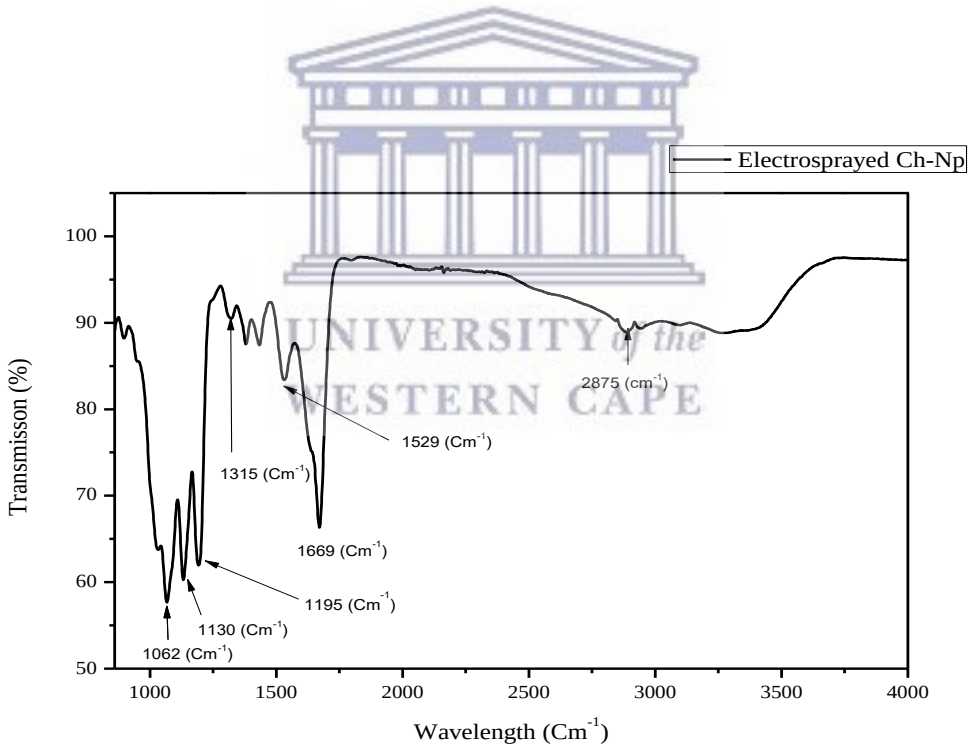

Figure 4-8: FTIR spectrum of the electrosprayed Ch-N showing the transmission peak of different functional groups.

c. Trifluoroacetic acid FTIR analysis

The obtained FTIR spectrum of the TFA surface is shown in

Figure 4-9. The sharp peak at 1770 cm^{-1} was assigned to C=O stretch while the peak at 1451 cm^{-1} was assigned to C-O stretch. The peak at 1331 cm^{-1} was assigned to HOC group. The high sharp peak at 1156 cm^{-1} was assigned to CF_3 group. The peaks at 812 cm^{-1} and 704 cm^{-1} were assigned to O-C=O stretching.

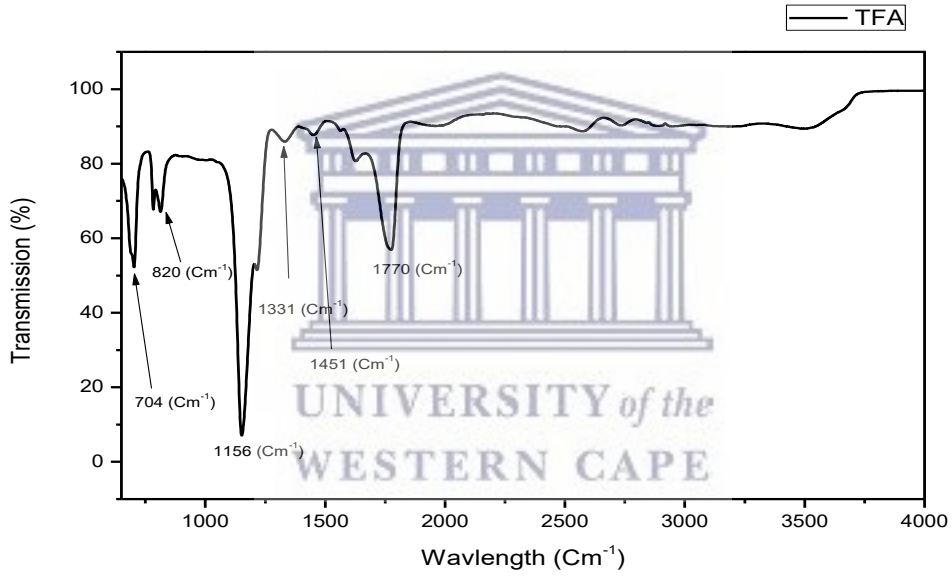

Figure 4-9: FTIR spectrum of the TFA showing the transmission peak of different functional groups.

4.6.3 Scanning electron microscopy analysis

The HR-SEM of the LMW-Ch and the electrosparyed chitosan at different magnifications showed a reduction in the particle size of LMW-Ch to a nano-scale level (Figure 4-10). Electrospraying of LMW-Ch resulted in a non-homogenous shape of Ch-Np with a higher tendency to agglomerate.

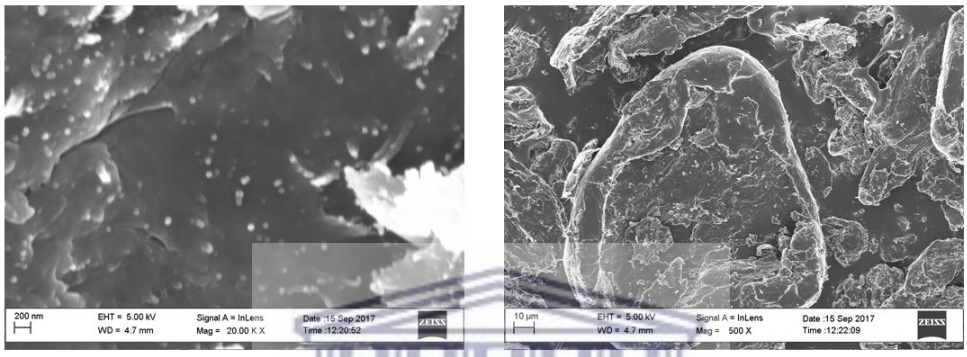

(A)

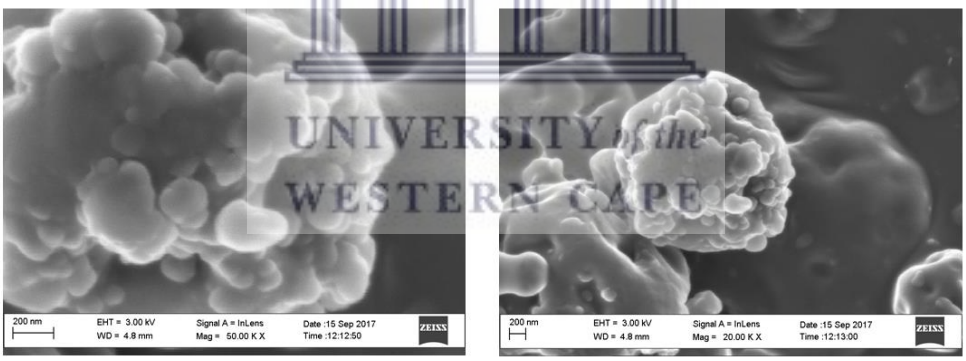

(B)

Figure 4-10: HR-SEM of (A) LMW-Ch (B) Ch-Np at different magnifications showing the difference in particle size and morphology.

4.7 Discussion

Chitosan nanoparticles are new materials recently introduced to the dental field. The ionic gelation method is the technique most commonly used to synthesize Ch-Np utilized in endodontic applications (Kishen *et al.*, 2008; DaSilva *et al.*, 2013; Shrestha and Kishen, 2014). However, one of the main shortcomings of this technique is the insolubility of the produced nanoparticles in water, which limits its applications in the dental field (Qi *et al.*, 2004). The main aim of this study was to synthesize Ch-Np to be used as an active component in a novel intra-canal medicament. The solubility of the Ch-Np will fulfil one of the ideal requirements of intra-canal medicaments (Abbott, 1990) and facilitate its removal from the root canal system when necessary. The choice of technique for synthesis of nanoparticles should be based on the intended application of the produced nanoparticles, particle size, stability and surface charge (Agnihotri *et al.*, 2004). Hence in this study the electrospraying technique was used because the newly synthesized Ch-Np should be water soluble if it is to be used as intra-canal medicament.

The selection of this technique was based on its advantages, such as its ability to produce high surface charged nanoparticles resulting from the ability of Ch-Np to retain the electrical current that passes through the LMW-Ch droplet during electrospraying, compared to the other methods used in the literature (Nguyen *et al.*, 2016). The highly positively charged nanoparticles may increase its affinity to the negatively charged microbial cell wall, enhancing its antimicrobial effect.

The selection of the solvent is also an important factor as it will determine the chemical properties of the synthesized nanoparticles. In this study trifluoroacetic acid ($C_2HF_3O_2$)

was used as a solvent. It is an organoflorine compound and considered as a non-aqueous volatile solvent (Hasegawa *et al.*, 1992). The use of trifluoroacetic acid is suggested to facilitate the formation of dry Ch-Np as it evaporates readily, allowing deposition of dry nanoparticles at the collector (Hasegawa *et al.*, 1992). Furthermore, TFA can break the intermolecular interaction between the chitosan molecule facilitating electrospraying (Hasegawa *et al.*, 1992; Lopez and Salazar, 2013).

4.7.1 Characterization findings

a. Hydrodynamic particle size (zeta-size)

The hydrodynamic particle size of the electrosprayed Ch-Np was evaluated using a zeta-sizer. The hydrodynamic particle size of the LMW-Ch showed an average of 3435 nm which was reduced to 419 nm when electrosprayed to form Ch-Np. This reduction in the hydrodynamic particle size of LMW-Ch is due to the action of the Coulomb force generated by the electrical current and acts on the chitosan solution droplet causing its breakage into nanoparticles (Bock *et al.*, 2011). Several factors may have an effect on the hydrodynamic particle size of the synthesized Ch-Np, such as the needle diameter, the electrical current, the distance between the needle tip and the collector, the flow rate and the viscosity of the chitosan solution.

This size of 419 nm falls within the definition of polymeric nanoparticles which states that polymeric nanoparticles can be within the range of 10 – 1000 nm (Bhatia, 2016; Jahangiri and Barghi, 2018). Furthermore, the term “nanoparticle” is a collective term and not restricted to the size of less than 100 nm when applied to biomedical research, due to the characteristic features of polymeric particles on a nano-scale level and may be determined by features such as cell permeability (Pinto Reis *et al.*, 2006; Zhang and

Kawakami, 2010). Hence the newly synthesized chitosan particles formed through electrospraying, produced particle sizes that fall within the range of nanoparticle sizes. Similar results showed hydrodynamic particle sizes of Ch-Np in a range of 200 – 1000 nm (Soppimath *et al.*, 2001), 101 – 348 nm (Yien *et al.*, 2012).

b. Particle size distribution (Polydispersity index)

The polydispersity index is used to measure the molecular weight distribution of a material (Rogošić *et al.*, 1996). The significance of measuring the polydispersity index of the electrosprayed Ch-Np is that it will determine the tendency of the material to agglomerate according to the ISO 22412:2017. Figure 4-5 shows a decrease in the PDI from 0.549 in LMW-Ch to 0.254 in Ch-Np. The decrease in the polydispersity index value of Ch-Np may be due to the reduction of the particle size and the lowering of the molecular weight. This result is supported by Rogošić *et al*., (1996) where it was shown that the reduction of the PDI indicates a decrease in the molecular weight width of a material, which confirms that chitosan was converted to chitosan nanoparticles in this study.

The higher values of PDI of both samples in this study (> 0.07) indicate broad size distribution of both samples and thus the presence of agglomeration as described by the ISO 22412:2017. The high PDI of Ch-Np indicates that the synthesized Ch-Np may have a tendency to agglomerate.

c. Surface charge (zeta-potential)

The synthesis of Ch-Np with high zeta potential (surface charge) was of interest as it would facilitate its intended application in this study. The results showed that the use of electrospraying increased the zeta potential of the LMW-Ch from 25.6 mV to 53.7 mV

in the electrosprayed Ch-Np (Figure 4-6). The increase in the zeta potential is considered due to the ability of Ch-Np to retain the electrical current that passes through the LMW-Ch droplet during electrospraying. The clinical importance of a higher zeta potential is that it will determine the affinity of the nanoparticles to the vital cells, such as the bacterial cell and it will influence its stability in a suspension (Qi *et al*., 2004), thus a higher zeta potential is expected to increase its antimicrobial properties.

d. Fourier-transform infrared spectroscopy analysis

Fourier transform infrared analysis was conducted on LMW-Ch, electrosprayed Ch-Np and TFA samples. The surface analysis of LMW-Ch was conducted by reflecting the infrared beam on the surface of the LMW-Ch in order to identify the functional groups present on the surface of the LMW-Ch. The main functional groups of LMW-Ch are amide I, amide II and amide II which peaked at 1643 cm^{-1}, 1568 cm^{-1} and 1311 cm^{-1} respectively (Figure 4-7). Similar results were obtained by Paulino *et al* (2006). They showed that chitosan had an amide I absorption peak at 1626 cm^{-1}, amide II peak at 1557 cm^{-1} and amide III peak at 1345 cm^{-1}.

The same functional groups were observed when LMW-Ch was electrosprayed. The transmission peaks of Ch-Np were in the range of the transmission peaks of the LMW-Ch. The three peaks 1669 cm^{-1}, 1529 cm^{-1} and 1319 cm^{-1} (Figure 4-8) were in the same range, amide I, amide II and amide II respectively confirming the newly formed particles are Ch-Np.

Furthermore, the intense sharp peak at 1669 cm^{-1} which was assigned to the trifluoroacetyl ester group (Figure 4-11) indicated the ability of TFA to form an amine salt (trifluoroacetyl ester) with the amine group of the chitosan. The formation of the

trifluoroacetyl ester group is supported by Hasegawa *et al.*, (1992) who reported formation of trifluoroacetyl ester when chitosan was dissolved in TFA, showing a transmission peak in the range of 1670 cm^{-1}.

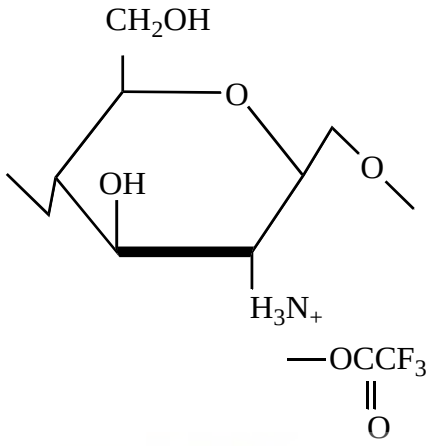

Figure 4-11: Formation of trifluoroacetyl ester group in electrosprayed Ch-Np. Chemical formula adapted from Hasegawa *et al.*, (1992).

The presence of a trifluoroacetyl ester functional group converts the state of Ch-Np from an acid soluble state into a water soluble form (Hasegawa *et al.*, 1992). Furthermore, the presence of the trifluoracetyl ester functional group in the electrosprayed Ch-Np may facilitate its solubility in water. This is an important feature as, for the newly synthesized Ch-Np to be used as an intra-canal medicament, it should be water soluble.

e. Scanning Electron Microscopy

The SEM analysis (Figure 4-10) showed that following electrospraying of LMW-Ch, Ch-Np was formed and particles had irregular shapes. Furthermore, the Ch-Np were agglomerated in large clusters. However, the LMW-Ch was in a non-particulate, irregular form, supporting the high PDI value. This irregularity is considered due to

evaporation of TFA during the synthesis procedure. A similar shape was obtained by Zhang and Kawakami (2010). Additionally, unlike a high molecular weight polymer, the literature showed that the use of a low molecular weight polymer produces irregular shapes when electrosprayed (Nguyen *et al.*, 2016).

4.8 Conclusion

The chitosan particles formed following electrospraying produced water soluble nanoparticles within an average size of 419.1 nm with high zeta potential which can therefore be a promising material for intra-canal medicament for the eradication of persistent root canal pathogens.

4.9 References

Abbott, P. V. (1990). Medicaments: aids to success in endodontics. Part 1. A review of the literature. *Australian Dental Journal*, 35(5): 438-448.

Agnihotri, S. A., Mallikarjuna, N. N., and Aminabhavi, T. M. (2004). Recent advances on chitosan-based micro-and nanoparticles in drug delivery. *Journal of Controlled Release*, 100(1): 5-28.

Ahmed, T. A., and Aljaeid, B. M. (2016). Preparation, characterization, and potential application of chitosan, chitosan derivatives, and chitosan metal nanoparticles in pharmaceutical drug delivery. *Drug Design, Development and Therapy*, 10: 483-507.

Arya, N., Chakraborty, S., Dube, N., and Katti, D. S. (2009). Electrospraying: A facile technique for synthesis of chitosan-based micro/nanospheres for drug delivery applications. *Journal of Biomedical Materials Research Part B: Applied Biomaterials*, 88(1): 17-31.

Bhardwaj, A., Bhardwaj, A., Misuriya, A., Maroli, S., Manjula, S., and Singh, A. K. (2014). Nanotechnology in dentistry: Present and future. *Journal of International Oral Health*, 6(1): 121-126.

Bhatia, S. (2016). Nanoparticles types, classification, characterization, fabrication methods and drug delivery applications, *Natural Polymer Drug Delivery Systems*. Springer, Cham, pp. 33-93.

Bock, N., Woodruff, M. A., Hutmacher, D. W., and Dargaville, T. R. (2011). Electrospraying, a reproducible method for production of polymeric microspheres for biomedical applications. *Polymers*, 3(1): 131-149.

Calvo, P., Remunan-Lopez, C., Vila-Jato, J. L., and Alonso, M. (1997). Novel hydrophilic chitosan-polyethylene oxide nanoparticles as protein carriers. *Journal of Applied Polymer Science*, 63(1): 125-132.

Croisier, F., and Jérôme, C. (2013). Chitosan-based biomaterials for tissue engineering. *European Polymer Journal*, 49(4): 780-792.

DaSilva, L., Finer, Y., Friedman, S., Basrani, B., and Kishen, A. (2013). Biofilm formation within the interface of bovine root dentin treated with conjugated chitosan and sealer containing chitosan nanoparticles. *Journal of Endodontics*, 39(2): 249-253.

Dizaj, S. M., Lotfipour, F., Barzegar-Jalali, M., Zarrintan, M. H., and Adibkia, K. (2014). Antimicrobial activity of the metals and metal oxide nanoparticles. *Materials Science and Engineering: C*, 44: 278-284.

Du, W.-L., Niu, S.-S., Xu, Y.-L., Xu, Z.-R., and Fan, C.-L. (2009). Antibacterial activity of chitosan tripolyphosphate nanoparticles loaded with various metal ions. *Carbohydrate Polymers*, 75(3): 385-389.

Ealia, S. A. M., and Saravanakumar, M. (2017). A review on the classification, characterisation, synthesis of nanoparticles and their application. *IOP Conference Series: Materials Science and Engineering*, 263: 032019.

Fan, W., Yan, W., Xu, Z., and Ni, H. (2012). Formation mechanism of monodisperse, low molecular weight chitosan nanoparticles by ionic gelation technique. *Colloids and Surfaces B: Biointerfaces*, 90: 21-27.

Fernández-Urrusuno, R., Calvo, P., Remuñán-López, C., Vila-Jato, J. L., and Alonso, M. J. (1999). Enhancement of nasal absorption of insulin using chitosan nanoparticles. *Pharmaceutical Research*, 16(10): 1576-1581.

Feynman, R. P. (1960). There's plenty of room at the bottom. *Engineering and Science*, 23(5): 22-36.

Gan, Q., Wang, T., Cochrane, C., and McCarron, P. (2005). Modulation of surface charge, particle size and morphological properties of chitosan–TPP nanoparticles intended for gene delivery. *Colloids and Surfaces B: Biointerfaces*, 44(2): 65-73.

Guarino, V., Altobelli, R., Cirillo, V., Cummaro, A., and Ambrosio, L. (2015). Additive electrospraying: a route to process electrospun scaffolds for controlled molecular release. *Polymers for Advanced Technologies*, 26(12): 1359-1369.

Hajipour, M. J., Fromm, K. M., Ashkarran, A. A., de Aberasturi, D. J., de Larramendi, I. R., Rojo, T., Serpooshan, V., Parak, W. J., and Mahmoudi, M. (2012). Antibacterial properties of nanoparticles. *Trends in Biotechnology*, 30(10): 499-511.

Hasegawa, M., Isogai, A., Onabe, F., and Usuda, M. (1992). Dissolving states of cellulose and chitosan in trifluoroacetic acid. *Journal of Applied Polymer Science*, 45(10): 1857-1863.

Helander, I., Nurmiaho-Lassila, E.-L., Ahvenainen, R., Rhoades, J., and Roller, S. (2001). Chitosan disrupts the barrier properties of the outer membrane of Gram-negative bacteria. *International Journal of Food Microbiology*, 71(2): 235-244.

ISO 22412. International Standards Organization. Particel size analysis - Dynamic light scattering. 2017.

Jadhav, A., Wang, L., and Padhye, R. (2013). Influence of applied voltage on droplet size distribution in electrospraying of thermoplastic polyurethane. *International Journal of Materials, Mechanics and Manufacturing*, 1(3): 287-289.

Jahangiri, A., and Barghi, L. (2018). Polymeric nanoparticles: review of synthesis methods and applications in drug delivery. *Journal of Advanced Chemical and Pharmaceutical Materials*, 1(2): 38-47.

Jaworek, A. (2007). Micro- and nanoparticle production by electrospraying. *Powder Technology*, 176(1): 18-35.

Jaworek, A., and Sobczyk, A. T. (2008). Electrospraying route to nanotechnology: An overview. *Journal of Electrostatics*, 66(3–4): 197-219.

Kawashima, Y., Handa, T., Kasai, A., Takenaka, H., and Lin, S. Y. (1985). The effects of thickness and hardness of the coating film on the drug release rate of theophylline granules coated with chitosan-sodium tripolyphosphate complex. *Chemical and Pharmaceutical Bulletin*, 33(6): 2469-2474.

Kishen, A., Shi, Z., Shrestha, A., and Neoh, K. G. (2008). An investigation on the antibacterial and antibiofilm efficacy of cationic nanoparticulates for root canal disinfection. *Journal of Endodontics*, 34(12): 1515-1520.

Liu, H., and Gao, C. (2009). Preparation and properties of ionically cross-linked chitosan nanoparticles. *Polymers for Advanced Technologies*, 20(7): 613-619.

Lopez, S. E., and Salazar, J. (2013). Trifluoroacetic acid: Uses and recent applications in organic synthesis. *Journal of Fluorine Chemistry*, 156: 73-100.

Nguyen, D. N., Clasen, C., and Van den Mooter, G. (2016). Pharmaceutical applications of electrospraying. *Journal of Pharmaceutical Sciences*, 105(9): 2601-2620.

Pancholi, K., Ahras, N., Stride, E., and Edirisinghe, M. (2009). Novel electrohydrodynamic preparation of porous chitosan particles for drug delivery. *Journal of Materials Science: Materials in Medicine*, 20(4): 917-923.

Paulino, A. T., Simionato, J. I., Garcia, J. C., and Nozaki, J. (2006). Characterization of chitosan and chitin produced from silkworm crysalides. *Carbohydrate Polymers*, 64(1): 98-103.

Pinto Reis, C., Neufeld, R. J., Ribeiro, A. J., and Veiga, F. (2006). Nanoencapsulation I. Methods for preparation of drug-loaded polymeric nanoparticles. *Nanomedicine: Nanotechnology, Biology and Medicine*, 2(1): 8-21.

Qi, L., Xu, Z., Jiang, X., Hu, C., and Zou, X. (2004). Preparation and antibacterial activity of chitosan nanoparticles. *Carbohydrate Research*, 339(16): 2693-2700.

Rogošić, M., Mencer, H. J., and Gomzi, Z. (1996). Polydispersity index and molecular weight distributions of polymers. *European Polymer Journal*, 32(11): 1337-1344.

Shrestha, A., and Kishen, A. (2014). Antibiofilm efficacy of photosensitizer-functionalized bioactive nanoparticles on multispecies Biofilm. *Journal of Endodontics*, 40(10): 1604-1610.

Shweta, A., and Sonia, P. (2013). Pharmaceutical relevance of crosslinked chitosan in microparticulate drug delivery. *International Research Journal of Pharmacy*, 4(2): 45-51.

Soppimath, K. S., Aminabhavi, T. M., Kulkarni, A. R., and Rudzinski, W. E. (2001). Biodegradable polymeric nanoparticles as drug delivery devices. *Journal of Controlled Release*, 70(1): 1-20.

Tapia-Hernández, J. A., Torres-Chávez, P. I., Ramírez-Wong, B., Rascón-Chu, A., Plascencia-Jatomea, M., Barreras-Urbina, C. G., Rangel-Vázquez, N. A., and Rodríguez-Félix, F. (2015). Micro-and nanoparticles by electrospray: advances and applications in foods. *Journal of Agricultural and Food Chemistry*, 63(19): 4699-4707.

Virlan, M. J. R., Miricescu, D., Radulescu, R., Sabliov, C. M., Totan, A., Calenic, B., and Greabu, M. (2016). Organic nanomaterials and their applications in the treatment of oral diseases. *Molecules*, 21(2): 207-230.

Wang, X., Du, Y., and Liu, H. (2004). Preparation, characterization and antimicrobial activity of chitosan–Zn complex. *Carbohydrate Polymers*, 56(1): 21-26.

Wu, Y., Yang, W., Wang, C., Hu, J., and Fu, S. (2005). Chitosan nanoparticles as a novel delivery system for ammonium glycyrrhizinate. *International Journal of Pharmaceutics*, 295(1): 235-245.

Xu, Y., and Du, Y. (2003). Effect of molecular structure of chitosan on protein delivery properties of chitosan nanoparticles. *International Journal of Pharmaceutics*, 250(1): 215-226.

Yien, L., Zin, N. M., Sarwar, A., and Katas, H. (2012). Antifungal activity of chitosan nanoparticles and correlation with their physical properties. *International Journal of Biomaterials*, 2012: 1-9.

Zhang, S., and Kawakami, K. (2010). One-step preparation of chitosan solid nanoparticles by electrospray deposition. *International Journal of Pharmaceutics*, 397(1): 211-217.

Zhao, L.-M., Shi, L.-E., Zhang, Z.-L., Chen, J.-M., Shi, D.-D., Yang, J., and Tang, Z.-X. (2011). Preparation and application of chitosan nanoparticles and nanofibers. *Brazilian Journal of Chemical Engineering*, 28(3): 353-362.

Chapter 5
Antimicrobial effects of chitosan nanoparticles

5.1 Review of the literature

Polymeric nanoparticles have gained significant interest as a result of their antimicrobial properties and biocompatibility (Virlan *et al.*, 2016). The presence of chitosan in a nano-scale form enhances its antimicrobial properties (Perinelli *et al.*, 2018). The mechanism of antimicrobial activity of Ch-Np starts with the ability of the nanoparticles to attach to the negatively charged microbial cell wall as a result of their highly positively charged surface (Chung *et al.*, 2004). This is enhanced by the large number of nanoparticles that attach to the microbial cell wall as a result of their small surface area (Mohammadi *et al.*, 2016; Sarwar *et al.*, 2014). After Ch-Np have bound to the microbial cell wall, they penetrate through the microbial cell membrane causing its rupture and finally apoptosis (Sarwar *et al.*, 2014). Finally, Ch-Np binds to the microbial DNA causing alteration in the mRNA and thus protein synthesis (Chávez de Paz *et al.*, 2011). As a result of these multiple actions, the presence of chitosan on a nano-scale level may enhance its antimicrobial properties by increasing its mechanism of action to kill the microbial cell (Pelgrift and Friedman, 2013).

The antimicrobial efficacy of Ch-Np to combat endodontic pathogens was evaluated in different forms such as solution, modification of existing root canal disinfectants or as a drug carrier for other antimicrobial agents. Kishan *et al*., (2008) and Shertha *et al*., (2010) showed that Ch-Np in a solution form completely eliminated *E. faecalis* pathogens present in a planktonic state and caused a significant reduction when present in a biofilm state.

Chávez de Paz *et al*., (2011) synthesized Ch-Np from HMW-Ch and LMW-Ch using an ionic gelation method and then compared the antimicrobial efficacy of the two nanoparticles against *S. mutans*. Ch-Np synthesized from LMW-Ch caused more the 95% of *S. mutans* damage. Additionally, Aliasghari *et al.,* (2016) showed that the antibacterial efficacy of Ch-Np against *S. mutans* is greater than chitosan on a macro-scale level, in which chitosan showed a minimal inhibitory concentration and minimal bactericidal concentration of 2.5 mg/mL and 1.25 mg/mL respectively compared to 1.25 mg/mL and 0.625 mg/mL in Ch-Np. They also showed that Ch-Np reduced *S. mutans* biofilm formation up to 93.4% (Chávez de Paz *et al*., 2011).

Chitosan nanoparticles can be used as a drug carrier (Kong *et al.*, 2010). This property of chitosan nanoparticles was utilized by Shrestha and Kishen (2014) by conjugating a photosensitizer material (Rose Bengal) to the chitosan structure and then evaluating its antimicrobial property against biofilms of *E. faecalis, Streptococcus oralis, Prevotella intermedia* and *Actinomyces naeslundii*. They showed that such a conjugation can destroy the bacterial cell membrane of the tested bacterial species and penetrate deep into the biofilm structure of the tested species, reducing the biofilm thickness and the number of microbial cells.

Chitosan nanoparticles were incorporated into a zinc oxide eugenol based sealer and were assessed for their antibacterial effect against *E. faecalis* biofilm on bovine root dentine treated by phosphorylated chitosan, chitosan conjugated with rose Bengal and a combination of phosphorylated chitosan and chitosan conjugated with rose Bengal, respectively. There was inhibition of *E. faecalis* biofilm formation, the degree of inhibitory effects varying with the different treatment solution used (DaSilva *et al.*, 2013).

Fluoridated dental varnish loaded with Ch-Np was able to inhibit the growth of *S. mutans* and it inhibited the growth of *S. mutans* especially in the first two days after application (Wassel and Khattab, 2017). Ch-Np incorporated into a calcium hydroxide intra-canal medicament increased its ability to reduce the number of viable *E. faecalis* in a biofilm state (Carpio-Perochena *et al.*, 2017).

The antifungal efficacy of Ch-Np against *C. albicans* was also demonstrated by Yien *et al.*, (2012). Ch-Np was a more effective antifungal component compared to chitosan on a macro-scale level. However, a high concentration of Ch-Np is needed to produce the antifungal effect (Yien *et al.*, 2012). Similar results by MubarakAli *et al.*, (2018) showed that Ch-Np possessed antifungal activity in higher concentrations (400 µg/mL ^{1}).

Most of the studies evaluated the antimicrobial efficacy of Ch-Np synthesized using the ionic gelation method which produced a non-water soluble Ch-Np, limiting its usage as antimicrobial intra-canal medicament which must be water soluble to facilitate its removal from the root canal wall.

5.2 Rationale of the study

Unlike other studies that evaluated the antimicrobial effect of non-water soluble Ch-Np synthesized using the ionic gelation method, the use of trifluoroacetic acid as a solvent of LMW-Ch before using electrospraying technique to synthesize Ch-Np, produced water soluble Ch-Np which may expand its use as intra-canal medicament. The antimicrobial effect of the water soluble Ch-Np produced by the electrospraying technique against endodontic pathogens was not evaluated.

5.3 Aim of the study

The aim of this study was to evaluate the antimicrobial effect of Ch-Np against three endodontic pathogens, namely *S. mutans*, *E. faecalis* and *C. albicans* in both the planktonic and biofilm state.

5.4 Objectives

i. To evaluate the antimicrobial effect of chitosan nanoparticles on the survival time of planktonic cells of *S. mutans*, *E. faecalis* and *C. albicans* using a Time-kill Test.

ii. To evaluate and compare the antimicrobial effect of Ch-Np with LMW-Ch for the survival time of planktonic cells of *S. mutans*, *E. faecalis* and *C. albicans* using a Time-kill Test.

iii. To evaluate the antimicrobial effect of Ch-Np on the biofilm biomass of *S. mutans*, *E. faecalis* and *C. albicans* using a microtiter plate biofilm assay.

5.5 Methodology

5.5.1 Antimicrobial effect of Ch-Np against endodontic pathogens in a planktonic state

a. Preparation of Ch-Np solution

For preparation of Ch-Np solution, 30 mg of the previously synthesized Ch-Np (chapter 4) was dissolved in distilled water to form a final concentration of 3% (w/v). The Ch-Np were allowed to dissolve completely by placing the mixture in an Eppendorf tube and mixed for 10 minutes.

b. Preparation of microbial suspension

The two bacterial species, *S. mutans* (ATCC 25175) and *E. faecalis* (ATCC 29212) and one fungal species, *C. albicans* (ATCC 90028) were obtained from American type culture collections.

The three microbial species were incubated in brain heart infusion broth (BHI) at 37°C for 24 hours. Following the overnight culture, *S. mutans*, *E. faecalis* and *C. albicans* were subcultured in brain heart infusion agar plates and incubated overnight at 37°C. The microbial cells were then suspended in phosphate buffer saline solution (PBS) and the concentration was adjusted to 0.5 McFarland standard (Mcf) using DensiCHEK Plus BioMérieux, Inc Durham, USA.

c. Antimicrobial assay

The survival time of the three pathogens in a planktonic state was evaluated using a Time-Kill Test following their exposure to 3% Ch-Np. 100 µL of 3% Ch-Np solution was dispensed in a sterile well of a 12-well cell culture plate to which 200 µL of

0.5 Mcf from each tested microbial species suspension and 1700 µL of BHI as a growth medium were added to form a total volume of 2000 µL in each well and labeled as either experimental group A (*S. mutans)*, group B (*E. faecalis*) and group C (*C. albicans*). The positive control group (D) consisted of 200 µL of the tested microbial species suspension added to 1700 µL of BHI and placed in a 12-well cell culture plate. The 12 well plate was incubated in an Orbital Shaker Incubator (Biocom Biotech, USA) at 37°C in an aerobic condition.

50 µL of PBS was added to each well and then 100 µL from each group was transferred and placed in a sterile 96-well microtiter plate. The suspension was diluted two-fold by transferring 50 µL from the first well to the second well and so forth up to the sixth well. The final volume of the last well was 100 µL. 2 µL from the final dilution of each group was then transferred and streaked in brain heart infusion agar plates and incubated at 37°C for 24 hours in an aerobic condition. The procedure of serial dilution was done at zero minute, 30 minutes, 1 hour, 2, 4, 6, 8 and 24 hours respectively. The test was repeated in triplicate.

After a 24 hour incubation period, the numbers of the colony forming units (CFU) in each plate were counted using an automated colony counter (Gerber, Switzerland). The number of colony forming units that exceeded 300 were considered as too numerous to count (TNTC) and recorded as 300 (CFU), while those less than 30 were considered as too low to count (TLTC) and recorded as zero except for *C. albicans* in which all values were recorded without any change based on the standard practice for colony counting (Sutton, 2011).

5.5.2 Effect of Ch-Np against biofilm biomass of endodontic pathogens

The effect of the synthesized Ch-Np against single microbial species endodontic biofilm was assessed by evaluating the ability of the Ch-Np to disrupt the biofilm biomass of *S. mutans*, *E. faecalis* and *C. albicans*.

a. Biofilm formation

S. mutans, *E. faecalis* and *C. albicans* were allowed to grow overnight by incubating them in brain heart infusion broth for 24 hours at 37°C. A cotton swab was taken from each microbial culture and streaked in a brain heart infusion agar plate and incubated overnight at 37°C to obtain substantial growth from each microorganism. A single colony from each microorganism was further suspended in a sterile phosphate buffer saline (PBS) solution and the concentration of each microorganism was adjusted to 0.5 Mcf standard.

50 µL from 0.5 Mcf standard of each microbial species was placed in a 96 well plate to which 150 µL of BHI was added. The microorganisms were allowed to grow and form biofilm by incubating the sterile 96 well plates for 24 hours at 37°C. The BHI was replaced after 24 hours to allow a constant supply of nutrient to the microorganisms. After 72 hours, the BHI was discarded and the biofilm that was formed was washed 5 times with sterile phosphate buffer saline (PBS) to remove any planktonic microbial cells and unattached microorganisms. For each microorganism, two groups were examined in which one was an experimental group and the other a control group. In each group the antibiofilm efficacy of Ch-Np was assessed 12 times (n=12).

b. Antimicrobial assay

The effect of the Ch-Np against the biofilm biomass of the microbial species was evaluated using a microtiter plate biofilm assay. 50 µL of 3% Ch-Np solution was placed in each well of the 96 wells of each experimental group to which 150 µL BHI was added. In the control group 50 µL of deionized water and 150 µL of BHI were added. The 96 well microtiter plate was incubated at 37°C for 24 hours. Following the incubation period, the BHI was removed and the wells were washed vigorously with phosphate buffer saline (PBS) solution to remove any remaining planktonic microbial cells and Ch-Np and disrupted biofilm, if present.

200 µL of 0.1% crystal violet was used to stain the remaining *S. mutans* and *E. faecalis* biofilms, while *C. albicans* was stained with 0.02% crystal violet for 10 minutes (Figure 5-1). Crystal violet's used at a lower concentration was due to the difference in the absorbance value of *C. albicans* compared to *S. mutans* and *E. faecalis* in which 0.02% is still within the dynamic range of the microtiter plate reader (Peeters *et al.*, 2008).

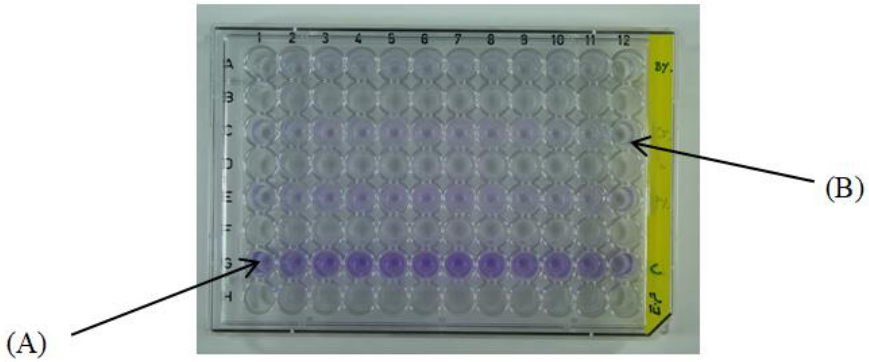

Figure 5-1: 96 well microtiter plate showing the difference in the colour density of stained microbial biofilm (A) control group, (B) experimental group treated with 3% Ch-Np.

After 10 minutes, the crystal violet was discarded and the plate allowed to air dry at room temperature for 30 minute. 180 µL of 30% acetic acid (v/v) was added to remove the crystal violet and 180 µL was added to avoid any interaction with any stained material at the liquid air interface which may not considered to be indicative of biofilm formation (Christensen *et al.*, 1985). The acetic acid was allowed to solubilize the crystal violet for 10 minutes before measuring the optical density of each sample at a wave length of 540 nm using a microplate reader (Rayto Rt–2100C, Germany) (Figure 5-2).

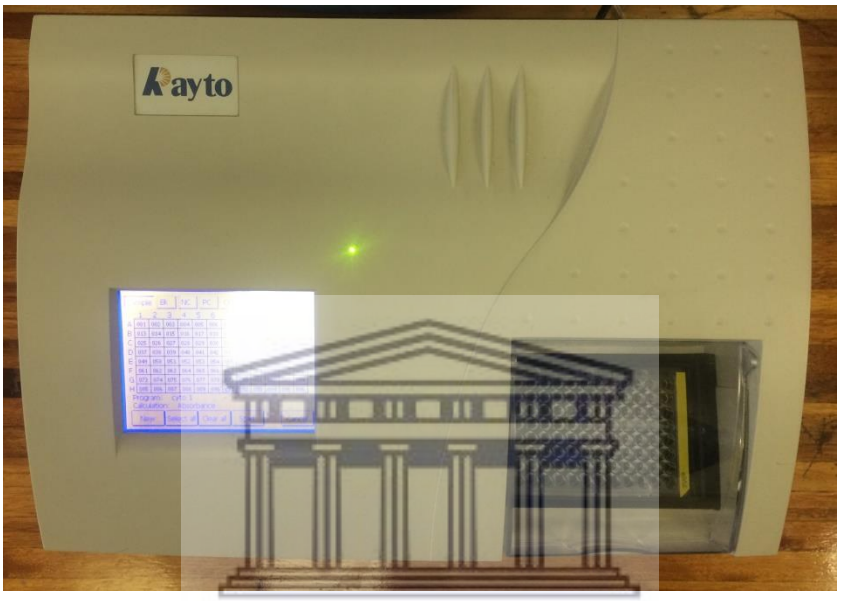

Figure 5-2: Rayto Microiter reader with 96 well microtiter plate showing the optical density of the stained biofilm in each well.

5.6 Data analysis

All results for each group were transferred to an Excel spreadsheet (Microsoft Corporation 2010, USA). To evaluate the effect of Ch-Np against planktonic cells of *S. mutans*, *E. faecalis* and *C. albicans* the data were expressed in Log CFU/mL and then analyzed using IBM SPSS statistical software (version 25, IBM, USA).

The survival time was tested using the Kaplan-Meier test by measuring the survival time of each microbial species when exposed to Ch-Np.

To evaluate the effect of Ch-Np on biofilm biomass of *S. mutans*, *E. faecalis* and *C. albicans* the data was expressed in optical density values and then analyzed using IBM SPSS statistical software. The effect was evaluated by comparing the optical density of each microbial species biofilm before and after their exposure to Ch-Np. A Mann-Whitney U test (non-parametric test for independent values) was used to determine a statistically significant difference, if any, between the groups. A p value of 0.05 was considered as a statistical difference.

5.7 Results

5.7.1 Effect of Ch-Np against endodontic pathogens in a planktonic state

The effect of Ch-Np against planktonic cells of *S. mutans, E. faecalis* and *C. albicans* was evaluated using the Time-kill Test. The data was analyzed using the Kaplan-Meir test. The mean, median and standard error of the survival rate of each microbial species when exposed to different concentrations of LMW-Ch is shown in Table 5-1.

Table 5-1: The Mean, median and standard error for the survival time of *S. mutans*, *E. faecalis* and *C. albicans* when exposed to 3% Ch-Np

Means and Medians for Survival Time								
Microorganism	**Mean**				**Median**			
	Estimate	**Std. Error**	**95% Confidence Interval**		**Estimate**	**Std. Error**	**95% Confidence Interval**	
			Lower Bound	**Upper Bound**			**Lower Bound**	**Upper Bound**
E. faecalis	7.00	1.25	4.56	9.44	4.00	1.03	1.98	6.02
S. mutans	6.50	1.18	4.18	8.82	4.00	1.07	1.90	6.10
C. albicans	17.00	1.77	13.52	20.47				
Overall	9.18	0.90	7.41	10.95	6.00	0.68	4.67	7.33

a. Antimicrobial effect of Ch-Np against planktonic cells of *S. mutans*

The Kaplan-Meir survival function curve showed that *S. mutans* was observed at zero minute only. At 30 minutes *S. mutans* was not observed when it was exposed to 3% Ch-Np (Figure 5-3).

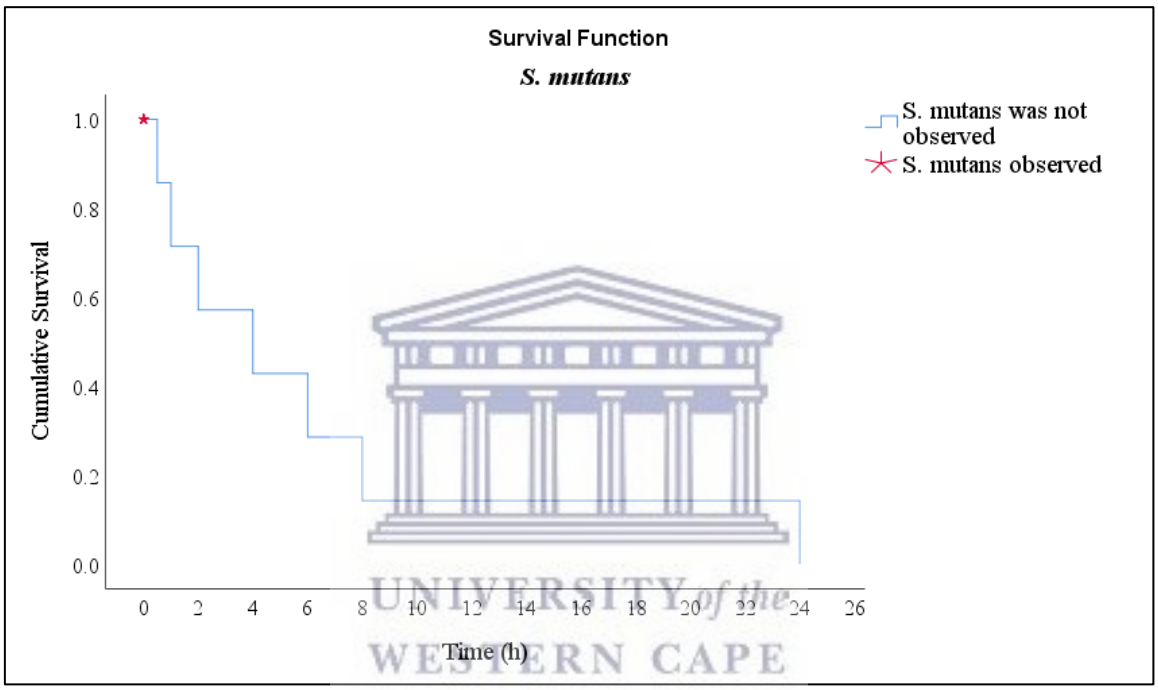

Figure 5-3: Survival function curve of *S. mutans* showing the time at which it was observed (zero minute) following its exposure to 3% Ch-Np.

At zero minute *S. mutans* showed a mean number of Log CFU/mL of 6.70 following its exposure to 3% Ch-Np. This number declined to zero at 30 minutes showing complete eradication even after 24 hours contact time. The mean number of the log CFU/mL of *S. mutans* when exposed to 3% Ch-Np compared to its normal growth rate represented by mean number of the Log CFU/mL are shown in Table 5-2.

Table 5-2: The mean number of the Log CFU/mL of *S. mutans* following its exposure to 3% Ch-Np compared to the positive control group

Time (h)	***S. mutans* exposed to 3% Ch-Np**	**Normal growth rate of *S. mutans* (control)**
0	6.70	6.97
0.5	0.00	6.86
1	0.00	6.83
2	0.00	6.92
4	0.00	6.97
6	0.00	6.94
8	0.00	6.98
24	0.00	6.98

The mean number of the Log CFU/mL of *S. mutans* following its exposure to 3% Ch-Np compared to the mean number of the Log CFU/mL of its normal growth rate are shown in Figure 5-4. There was complete eradication of *S. mutans* at 30 minutes following its exposure to 3% Ch-Np. The colony forming units of *S. mutans* when exposed to 1% and 3% LMW-Ch are shown in Figure 5-5.

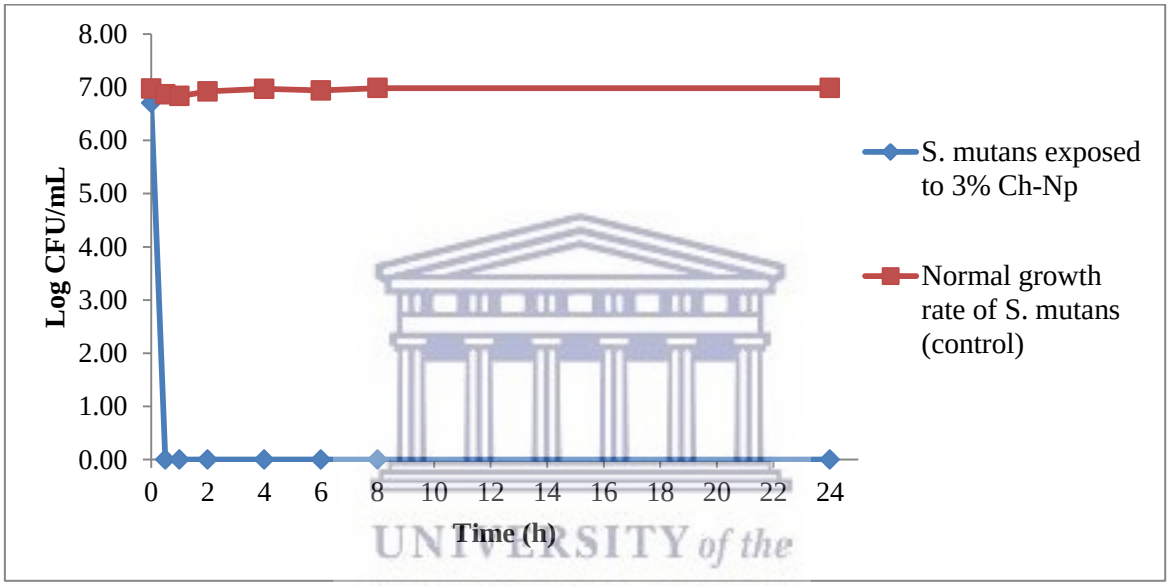

Figure 5-4: The mean Log CFU/mL of *S. mutans* following its exposure to 3% Ch-Np and 3% LMW-Ch overtime.

Figure 5-5: The colony forming units of *S. mutans* over-time following its exposure to 3% Ch-Np.

b. Antimicrobial effect of Ch-Np against planktonic cells of *E. faecalis*

The Kaplan-Meir survival function curve showed that *E. faecalis* was observed at zero and 30 minutes only. After 1 hour *E. faecalis* was not observed when it was exposed to 3% Ch-Np (Figure 5-6).

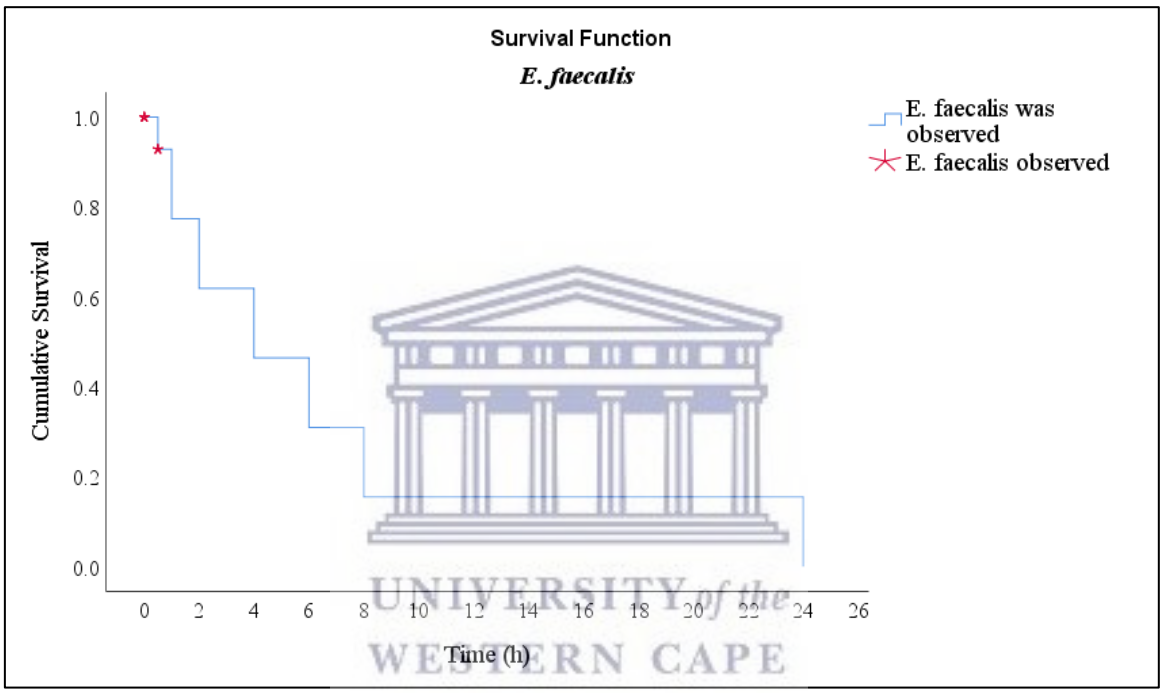

Figure 5-6: Survival function curve of *E. faecalis* showing the time at which it was observed (zero and 30 minutes) following its exposure to 3% Ch-Np.

At zero minute *E. faecalis* showed a mean number of Log CFU/mL of 6.55 following its exposure to 3% Ch-Np. This number declined to 3.07 at 30 minutes. At 1 hour complete eradication of *E. faecalis* was observed and continued even after 24 hours contact time. The mean number of the log CFU/mL of *E. faecalis* following its exposure to 3% Ch-Np compared to its normal growth rate represented by mean number of the Log CFU/mL are shown in Table 5-3.

Table 5-3: The mean number of the Log CFU/mL of *E. faecalis* following its exposure to 3% Ch-Np compared to the positive control group

Time (h)	***E. faecalis* exposed to 3% Ch-Np**	**Normal growth rate of *E. faecalis* (control)**
0	6.55	6.98
0.5	3.07	6.98
1	0.00	6.98
2	0.00	6.98
4	0.00	6.98
6	0.00	6.98
8	0.00	6.98
24	0.00	6.98

The number of the Log CFU/mL of *E. faecalis* following its exposure to 3% Ch-Np compared to the mean number of the Log CFU/mL of its normal growth rate are shown in Figure 5-7. There was complete eradication of *E. faecalis* at 1 hour following its exposure to 3% Ch-Np. The colony forming units of *E. faecalis* when exposed to 1% and 3% LMW-Ch are shown in Figure 5-8.

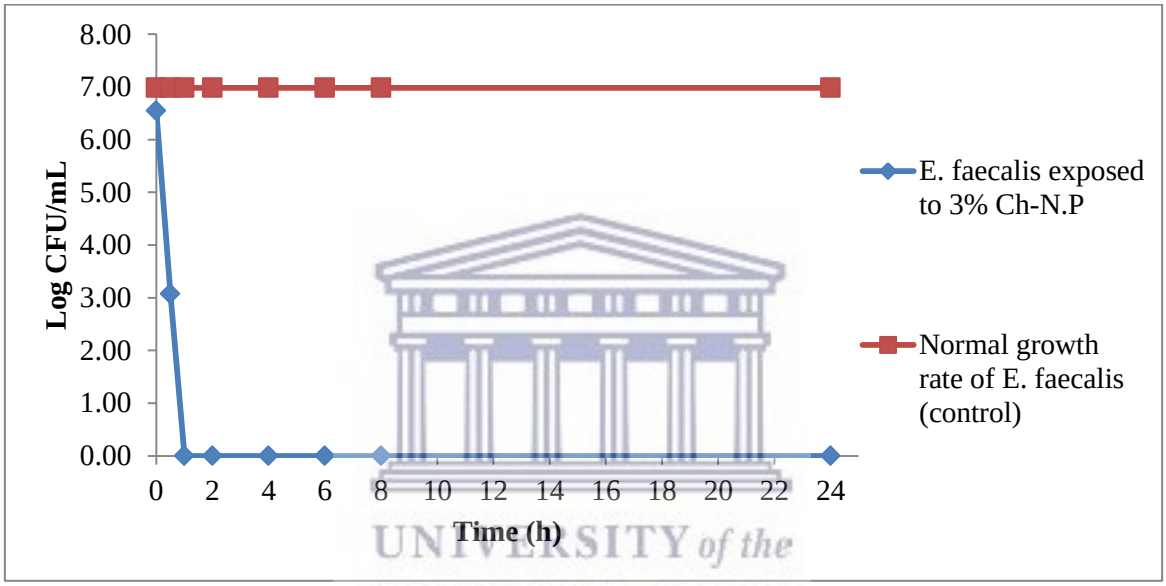

Figure 5-7: The mean Log CFU/mL of *E. faecalis* following its exposure to 3% Ch-Np over time.

Figure 5-8: The colony forming units of *E. faecalis* over time following its exposure to 3% Ch-Np.

c. Antimicrobial effect of Ch-Np against planktonic cells of *C. albicans*

The Kaplan-Meir survival function curve showed that *C. albicans* was observed at all times when it was exposed to 3% Ch-Np (Figure 5-9).

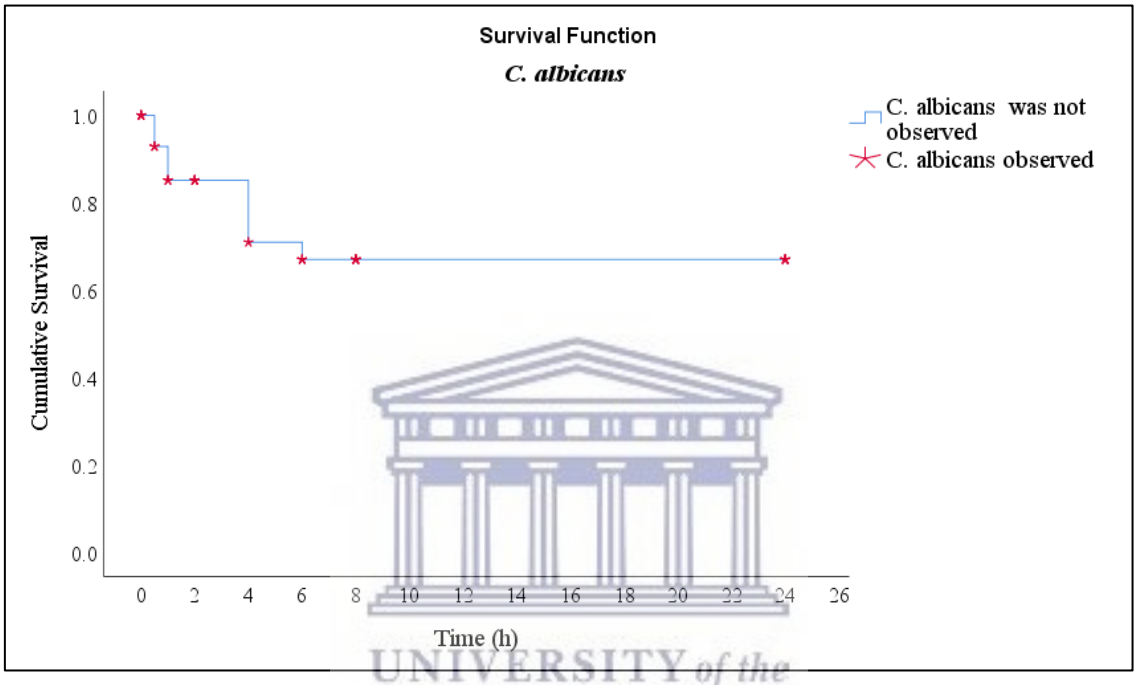

Figure 5-9: Survival function curve of *C. albicans* showing the time at which it was observed at all times following its exposure to 3% Ch-Np.

At zero minute *C. albicans* showed a mean number of Log CFU/mL of 4.84 following its exposure to 3% Ch-Np. This number declined initially at 30 minute to an average of 2.38 to reach a minimum of 1.55 at 4 hours contact time. At 6 hour contact time there was an increase in the log CFU/mL to reach a maximum of 6.93 CFU/mL at 24 hours contact time. The mean number of the log CFU/mL of *C. albicans* following its exposure to 3% Ch-Np compared to its normal growth rate represented by mean number of the Log CFU/mL are shown in (Table 5-4).

Table 5-4: The mean number of the Log CFU/mL of *C. albicans* following its exposure to 3% Ch-Np compared to the positive control group

Time (h)	***C. albicans* exposed to 3% Ch-Np**	**Normal growth rate of *C. albicans* (control)**
0	4.84	5.41
0.5	2.38	5.28
1	2.30	5.11
2	4.74	4.51
4	1.55	5.51
6	4.27	6.65
8	5.60	6.98
24	6.93	6.98

The mean number of the Log CFU/mL of *C. albicans* following its exposure to 3% Ch-Np compared to the mean number of the Log CFU/mL of its normal growth rate are shown in Figure 5-10. The colony forming units of *C. albicans* when exposed to 1% and 3% LMW-Ch are shown in Figure 5-11.

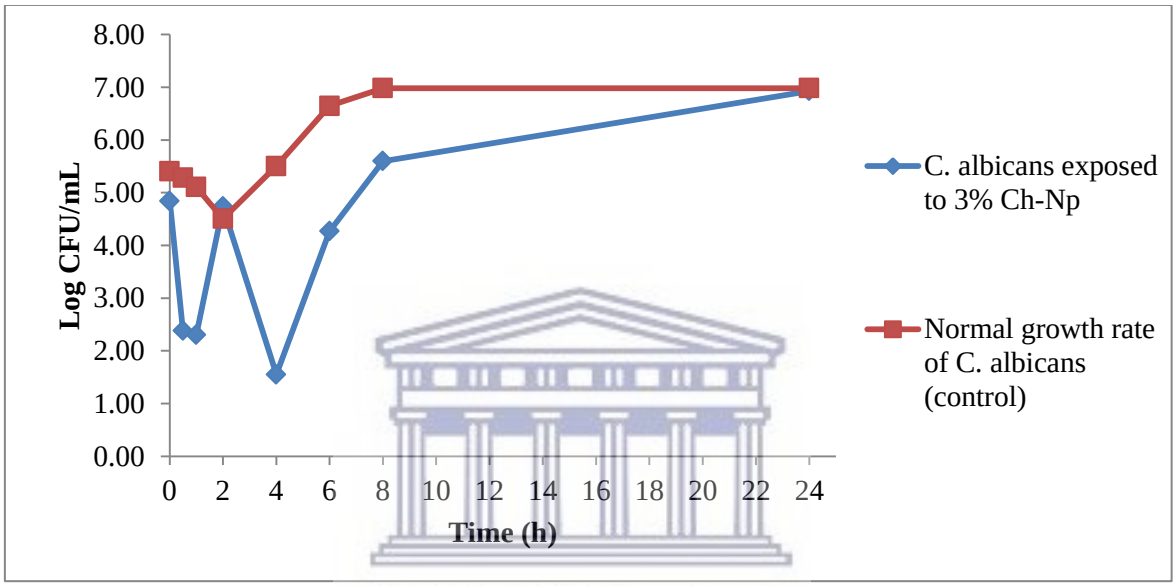

Figure 5-10: The mean Log CFU/mL of *C. albicans* following its exposure to 3% Ch-Np overtime.

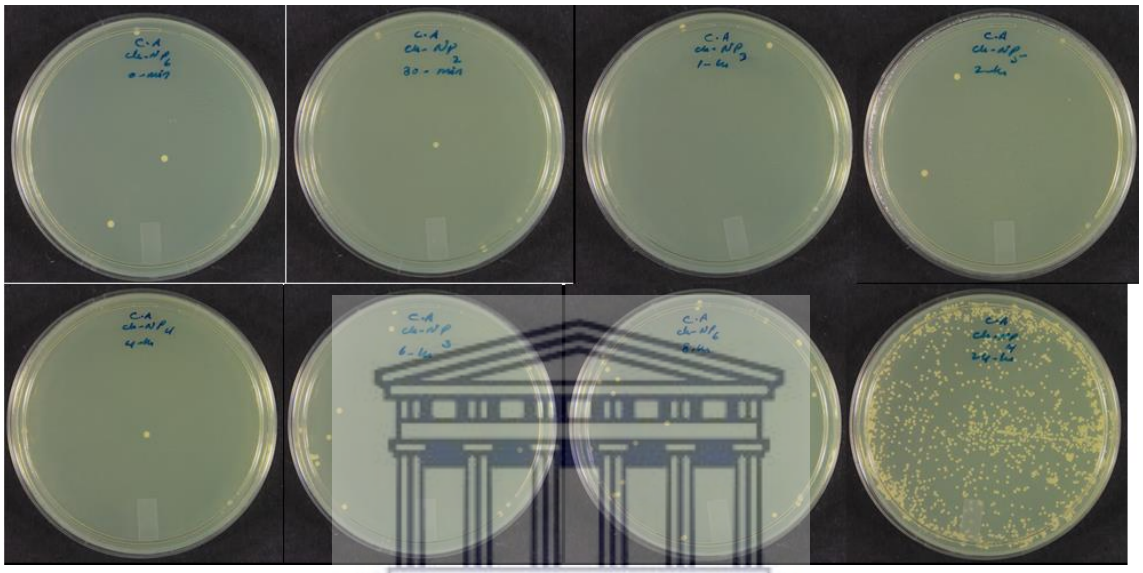

Figure 5-11: The colony forming units of *C. albicans* over time following its exposure to 3% Ch-Np.

5.7.2 Comparison between the antimicrobial effect of Ch-Np to LMW-Ch

The effect of Ch-Np against planktonic cells of *S. mutans*, *E. faecalis* and *C. albicans* was compared to the effect of 3% LMW-Ch (chapter 3). The data was analyzed using the Kaplan-Meir test. The mean, median and standard error of the survival rate of each microbial species when exposed to 3% Ch-Np and 3% LMW-Ch are shown in Table 5-5.

Table 5-5: The Mean, median and standard error for the survival time of *S. mutans*, *E. faecalis* and *C. albicans* when exposed to 3% Ch-Np and 3% LMW-Ch.

Means and Medians for Survival Time									
Microorganism	Particle size	Mean				Median			
		Estimate	Std. Error	95% Confidence Interval		Estimate	Std. Error	95% Confidence Interval	
				Lower Bound	Upper Bound			Lower Bound	Upper Bound
S. mutans	Ch-Np	6.5	1.18	4.18	8.82	4	1.07	1.91	6.1
	LMW-Ch	8.03	1.37	5.34	10.73	6	0.91	4.21	7.79
	Overall	7.24	0.9	5.48	9	4	0.71	2.61	5.39
E. faecalis	Ch-Np	7	1.25	4.56	9.44	4	1.03	1.98	6.02
	LMW-Ch	9.69	1.56	6.62	12.8	6	0.85	4.3	7.66
	Overall	8.27	0.99	6.34	10.2	6	0.64	4.75	7.25
C. albicans	Ch-Np	17	1.77	13.52	20.47	.	.	.	.
	LMW-Ch	11.65	1.85	8.02	15.27	8	1.34	5.37	10.63
	Overall	14.13	1.37	11.44	16.83	8	4.73	0	17.27
Overall	Overall	9.45	0.64	8.19	10.72	6	0.47	5.07	6.93

a. Comparison between the antimicrobial effect of Ch-Np and LMW-Ch against planktonic cells of *S. mutans*

The Kaplan-Meir survival function curve showed that *S. mutans* was observed at zero minute only when exposed to 3% Ch-Np. It was observed up to 4 hours following its exposure to 3% LMW-Ch (Figure 5-12).

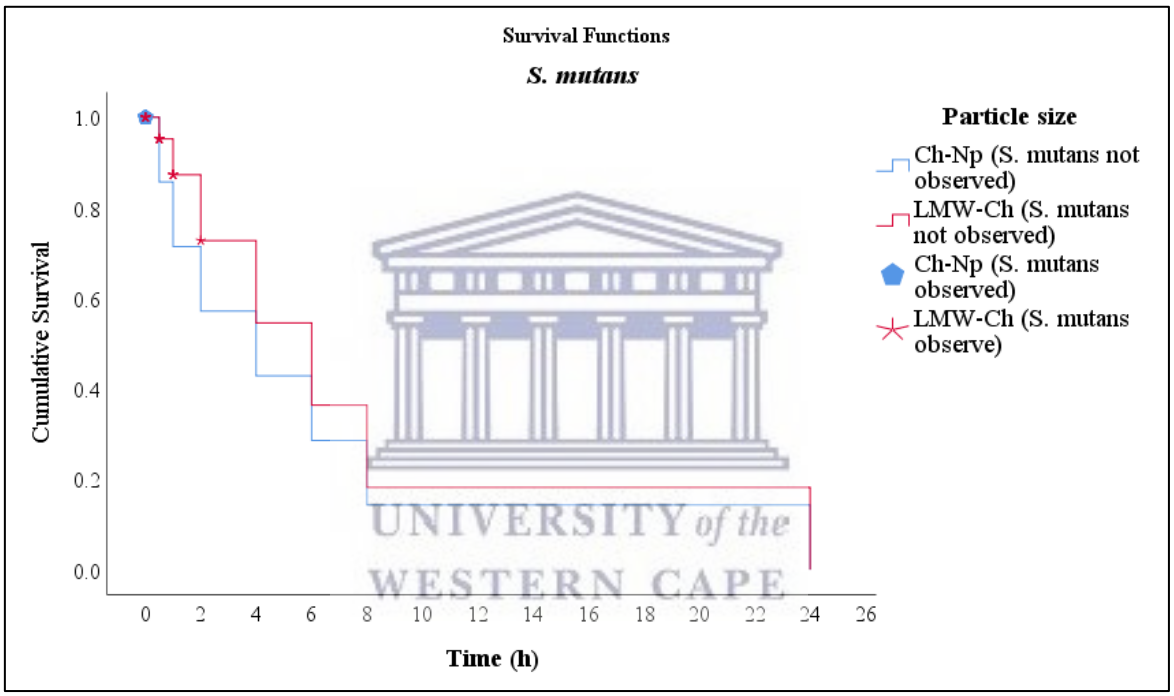

Figure 5-12: Survival function curve of *S. mutans* showing the time at which it was observed following its exposure to 3% Ch-Np and 3% LMW-Ch.

At zero minute *S. mutans* showed a mean number of Log CFU/mL of 6.70 following its exposure to 3% Ch-Np. This number declined to zero at 30 minutes showing complete eradication even after 24 hours contact time. The mean number of the log CFU/mL of *S. mutans* when exposed to 3% LMW-Ch at zero minute was 6.72 and declined to 1.03 at 2 hours and showed complete eradication at 4 hour contact time. The mean number of the Log CFU/mL of *S. mutans* following its exposure to 3% Ch-Np and 3% LMW-Ch compared to its normal growth rate are shown in Table 5-6.

Table 5-6: The mean number of the Log CFU/mL of *S. mutans* following its exposure to 3% Ch-Np and 3% LMW-Ch compared to the positive control group

Time (h)	***S. mutans* exposed to 3% Ch-Np**	***S. mutans* exposed to 3% LMW-Ch**	**Normal growth rate of *S. mutans* (control)**
0	6.70	6.72	6.97
0.5	0.00	4.30	6.86
1	0.00	3.20	6.83
2	0.00	1.03	6.92
4	0.00	0.00	6.97
6	0.00	0.00	6.94
8	0.00	0.00	6.98
24	0.00	0.00	6.98

The mean number of the Log CFU/mL of *S. mutans* following its exposure to 3% Ch-Np and 3% Ch-Np compared to the mean number of the Log CFU/mL of its normal growth rate are shown in Figure 5-13. Complete eradication of *S. mutans* at 30 minutes following its exposure to 3% Ch-Np compared to 4 hours following its exposure to 3% LMW-Ch was observed.

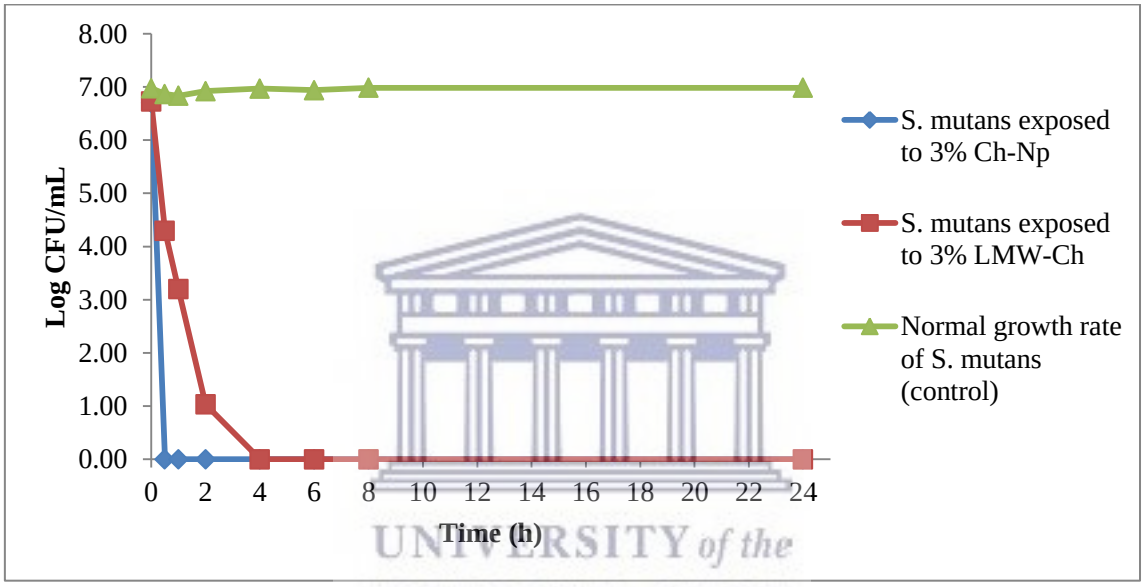

Figure 5-13: The mean Log CFU/mL of *S. mutans* following its exposure to 3% Ch-Np and 3% LMW-Ch over time.

b. Comparison between the antimicrobial effect of Ch-Np and LMW-Ch against planktonic cells of *E. faecalis*

The Kaplan-Meir survival function curve showed that *E. faecalis* was observed at zero and 30 minutes when exposed to 3% Ch-Np. It was observed up to 4 hours following its exposure to 3% LMW-Ch (Figure 5-14).

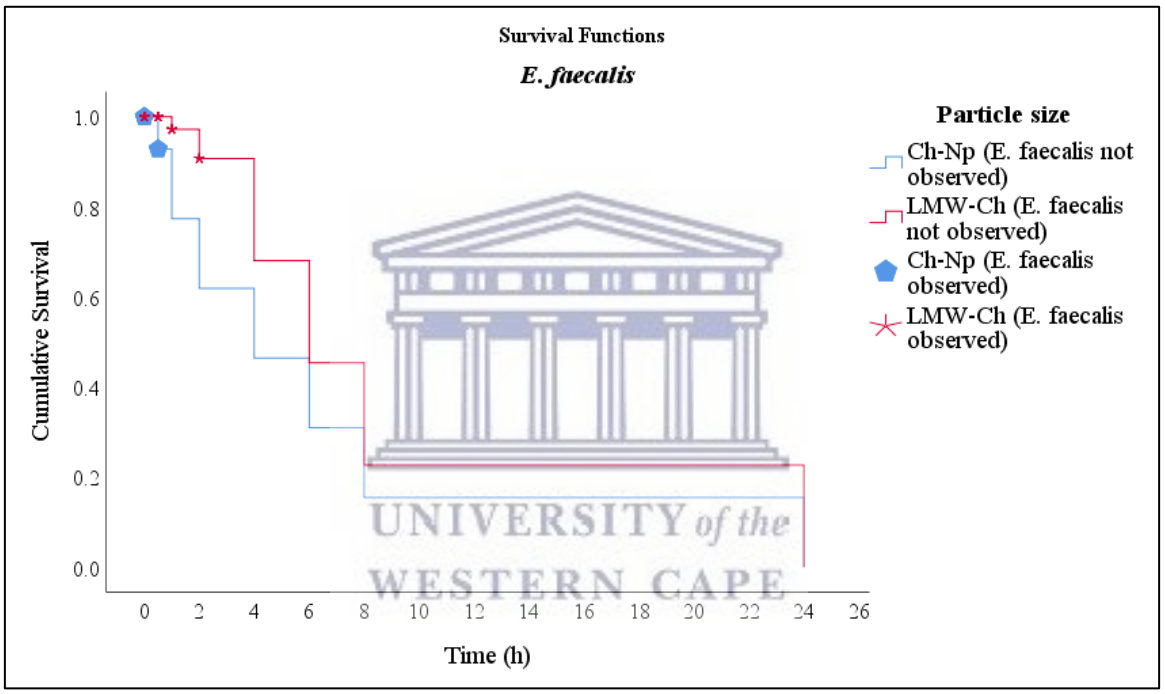

Figure 5-14: Survival function curve of *E. faecalis* showing the time at which it was observed following its exposure to 3% Ch-Np and 3% LMW-Ch.

At zero minute *E. faecalis* showed a mean number of Log CFU/mL of 6.55 following its exposure to 3% Ch-Np. This number declined to 3.07 at 30 minutes and showed complete eradication of *E. faecalis* at 1 hour contact time that continued after 24 hours contact time. When *E. faecalis* was exposed to 3% LMW-Ch it showed a mean number of the Log CFU/mL at zero minute of 6.98. This number declined to a minimum of 4.11 at 2 hours contact time and showed complete eradication at 4 hours contact time. The mean number of the log CFU/mL of *E. faecalis* following its exposure to 3% Ch-Np and 3% LMW-Ch compared to its normal growth rate, represented by mean number of the Log CFU/mL, are shown in Table 5-7.

Table 5-7: The mean number of the Log CFU/mL of *E. faecalis* following its exposure to 3% Ch-Np and LMW-Ch compared to the positive control group

Time (h)	***E. faecalis* exposed to 3% Ch-N.P**	***E. faecalis* exposed to 3% LMW-Ch**	**Normal growth rate of *E. faecalis* (control)**
0	6.55	6.98	6.98
0.5	3.07	6.86	6.98
1	0.00	5.48	6.98
2	0.00	4.11	6.98
4	0.00	0.00	6.98
6	0.00	0.00	6.98
8	0.00	0.00	6.98
24	0.00	0.00	6.98

The mean number of the Log CFU/mL of *E. faecalis* following its exposure to 3% Ch-Np and 3% LMW-Ch compared to the mean number of the Log CFU/mL of its normal growth rate are shown in Figure 5-15. Complete eradication of *E. faecalis* was observed at 1 hour following its exposure to 3% Ch-Np compared to 4 hours following its exposure to 3% LMW-Ch.

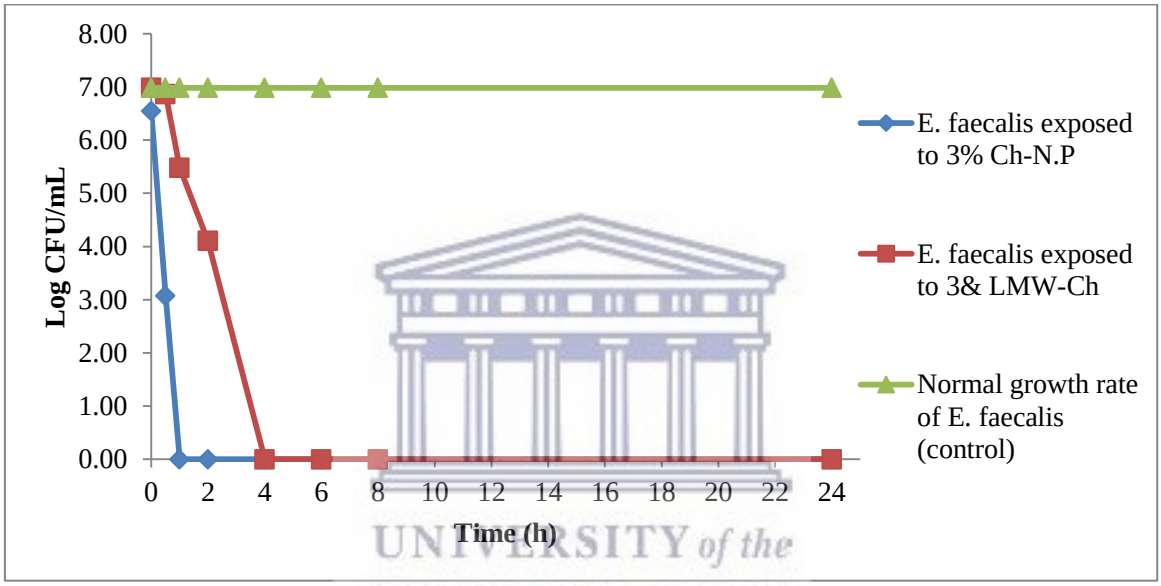

Figure 5-15: The mean Log CFU/mL of *E. faecalis* following its exposure to 3% Ch-Np and 3% LMW-Ch overtime.

c. Comparison between the antimicrobial effect of Ch-Np and LMW-Ch against planktonic cells of *C. albicans*

The Kaplan-Meir survival function curve showed that *C. albicans* was observed at all times when it was exposed to 3% Ch-Np. When it was exposed to LMW-Ch it was observed at zero minute, 30 minutes, 1 and 2 hours and not observed at 4 hours contact time. It was re-observed again at 6 hours contact time and continued to be observed until 24 hours contact time (Figure 5-16).

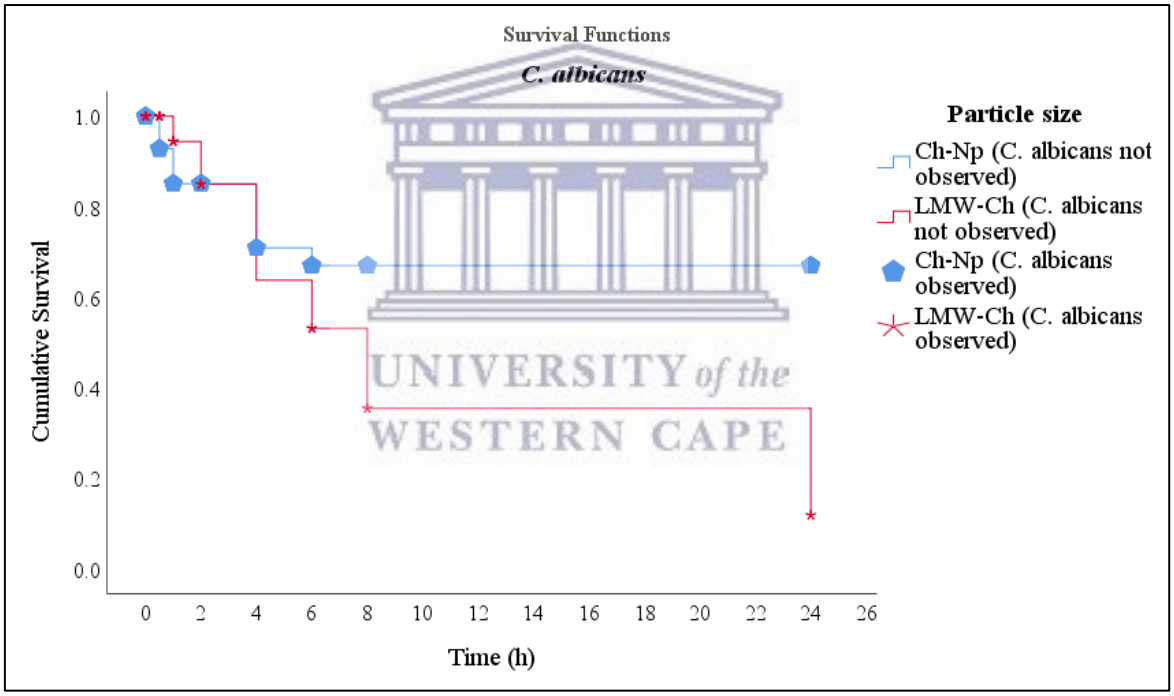

Figure 5-16: Survival function curve of *C. albicans* showing the time at which it was observed following its exposure to 3% Ch-Np and 3% LMW-Ch.

At zero minute *C. albicans* showed a mean number of Log CFU/mL of 4.84 following its exposure to 3% Ch-Np. This number declined initially at 30 minutes to an average of 2.38 to reach a minimum of 1.55 at 4 hours contact time. However, it started to increase again at 6 hour contact time to reach a maximum of 6.93 CFU/mL at 24 hours contact time. However, when *C. albicans* was exposed to 3% LMW-Ch it showed a mean number of Log CFU/mL at zero minute of 5.10. This number declined to a minimum of 2.33 at 2 hours contact time and reached zero at 4 hours contact time. The number of the Log CFU/mL started to increase again at 6 hour contact time to be 2.62 and reached a maximum of 2.22 at 24 hours contact time. The mean number of the log CFU/mL of *C. albicans* following its exposure to 3% Ch-Np and 3% LMW-Ch compared to its normal growth rate represented by mean number of the Log CFU/mL are shown in Table 5-8.

Table 5-8: The mean number of the Log CFU/mL of *C. albicans* following its exposure to 3% Ch-Np compared to the positive control group

Time (h)	***C. albicans* exposed to 3% Ch-Np**	***C. albicans* exposed to 3% LMW-Ch**	**Normal growth rate of *C. albicans* (control)**
0	4.84	5.10	5.41
0.5	2.38	5.09	5.28
1	2.30	3.16	5.11
2	4.74	2.33	4.51
4	1.55	0.00	5.51
6	4.27	2.62	6.65
8	5.60	1.62	6.98
24	6.93	2.22	6.98

The mean number of the Log CFU/mL of *C. albicans* following its exposure to 3% Ch-Np and 3% LMW-Ch compared to the mean number of the Log CFU/mL of its normal growth rate are shown in Figure 5-17. Ch-Np showed fungistatic activity at 4 hours contact time.

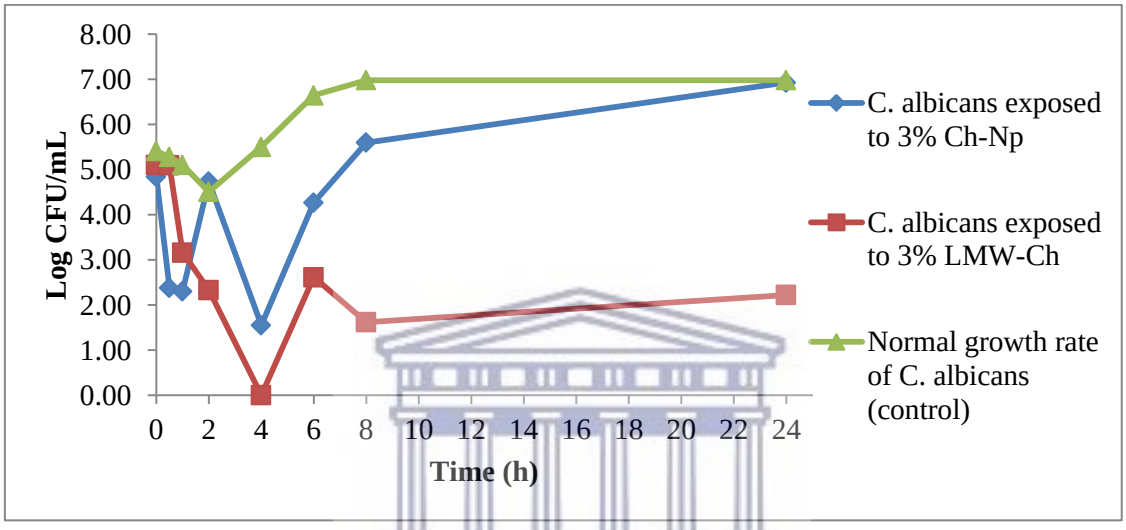

Figure 5-17: The distribution of the mean Log CFU/mL of *C. albicans* following its exposure to 3% Ch-Np and 3% LMW-Ch over time.

Comparison between the effect of 3% Ch-Np and 3% LMW-Ch among each microbial species was tested using the Breslow (generalized Wilcoxon) test. The Breslow test showed a statistical difference between the effect of 3% Ch-Np and 3% LMW-Ch against *E. faecalis* ($p < 0.05$). There was no statistical difference between the effect of 3% Ch-Np and 3% LMW-Ch against *S. mutans* and *C. albicans* ($p < 0.02$) (Table 5-9*)*.

Table 5-9: Pairwise comparison between the antimicrobial effect of 3% Ch-Np and 3% LMW-Ch against *S. mutans*, *E. faecalis* and *C. albicans*.

Pairwise Comparisons						
	Microorganism	Particle size	Ch-Np		LMW-Ch	
			Chi-Square	Sig.	Chi-Square	Sig.
Breslow (Generalized Wilcoxon)	*S. mutans*	Ch-Np			2.32	0.13
		LMW-Ch	2.32	0.13		
	E. faecalis	Ch-Np			6.33	0.01
		LMW-Ch	6.33	0.01		
	C. albicans	Ch-Np			0.35	0.56
		LMW-Ch	0.35	0.56		

5.7.3 Effect of Ch-Np against biofilm biomass of endodontic pathogens

The effect of Ch-Np against the biofilm biomass of *S. mutans*, *E. faecalis* and *C. albicans* was evaluated using microtiter plate biofilm assay. The data was analyzed using the Mann Whitney U test. The mean, median and standard error of the optical density of each microbial species biofilm in a control condition and following its exposure to 3% Ch-Np are shown in Table 5-10. The biofilm of *S. mutans* showed a mean optical density of 1.14 before exposure to 3% Ch-Np which decreased to 0.48 after it was exposed to 3% Ch-Np. The biofilm of *E. faecalis* showed a mean optical density of 0.34 before exposure to 3% Ch-Np which decreased to 0.09 after it was

exposed to 3% Ch-Np. The biofilm of *C. albicans* showed a mean optical density of 0.14 before exposure to 3% Ch-Np which decreased to 0.09 after it was exposed to 3% Ch-Np.

Table 5-10: The Mean, median and standard error for the optical density of *S. mutans*, *E. faecalis* and *C. albicans* biofilm in normal conditions (control) and following its exposure to 3% Ch-Np

	Mean	**Median**	**Std. Error of Mean**	**Range**	**Skewness**	**Std. Error Skewness**
S. mutans	0.48	0.48	0.01	0.14	-0.28	0.64
S. mutans **(control)**	1.14	1.23	0.20	1.69	-0.25	0.64
E. faecalis	0.09	0.09	0.00	0.04	0.69	0.66
E. faecalis **(control)**	0.34	0.34	0.01	0.07	0.27	0.64
C. albicans	0.09	0.08	0.01	0.10	0.72	0.66
C. albicans **(control)**	0.14	0.13	0.01	0.06	0.41	0.64

There was a difference in the distribution of the biofilm optical density of *S. mutans*, *E. faecalis* and *C. albicans* before and after exposure to 3% Ch-Np (Figure 5-18).

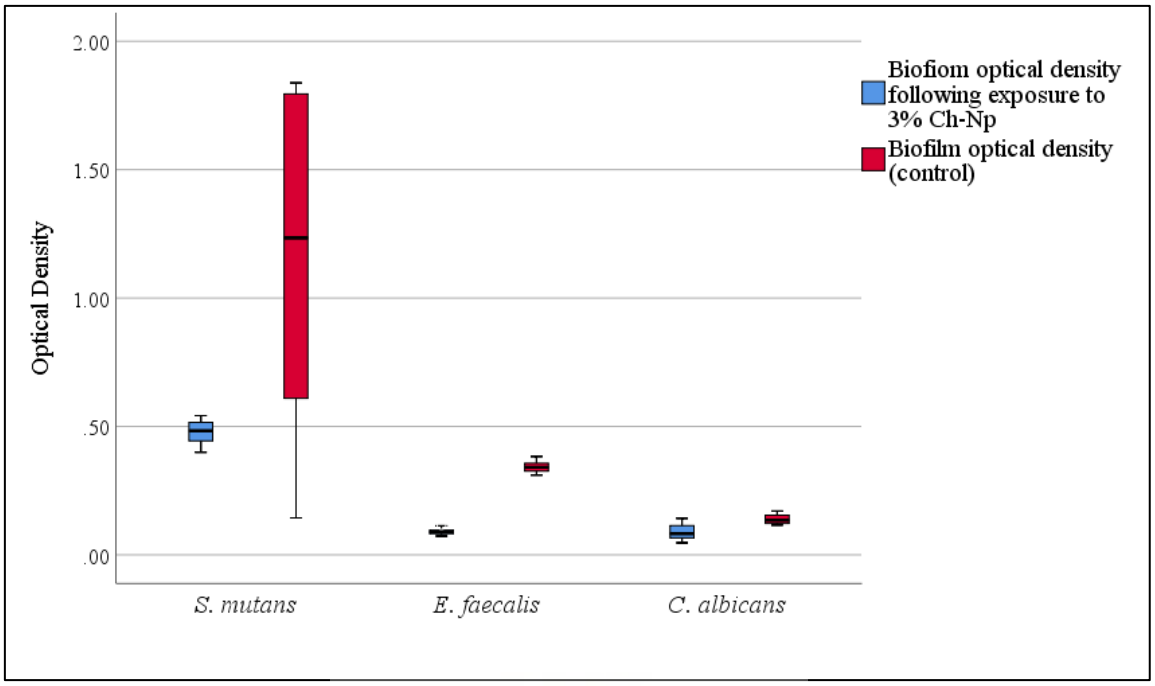

Figure 5-18: Box and Whisker plots demonstrating the median, distribution, maximum and minimum values of the biofilm optical density of *S. mutans*, *E. faecalis* and *C. albicans* in normal conditions (control) and following its exposure to 3% Ch-Np.

The Mann Whitney U test was used to compare the effect of 3% Ch-Np against biofilms of *S. mutans*, *E. faecalis* and *C. albicans* with the biofilms of *S. mutans*, *E. faecalis* and *C. albicans* in a control condition. 3% Ch-Np showed a statistically significant difference in the biofilm biomass of *S. mutans* (p = 0.007), *E. faecalis* (p = 0.000) and *C. albicans* (p = 0.004) as shown in Table 5-11.

Table 5-11: The effect of 3% Ch-Np on the biofilm biomass of *S. mutans*, *E. faecalis* and *C. albicans* (statistical analysis using the Mann-Whitney U test).

	E. faecalis	***S. mutans***	***C. albicans***
Z	-4.161	-2.714	-2.829
Asymp. Sig. (2-tailed)	0	0.007	0.005
Exact Sig. [2*(1-tailed Sig.)]	.000b	.006b	.004b

5.8 Discussion

Although LMW-Ch showed antimicrobial activity against *S. mutans, E. faecalis* and *C. albicans*, its main drawback as active antimicrobial component of intra-canal medicament is its large particle size which may limit its ability to diffuse inside the dentinal tubules. Furthermore, the inability of chitosan to dissolve in water may render it difficult to be removed from the root canal system. Hence in this study LMW-Ch was converted to water soluble Ch-Np using the electrospraying method (chapter 4).

The presence of chitosan on a nano-scale level may enhance its ability to diffuse inside the dentinal tubules which have a diameter ranging between 2.5 µm near the pulp chamber and 1.2 µm in the middle of the dentine (Garberoglio and Brännström, 1976), this ability to be small enough to enter the dentinal tubules may enhance its antimicrobial activity inside the root canal system. The presence of chitosan on a nano-scale level may overcome the antimicrobial resistance of some of the currently available antimicrobial agents as it possesses different mechanisms to eradicate the microbial cells (Pelgrift and Friedman, 2013).

Endodontic pathogens are present inside the root canal system in planktonic and biofilm forms (Usha, 2010; Siqueira *et al.*, 2010). This requires an antimicrobial agent that is able to act against both forms of microbial contamination. Hence in this study Ch-Np was evaluated against *S. mutans*, *E. faecalis* and *C. albicans* in planktonic and biofilm states. For planktonic cells the method used to evaluate the antimicrobial effect of Ch-Np was a Time-Kill Test, which also allows for comparing its antimicrobial effect to LMW-Ch. For microbial biofilm biomass the method used to evaluate the antimicrobial effect of Ch-Np was a microtiter biofilm assay which observed the attachment of

microbial biofilm to a surface (Merritt *et al.*, 2011). Furthermore, the microtiter plate assay is more reliable and provided more clinical significance compared to other methods used to evaluate the biofilm biomass such as the tube test (Deighton and Balkau, 1990).

Antimicrobial effect of Ch-Np against endodontic pathogens in a planktonic state

Ch-Np eradicated *S. mutans* and *E. faecalis* completely in a planktonic state. One of the main factors that may contribute to the bactericidal effect of Ch-Np is its high positively charged surface that resulted from the electrical current during the electrospraying process. The high positive surface charge of Ch-Np may facilitate its binding to the negatively charged bacterial cell wall (Qi *et al.*, 2004) which may disrupt its function such as cell permeability. Additionally, the presence of chitosan on a nano-scale level may facilitate its penetration inside the bacterial cells causing more damage as suggested by Sarwar *et al*., (2014).

The difference in the time required by Ch-Np to completely eradicate planktonic cells of *S. mutans* and *E. faecalis* may be due to the morphological difference between these species. For instance, *S. mutans* and *E. faecalis* are both Gram positive bacteria, but, they showed differences in their genetic mapping (Hardie and Whiley, 1997; Schleifer and Kilpper-Bälz, 1984). This may be reflected in their defence mechanisms against Ch-Np used in this experiment and thus their eradication time.

Chitosan nanoparticles could not completely eradicate planktonic cells of *C. albicans*. This may be due to the rigid cell wall of *C. albicans* which may prevent the penetration of the Ch-Np into the fungal cell. An important factor that may explain the ability of planktonic cells of *C. albicans* to re-grow is the possible development of a resistance

mechanism by *C. albicans* to Ch-Np. *C. albicans* has the ability to adapt to any environmental changes and produce genetically altered species for better adaptation to the new stressed environment (Kim *et al.*, 2015). This assumption is shown in Figure 5-10 as the mean number of Log CFU/mL showed initial reduction followed by increase in the mean Log CFU/mL. The fluctuation in the mean number Log CFU/mL over time may indicate injury of some of *C. albicans* cells while other cells start to produce a new strain that is resistant to the effect of Ch-Np.

Another factor that may explain the inability of Ch-Np to eliminate *C. albicans* is the low concentration used in this study. Higher concentrations of Ch-Np are required to eliminate the planktonic cells of *C. albicans* (MubarakAli *et al.*, 2018; Yien *et al.*, 2012). Furthermore, the high growth rate of *C. albicans* following its exposure to water soluble Ch-Np suggests that water soluble Ch-Np promoted the growth of *C. albicans*. This assumption was also reported by Qin *et al* (2006) who showed that *C. albicans* growth rate increased in the presence of water-soluble chitosan.

The antimicrobial effect of chitosan nanoparticles *vs*. chitosan

The effect of the particle size of chitosan was evaluated by comparing the survival time of *S. mutans*, *E. faecalis* and *C. albicans* following their exposure to 3% Ch-Np and 3% LMW-Ch.

Ch-Np eradicated *S. mutans* and *E. faecalis* more rapidly compared to LMW-Ch at the same concentration indicating that, the small particle size of chitosan may result in a better antimicrobial effect. This effect may be due to the multiple antimicrobial mechanisms adopted by Ch-Np (Pelgrift and Friedman, 2013) compared to LMW-Ch which may produce an antimicrobial effect through its binding to the microbial cell wall

(Chung *et al.*, 2004). Ch-Np may diffuse through the microbial cell wall as a result of their small particle size enhancing their action by producing multiple activities inside the microbial cells (Pelgrift and Friedman, 2013; Chávez de Paz *et al.*, 2011).

A greater antimicrobial effect of Ch-Np compared to LMW-Ch against *C. albicans* may be suggested as Ch-Np showed a reduction in the mean number of the Log CFU/mL of *C. albicans* at two time interval (1 and 4 hours) compared to only one time interval (4 hours) when it was exposed to LMW-Ch indicating a better antifungal effect of chitosan on a nano-scale level.

Unlike LMW-Ch which possess antimicrobial activity in acidic medium (Kong *et al.*, 2010), Ch-Np was able to produce a greater antimicrobial effect at neutral pH which may indicate that the antimicrobial effect resulted from the small particle size rather than the presence of chitosan in an acidic medium. Similar results that showed the effect of the particle size of chitosan on its antimicrobial efficacy was shown by Aliasghari *et al.*, (2016).

Effect of Ch-Np against biofilm biomass of endodontic pathogens

S. mutans, *E. faecalis* and *C. albicans* showed significant reduction in their biofilm biomass when exposed to 3% Ch-Np. The significant effect of Ch-Np in reducing the biofilm biomass of all tested pathogens may be due to the ability of the nanoparticles to penetrate the extracellular polysaccharide biofilm's matrix as a result of its small particle size and ability to attach to the negatively charged microbial cell wall as a result of its highly positively charged surface. Furthermore, the antimicrobial mechanism of nanoparticles against the integrity of microbial biofilm may be due to changes in the structural integrity and electrochemical interaction on the surface and in the enzymes of

the microbial cells, following their penetration through the extracellular polymeric matrix. Similar explanation on the effect of Ch-Np against the biofilm structure was demonstrated by Lee *et al*., (2018) and Chung *et al*., (2004).

E. faecalis biofilm formation is enhanced by the presence of *S. mutans* (Deng *et al.*, 2009). As a result, the antimicrobial activity of Ch-Np shown in this study may further contribute to the elimination of *E. faecalis* through its antimicrobial effect against *S. mutans* and its ability to disrupt the biofilm biomass of the two pathogens. The significant reduction in the biofilm biomass formation of *C. albicans* following its exposure to Ch-Np may enhance the antimicrobial effect of other antimicrobial irrigant solutions.

The results of this study were similar to the results obtained by Kishan *et al*., (2008) and Shertha *et al*., (2010) who showed that Ch-Np synthesized by the ionic gelation method caused a significant reduction of its biofilm state.

5.9 Conclusion

The use of water soluble chitosan nanoparticles as antimicrobial agent resulted in complete eradication of *S. mutans* and *E. faecalis* and showed a reduction in the colony forming unit of *C. albicans* when tested in a planktonic state. Furthermore, it produced a significant reduction on the biofilm biomass of *S. mutans*, *E. faecalis* and *C. albicans*.

The use of chitosan on a nano-scale level showed enhanced antimicrobial activity. Hence it can be considered a plausible antimicrobial agent to act as new intra-canal medicament against endodontic pathogens.

5.10 References

Aliasghari, A., Khorasgani, M. R., Vaezifar, S., Rahimi, F., Younesi, H., and Khoroushi, M. (2016). Evaluation of antibacterial efficiency of chitosan and chitosan nanoparticles on cariogenic streptococci: an *in vitro* study. *Iranian Journal of Microbiology*, 8(2): 93-100.

Carpio-Perochena, A. d., Kishen, A., Felitti, R., Bhagirath, A. Y., Medapati, M. R., Lai, C., and Cunha, R. S. (2017). Antibacterial properties of chitosan nanoparticles and propolis associated with calcium hydroxide against single-and multispecies biofilms: an *in vitro* and *in situ* study. *Journal of Endodontics*, 43(8): 1332-1336.

Chávez de Paz, L. E., Resin, A., Howard, K. A., Sutherland, D. S., and Wejse, P. L. (2011). Antimicrobial effect of chitosan nanoparticles on *Streptococcus mutans* biofilms. *Applied and Environmental Microbiology*, 77(11): 3892-3895.

Christensen, G. D., Simpson, W., Younger, J., Baddour, L., Barrett, F., Melton, D., and Beachey, E. (1985). Adherence of coagulase-negative staphylococci to plastic tissue culture plates: a quantitative model for the adherence of staphylococci to medical devices. *Journal of Clinical Microbiology*, 22(6): 996-1006.

Chung, Y.-C., Su, Y. P., Chen, C.-C., Jia, G., Wang, H. L., Wu, J. G., and Lin, J. G. (2004). Relationship between antibacterial activity of chitosan and surface characteristics of cell wall. *Acta Pharmacologica Sinica*, 25(7): 932-936.

DaSilva, L., Finer, Y., Friedman, S., Basrani, B., and Kishen, A. (2013). Biofilm formation within the interface of bovine root dentin treated with conjugated chitosan and sealer containing chitosan nanoparticles. *Journal of Endodontics*, 39(2): 249-253.

Deighton, M. A., and Balkau, B. (1990). Adherence measured by microtiter assay as a virulence marker for *Staphylococcus epidermidis* infections. *Journal of Clinical Microbiology*, 28(11): 2442-2447.

Deng, D. M., Hoogenkamp, M. A., Exterkate, R. A. M., Jiang, L. M., van der Sluis, L. W. M., ten Cate, J. M., and Crielaard, W. (2009). Influence of *Streptococcus mutans* on *Enterococcus faecalis* Biofilm Formation. *Journal of Endodontics*, 35(9): 1249-1252.

Garberoglio, R., and Brännström, M. (1976). Scanning electron microscopic investigation of human dentinal tubules. *Archives of Oral Biology*, 21(6): 355-362.

Hardie, J., and Whiley, R. (1997). Classification and overview of the genera *Streptococcus* and *Enterococcus*. *Journal of Applied Microbiology*, 83(S1): 1-11.

Kim, S. H., Clark, S. T., Surendra, A., Copeland, J. K., Wang, P. W., Ammar, R., Collins, C., Tullis, D. E., Nislow, C., and Hwang, D. M. (2015). Global analysis of the fungal microbiome in cystic fibrosis patients reveals loss of function of the transcriptional repressor Nrg1 as a mechanism of pathogen adaptation. *PLoS Pathogens*, 11(11): 1-26.

Kishen, A., Shi, Z., Shrestha, A., and Neoh, K. G. (2008). An investigation on the antibacterial and antibiofilm efficacy of cationic nanoparticulates for root canal disinfection. *Journal of Endodontics*, 34(12): 1515-1520.

Kong, M., Chen, X. G., Xing, K., and Park, H. J. (2010). Antimicrobial properties of chitosan and mode of action: a state of the art review. *International Journal of Food Microbiology*, 144(1): 51-63.

Lee, D., Seo, Y., Khan, M. S., Hwang, J., Jo, Y., Son, J., Lee, K., Park, C., Chavan, S., and Gilad, A. A. (2018). Use of nanoscale materials for the effective prevention and extermination of bacterial biofilms. *Biotechnology and Bioprocess Engineering*, 23(1): 1-10.

Merritt, J. H., Kadouri, D. E., and O'Toole, G. A. (2011). Growing and analyzing static biofilms. *Current Protocols in Microbiology*, 22(1): 1B. 1.1-1B. 1.18.

Mohammadi, A., Hashemi, M., and Hosseini, S. M. (2016). Effect of chitosan molecular weight as micro and nanoparticles on antibacterial activity against some soft rot pathogenic bacteria. *LWT-Food Science and Technology*, 71: 347-355.

MubarakAli, D., LewisOscar, F., Gopinath, V., Alharbi, N. S., Alharbi, S. A., and Thajuddin, N. (2018). An inhibitory action of chitosan nanoparticles against pathogenic bacteria and fungi and their potential applications as biocompatible antioxidants. *Microbial pathogenesis*, 114: 323-327.

Peeters, E., Nelis, H. J., and Coenye, T. (2008). Comparison of multiple methods for quantification of microbial biofilms grown in microtiter plates. *Journal of Microbiological Methods*, 72(2): 157-165.

Pelgrift, R. Y., and Friedman, A. J. (2013). Nanotechnology as a therapeutic tool to combat microbial resistance. *Advanced Drug Delivery Reviews*, 65(13): 1803-1815.

Perinelli, D. R., Fagioli, L., Campana, R., Lam, J. K. W., Baffone, W., Palmieri, G. F., Casettari, L., and Bonacucina, G. (2018). Chitosan-based nanosystems and their exploited antimicrobial activity. *European Journal of Pharmaceutical Sciences*, 117: 8-20.

Qi, L., Xu, Z., Jiang, X., Hu, C., and Zou, X. (2004). Preparation and antibacterial activity of chitosan nanoparticles. *Carbohydrate Research*, 339(16): 2693-2700.

Qin, C., Li, H., Xiao, Q., Liu, Y., Zhu, J., and Du, Y. (2006). Water-solubility of chitosan and its antimicrobial activity. *Carbohydrate Polymers*, 63(3): 367-374.

Sarwar, A., Katas, H., and Zin, N. M. (2014). Antibacterial effects of chitosan–tripolyphosphate nanoparticles: impact of particle size molecular weight. *Journal of Nanoparticle Research*, 16(7): 2517-2531.

Schleifer, K. H., and Kilpper-Bälz, R. (1984). Transfer of *Streptococcus faecalis* and *Streptococcus faecium* to the *Genus Enterococcus* nom. rev. as *Enterococcus faecalis* comb. nov. and *Enterococcus faecium* comb. nov. *International Journal of Systematic and Evolutionary Microbiology*, 34(1): 31-34.

Shrestha, A., and Kishen, A. (2014). Antibiofilm efficacy of photosensitizer-functionalized bioactive nanoparticles on multispecies Biofilm. *Journal of Endodontics*, 40(10): 1604-1610.

Shrestha, A., Zhilong, S., Gee, N. K., and Kishen, A. (2010). Nanoparticulates for antibiofilm treatment and effect of aging on its antibacterial activity. *Journal of Endodontics*, 36(6): 1030-1035.

Siqueira, J. F., Rôças, I. N., and Ricucci, D. (2010). Biofilms in endodontic infection. *Endodontic Topics*, 22(1): 33-49.

Sutton, S. (2011). Accuracy of plate counts. *Journal of Validation Technology*, 17(3): 42-46.

Usha, H. (2010). Biofilm in endodontics: New understanding to an old problem. *International Journal of Contemporary Dentistry*, 1(3): 44-51.

Virlan, M. J. R., Miricescu, D., Radulescu, R., Sabliov, C. M., Totan, A., Calenic, B., and Greabu, M. (2016). Organic nanomaterials and their applications in the treatment of oral diseases. *Molecules*, 21(2): 207-230.

Wassel, M. O., and Khattab, M. A. (2017). Antibacterial activity against *Streptococcus mutans* and inhibition of bacterial induced enamel demineralization of propolis, miswak, and chitosan nanoparticles based dental varnishes. *Journal of Advanced Research*, 8(4): 387-392.

Yien, L., Zin, N. M., Sarwar, A., and Katas, H. (2012). Antifungal activity of chitosan nanoparticles and correlation with their physical properties. *International Journal of Biomaterials*, 2012: 1-9.

Chapter 6
Antimicrobial effects of a novel chitosan nanoparticle based intra-canal medicament

6.1 Review of the literature

Intra-canal medicaments are defined as the " temporary placement of strong disinfection medical agents in an attempt to sterilize the intra-canal space and to act as a physical and chemical blockage against coronal leakage from temporary filling material and at the same time to be biocompatible" (Kawashima *et al.*, 2009).

Several intra-canal medicaments are available, however they showed certain shortcomings such as the development of resistant microbial species (Chockattu *et al.*, 2018; Balasubramaniam and Jayakumar, 2017; Valera *et al.*, 2016). Most of the intra-canal medicaments lose their antimicrobial effectiveness when they are within the root canal system (Haapasalo *et al.*, 2007). Various mechanisms were suggested to explain the mechanism by which the antimicrobial effectiveness of these medicaments can be inhibited inside the root canal system. Haapasalo *et al*., (2007) proposed that inactivation of intra-canal medicaments inside the root canal system may result from their interaction with the hydroxyapatite of the dentine structure. Dentine can act as a

buffering agent to inhibit the effect of H^+ that is released from calcium hydroxide causing protein denaturation of the bacterial cell wall (Estrela *et al.*, 1995). Others suggested that inactivation of intra-canal medicaments may result from the chemical interaction that occurs between some of the intra-canal medicaments and the organic component (protein) in the root dentin or with the root canal system such as inflammatory exudate and remnants of pulp tissue (Portenier *et al.*, 2001). Chlorhexidine was found to lose its antimicrobial activity when in contact with saliva that already contains proteins such as albumin and mucin (Spijkervet *et al.*, 1990).

The effect of dentine on the antimicrobial activity of various intra-canal medicaments was evaluated by Portenier *et al.*, (2001). It was shown that the antimicrobial effectiveness of calcium hydroxide, iodine potassium and chlorhexidine against *E. faecalis* were inhibited in the presence of dentine and serum albumin. Furthermore, Haapasalo *et al.*, (2000) also showed that the antimicrobial effect of saturated calcium hydroxide, 0.5% and 0.05% chlorhexidine acetate, iodine potassium iodide and 1% sodium hypochlorite against *E. faecalis* was inhibited when it came in contact with dentine powder. Portenier *et al.*, (2006) also reported a delay in the killing time of *E. faecalis* when treated by 0.2% chlorhexidine and MTAD in the presence of dentine powder and serum albumin.

Intra-canal medicament vehicles

Several vehicles are available to carry the antimicrobial active component of intra-canal medicaments. Such vehicles can be categorized into aqueous, viscous and oily vehicles (Fava and Saunders, 1999). According to Fava and Saunders (1999), the ideal properties of intra-canal medicaments' vehicles include; (i) the ability to release the antimicrobial

agent gradually into the root canal system, (ii) ability to dissolve in tissue fluids and (iii) they do not induce hard tissue formation.

Aqueous vehicles are usually prepared by mixing the active component of the intra-canal medicament such as calcium hydroxide with different derivatives of water such as distilled water, saline or anaesthetic solutions. The intra-canal medicament is mixed with the aqueous vehicles until a desired paste consistency is formed (Fava and Saunders, 1999).

Viscous vehicles such as glycerine and propylene glycol were used to carry the active components of intra-canal medicaments (Srinivas *et al.*, 2016; Yücel *et al.*, 2007). Yücel *et al.*, (2007) used glycerine as a vehicle for calcium hydroxide and evaluated its effect on the pH of calcium hydroxide over time since the main antimicrobial mechanism of calcium hydroxide is its high pH. It was shown that the pH of calcium hydroxide increased following mixing with glycerine to show a maximum of an average pH of 12.13 which may increase its antimicrobial efficacy (Yücel *et al.*, 2007)

Oils such as silicon oil and eugenol were also used as vehicles for intra-canal medicaments. Metapex is a calcium hydroxide based intra-canal medicament that uses silicon oil as a vehicle (Sridhar and Tandon, 2010). Mustafa *et al.*, (2018) evaluated the root canal pH following its treatment with Metapex over time and compare it with calcium hydroxide mixed with saline since the antimicrobial effectiveness of calcium hydroxide is based on its pH. It was shown that the mixing of calcium hydroxide with saline has a significantly higher pH initially which starts to decrease after 14 days becoming lower than the pH of Metapex (Mustafa *et al.*, 2018).

Zeolites

Zeolites (Ze) are natural inorganic microporous crystalline hydrated sodium aluminosilicate materials (Gougazeh and Buhl, 2014). They are composed of ($Na_{12}[(-SiO_2)_{12}(AlO_2)_{12}]\cdot 27H_2O$) (Laurino and Palmieri, 2015). Their structure is found in a network form composed of SiO_4 and AlO_4 tetrahedra that are corner-shared to form a porous (cage) material with sizes ranging between 0.30 – 0.45 nm (small pore zeolites), 0.45 -0.60 nm (medium pore zeolites) and 0.60 – 0.80 nm (large pore zeolites) (Dusselier and Davis, 2018).

Various types of synthetic zeolites are available such as erionite, clinoptilolite, mordenite, and faujasite, based on their chemical and structural framework (Hedström, 2001). Zeolite Y is a type of faujasite zeolite with a pore diameter of 7.4 Å. The structure of zeolite Y is formed from primary units known as solidate cages that are arranged to from super-cages that can contain a material with 1.2 nm diameter (Taufiqurrahmi *et al.*, 2011). The chemical structure of zeolite Y is similar to the other types of zeolite except that it contains a Si:Al ratio of 2.5 to infinity (Verboekend *et al.*, 2016).

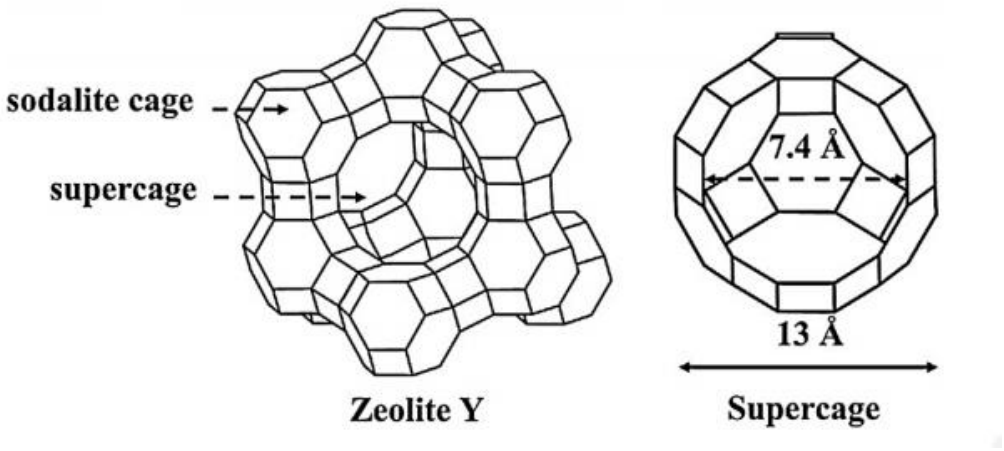

Figure 6-1: Framework structure of Zeolite-Y showing the primary unit (solidate cage) and the super-cage with a pore diameter of 7.4 Å. Chemical frame structure adapted from Kim and Yoon (2014).

Zeolite Y has a negative charge surface resulting from isomorphous substitution of Al^{3+} for Si^{4+} in its framework. This substitution needs to be balanced by a cation such as Na^{+}, NH^{4+} or H^{+} when the two charges are in close proximity (Dusselier and Davis, 2018). As a result of these properties zeolites are involved in various applications such as ion exchange, adsorption and catalysis (Taufiqurrahmi *et al.*, 2011).

In chemical and medical sciences, composite materials were synthesized by combining zeolites with different organic materials such as chitosan. The synthesized zeolite composite was able to adsorb copper while maintaining the properties of each element (Wan Ngah *et al.*, 2012b). Chitosan-zeolite nanocomposite was synthesized by Akmammedov *et al.*, (2018) and used as scaffold for bone tissue engineering. The newly synthesized nanocomposite caused proliferation of the bone marrow mesenchymal cell while maintaining its biodegradability and biocompatibility.

Antimicrobial cotton was synthesized by Scacchetti *et al.*, (2018) through its functionalization with chitosan-zeolite composite. Its antimicrobial properties were evaluated against *E. coli*, *S. aureus*, *C. albicans* and *Trichophyton rubrum*. Scacchetti *et al.*, showed that the newly synthesized cotton possessed antimicrobial activity against *S. aureus* and *T. ruburn*.

The cationic nature of zeolite which provides adsorption capability in addition to their porous structure, render them a suitable material to carry the antimicrobial Ch-Np to serve as intra-canal medicament.

6.2 Rationale of the study

The electrosprayed Ch-Np showed promising antimicrobial activity against *S. mutans*, *E. faecalis* and *C. albicans* in a planktonic and biofilm state. Hence, in order to be used as an intra-canal medicament it needs a vehicle which does not affect its antimicrobial properties. Furthermore, it should be able to maintain its antimicrobial activity even in the presence of tissue inhibitors such as dentine powder and serum albumin.

6.3 Aim of the study

The aim of the study was to synthesize a novel chitosan nanoparticle based intra-canal medicament using Zeolite-Y as a carrier and to evaluate its antimicrobial activity in the presence of tissue inhibitors.

6.4 Objectives

i. To synthesize a novel intra-canal medicament by loading chitosan nanoparticles into zeolite-Y.
ii. To evaluate the antimicrobial effect of the chitosan nanoparticles-zeolite nanocomposite against *S. mutans*, *E. faecalis* and *C. albicans* using an agar diffusion test.
iii. To evaluate the effect of tissue inhibitors such as dentine powder and serum albumin on the antimicrobial activity of the novel chitosan nanoparticles-zeolite nanocomposite using a Time-Kill Test.

6.5 Methodology

6.5.1 Synthesis and characterization of Ch-Np-Zeolite nanocomposite

To synthesize the novel chitosan nanoparticles-zeolite (Ch-Np-Zeolite) nanocomposite, 0.09 g of Ch-Np powder was dissolved in 3 mL of deionized water and stirred for 1 hour using a magnetic stirrer to allow complete dissolution of the Ch-Np. 1.6 g of Zeolite-Y (Zeolyst international, Netherland) was mixed with 3 mL of 3% (w/v) Ch-Np incrementally using a plastic spatula and a paper pad at room temperature for 30 seconds until a paste like consistency was formed. The paste was then loaded into a 5 mL disposable plastic syringe for ease of use within the root canal system.

a. Scanning electron microscopy (HRSEM)

The surface morphology of Zeolite-Y before and after mixing with Ch-Np was analyzed using high resolution scanning electron microscopy (HR-SEM). High resolution scanning electron microscopy images, using a Zeiss Gemini Auriga Scanning Electron Microanalyser equipped with a CDU – led detector at 3.00 kV with tungsten filament, of zeolite-Y before and after mixing with Ch-Np were generated. A small amount of zeolite-Y and Ch-Np-Zeolite nanocomposite was placed on stubs coated with carbon and the samples were then coated with a thin gold film to make the surface conductive and to prevent charging in the samples' morphology and to enhance the resolution of the samples' images. SEM images were taken with different magnification levels and at various points.

b. Energy dispersive spectroscopy (EDS) analysis

Following mixing of Ch-Np with zeolite Y, quantitative elemental analysis was done for the zeolite before and after mixing using energy-dispersive X-ray spectroscopy (EDS) (Field Emission High Resolution, Zeiss Gemini Auriga, Germany) to evaluate any changes in their elemental composition and mapping.

6.5.2 Antimicrobial effect of Ch-Np-Zeolite nanocomposite

The antimicrobial activity of the newly synthesized Ch-Np-Zeolite nanocomposite was evaluated against *S. mutans* (ATCC 25175), *E. faecalis* (ATCC 29212) and *C. albicans* (ATCC 90028) using an agar diffusion test.

The microbial species were incubated in brain heart infusion broth (BHI) at 37°C for 24 hours. Following the overnight culture, *S. mutans* and *E. faecalis* were subcultured in brain heart infusion agar plates and incubated overnight at 37°C. The microbial cells

were then suspended in phosphate buffer saline solution (PBS) and the concentration was adjusted to 0.5 Mcf using DensiCHEK Plus BioMérieux, Inc Durham.

A volume of 25 mL sterile brain heart infusion agar was poured into sterile petri dishes and allowed to harden at room temperature. A cotton swab from each microbial species was streaked in the poured agar plates. In each agar plate five holes (5 mm diameter each) were made (n = 15 for each species) and completely filled with the novel Ch-Np-Ze nanocomposite paste. The agar plates were incubated at 37°C for 24 hours. The zone of inhibition around each hole was measured in millimetres using an electronic digital caliper (Grip, RSA) (Figure 6-2).

Figure 6-2: Digital caliper used to measure the size of inhibition zone in millimetres around each hole

6.5.3 Effect of tissue inhibitors on the antimicrobial activity of Ch-Np-Zeolite nanocomposite

To determine whether tissue inhibitors like dentine powder or serum albumin have a negative effect on Ch-Np-Zeolite nanocomposite, the antimicrobial activity was further

tested against *S. mutans* and *E. faecalis* in the presence of dentine powder and serum albumin.

The antimicrobial activity of the Ch-Np-Zeolite nanocomposite was evaluated using a methodology adapted from Haapasalo *et al*., (2000) and Portenier *et al*., (2001) by measuring the number of CFU/mL before and after their exposure to Ch-Np-Ze nanocomposite in the presence or absence of tissue inhibitors over time.

a. Preparation of tissue inhibitors

i. Dentine powder preparation

Dentine powder was prepared from freshly extracted human teeth obtained from the Department of Oral Surgery, Faculty of Dentistry, University of the Western Cape. The teeth were extracted for orthodontic purposes. The teeth were kept in 5% sodium hypochlorite solution (Milton, RSA) to prevent any microbial growth and to remove all the soft tissue. The crowns of the teeth were cut off using a diamond bur at high speed handpiece. The pulp tissue was extirpated from all roots canals using barbed broach and the roots were rinsed thoroughly with distilled water to remove any excess sodium hypochlorite. The teeth roots were serialized by placing them in an autoclave (Hirayama, Japan) at 121°C for 15 minutes. The roots of the teeth were crushed into fine powder using a ball milling machine (Fritsch pulverisette, Germany) (Figure 6-3).

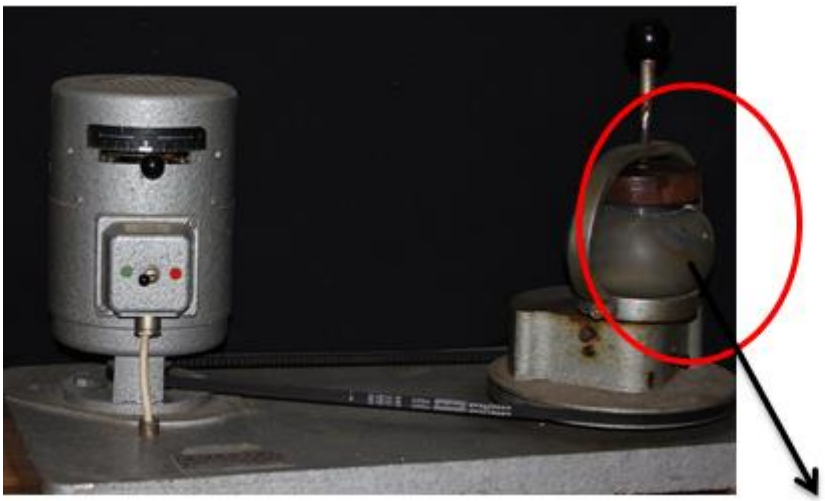

(A)

(B)

Figure 6-3: Photograph showing (A) Fritsch pulverisette ball milling machine, (B) two marble balls inside the chamber to crush the dentine.

ii. Bovine serum albumin

The effect of serum albumin was evaluated using bovine serum albumin purchased from Thermo Scientific (South Africa) (Lot No: RZB35918).

b. Antimicrobial assay

The prepared dentine powder was suspended in 150 µL sterile brain heart infusion broth to form a final concentration of 56% (w/v). A volume of 150 µL Ch-Np-Zeolite

nanocomposite was added to 150 µL dentine powder suspension (Figure 6-4). The mixtures were allowed to mix for two hours before adding 150 µL from the previously prepared 0.5 Mcf standard of *S. mutans* (experimental group A) and *E. faecalis* (experimental group B). The control group contained dentine powder suspension to which either *S. mutans* (control group C) or *E. faecalis* (control group D) was added. The mixture was incubated in an Orbital Shaker Incubator (Biocom Biotech, USA) at 37°C under aerobic conditions.

A volume of 150 µL Ch-Np-Zeolite nanocomposite was added to 150 µL bovine serum albumin suspension. The mixtures were allowed to mix for two hours before adding 150 µL from the previously prepared 0.5 Mcf standard of *S. mutans* (experimental group E) and *E. faecalis* (experimental group F). The control group contained serum albumin suspension to which either *S. mutans* (control group G) or *E. faecalis* (control group H) was added. The mixture was incubated in an Orbital Shaker Incubator (Biocom Biotech, USA) at 37°C under aerobic conditions.

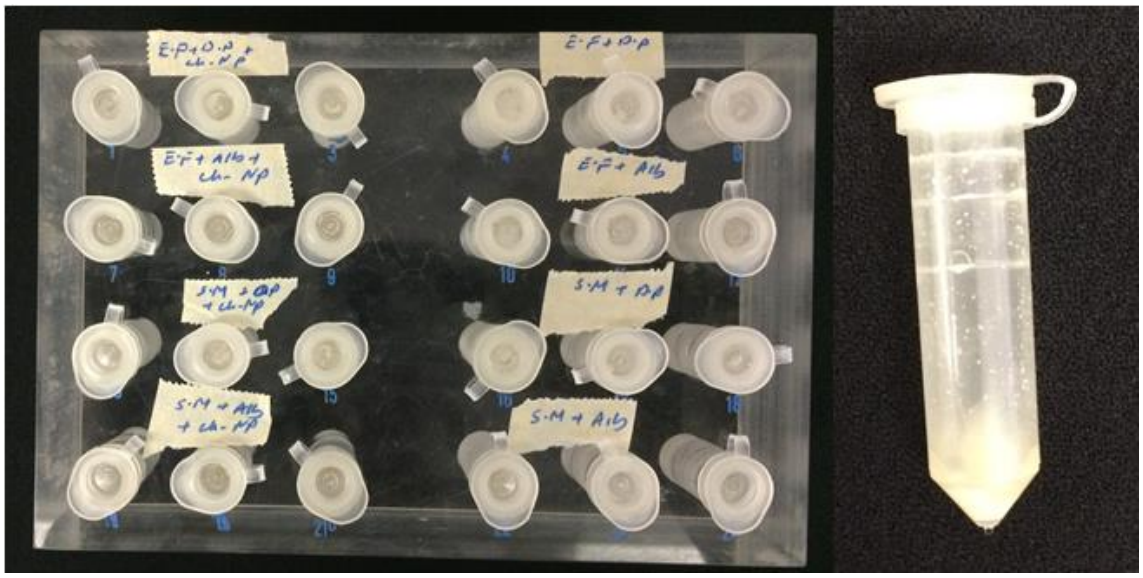

Figure 6-4: Eppendorf tube containing Ch-Np-Zeolite nanocomposite and dentine powder suspension.

50 µL PBS was added to each well and then 50 µL from each group was transferred and placed in a sterile 96-well microtiter plate. The suspension was diluted two-fold by transferring 50 µL from the first well to the second well proceeding up to the fifth well. The procedure of serial dilution was done at zero minute, 30 minutes, 1 hour and 24 hours. 2 µL from the final dilution of each group at each time was then transferred and streaked in brain heart infusion agar plate and incubated at 37°C for 24 hours under aerobic conditions. The numbers of the colony forming units (CFU) in each plate were counted following a standard protocol for microbial counting of colony forming units. The number of colony forming units that exceeded 300 were considered as too numerous to count (TNTC) and recorded as 300 (CFU), while those less than 30 were considered as too low to count (TLTC) and recorded as standard protocol for a microbial colony (Sutton, 2011). All tests were repeated in triplicate.

6.6 Data analysis

Results from each group were transferred to an Excel spreadsheet (Microsoft Corporation 2010, USA) and analysed using IBM SPSS statistics software (version 25, IBM, USA).

The difference between the antimicrobial effect of Ch-Np-Zeolite nanocomposite against *S. mutans*, *E. faecalis* and *C. albicans* was analysed using the Mann Whitney U test. A probability value of $p < 0.05$ was considered as a significant difference.

To evaluate the effect of tissue inhibitors on the antimicrobial activity of Ch-Np-Zeolite nanocomposite against *S. mutans* and *E. faecalis*, the data were expressed in Log CFU/mL and then analysed by measuring the number of the Log CFU/mL.

6.7 Results

6.7.1 Synthesis and characterization of Ch-Np-Zeolite nanocomposite

Mixing Ch-Np with Zeolite produced a white, creamy paste like consistency (Figure 6-5) that was easily dispensed into a syringe.

Figure 6-5: Consistency of the novel Ch-Np-Zeolite nanocomposite intra-canal medicament.

a. Scanning electron microscopy (HRSEM)

The HR-SEM analysis of Zeolite-Y before and after mixing with Ch-Np at different magnifications showed no change in its structural morphology (Figure 6-6). Furthermore, the SEM analysis showed that Zeolite-Y had a crystalline form.

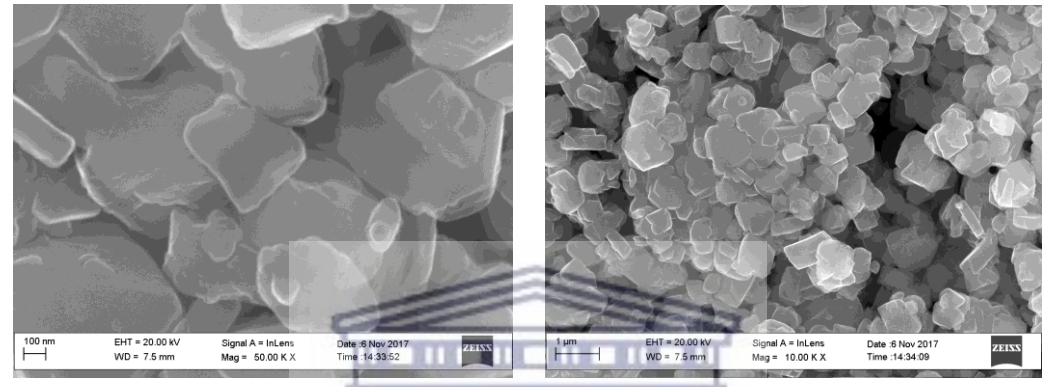

A

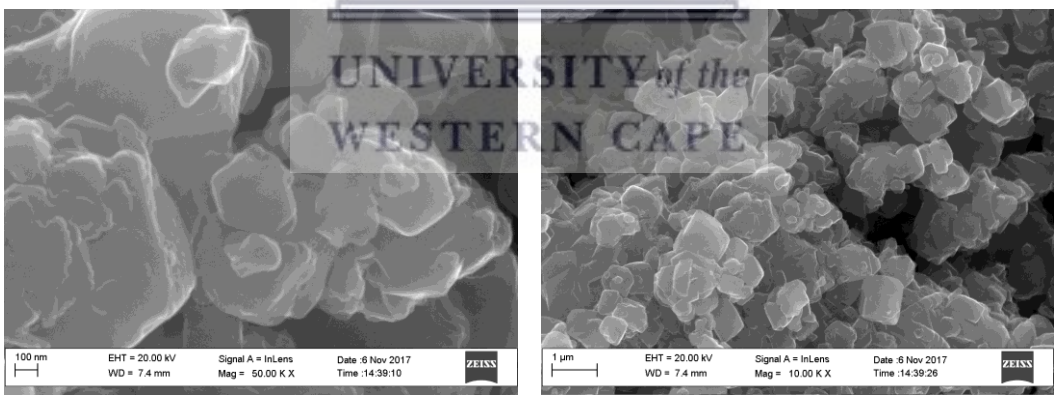

B

Figure 6-6: HR-SEM analysis of (A) Zeolite-Y before mixing with Ch-Np, (B) Zeolite-Y after mixing with Ch-Np. There was no change in the structural morphology of zeolite-Y before and after mixing with Ch-Np.

b. Energy dispersive spectroscopy (EDS) analysis

The elemental composition of zeolite-Y and Ch-Np-Zeolite nanocomposite was determined using energy dispersive spectroscopy. Figure 6-7 shows the peak signals and the atomic percentages of each element in zeolite-Y. The Si:Al was 2.71. Furthermore the Na^+ atomic percentage was 2.4.

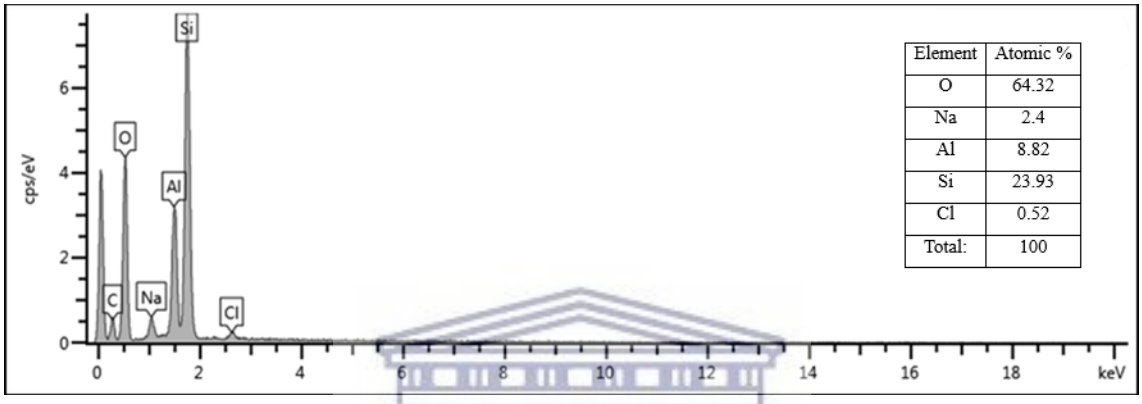

Element	Atomic %
O	64.32
Na	2.4
Al	8.82
Si	23.93
Cl	0.52
Total:	100

Figure 6-7: SEM-EDS of zeolite-Y showing the peak signal and atomic percentages of each element.

The peaks signals and the atomic percentages of each element in the Ch-Np-Zeolite nanocomposite are shown in Figure 6-8. The Si:Al ratio was reduced to 2.69. Na^+ atomic percentage was reduced to 2.58.

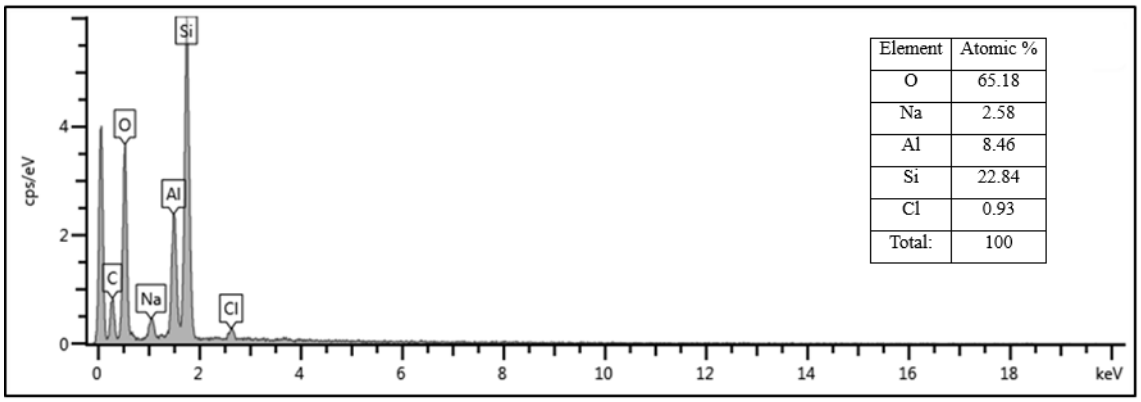

Element	Atomic %
O	65.18
Na	2.58
Al	8.46
Si	22.84
Cl	0.93
Total:	100

Figure 6-8: SEM-EDS of Ch-Np-Zeolite nanocomposite showing the peak signal and atomic percentages of each element.

6.7.2 Antimicrobial effect of Ch-Np-Zeolite nanocomposite

The antimicrobial activity of Ch-Np-Ze nanocomposite against *S. mutans*, *E. faecalis* and *C. albicans* was evaluated using an agar diffusion test. Zeolite-Y was used as a control. The mean sizes of the inhibition zones around each microbial species when treated with Ch-Np-Zeolite nanocomposite or Zeolite are shown in Table 6-1.

Table 6-1: Descriptive analysis showing the mean and standard deviation of the size of inhibition zones of Ch-Np-Ze nanocomposite around each tested microbial species

Size of inhibition zone (mm)			
Treatment	**Microorganism**	**Mean**	**Std. Deviation**
3% Ch-Np-Zeolite nanocomposite	*S. mutans*	9.57	0.80
	E. faecalis	7.85	0.59
	C. albicans	0.00	0.00
	Total	5.80	4.25
Zeolite	*S. mutans*	0.00	0.00
	E. faecalis	0.00	0.00
	C. albicans	0.00	0.00
	Total	0.00	0.00
Total	*S. mutans*	4.78	4.90
	E. faecalis	3.92	4.01
	C. albicans	0.00	0.00
	Total	2.90	4.18

The results showed that there was no antimicrobial activity when using zeolite-Y as a carrier against the three tested microbial species. This is demonstrated by the absence of an inhibition zone around zeolite-Y when tested against the three microbial species (Figure 6-10).

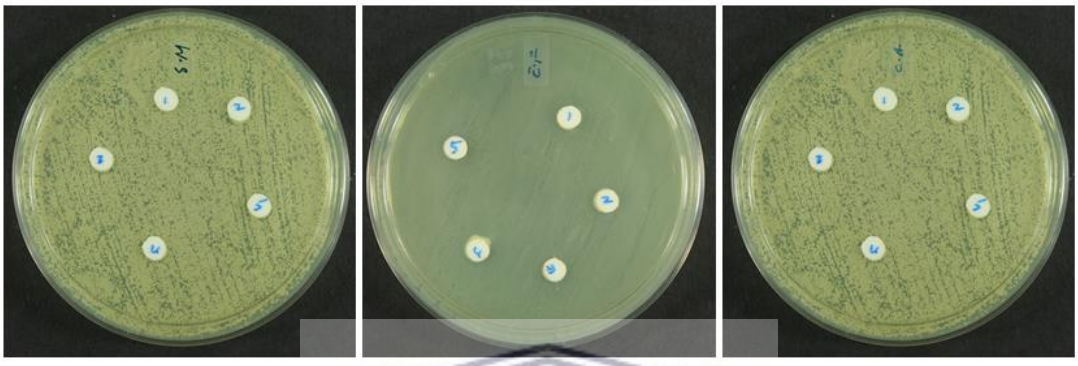

Figure 6-9: Brain heart infusion agar plate of (A) *S. mutans*, (B) *E. faecalis* and (C) *C. albicans* with holes filled with zeolite-Y showing no inhibition zone around them indicating the negative antimicrobial effect against them.

A similar effect was observed when Ch-Np-Zeolite nanocomposite was tested against *C. albicans* in which no zone of inhibition was observed (Figure 6-10).

Figure 6-10: Brain heart infusion agar plate streaked with *C. albicans* showing 5 holes containing 3% Ch-Np-Zeolite nanocomposite with no inhibition zone around them.

The control condition (Zeolite-Y mixed with distilled water) and the experimental group (*C. albicans*) had a mean size inhibition zone of zero and zero variance. Therefore, these observations were excluded from further statistical analysis.

Ch-Np-Zeolite nanocomposite showed activity against *S. mutans* and *E. faecalis* as a zone of inhibition was observed. The mean size of the inhibition zone when *S. mutans* and *E. faecalis* were exposed to the novel Ch-Np-Zeolite nanocomposite was 9.57 mm and 7.85 mm respectively (Figure 6-11). The mean, median and standard error of the size of the inhibition zone around each microbial species are shown in Table 6-2.

Figure 6-11: Brain heart infusion agar plate streaked with (A) *S. mutans*, (B) *E. faecalis* showing the inhibition zone around holes filled with 3% Ch-Np-Zeolite nanocomposite.

Table 6-2: Descriptive analysis showimg the mean, median , standard error of mean, range, skweness and standard error of skewness of the size of the inhibition zone around *S. mutans* and *E. faecalis*.

Size of inhibition zone (mm)						
Microorganism	Mean	Median	Std. Error of Mean	Range	Skewness	Std. Error of Skewness
S. mutans	9.57	9.45	0.21	3.22	0.8	0.58
E. faecalis	7.85	7.87	0.15	2.2	0.19	0.58

The distribution of the size of the inhibition zone around *S. mutans* and *E. faecalis* is shown in Figure 6-12.

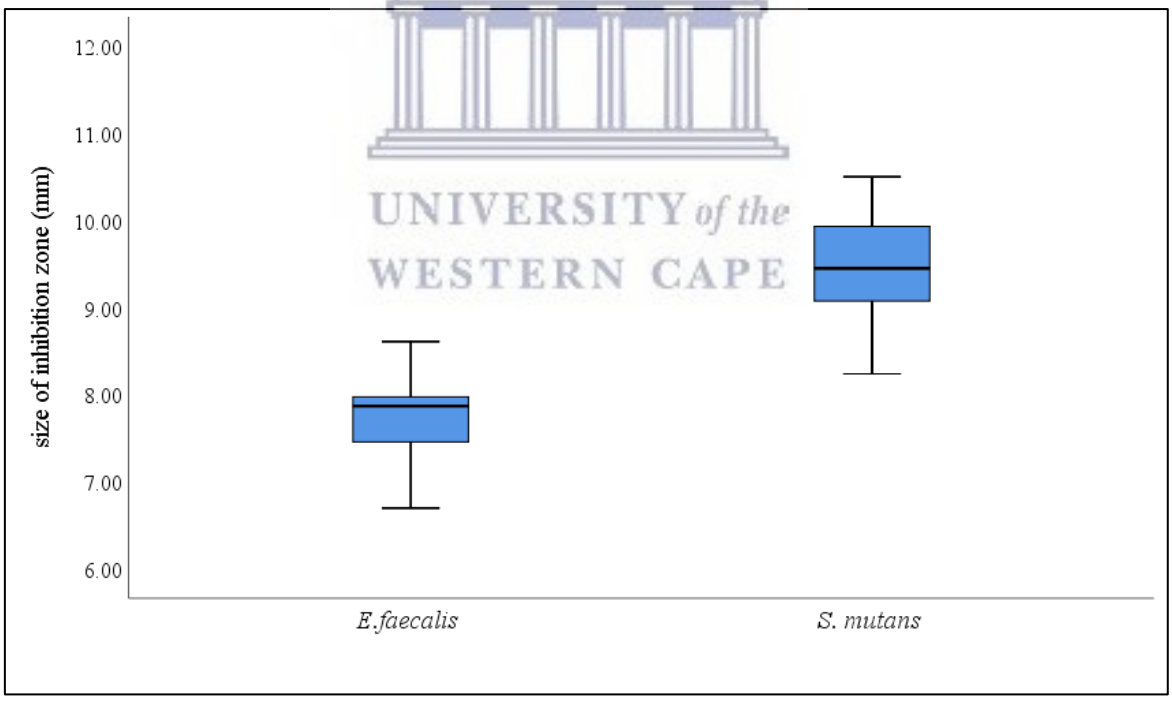

Figure 6-12: Box and Whisker plots showing the median, distribution, maximum and minimum values of the size of the inhibiton zone around *S. mutans* and *E. faecalis* produced by 3% Ch-Np-Zeolite nanocomposite.

A non-parametric Mann-Whitney U-test was used to evaluate the difference in the antimicrobial activity of Ch-Np-Ze nanocomposite against *S. mutans* and *E. faecalis*. There was no significant difference in the effect of the antimicrobial activity of the nanocomposite against the two tested microbial species (p= 0.089) (Table 6-3).

Table 6-3: Mann-Whitney U test showing the effect of Ch-Np-Ze nanocomposite against the tested microbial species

Independent-Samples Mann-Whitney U Test Summary	
Total N	60
Mann-Whitney U	557.500
Standard Error	63.273
Standardized Test Statistic	1.699
Asymptotic Sig.(2-sided test)	.089

6.7.3 Effect of tissue inhibitors on the antimicrobial activity of Ch-Np-Zeolite nanocomposite

The antimicrobial activity of Ch-Np-Ze nanocomposite in the presence of tissue inhibitors (dentine powder and serum albumin) was evaluated against *S. mutans* and *E. faecalis* by measuring the number of CFU/mL over a period of time.

The presence of tissue inhibitors did not alter the antimicrobial activity of Ch-Np-Zeolite nanocomposite as antimicrobial agent against planktonic cells of *S. mutans*. Ch-Np-Zeolite nanocomposite showed complete eradication of *S. mutans* after 1 hour in the presence of dentine powder. At zero minute the mean number of the

Log CFU/mL of *S. mutans* was 6.98 for both the control group and when exposed to Ch-Np-Zeolite nanocomposite in the presence of dentine powder. However, this number declined to 6.27 at 30 minutes and showed complete eradication at 1 hour when exposed to Ch-Np-Zeolite nanocomposite compared to 6.98 at 30 minutes and 1 hour in the control group. The activity of Ch-Np-Zeolite nanocomposite continued even after 24 hours contact time (Figure 6-13). The colony forming units of *S. mutans* when exposed to Ch-Np-Zeolite nanocomposite in the presence of dentine powder are shown in Figure 6-14.

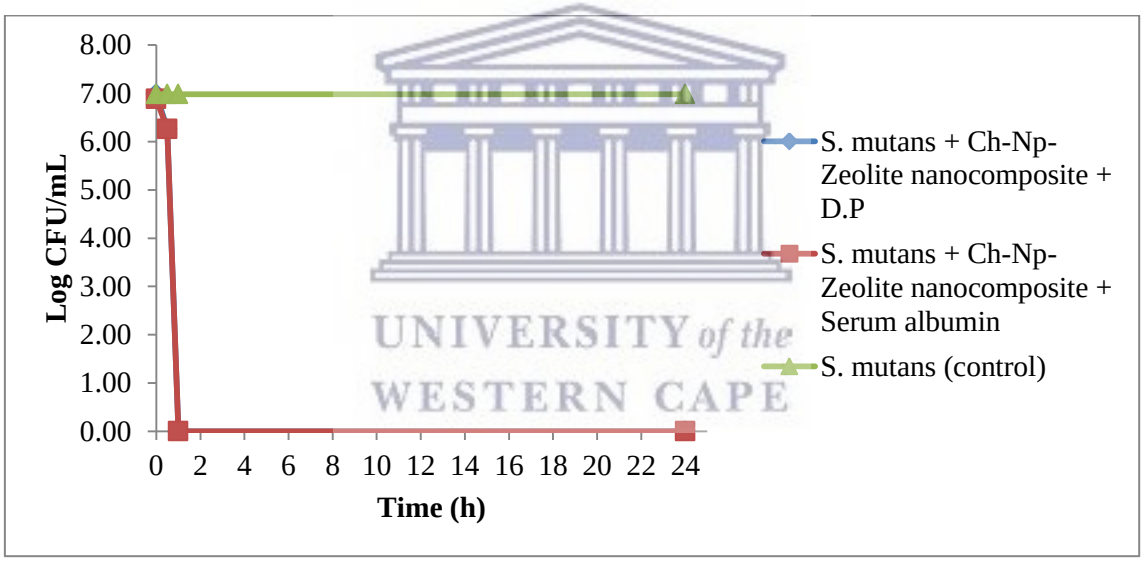

Figure 6-13: The mean Log CFU/mL of *S. mutans* when exposed to 3% Ch-Np-Zeolite nanocomposite in the presence of dentine powder (D.P) and serum albumin. The effect of the tissue inhibitors on *S. mutans* produced similar results causing the graph to be superimpose on each other.

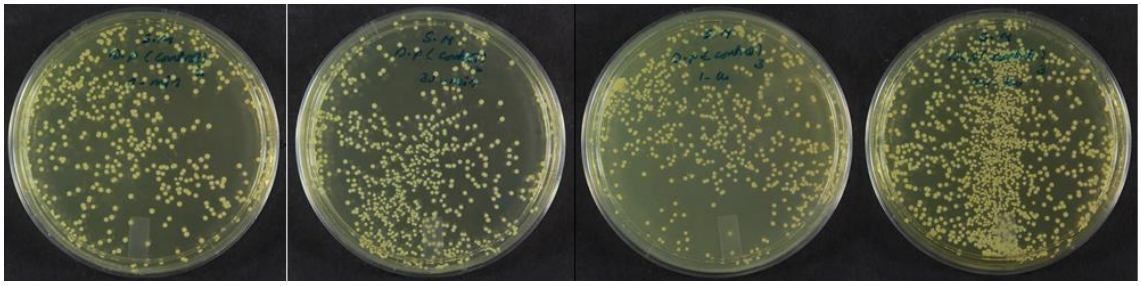

(A)

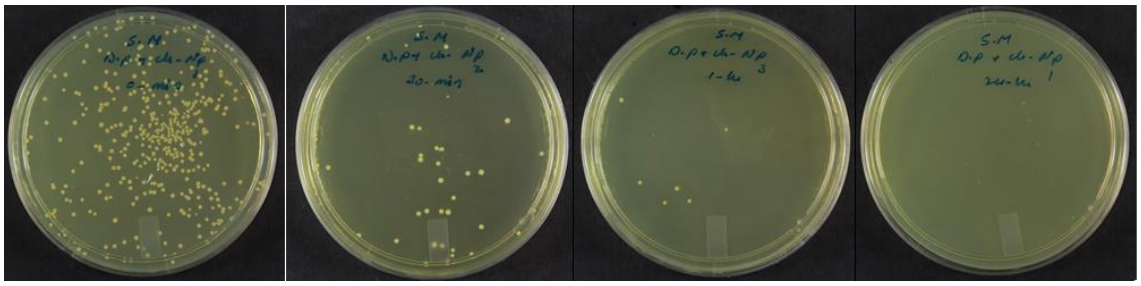

(B)

Figure 6-14: The colony forming units of *S. mutans* when exposed to Ch-Np-Zeolite nanocomposite over time in the presence of dentine powder (A) control group (B) experimental group.

The use of 3% Ch-Np-Zeolite nanocomposite completely eradicated *S. mutans* at 1 hour contact time in the presence of serum albumin. At zero minute, the mean number of the Log CFU/mL was 6.88. This number reduced to 6.26 at 30 minutes and showed complete eradication at 1 hour which continued even after 24 hour contact time (Figure 6-13). The colony forming units of *S. mutans* when exposed to Ch-Np-Zeolite nanocomposite in the presence of serum albumin are shown in Figure 6-15.

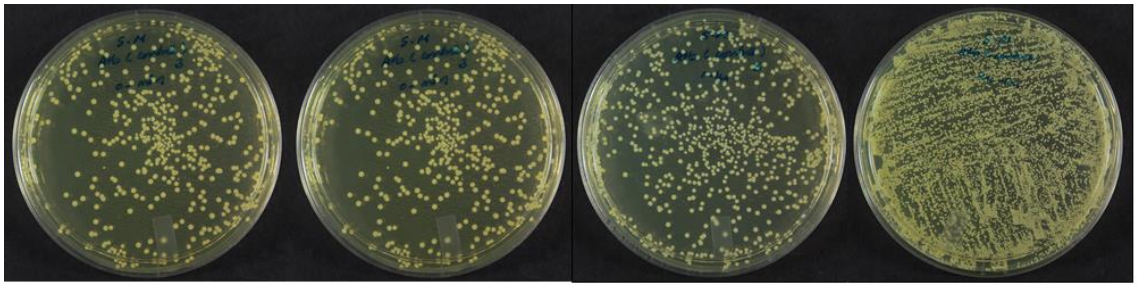

(A)

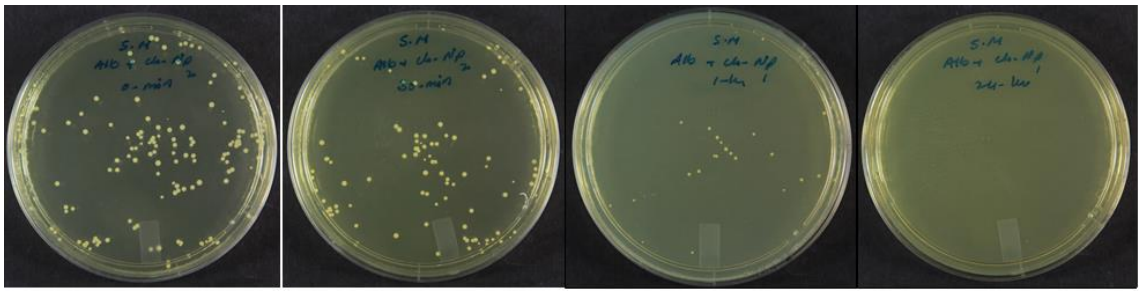

(B)

Figure 6-15: The colony forming units of *S. mutans* when exposed to Ch-Np-Zeolite nanocomposite over time in the presence of serum albumin (A) control group (B) experimental group.

The mean numbers of the Log CFU/mL of *S. mutans* following its exposure to 3% Ch-Np-Zeolite nanocomposite in the presence of dentine powder and serum albumin over time are shown in Table 6-4.

Table 6-4: The mean number of the Log CFU/mL of *S. mutans* following its exposure to 3% Ch-Np in the presence of dentine powder and serum albumin compared to the positive control group

Time (h)	*S. mutans* + Ch-Np-Zeolite nanocomposite + D.P	*S. mutans* + Ch-Np-Zeolite nanocomposite + Serum albumin	*S. mutans* (control)
0	6.98	6.88	6.98
0.5	6.27	6.26	6.98
1	0.00	0.00	6.98
24	0.00	0.00	6.98

The presence of tissue inhibitors did not alter the antimicrobial activity of the 3% Ch-Np-Zeolite nanocomposite as an antimicrobial agent against planktonic cells of *E. faecalis*. Ch-Np-Zeolite nanocomposite completely eradicated *E. faecalis* after 1 hour in the presence of dentine powder. At zero minute the mean number of the Log CFU/mL of *E. faecalis* was 6.98 for both the control group and when exposed to Ch-Np-Zeolite nanocomposite in the presence of dentine powder. This number declined to 2.01 at 30 minutes and showed complete eradication at 1 hour when exposed to Ch-Np-Zeolite nanocomposite compared to 6.98 at 30 minutes and 1 hour in the control group. The activity of Ch-Np-Zeolite nanocomposite continued even after 24 hours contact time (Figure 6-16). The colony forming units of *E. faecalis* when exposed to Ch-Np-Zeolite nanocomposite in the presence of dentine powder are shown in Figure 6-17.

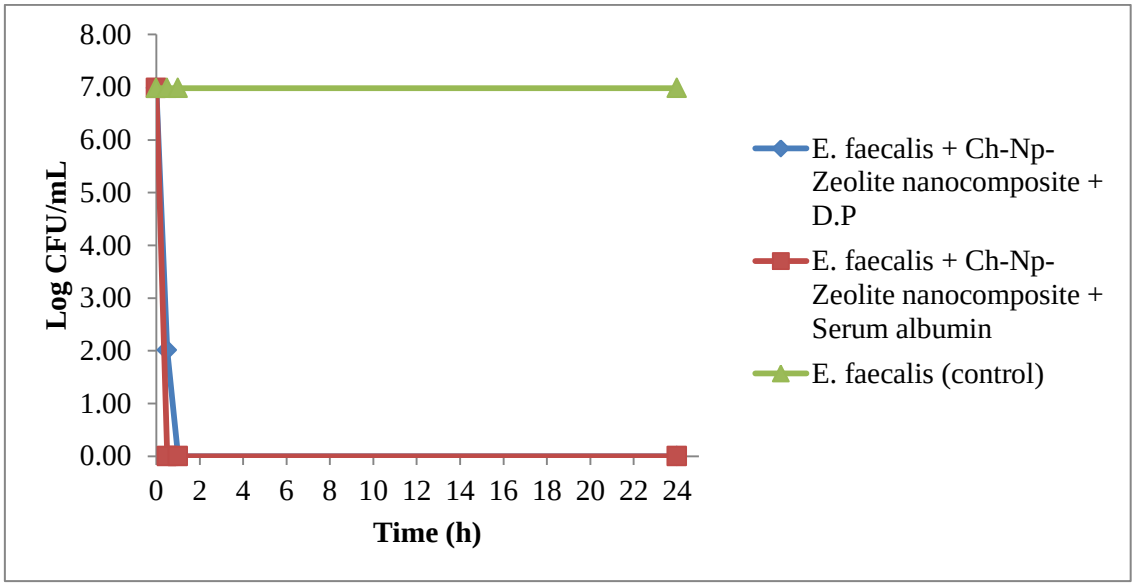

Figure 6-16: The mean Log CFU/mL of *E. faecalis* when exposed to 3% Ch-Np-Zeolite nanocomposite in the presence of dentine powder (D.P) and serum albumin.

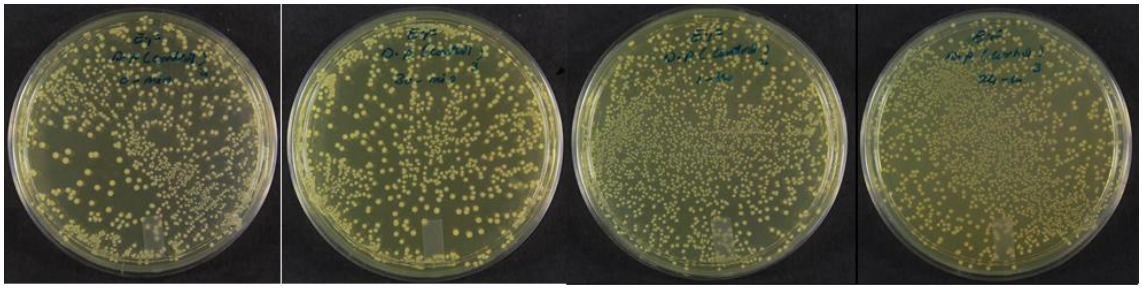

(A)

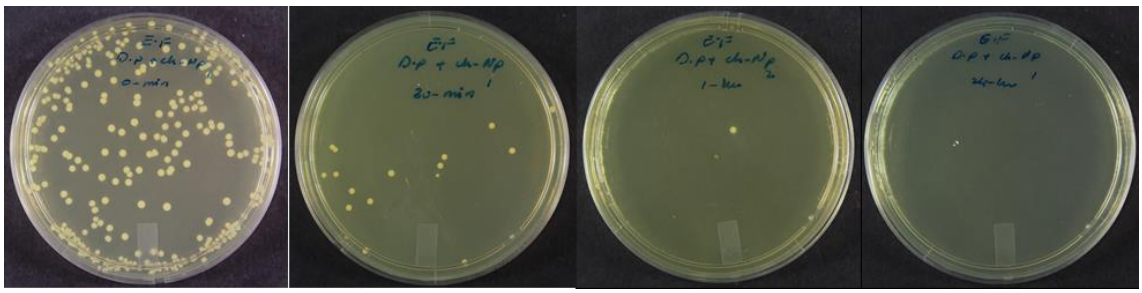

(B)

Figure 6-17: The colony forming units of *E. faecalis* when exposed to Ch-Np-Zeolite nanocomposite over time in the presence of dentine powder (A) control group (B) experimental group.

The use of 3% Ch-Np-Zeolite nanocomposite completely eradicated *E. faecalis* at 30 minutes in the presence of serum albumin. At zero minute, the mean number of the Log CFU/mL was 6.98. This number showed immediate reduction to zero showing complete eradication of *E. faecalis* at 30 minutes which continued even after 24 hours contact time (Figure 6-16). The colony forming units of *E. faecalis* when exposed to Ch-Np-Zeolite nanocomposite in the presence of dentine powder are shown in Figure 6-18.

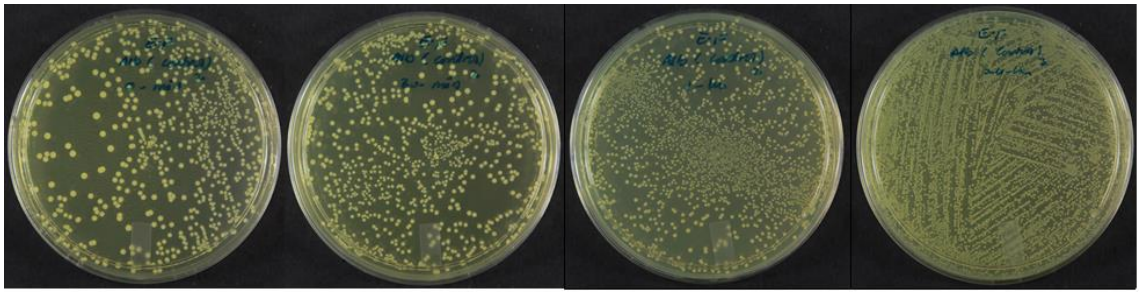

(A)

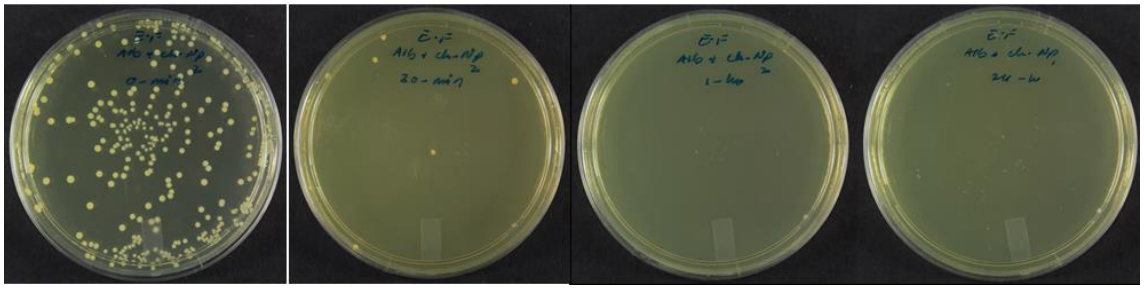

(B)

Figure 6-18: The colony forming units of *E. faecalis* when exposed to Ch-Np-Zeolite nanocomposite over time in the presence of serum albumin (A) control group (B) experimental group.

The mean numbers of the Log CFU/mL of *E. faecalis* following its exposure to 3% Ch-Np-Zeolite nanocomposite in the presence of dentine powder and serum albumin over time are shown Table 6-5.

Table 6-5: The mean number of the Log CFU/mL of *E. faecalis* following its exposure to 3% Ch-Np in the presence of dentine powder and serum albumin compared to the positive control group

Time (h)	*E. faecalis* + Ch-Np-Zeolite nanocomposite + D.P	*E. faecalis* + Ch-Np-Zeolite nanocomposite + Serum albumin	*E. faecalis* (control)
0	6.98	6.98	6.98
0.5	2.01	0.00	6.98
1	0.00	0.00	6.98
24	0.00	0.00	6.98

6.8 Discussion

Chitosan nanoparticles eradicated planktonic cells of *S. mutans* and *E. faecalis* and significantly reduced the biofilm biomass of *S. mutans, E. faecalis,* and *C. albicans* (chapter 5). However, a need for a carrier is mandatory to deliver the antimicrobial water soluble chitosan nanoparticles within the root canal system while maintain their antimicrobial activity. The aim of this study was to create a novel bioactive Ch-Np-Zeolite nanocomposite to serve as intra-canal medicament. This was done by loading Ch-Np into zeolite-Y as a carrier. One of the main drawbacks of the commonly available intra-canal medicaments is their tendency to lose their antimicrobial activity inside the root canal system as a result of the presence of tissue inhibitors such as dentine powder and serum albumin. As a result the antimicrobial activity of the novel Ch-Np-Zeolite nanocomposite was further evaluated in the presence of tissue inhibitors.

The first part of this study involved loading the synthesized antimicrobial water soluble Ch-Np onto a carrier. Zeolite- Y was selected as a carrier because of its unique properties such as its ability to adsorb the positively charged materials such as Ch-Np (Taufiqurrahmi *et al.*, 2011). Furthermore, Zeolite-Y is a porous material that allows the

entrapment of various materials inside its porosity (Missengue *et al.*, 2016). As a result of these properties Zeolite-Y was selected as a carrier for Ch-Np. The used Ch-Np concentration (3% w/v) was based on the positive results that were obtained when it was used against planktonic cells of *S. mutans, E. faecalis* and *C. albicans* and against the biofilm biomass of the same microbial species.

The second part of this experiment was aimed at evaluating the effect of loading Ch-Np in a soluble form onto zeolite-Y on its antimicrobial properties. The agar diffusion method was used as antimicrobial test as it provides a qualitative result by means of determining the susceptibility or resistance of a material against certain microbial species (Reller *et al.*, 2009). The agar diffusion test is an antimicrobial assay that does not provide information regarding the antimicrobial activity of a material such as bactericidal or bacteriostatic. However, this was not of great concern in this experiment since the bactericidal effect of Ch-Np was proved in Chapter 5 by using a Time-Kill Test.

The third part of this study was aimed evaluating the effect of tissue inhibitors on the antimicrobial activity of the novel Ch-Np-Zeolite intra-canal medicament. This was evaluated by following the standard protocol adopted by Haapasalo *et al.*, (2000) for evaluation of the effect of tissue inhibitors against the antimicrobial activity of intra-canal medicaments. In this method the intra-canal medicament was allowed to interact with the tissue inhibitors before evaluating its activity against planktonic microbial cells.

6.8.1 Synthesis and characterization of Ch-Np-Zeolite nanocomposite

Ch-Np were loaded into zeolite-Y as carrier through mixing of Ch-Np solution with the zeolite-Y powder. A ratio of 1:2 was evaluated which gave a proper paste like consistency. Zeolite-Y possesses negatively charged surfaces as a result of the presence of negatively charged AlO_4^- in their structure which is charge balanced by the presence of Na^+ (Lutz, 2014). The presence of Na^+ allows cation exchange and neutralization of the surface charge through adsorption of Ch-Np. This was shown in the EDS analysis of zeolite-Y before and after mixing with Ch-Np. The atomic percent of Na^+ in zeolite-Y before it was mixed with Ch-Np was 19.88. This value was reduced to 2.57% indicating cation exchange with Ch-Np and possibly due to the dilution effect. The process of Ch-Np adsorption is facilitated by the highly positively charged Ch-Np that resulted from the electrospraying process during synthesis. Another possible mechanism that facilitates the adsorption of Ch-Np may be the result of binding of the amino group of Ch-Np to zeolite-Y. A similar effect was observed by Xie *et al.*, (2013). Wan Ngah *et al.*, (2012a) synthesized chitosan-zeolite composite either by crosslinking with chitosan or the use of other crosslinkers such as sodium tripolyphosphate. It was shown that chitosan can be crosslinked with zeolite forming a new composite material.

The SEM analysis showed that the novel Ch-Np-Zeolite nanocomposite has a crystal like structure similar to zeolite while the Ch-Np was not shown on the SEM analysis (Figure 6-6). This may be due to the presence of Ch-Np in a soluble form.

6.8.2 Antimicrobial effect of Ch-Np-Zeolite nanocomposite

The use of zeolite as a carrier for Ch-Np did not affect its antimicrobial activity. The antimicrobial effect of the novel Ch-Np-Zeolite intra-canal medicament may be due to

the direct contact between the Ch-Np found on the surface of the zeolite and the microbial cells, the ability of the Ch-Np to be released from the zeolite structure or presence of unbound Ch-Np which may directly interact with the microbial cells.

The agar diffusion test showed a mean size inhibition zone of 9.57 mm when *S. mutans* was exposed to Ch-Np-Zeolite nanocomposite compared to 7.85 mm against *E. faecalis*. The larger inhibition zone around *S. mutans* compared to *E. faecalis* may be due to the greater antimicrobial effect of Ch-Np-Zeolite nanocomposite on *S. mutans* compared to *E. faecalis*. A similar effect was obtained by Scacchetti *et al*., (2018). The absence of an inhibition zone around *C. albicans* may be due to its planktonic form when agar diffusion test was used. However, this cannot exclude the fungistatic effect of Ch-Np-Zeolite intra-canal medicament.

6.8.3 Effect of tissue inhibitors on the antimicrobial activity of Ch-Np-Zeolite nanocomposite

The antimicrobial activity of the novel Ch-Np-Zeolite nanocomposite was not altered by the presence of tissue inhibitors. This is possibly due to the different mechanism of action adapted by the novel chitosan nanoparticles based intra-canal medicament compared to the currently available intra-canal medicaments such as the antibiotic based intra-canal medicament which is mainly based on the effect of the antibiotic used within the intra-canal medicament. However, the development of antibiotic resistant microbial species such as *E. faecalis* is one of the main drawbacks of such intra-canal medicaments (Balasubramaniam and Jayakumar, 2017). Furthermore, the antimicrobial mechanism of the calcium hydroxide and chlorhexidine based intra-canal medicaments was found to be inhibited in the presence of tissue inhibitors as a result of the buffering

effect of the inorganic and organic part of the root canal system (Haapasalo *et al.*, 2000; Spijkervet *et al.*, 1990).

As a result of all these shortcomings of other intra-canal medicaments, the novel Ch-Np-Zeolite nanocomposite may hold promise as its antimicrobial activity is based on the effect of Ch-Np. The antimicrobial mechanism of Ch-Np is multifactorial based on the ability of the nanoparticles to attach to the microbial cell wall disturbing its function and diffusing inside the microbial cell where it produced reactive oxygen species that damage the microbial DNA (Chávez de Paz *et al.*, 2011).

6.9 Conclusion

The use of zeolite Y as a carrier for Ch-Np produced a paste like consistency nanocomposite material that can easily be placed within the root canal system to serve as a novel intra-canal medicament. The loading of Ch-Np into zeolite maintained its antimicrobial activity in the presence or absence of tissue inhibitors showing superiority to the currently available intra-canal medicament.

6.10 References

Akmammedov, R., Huysal, M., Isik, S., and Senel, M. (2018). Preparation and characterization of novel chitosan/zeolite scaffolds for bone tissue engineering applications. *International Journal of Polymeric Materials and Polymeric Biomaterials*, 67(2): 110-118.

Balasubramaniam, R., and Jayakumar, S. (2017). Antibiotics in endodontics-A concise review. *International Journal of Applied Dental Sciences*, 3(4): 323-329.

Chávez de Paz, L. E., Resin, A., Howard, K. A., Sutherland, D. S., and Wejse, P. L. (2011). Antimicrobial effect of chitosan nanoparticles on *Streptococcus mutans* biofilms. *Applied and Environmental Microbiology*, 77(11): 3892-3895.

Chockattu, S. J., Deepak, B., and Goud, K. M. (2018). Comparison of anti-bacterial efficiency of ibuprofen, diclofenac, and calcium hydroxide against *Enterococcus faecalis* in an endodontic model: An in vitro study. *Journal of Conservative Dentistry*, 21(1): 80-84.

Dusselier, M., and Davis, M. E. (2018). Small-Pore Zeolites: Synthesis and Catalysis. *Chemical reviews*, 118: 5265-5329.

Estrela, C., Sydney, G. B., Bammann, L. L., and Felippe Jr, O. (1995). Mechanism of action of calcium and hydroxyl ions of calcium hydroxide on tissue and bacteria. *Brazilian Dental Journal*, 6(2): 85-90.

Fava, L., and Saunders, W. (1999). Calcium hydroxide pastes: classification and clinical indications. *International Endodontic Journal*, 32(4): 257-282.

Gougazeh, M., and Buhl, J. C. (2014). Synthesis and characterization of zeolite A by hydrothermal transformation of natural Jordanian kaolin. *Journal of the Association of Arab Universities for Basic and Applied Sciences*, 15(1): 35-42.

Haapasalo, H. K., Sirén, E. K., Waltimo, T. M. T., Òrstavik, D., and Haapasalo, M. P. P. (2000). Inactivation of local root canal medicaments by dentine: an *in vitro* study. *International Endodontic Journal*, 33(2): 126-131.

Haapasalo, M., Qian, W., Portenier, I., and Waltimo, T. (2007). Effects of dentin on the antimicrobial properties of endodontic medicaments. *Journal of Endodontics*, 33(8): 917-925.

Hedström, A. (2001). Ion exchange of ammonium in zeolites: a literature review. *Journal of Environmental Engineering*, 127(8): 673-681.

Kawashima, N., Wadachi, R., Suda, H., Yeng, T., and Parashos, P. (2009). Root canal medicaments. *International Dental Journal*, 59(1): 5-11.

Kim, H. S., and Yoon, K. B. (2014). Preparation and characterization of CdS and PbS quantum dots in zeolite Y and their applications for nonlinear optical materials and solar cell. *Coordination Chemistry Reviews*, 263-264: 239-256.

Laurino, C., and Palmieri, B. (2015). Zeolite:"the magic stone"; main nutritional, environmental, experimental and clinical fields of application. *Nutricion Hospitalaria*, 32(2): 573-581.

Lutz, W. (2014). Zeolite Y: Synthesis, modification, and properties—A case revisited. *Advances in Materials Science and Engineering*, 2014: 1-20.

Missengue, R. N., Musyoka, N. M., Madzivire, G., Babajide, O., Fatoba, O. O., Tuffin, M., and Petrik, L. F. (2016). Leaching and antimicrobial properties of silver nanoparticles loaded onto natural zeolite clinoptilolite by ion exchange and wet impregnation. *Journal of Environmental Science and Health, Part A*, 51(2): 97-104.

Mustafa, M., Alaajam, W. H., Azeim, A. A., Alfayi, N. A., Alqobty, R. M., and Alghannam, S. (2018). Diffusion of calcium hydroxide through dentinal tubules of retreated root canals: An *in vitro* study. *European Journal of Dentistry*, 12(3): 386.

Portenier, I., Haapasalo, H., Rye, A., Waltimo, T., Ørstavik, D., and Haapasalo, M. (2001). Inactivation of root canal medicaments by dentine, hydroxylapatite and bovine serum albumin. *International Endodontic Journal*, 34(3): 184-188.

Portenier, I., Waltimo, T., Ørstavik, D., and Haapasalo, M. (2006). Killing of *Enterococcus faecalis* by MTAD and Chlorhexidine Digluconate with or without Cetrimide in the Presence or Absence of Dentine Powder or BSA. *Journal of Endodontics*, 32(2): 138-141.

Reller, L. B., Weinstein, M., Jorgensen, J. H., and Ferraro, M. J. (2009). Antimicrobial susceptibility testing: a review of general principles and contemporary practices. *Clinical Infectious Diseases*, 49(11): 1749-1755.

Scacchetti, F. A., Pinto, E., and Soares, G. M. (2018). Thermal and antimicrobial evaluation of cotton functionalized with a chitosan–zeolite composite and microcapsules of phase-change materials. *Journal of Applied Polymer Science*, 135(15): 46135.

Spijkervet, F. K. L., van Saene, J. J. M., van Saene, H. K. F., Panders, A. K., Vermey, A., and Fidler, V. (1990). Chlorhexidine inactivation by saliva. *Oral Surgery, Oral Medicine, Oral Pathology*, 69(4): 444-449.

Sridhar, N., and Tandon, S. (2010). Continued Root-Growth and Apexification Using a Calcium Hydroxide and Iodoform Paste (Metapex): Three Case Reports. *Journal of Contemporary Dental Practice*, 11(5): 063-070.

Srinivas, S., Jibhkate, N., Baranwal, R., Avinash, A., and Rathi, S. (2016). Propylene glycol: a new alternative for an intracanal medicament. *Journal of International Oral Health*, 8(5): 611.

Sutton, S. (2011). Accuracy of plate counts. *Journal of Validation Technology*, 17(3): 42-46.

Taufiqurrahmi, N., Mohamed, A. R., and Bhatia, S. (2011). Nanocrystalline zeolite Y: synthesis and characterization. *IOP Conference Series: Materials Science and Engineering*, 17: 012030.

Valera, M. C., Oliveira, S., Maekawa, L., Cardoso, F., Chung, A., Silva, S., and Carvalho, C. (2016). Action of chlorhexidine, Zingiber officinale, and calcium hydroxide on *Candida albicans*, *Enterococcus faecalis*, *Escherichia coli*, and endotoxin in the root canals. *The Journal of Contemporary Dental Practice*, 17(2): 114-8.

Verboekend, D., Nuttens, N., Locus, R., Van Aelst, J., Verolme, P., Groen, J., Pérez-Ramírez, J., and Sels, B. (2016). Synthesis, characterisation, and catalytic evaluation of hierarchical faujasite zeolites: milestones, challenges, and future directions. *Chemical Society Reviews*, 45(12): 3331-3352.

Wan Ngah, W., Teong, L., Wong, C., and Hanafiah, M. (2012a). Preparation and characterization of chitosan–zeolite composites. *Journal of Applied Polymer Science*, 125(3): 2417-2425.

Wan Ngah, W. S., Teong, L. C., Toh, R. H., and Hanafiah, M. A. K. M. (2012b). Utilization of chitosan–zeolite composite in the removal of Cu(II) from aqueous solution: Adsorption, desorption and fixed bed column studies. *Chemical Engineering Journal*, 209: 46-53.

Xie, J., Li, C., Chi, L., and Wu, D. (2013). Chitosan modified zeolite as a versatile adsorbent for the removal of different pollutants from water. *Fuel*, 103: 480-485.

Yücel, A. Ç., Aksoy, A., Ertaş, E., and Güvenç, D. (2007). The pH changes of calcium hydroxide mixed with six different vehicles. *Oral Surgery, Oral Medicine, Oral Pathology, Oral Radiology, and Endodontology*, 103(5): 712-717.

Chapter 7
Cytotoxicity of the novel Ch-Np-Zeolite nanocomposite on 3T3 fibroblast cell line

7.1 Review of the literature

The use of biocompatible dental material is an important factor for use in endodontics. Biocompatibility is defined by Williams (2008) as "the ability of a biomaterial to perform its desired function with respect to a medical therapy, without eliciting any undesirable local or systemic effect in the recipient or beneficiary of that therapy, but generating the most appropriate beneficial cellular or tissue response in that specific situation, and optimising the clinically relevant performance of that therapy". Biocompatibility is a collective term that includes mutagenicity, genotoxicity carcinogenicity, histocompatibility, cytotoxicity and microbial effect (Hauman and Love, 2003).

One of the requirements of an ideal intra-canal medicament is its ability to produce an antimicrobial effect while remaining biologically compatible with the periapical tissue and not provoke irritation (Harrison *et al.*, 1979). The cytotoxic effect of various intra-canal medicaments was evaluated by many authors. Leonardo *et al*., (2002) showed that

calcium hydroxide as intra-canal medicament caused an initial inflammatory response and inhibition of bone healing in the first 7 days, which was resolved showing bone replacement within 15 to 30 days. Breault *et al.*, (1995) suggested that calcium hydroxide as intra-canal medicament should be avoided in cases where regeneration of new gingival attachment is desired as it can inhibit the gingival fibroblast attachment. Furthermore, the use of calcium hydroxide mixed with barium sulphate as intra-canal medicament may delay the healing process of the periapical area if extruded beyond the root apex (Orucoglu and Cobankara, 2008). More recently Lim *et al*., (2017) found that calcium hydroxide based intra-canal medicament that uses *N*-2-methyl-pyrrolidone as a vehicle, produced a cytotoxic effect against the L929 cell line.

Other intra-canal medicaments such as chlorhexidine based intra-canal medicament showed a cytotoxic effect when tested on embryonic fibroblasts (Sanchez *et al.*, 1988). Furthermore, chlorhexidine was shown to produce 100% apoptosis of human fibroblast, transformed keratinocyte cell lines and basal keratinocytes (Tatnall *et al.*, 1990). Chlorhexidine was also found to induce a cytotoxic effect on stem cells extracted from deciduous teeth (Tu *et al.*, 2015).

Various methods can be used according to the ISO 10993-5 to evaluate the cytotoxicity of dental materials in *in vitro* studies, such as; barrier screening assay, direct cell culture and culture extract testing, dentine barrier testing, filter diffusion testing and agar diffusion testing (Murray *et al.*, 2007). Various cell culture techniques are available for cytotoxicity testing. The most commonly used cells for *in vitro* cell culture studies are permanent mouse fibroblasts (3T3 and L-929) and human epithelium cells (HeLa) (Silva *et al.*, 2013; Geurtsen *et al.*, 1998).

The biocompatibility of nanoparticles is not certain as a result of their small particle size that allows their diffusion through various biological barriers, reaching sensitive organs such as the liver, lungs and kidneys (Pourmand and Abdollahi, 2012). Silver and gold nanoparticles were detected in multiple organs following their exposure to rats suggesting their toxic potential (Lee *et al.*, 2018).

Polymeric nanoparticles are biodegradable and have non-inflammatory and non-immunologic tissue effects in addition to the low potentiality to produce cytotoxic effect (Bahadar *et al.*, 2016). Ch-Np are synthesized using various techniques. The use of the ionic gelation technique resulted in a non-toxic Ch-Np that was tested against A549 cells (Huang *et al.*, 2004). A similar effect was obtained by Qi *et al*., (2005) in which the number of the viable cells of BEL7402, BGc823 and Colo320 tumour cells was not reduced following their exposure to Ch-Np. However, Grabowski *et al*., (2015) showed that the use of different chemicals during polymeric nanoparticles synthesis may affect their biocompatibility.

7.2 Rationale of the study

The novel Ch-Np-Zeolite nanocomposite showed promising antimicrobial activity against some endodontic pathogens even in the presence of tissue inhibitors. However, with the increased concern regarding the cytotoxic effect of using nanoparticles in human tissue, cytotoxicity testing is essential to validate the use of the novel Ch-Np-Zeolite nanocomposite as intra-canal medicament.

7.3 Aim of the study

The aim of this study was to evaluate the effect of each component in the novel Ch-Np Zeolite nanocomposite separately and when mixed together forming the novel Ch-Np-Zeolite nanocomposite.

7.4 Objectives

i. To evaluate the cytotoxic effect of LMW-Ch, Ch-Np, Zeolite Y and Ch-Np-Zeolite nanocomposite against 3T3 mouse fibroblasts cell lines using a MTT assay.

7.5 Null hypothesis

i. There is a cytotoxic effect of using LMW-Ch, Ch-Np, Zeolite-Y and the novel Ch-Np-Zeolite nanocomposite on 3T3 mouse fibroblast cells.

7.6 Methodology

7.6.1 Cells lines

The cytotoxicity test was done by measuring the survival rate of Balb/c 3T3 mouse fibroblast cell-lines obtained from the National Repository for Biological Materials (Sandringham South Africa). The Balb/c 3T3 mouse fibroblast cells were grown as described by Grobler *et al.*, (2008). The cells were incubated at 37°C under 5% carbon dioxide and 95% humidity in Dulbecco's Modified Eagle's medium (DMEM). The medium was mixed with 1% Penicillin/Streptomycin mix (Cambrex Bio Science) and 10% fetal bovine serum as supplement. The cells were subcultured every 48 hours using trypsin/ethylenediaminetetra acetic acid (EDTA) and DMEM. The pH of the growth medium was adjusted to 8.

7.6.2 Cytotoxicity testing

The 3T3 cells were allowed to grow to near confluency. The cells were diluted to final suspension containing approximately 3×10^5 cells/mL. 100 µL of the Balb/c 3T3 cells was plated in 96-well plates and allowed to grow and attach to the well surface for 24 hours.

The medium was replaced by 100 µL of LMW-Ch (group A), Ch-Np (group B), Zeolite-Y (group C) and Ch-Np-Zeolite nanocomposite (group D) and incubated for 24 hours. The control group (E) contained DMEM medium (n=16). The survival rate of Balb/c 3T3 mouse fibroblast cells was evaluated using the MTT colorimetric assay as described by Mosmann (1983). This assay is based on the ability of the mitochondria in the living cells to convert the yellow water-soluble MTT into a dark blue insoluble formazan product which is directly proportional to the number of surviving cells.

7.6.3 MTT assay

5 mg of MTT (3-(4,5-dimethylethylthiazol-2-yl)-2,5-diphenyl tetrazolium bromide, SigmaAldrich, South Africa) was dissolved in 1 mL of PBS and sterilized. 10 µL of the MTT was added to each well of each group and incubated at 37°C. After 3 hours the medium that contained the MTT was discarded in all groups. 100 µL of di-methylsulfoxide (DMSO) was added to each well to solubilize the Fromazan crystal before measuring the color change (Figure 7-1) as represented by optical density of the living cells when absorbed at a wave length of 540 nm using a microplate reader (Rayto Rt–2100C, Germany). The test was repeated in triplicate.

Figure 7-1: 96 well-plate showing the difference in colour between the control group (control wells) and the experimental group (test samples). The change in colour density indicates increase in the growth rate of the Balb/c 3T3 fibroblast cells.

7.7 Data analysis

Results for each group were transferred to an Excel spreadsheet (Microsoft Corporation 2010, USA). The data was expressed as a mean of optical density values and then analyzed using IBM SPSS statistics software (version 25, IBM, USA). The mean of each group was compared to the control group and expressed as a percentage of the control which represents 100%. The assay was repeated 4 times. A t-test was used to evaluate the statistical difference between each group and the control group.

7.8 Results

7.8.1 Cytotoxic effect of LMW-Ch

Following exposure of Balb/c 3T3 mouse fibroblast cells to LMW-Ch, the mean of the optical density values of the Balb/c 3T3 mouse fibroblast cells increased to 0.74 compared to their control which is 0.69 (Table 7-1).

Table 7-1: The mean, standard deviation and standard error of the mean of the optical density of Balb/c 3T3 mouse fibroblast cells in control condition and when exposed to LMW-Ch.

Group	Mean	Std. Deviation	Std. Error Mean
LMW-Ch	0.74	0.10	0.01
Control	0.69	0.10	0.01

Comparison was made between the mean growth rates of Balb/c 3T3 mouse fibroblast cells in each group using a t-test to determine if there is any statistically significant difference between the two groups. There was a statistical difference ($p = 0.00$) between

the growth rate of 3T3 fibroblast cells in normal conditions and following their exposure to LMW-Ch (Table 7-2).

Table 7-2: Comparison between the growth rate of the control of Balb/c 3T3 mouse fibroblast cells and LMW-Ch group using a t-test showing statistical difference between the two groups.

Levene's Test for Equality of Variances		t-test for Equality of Means						
F	Sig.	t	degree of freedom	Sig. (2-tailed)	Mean Difference	Std. Error Difference	95% Confidence Interval of the Difference	
							Lower	Upper
0.58	0.45	2.95	126.00	0.00	0.05	0.02	0.02	0.09

7.8.2 Cytotoxicity of Ch-Np

Following exposure of Balb/c 3T3 mouse fibroblast cells to Ch-Np, the mean of the optical density values of the Balb/c 3T3 mouse fibroblast cells was similar (0.67) in both groups (Table 7-3).

Table 7-3: The mean, standard deviation and standard error of the mean of the optical density of Balb/c 3T3 mouse fibroblast cells in control condition and when exposed to Ch-Np.

Group	Mean	Std. Deviation	Std. Error Mean
Ch-Np	0.67	0.11	0.01
Control	0.67	0.13	0.02

A comparison was made between the mean growth rates of Balb/c 3T3 mouse fibroblast cells in each group using a t-test to determine if there is any statistically significant difference between the two groups. There was no statistical difference (p = 0.89) between the growth rate of 3T3 fibroblast cells in normal conditions and following their exposure to Ch-Np (Table 7-4).

Table 7-4: Comparison between the growth rate of the control of Balb/c 3T3 mouse fibroblast cells and Ch-Np group using a t-test showing no statistical difference between the two groups.

Levene's Test for Equality of Variances		t-test for Equality of Means						
F	Sig.	t	degree of freedom	Sig. (2-tailed)	Mean Difference	Std. Error Difference	95% Confidence Interval of the Difference	
							Lower	Upper
9.12	0.00	0.15	126.00	0.89	0.00	0.02	-0.04	0.04

7.8.3 Cytotoxicity of Zeolite-Y

Following exposure of Balb/c 3T3 mouse fibroblast cells to zeolite-Y, the mean of the optical density values of the Balb/c 3T3 mouse fibroblast cells increased to 0.69 compared to their control which is 0.66 (Table 7-5).

Table 7-5: The mean, standard deviation and standard error of the mean of the optical density of Balb/c 3T3 mouse fibroblast cells in control condition and when exposed to zeolite-Y

Group	Mean	Std. Deviation	Std. Error Mean
Zeolite-Y	0.69	0.08	0.01
Control	0.66	0.09	0.01

A comparison was made between the mean growth rates of Balb/c 3T3 mouse fibroblast cells in each group using a t-test to determine if there is any statistically significant difference between the two groups. There was no statistical difference ($p = 0.05$) between the growth rate of 3T3 fibroblast cells in normal conditions and following their exposure to zeolite-Y (Table 7-6).

Table 7-6: Comparison between the growth rate of the control of Balb/c 3T3 mouse fibroblast cells and zeolite-Y group using a t-test showing no statistical difference between the two groups.

Levene's Test for Equality of Variances		t-test for Equality of Means						
F	Sig.	t	degree of freedom	Sig. (2-tailed)	Mean Difference	Std. Error Difference	95% Confidence Interval of the Difference	
							Lower	Upper
0.19	0.66	1.98	126.00	0.05	0.03	0.02	-	0.06

7.8.4 Cytotoxicity of Ch-Np-Zeolite nanocomposite

Following exposure of Balb/c 3T3 mouse fibroblast cells to Ch-Np-Zeolite nanocomposite, the mean of the optical density values of the Balb/c 3T3 mouse fibroblast cells increased to 0.69 compared to their control which is 0.66 (Table 7-7).

Table 7-7: The mean, standard deviation and standard error of the mean of the optical density of Balb/c 3T3 mouse fibroblast cells in control condition and when exposed to Ch-Np-Zeolite nanocomposite

Group	Mean	Std. Deviation	Std. Error Mean
Ch-Np-Zeolite nanocomposite	0.58	0.06	0.01
Control	0.51	0.04	0.01

Comparison was made between the mean growth rates of Balb/c 3T3 mouse fibroblast cells in each group using a t-test to determine if there is any statistically significant difference between the two groups. There was a statistical difference ($p = 0.00$) between the growth rate of 3T3 fibroblast cells in normal conditions and following their exposure to Ch-Np-Zeolite nanocomposite (Figure 7-2) when analyzed using a t test (Table 7-8).

Table 7-8: Comparison between the growth rate of the control of Balb/c 3T3 mouse fibroblast cells and Ch-Np-Zeolite nanocomposite group using a t-test showing statistical difference between the two groups.

Levene's Test for Equality of Variances		t-test for Equality of Means						
F	Sig.	t	degree of freedom	Sig. (2-tailed)	Mean Difference	Std. Error Difference	95% Confidence Interval of the Difference	
							Lower	Upper
6.00	0.02	8.57	126.00	0.00	0.07	0.01	0.06	0.09

(A) (B)

Figure 7-2: Balb/c 3T3 mouse fibroblast cells showing (A) increased growth rate following their exposure to Ch-Np-Zeolite nanocomposite compared to (B) their growth rate in normal conditions.

7.8.5 Survival rate of Balb/c 3T3 fibroblast cell

All groups, that is cells exposed to LMW-Ch, Ch-Np, zeolite-Y and Ch-Np-Zeolite nanocomposite showed positive growth. 3T3 cells showed 100% growth rate in the control group. The growth rate increased to 100.45 % and 104.57 % when exposed to Ch-Np and zeolite-Y respectively, which was not statistically different to the control group ($p > 0.05$, t – test). The growth rate of 3T3 cells when exposed to LMW-Ch and Ch-Np-Zeolite nanocomposite increased to 107.48 and 114.68 respectively, which was statistically significant to the control group ($p < 0.05$, t – test) as shown in Figure 7-3.

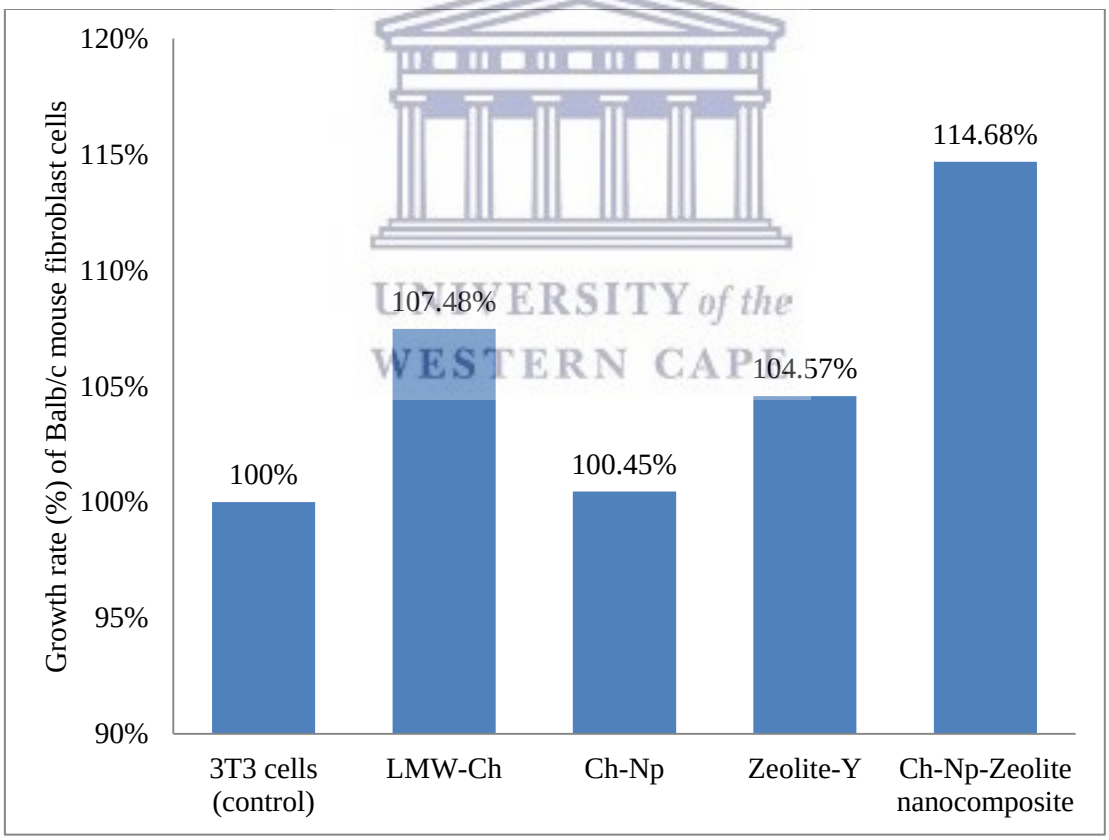

Figure 7-3: Bar graph showing the growth rate of Balb/c 3T3 mouse fibroblast cells when exposed to LMW-Ch, Ch-Np, zeolite-Y and Ch-Np-Zeolite nanocomposite.

7.9 Discussion

The biocompatibility of any new material is an important factor that determines its applicability for use in humans. There are various tests that are followed starting from *in vitro* initial tests such as cytotoxicity and mutagenicity followed by animal studies and finally preclinical and clinical testing on humans (Hauman and Love, 2003). Hence, cytotoxicity is the frontline of biocompatibility testing. The novel Ch-Np-Zeolite nanocomposite was cytotoxic for endodontic pathogens showing complete eradication of some endodontic pathogens in a short period of time. However, similar effects on human cells should be excluded. The purpose of this study was to exclude any cytotoxic effect when using the novel Ch-Np-Zeolite nanocomposite or its component for *in vitro* cell culture studies.

The ISO standard (10993-5) categorized the end point when measuring cytotoxicity of a material by either; (i) evaluating the cell damage by morphological means with morphological assessment, (ii) measuring the cell damage, (iii) measuring the cell growth and (iv) measuring specific aspects of cellular metabolism (Kirkpatrick *et al.*, 1998). The MTT colorimetric assay is a qualitative assay that provides sensitivity and reliability in measuring the growth, viability and activation of cells (Foldbjerg *et al.*, 2011). This assay provided information regarding the effect of LMW-Ch, Ch-Np, zeolite-Y and Ch-Np-Zeolite nanocomposite on fibroblast cells.

The Balb/c 3T3 mouse fibroblast cells were selected as a testing cell line in this study. 3T3 cells are permanent cell lines that have the ability to replicate without specific metabolic potential (Roberta *et al.*, 2003). Furthermore, the 3T3 cells were shown to be

the most commonly used cell line to evaluate the cytotoxicity of endodontic materials *in vitro* (Hassan and Khallaf, 2018; Geurtsen *et al.*, 1998).

In this study, LMW-Ch showed a statistically significant higher growth rate of 3T3 cells compared to their control. Although the exact mechanism that resulted in increased cell growth was not evaluated, it may be due to chitosan's molecular weight and high degree of deacetylation (75% - 85%) which may influence this effect. This assumption is supported by another study that showed chitosan as a biocompatible material (Tripathi and Singh, 2018). Various factors may affect the biocompatibility of chitosan such as its molecular weight which was shown to affect the survival rate of a Balb/c 3T3 cell line in which higher growth rate was observed as the molecular weight increased although different molecular weights tested showed positive results (Grobler and Perchyonok, 2018). The degree of deacetylation of chitosan was found to reduce the survival rate of a 3T3 mouse fibroblast cell line in which the lower the degree of deacetylation the more cytotoxic the effect (Grobler *et al.*, 2016).

The change in particle size of LMW-Ch into nanoparticles resulted in reduction in its polydispersity index and thus molecular weight (Rogošić *et al.*, 1996). The synthesized Ch-Np did not increase the growth rate of the 3T3 mouse fibroblast cell line significantly compared to LMW-Ch which may be due to the reduction in its molecular weight.

Similarly, zeolite-Y did not affect the growth rate of 3T3 cells positively or negatively. A similar result was observed by Thom *et al.*, (2003) where the cytotoxic effect of zeolite containing endodontic sealer on a Hela cell line was tested.

The Ch-Np Zeolite nanocomposite seems to promote the growth of 3T3 fibroblast cells in culture. Although the exact mechanism that resulted in increased cell growth is not known, this result may be due to the combined activity of Ch-Np and zeolite-Y. Furthermore, this result suggests the ability of the novel Ch-Np-Zeolite nanocomposite to promote healing of the injured periapical area if accidentally passed to the periapical tissue.

7.10 Conclusion

None of the tested materials showed any cytotoxic effect when tested against 3T3 fibroblast cells. However, the Ch-Np Zeolite nanocomposite seemed to promote the growth of 3T3 fibroblast cells in culture suggesting its ability to promote healing of the injured periapical area if accidentally passed to the periapical tissue.

7.11 References

Bahadar, H., Maqbool, F., Niaz, K., and Abdollahi, M. (2016). Toxicity of nanoparticles and an overview of current experimental models. *Iranian Biomedical Journal*, 20(1): 1-11.

Breault, L. G., Schuster, G. S., Billman, M. A., Hanson III, B. S., Kudryk, V. L., Pashley, D. H., Runner, R. R., and McPherson III, J. C. (1995). The effects of intracanal medicaments, fillers, and sealers on the attachment of human gingival fibroblasts to an exposed dentin surface free of a smear layer. *Journal of periodontology*, 66(7): 545-551.

Foldbjerg, R., Dang, D. A., and Autrup, H. (2011). Cytotoxicity and genotoxicity of silver nanoparticles in the human lung cancer cell line, A549. *Archives of Toxicology*, 85(7): 743-750.

Geurtsen, W., Leinenbach, F., Krage, T., and Leyhausen, G. (1998). Cytotoxicity of four root canal sealers in permanent 3T3 cells and primary human periodontal ligament fibroblast cultures. *Oral Surgery, Oral Medicine, Oral Pathology, Oral Radiology, and Endodontology*, 85(5): 592-597.

Grabowski, N., Hillaireau, H., Vergnaud, J., Tsapis, N., Pallardy, M., Kerdine-Römer, S., and Fattal, E. (2015). Surface coating mediates the toxicity of polymeric nanoparticles towards human-like macrophages. *International Journal of Pharmaceutics*, 482(1-2): 75-83.

Grobler, S., Olivier, A., Kruijsse, H., and Perchyonok, V. (2016). Cytotoxicity of different degrees of de-acetylated chitosan on 3T3-and two human tooth fibroblast cell-lines. *International Journal of Dentistry and Oral Sciences*, 3(10): 337-339.

Grobler, S. R., Oliver, A., Moodley, D., and Van Wyk Kotze, T. J. (2008). Cytotoxicity of recent dentin bonding agents on mouse fibroblast cells. *Quintessence International*, 39(6): 511-516.

Grobler, S. R., and Perchyonok, V. (2018). Cytotoxicity of Low, Medium and High Molecular weight Chitosan's on Balb/c 3T3 Mouse Fibroblast Cells at a 75-85% De-acetylation Degree. *Material Science and Engineering with Advanced Research*, 2(2): 27-30.

Harrison, J. W., Bellizzi, R., and Osetek, E. M. (1979). The clinical toxicity of endodontic medicaments. *Journal of Endodontics*, 5(2): 42-47.

Hassan, R., and Khallaf, M. (2018). Effect of a silver nanoparticle intracanal-based medicament on the microhardness of human radicular dentine. *Endodontic Practice Today*, 12(2): 125-131.

Hauman, C., and Love, R. (2003). Biocompatibility of dental materials used in contemporary endodontic therapy: a review. Part 1. Intracanal drugs and substances. *International Endodontic Journal*, 36(2): 75-85.

Huang, M., Khor, E., and Lim, L.-Y. (2004). Uptake and cytotoxicity of chitosan molecules and nanoparticles: effects of molecular weight and degree of deacetylation. *Pharmaceutical Research*, 21(2): 344-353.

ISO10993. International Standards Organization. Biological evaluation of medical devices-part 5: tests for *in vitro* cytotoxicity. 2017.

Kirkpatrick, C., Bittinger, F., Wagner, M., Köhler, H., Van Kooten, T., Klein, C., and Otto, M. (1998). Current trends in biocompatibility testing. *Proceedings of the Institution of Mechanical Engineers, Part H: Journal of Engineering in Medicine*, 212(2): 75-84.

Lee, J. H., Sung, J. H., Ryu, H. R., Song, K. S., Song, N. W., Park, H. M., Shin, B. S., Ahn, K., Gulumian, M., and Faustman, E. M. (2018). Tissue distribution of gold and silver after subacute intravenous injection of co-administered gold and silver nanoparticles of similar sizes. *Archives of Toxicology*, 92(4): 1393-1405.

Leonardo, M. R., Silveira, F. F., Silva, L. A. B. d., Tanomaru Filho, M., and Utrilla, L. S. (2002). Calcium hydroxide root canal dressing. Histopathological evaluation of periapical repair at different time periods. *Brazilian Dental Journal*: 17-22.

Lim, M.-J., Jang, H.-J., Yu, M.-K., Lee, K.-W., and Min, K.-S. (2017). Removal efficacy and cytotoxicity of a calcium hydroxide paste using N-2-methyl-pyrrolidone as a vehicle. *Restorative Dentistry & Endodontics*, 42(4): 290-300.

Mosmann, T. (1983). Rapid colorimetric assay for cellular growth and survival: application to proliferation and cytotoxicity assays. *Journal of Immunological Methods*, 65(1-2): 55-63.

Murray, P. E., García Godoy, C., and García Godoy, F. (2007). How is the biocompatibilty of dental biomaterials evaluated? *Medicina Oral, Patología Oral Y Cirugía Bucal*, 12(3): 258-266.

Orucoglu, H., and Cobankara, F. K. (2008). Effect of unintentionally extruded calcium hydroxide paste including barium sulfate as a radiopaquing agent in treatment of teeth with periapical lesions: report of a case. *Journal of Endodontics*, 34(7): 888-891.

Pourmand, A., and Abdollahi, M. (2012). Current Opinion on Nanotoxicology. *DARU Journal of Pharmaceutical Sciences*, 20(1): 95.

Qi, L., Xu, Z., Jiang, X., Li, Y., and Wang, M. (2005). Cytotoxic activities of chitosan nanoparticles and copper-loaded nanoparticles. *Bioorganic & Medicinal Chemistry Letters*, 15(5): 1397-1399.

Roberta, T., Federico, M., Federica, B., Antonietta, C. M., Sergio, B., and Ugo, C. (2003). Study of the potential cytotoxicity of dental impression materials. *Toxicology in Vitro*, 17(5-6): 657-662.

Rogošić, M., Mencer, H. J., and Gomzi, Z. (1996). Polydispersity index and molecular weight distributions of polymers. *European Polymer Journal*, 32(11): 1337-1344.

Sanchez, I. R., Nusbaum, K. E., Swaim, S. F., Hale, A. S., Henderson, R. A., and McGurie, J. A. (1988). Chlorhexidine diacetate and povidone-iodine cytotoxicity to canine embryonic fibroblasts and *Staphylococcus aureus*. *Veterinary Surgery*, 17(4): 182-185.

Silva, E. J. N. L., Rosa, T. P., Herrera, D. R., Jacinto, R. C., Gomes, B. P. F. A., and Zaia, A. A. (2013). Evaluation of Cytotoxicity and Physicochemical Properties of Calcium Silicate-based Endodontic Sealer MTA Fillapex. *Journal of Endodontics*, 39(2): 274-277.

Tatnall, F., Leigh, I., and Gibson, J. (1990). Comparative study of antiseptic toxicity on basal keratinocytes, transformed human keratinocytes and fibroblasts. *Skin Pharmacology and Physiology*, 3(3): 157-163.

Thom, D. C., Davies, J. E., Santerre, J. P., and Friedman, S. (2003). The hemolytic and cytotoxic properties of a zeolite-containing root filling material *in vitro*. *Oral Surgery, Oral Medicine, Oral Pathology, Oral Radiology, and Endodontology*, 95(1): 101-108.

Tripathi, K., and Singh, A. (2018). Chitin, chitosan and their pharmacological activities: A review. *International Journal of Pharmaceutical Sciences and Research* 9(7): 2626-2635.

Tu, Y.-Y., Yang, C.-Y., Chen, R.-S., and Chen, M.-H. (2015). Effects of chlorhexidine on stem cells from exfoliated deciduous teeth. *Journal of the Formosan Medical Association*, 114(1): 17-22.

Williams, D. F. (2008). On the mechanisms of biocompatibility. *Biomaterials*, 29(20): 2941-2953.

Chapter 8
Summary, conclusion, limitations and recommendations

8.1 Summary of the thesis

The ultimate goal of treating root canal infection is to establish complete disinfection of the root canal system. This is achieved through a series of clinical steps starting from mechanical preparation of the root canal system using various endodontic instruments that mechanically remove some of the infected root canal dentine. The mechanical preparation is followed by chemical preparation which includes the use of antimicrobial endodontic irrigant solutions which attempt to eradicate the remaining endodontic pathogens. However, complete eradication of endodontic pathogens using various irrigant solutions was not reported in the literature. Intra-canal medicaments are antimicrobial agents that are placed inside the root canal system for a period of time to eradicate the remaining and persistent endodontic pathogens within the root canal system. However, the antimicrobial activity of most intra-canal medicaments is reduced inside the root canal system as a result of the effect of tissue inhibitors.

The introduction of nanotechnology which is based on the concept of using a material on a nano-scale level has expanded the application of different materials in various areas. One of these applications is the use of nanoparticles as antimicrobial agents

which gained much attention as a result of the multiple mechanisms adopted by the nanoparticles to eradicate the microbial cell and thus overcoming one of the main shortcomings of the common antimicrobial agents currently available, namely the development of microbial resistance.

The aim of this study was to develop a novel nanoparticle based intra-canal medicament to overcome the shortcomings of the currently available intra-canal medicaments. To achieve this aim a series of laboratory experiments were performed starting from the selection of a suitable material for synthesis of nanoparticles and evaluate its antimicrobial effect against three endodontic pathogens and to evaluate whether the activity is concentration dependent. Chitosan was selected because of its ability to produce an antimicrobial effect against microbial species in medicine. In this study, chitosan showed an antimicrobial effect against endodontic pathogens tested and showed complete eradication of *S.* mutans and *E. faecalis* as well as fungistatic effect against *C. albicans*. For this to be used as intra-canal medicament it needs to be made water soluble. Furthermore, the chitosan needed to be converted to nanoparticles size to enable penetration into the dentinal tubules and possibly enhances its activity to a wider area within the root canal system.

Therefore, synthesis of water soluble chitosan nanoparticles was necessary. Chitosan nanoparticles was synthesized using the electrospraying technique which was able to produce water soluble and highly positively charged nanoparticles as a result of the electrical current generated during the electrospraying process. The highly positively charged Ch-Np enhanced its antimicrobial activity. Furthermore, the use of trifluoroacetic acid as a solvent renders the chitosan water soluble while maintaining the

main chemical structure of the chitosan. This was confirmed through dynamic light scattering analysis, FTIR and SEM.

Once chitosan nanoparticles were formed and characterized, the antimicrobial effect against endodontic pathogens was evaluated and compared to the effect of LMW-Ch. The results showed that Ch-Np had a better antimicrobial effect compared to LMW-Ch, and was able to eradicate *S. mutans* and *E. faecalis* in a shorter time period and showed a reduction in the colony forming units of *C. albicans*. Furthermore, the synthesized Ch-Np showed a statistically significant reduction in the biofilm biomass of the three tested pathogens.

Once the antimicrobial activity of Ch-Np was proven, hence, the next step was to load the Ch-Np into a carrier to form a novel intra-canal medicament while maintaining the antimicrobial properties of Ch-Np. Zeolite-Y is a microporous crystalline hydrated sodium aluminosilicate material that was shown to have the capacity to adsorb various materials inside it as a result of its porosity and cationic action. Ch-Np was successfully loaded onto zeolite-Y forming a new intra-canal medicament that maintained its antimicrobial activity.

One of the problems with the current intra-canal medicaments is that they are inhibited within the root canal system by the effect of tissue inhibitors such as dentine powder and serum albumin. Hence the newly created Ch-Np-Zeolite intra-canal medicament was further tested for its antimicrobial activity in the presence of tissue inhibitors. It was shown that the newly created intra-canal medicament was not affected by the presence of tissue inhibitors, showing its ability to maintain its activity inside the root canal system.

Considering that the novel intra-canal medicament will be used in human tissue, it is imperative that it should be biocompatible. Hence the need of cytotoxicity testing is mandatory. Therefore, the cytotoxicity of the novel Ch-Np-Zeolite nanocomposite and its components were evaluated against Balb/c 3T3 mouse fibroblast cells, one of the most commonly used cell lines to evaluate the cytotoxicity of endodontic material. This experiment showed that none of the tested materials showed any cytotoxic effect when tested against 3T3 fibroblast cells. The Ch-Np-Zeolite intra-canal medicament seemed to promote the growth of 3T3 fibroblast cells in culture suggesting its ability to promote healing of the injured periapical area if accidentally passed to the periapical tissue.

Based on the results of these experiments this newly created Ch-Np-Zeolite nanonanocomposite can therefore be used as advanced treatment modalities to disinfect the root canal system.

8.2 Conclusion

Chitosan nanoparticles completely eradicated planktonic cells of *S. mutans* and *E. faecalis* of which the latter is one of the most resistant endodontic pathogens, and showed fungistatic activity against *C. albicans*. Furthermore, chitosan nanoparticles disrupt the biofilm integrity of the three pathogens showing the possibility of broader antimicrobial affect against planktonic and biofilm states of microbial contamination.

In order to provide a clinical application for the antimicrobial chitosan nanoparticles, a novel chitosan nanoparticle based intra-canal medicament was created by loading Ch-Np onto Zeolite-Y as a carrier. The loading of Ch-Np onto Zeolite-Y resulted in a paste like material that can easily be maintained within the root canal system while providing the antimicrobial activity of Ch-Np. One of the characteristic properties of the

novel Ch-Np-Zeolite intra-canal medicament is its ability to maintain its antimicrobial activity in the presence of tissue inhibitors such as dentine powder and serum albumin, overcoming one of the main disadvantages of the currently available intra-canal medicaments. Another advantage of the novel Ch-Np-Zeolite intra-canal medicament is its ability to enhance the growth of the 3T3 fibroblast cells which may contribute to the healing process of the injured periapical tissue.

8.3 Limitations of the study

i. This is an *in vitro* study which needs to be tested *in vivo*.

ii. This novel intra-canal medicament was tested on three endodontic pathogens. Perhaps more endodontic microbial species should be evaluated.

iii. The depth of antimicrobial activity of the Ch-Np-Zeolite intra-canal medicament within the dentinal tubules over extended time period was not evaluated.

8.4 Recommendations for further research projects

i. A randomized clinical trial is recommended to test and verify the *in vitro* results.

ii. The depth of activity of the novel Ch-Np-Zeolite nanocomposite inside the dentinal tubules needs further investigation.

iii. The effect of adding radiopaque material into the novel Ch-Np-Zeolite nanocomposite and its effect on its antimicrobial activity is an area that requires further investigations.

iv. The antimicrobial activity of the newly created intra-canal medicament needs to be tested in wide variety of endodontic pathogens.